



UNIVERSITÀ DEGLI STUDI DI SALERNO



UNIVERSITÀ DEGLI STUDI DI SALERNO
Dipartimento di Farmacia

PhD Program
in **Drug Discovery and Development**
XXX Cycle — Academic Year 2017/2018

PhD Thesis in

***Design and synthesis of bioactive small
molecules by traditional and innovative
methods***

Candidate

Tania Ciaglia

Supervisor

Prof. *Pietro Campiglia*

PhD Program Coordinator: Prof. Dr. *Gianluca Sbardella*

INDEX

Abstract

CHAPTER 1: Design, synthesis and biological evaluation of new TRPM8 modulators	1
1.1 Introduction: TRP, an overview	2
1.2 TRPM8: features, structure and localization	6
1.3 TRPM8: physiopathological role	8
1.3.1 TRPM8 and cancer	
1.3.2 TRPM8 and pain	
1.3.3 TRPM8 in overactive bladder and painful bladder syndrome	
1.4 TRPM8 modulation	11
1.4.1 TRPM8 activators	
1.4.2 TRPM8 inhibitors	
2.1 Tryptamine-based derivatives as TRPM8 channel modulators: Background	15
2.2 Synthesis of 1st series	17
2.3 Activity and binding evaluation of the N-substituted Tryptamines synthesized	20
2.3.1 Screening of the activity of the 1 st series by Ca ²⁺ -Imaging experiments on TRPM8	
2.3.2 Screening of the activity of the 1 st series by Ca ²⁺ -Imaging experiments on TRPA1 and TRPV1	
2.3.3 Patch-Clamp Electrophysiology of the 1 st series	
2.3.4 Molecular modeling studies	
3.1 Tetrahydro-β-carboline and tetrahydroisoquinoline-based TRPM8 modulators (series III, IV, V): Background and design	30
3.2 Synthesis of series III-V	31
3.3 Activity evaluation of series III-V	34
3.3.1 Screening of the activity of series III-V by Ca ²⁺ -Imaging experiments on TRPM8	
3.3.2 Patch-Clamp Electrophysiology of series III-V	

4.1	Tetrahydro- β -carboline and tetrahydroisoquinoline-based TRPM8 modulators (series III, IV, V, and VI): Background and design of series III-VI	36
4.2	Synthesis of series III-VI	37
4.3	Activity evaluation of series III-VI	45
5.1	Conclusions	45
6.1	Chemistry	46
6.2	Pharmacology and molecular modeling	77
	CHAPTER II: Ring fused cyclic aminals from THβC-based dipeptide compounds	83
1.	Background	84
2.	Chemistry and computational studies	86
3.	Conclusions	93
4.1	Chemistry	94
4.2	Computational details	123
	CHAPTER III: Indole-based derivatives as varicella zoster virus (VZV) inhibitors	127
1.1	Introduction	128
1.2	Pathogenesis of Varicella-Zoster Virus	128
1.3	Epidemiology of Varicella-Zoster Virus	129
1.4	Treatment and resistance	129
2.1	Background and design: 1 st series	132
2.2	Synthesis of 1 st series	133
3.1	Antiviral activity against Varicella zoster virus: 1 st series	135
3.2	Antiviral activity against other members of the Herpesviridae family: 1 st series	137
4.1	Background and design: 2 nd and 3 rd series	139
4.2	Synthesis 2 nd and 3 rd series	140
5.	Antiviral activity against Varicella zoster virus: 2 nd and 3 rd series	141
6.	Conclusions	142
7.1	Chemistry	143

7.2	Pharmacology	155
 CHAPTER IV: Design and synthesis of potential GRK2 inhibitors		157
1.1	Introduction: GPCR main features	158
1.2	GRKs: main features	160
1.3	GRK2: physiopathological role	161
1.3.1	GRK2 and the cardiovascular system	
1.3.2	GRK2 and the immune system	
1.3.3	GRK2: role in cancer	
1.3.4	GRK2 and the insuline resistance	
2.1	Background and design: 1st series	166
2.2	Synthesis of 1st series	169
3.	Activity of the thiazolidine derivatives of the 1st series	172
4.1	Background and design: 2nd series	173
4.2	Synthesis of 2nd series	174
5.	Activity of the thiazolidine derivatives of the 2nd series	176
6.	Conclusions	176
7.1	Chemistry	177
7.2	Pharmacology: GRK2 activity in rhodopsin phosphorylation assay	186
 CHAPTER V: A continuos flow procedure for the difluoromethylation of aminoacids		189
1.	Introduction	190
2.	Aim of the study	193
3.	Synthesis	196
4.	Conclusions	201
5.	Chemistry	202
 REFERENCES		211

ABSTRACT

Abstract

My PhD research plan concerns the exploration of the structural requirements determining TRPM8 modulation. We prepared a series of N-substituted tryptamines and identified two compounds acting, respectively, as an activator (21) or an inhibitor (12) of calcium influx in HEK293 cells. To develop more potent and selective derivatives we designed and synthesized new series of potential tetrahydroisoquinoline- and tetrahydro- β -carboline-based TRPM8 modulators. The synthetic approach used for the preparation of these compounds led to indole-fused aminoacetal derivatives. Optimization of reaction conditions allow us to obtain ring-fused aminals, which could be useful for preparing analogues of biologically active natural and synthetic products.

At the same time I worked on the synthesis of potential varicella zoster virus replication inhibitors: tryptamine derivative 17a was found to have a selective activity against this herpesvirus family member. A second part of my PhD was dedicated to the identification of small heterocyclic compounds as GRK2 inhibitors.

Lastly, I spent an abroad semester in the University of Graz, where I collaborated to the development of a continuous flow difluoromethylation protocol employing fluoroform as reagent. The protocol is applicable for the direct α -difluoromethylation of protected α -amino acids, and enables a highly atom efficient synthesis of the active pharmaceutical ingredient eflornithine.

CHAPTER I:
Design, synthesis and biological evaluation of new
TRPM8 modulators

1.1 Introduction: TRP, an overview

Transient receptor potential channels (TRP) play critical roles in the responses to all major classes of external stimuli, including light, sound, chemicals, temperature, and touch. TRP channels also imbue individual cells with the ability to sense changes in the local environment, such as alterations in osmolarity. Voltage and pH interact allosterically with temperature to activate the channel.¹ TRP genes were first described in the fruit fly *Drosophila melanogaster*. In some of these flies, prolonged exposure to light induced transient photoreceptor depolarisation, whereas in the wild type the response was sustained. This difference was attributed to mutant TRP gene expression. Genetic ablation studies in worms, flies and mice indicate that TRPs serve as sensors to elicit responses to a variety of stimuli, ranging from temperature, osmotic pressure, olfaction, taste, mechanical stress, light and injury-induced inflammation mediating pain.² Currently, more than 100 TRP genes have been identified in various animals (Table 1). Human TRP genes are diverse in length and range between 11.4 and about 911 kb. The overall protein sequence homology between subfamily members in the same species is usually about 35%.³

Table 1. TRP channel family^a.

	<i>Drosophila melanogaster</i>	<i>Caenorhabditis elegans</i>	<i>Ciona intestinalis</i>	<i>Fugu rubripes</i>	<i>Danio rerio</i>	<i>Mus musculus</i>	<i>Homo sapiens</i>
TRPC	3	3	8	8	8	7	6
TRPV	3	5	2	4	4	6	6
TRPM	1	4	2	6	6	8	8
TRPA	4	2	4	1	2	1	1
TRPN	1	1	1	-	1	-	-
TRPML	4	1	9	2	2	3	3
TRPP	1	1	1	4	4	3	3
Total	17	17	27	25	27	28	27

^aTRP channel in the fruit fly *Drosophila melanogaster*, the worm *Caenorhabditis elegans*, the sea squirt *Ciona intestinalis*, the puffer fish *Fugu rubripes*, the zebrafish *Danio rerio*, mouse and human. The numbers correspond to proteins with distinct channel properties within each subfamilies.

Based on protein homology, members of the TRP channel family can be seen to fall into seven subfamilies: TRPC, TRPV, TRPM, TRPA, TRPP, TRPML e TRPN. The number of channels within each subfamily varies across species (Figure 1), while the transmembrane segments tend to share the greatest homology within a particular subfamily.⁴

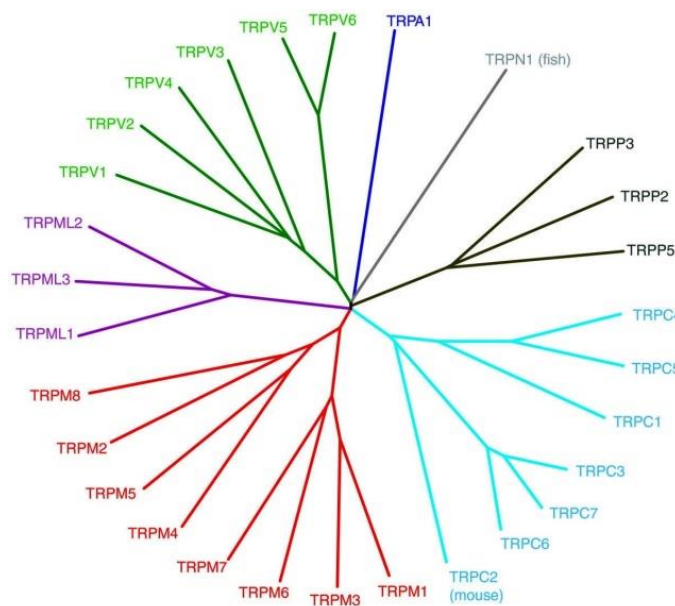


Figure 1. TRP subfamilies. (Adapted from Nilius et al., 2011).

The TRPV, TRPM, TRPA, and TRPN subfamilies are so called based on the original name of the initially described member of each subfamily. TRPVs (‘vanilloid’) are named after a founding member vanilloid receptor 1 (now TRPV1). The TRPM subfamily groups, with eight members (TRPM1–8), named after the original member, melastatin (now TRPM1). All members of the TRPA subfamily are nociceptive channels characterized by the presence of about 14 ankyrin repeats. The TRPN subfamily is named after the ‘NO-mechano-potential C’ (NOMP-C) channel of *Caenorhabditis elegans*. The TRPC subfamily (‘canonical’) comprises closest homologs of *Drosophila* TRP channels. TRPMLs and TRPPs include mucolipins and polycystins, respectively. The structure of the

integral channel endows the receptor with its characteristic nonselective cationic behavior and also potentially defines the outwardly rectifying current-voltage profile noted for many of these channels.⁵

All members of TRP family share a similar molecular architecture, most likely consisting of a symmetrical arrangement of four subunits, each of six transmembrane-spanning domains (TM1–TM6) and cytosolic N- and C-terminal tails that tetramerize to form a functional channel. TM5, TM6 and the connecting pore loop form the central cation-conducting pore, whereas TM1–TM4 and the cytoplasmic N- and C-terminal parts are thought to contain the regulatory domains that control channel gating.⁶

Compared with the six TM channels, TRP channels can have extremely long cytoplasmic N- and C-terminal tails containing several regulatory modules and, as in TRPM2, TRPM6 and TRPM7, can even contain entire functional enzymes. The relevance of these different cytoplasmic domains to channel functioning is poorly understood.⁷

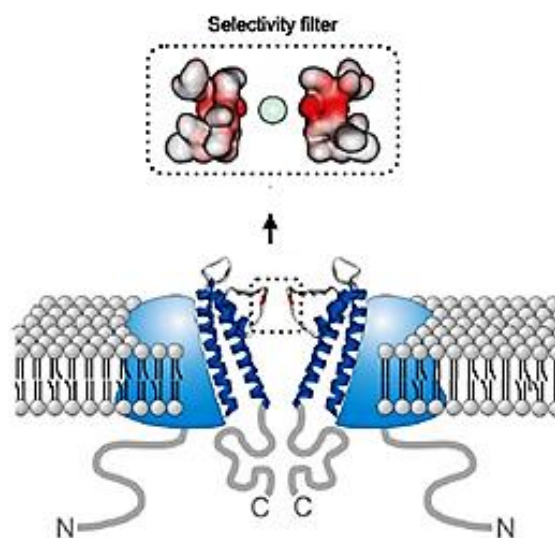


Figure 2. TRP channel.

The heat-activated TRPV1 was first among a group of eight temperature-activated TRP ion channels called thermoTRPs (Figure 3). TRPV1 could be activated by elevated temperatures with a discrete threshold near 43°C.⁸ Three other TRPV channels TRPV2 (also known as VRL-1), TRPV3, and TRPV4 (also known as

VROAC or OTRPC4) have been cloned and characterized as heat or warm thermosensors.⁷⁻⁹ In addition, two TRPM channels (TRPM4 and TRPM5) have been recently reported to be thermosensitive.¹⁰ The threshold temperatures for the activation of these channels range from relatively warm (TRPV3, TRPV4, TRPM4, and TRPM5) to extremely hot (TRPV2). In contrast to these warmth- or heat-activated TRP channels, two other TRP channels TRPM8 and TRPA1 are activated by cold stimuli. All eight, when expressed in native cells (human embryonic kidney cells, chinese hamster ovary cells, *Xenopus oocytes*) have the property of rendering the cells temperature sensitive. Each one has unique characteristics, highlighted by distinct temperature thresholds of activation. Sensitization or desensitization to repeated thermal stimuli and the ability to be modulated by distinct signaling mechanisms further distinguish thermoTRPs.¹¹

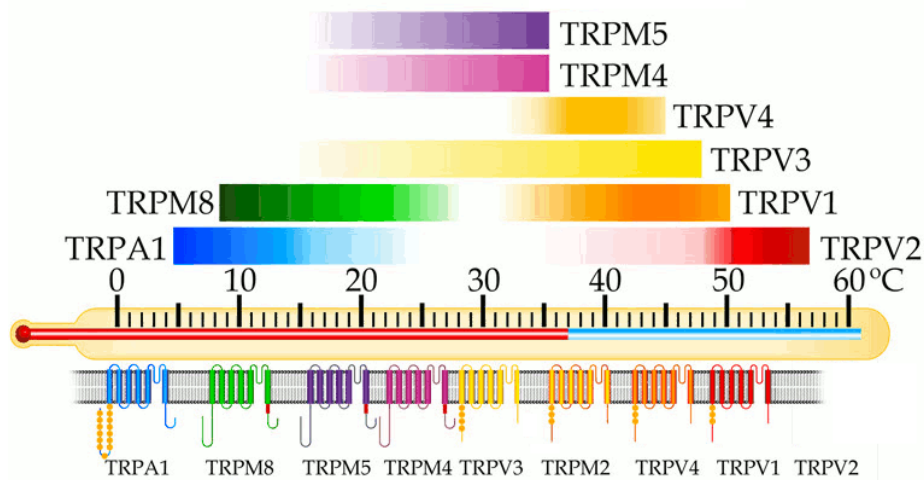


Figure 3. ThermoTRPs. (Adapted from Vay et al., 2012).

1.2 TRPM8: features, structure and localization

Transient receptor potential melastatin type 8 (TRPM8) is a non-selective Ca^{2+} permeable channel, that behaves as a polymodal receptor and exhibits highly complicated gating behavior that is regulated by a variety of factors.³ It has been demonstrated that cool temperature opens TRPM8 channels localized on the membranes of somatic sensory nerves, causing sensory nerve excitation. TRPM8 was the first cold-activated ion channel to be identified and it established the general role for TRP ion channels in thermosensation. When expressed on heterologous cell systems, cooling temperatures below 24–28°C start to evoke depolarizing currents. TRPM8-mediated currents increase with decreasing temperatures and reach maximum currents near 10°C.⁵

Electrophysiological studies have indicated that TRPM8 activation results in a large increase of intracellular Ca^{2+} levels through both Ca^{2+} entry from extracellular sites and Ca^{2+} release from intracellular Ca^{2+} stores. TRPM8 is activated by endogenous agonists or mechanisms other than temperature, such as depolarizing voltages.^{12,13}

The human TRPM8 polypeptide consists of 1104 amino acids.¹⁴ The channel is formed by four identical subunits. Each subunit shows 6 transmembrane domains (S1-S6) that surround the central pore, with S5 and S6 forming the gate and selective filter, while the S1–S4 transmembrane domains exhibit weak voltage-sensing properties. The N- and C-terminal domains are in the cytoplasmic side.¹⁵ The C-terminal domain, which confers temperature sensitivity on TRPM8, appears involved in tetramer stabilization since some mutations within the coiled region of C-terminus (978–1104) markedly reduce the ability of the TRPM8 monomers to form oligomeric channels. Single-point mutation in this region, Leu-1089 into Pro, disrupts this interaction and reduces oligomerization and surface expression of TRPM8, without affecting total protein. The "TRP box", in common with all the TRP family members, and a binding site for phosphatidylinositol 4,5-bisphosphate, are located in this C-terminal tail. Functional TRPM8 channels require the presence of the C-terminal as well as the region compromised between amino acids 40 to 86 of the N-terminal which are essential for the localization to the plasma membrane.¹⁶ On the other hand, N-terminus should not play a

significant role in tetramerization since the analysis of deletion mutants shows that the transmembrane domain is sufficient for TRPM8 assembly into tetramers (Figure 4).¹⁷

The protein shows 8 putative glycosylation sites and an immunogenic epitope that will facilitate the future design of peptide vaccination.¹⁶

The first four helices (S1–S4) constitute the voltage sensor module and include the binding sites for activators as menthol and icilin, although they do not fully overlap, since most residues involved in menthol recognition are located in S2, whereas icilin interacts also with residues of S3.¹⁸

The last two TM helices (S5–S6) constitute the pore module, which is characterized by a highly conserved hydrophobic region and a conserved aspartate residue, whose neutralization results in a non-functional channel. Moreover, the S6 helix is responsible for the ion selectivity of TRPM8 since the introduction of positively charged residues switches from cation to anion selectivity.¹⁹

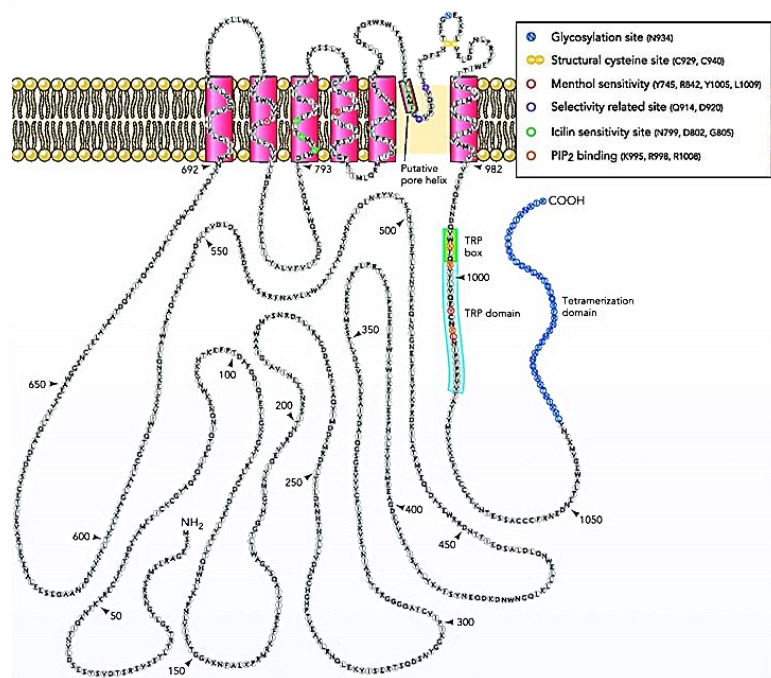


Figure 4. Schematic representation of TRPM8 protein.

(Adapted from Latorre et al., 2011).

TRPM8 is expressed mainly in a subpopulation of primary afferent neurons from both, dorsal root and trigeminal ganglia, and in the nodose and geniculate ganglia in the peripheral nervous system. The protein has been also identified in prostate and genitourinary tract, bladder, sperm, vascular smooth muscle, liver, lung and odontoblasts. Moreover the channel is expressed in the plasma membrane, in the membrane rafts and in the endoplasmic reticulum membrane of prostate cancer cells.²⁰

1.3 TRPM8: physiopathological role

1.3.1 TRPM8 and cancer

The role of TRP channels in cancer is highly heterogeneous, ranging from the control of Ca²⁺ homeostasis to regulation of tumorigenic and metastatic events. Tumour progression can be generally associated with misregulation of either one or more TRP channels.

TRPM8 is overexpressed in many prostate, breast, colon, lung and skin cancers,²¹ and this behaviour makes it an attractive target for cancer modulation.²² Moreover, TRPM8 may be effectively used in prostate cancer diagnosis and staging.^{23,24}

Several studies suggest that TRPM8 expression is regulated by androgens, thus the channel levels decrease when prostate cancer cells become androgen-independent. This has been confirmed in recent more direct experiments which reported androgen-dependent TRPM8 expression in the androgen-responsive LNCaP (androgen-sensitive human prostate adenocarcinoma cells) cell line, but not in the androgen-unresponsive PC-3 cell line.²⁵

It has been recognized that the androgen receptor (AR)2 protein is an important transcription factor for TRPM8 expression in prostate cells.²⁶ In general, androgens are important regulators of reproductive organs and are also involved in the pathogenesis of prostate cancer, including progression and metastasis.²⁷ An intensive colocalization pattern of the TRPM8 protein with endogenous androgens in human prostate tissues obtained from healthy individuals and patients with prostate cancer at various stages of the disease, as well as in cultured cells, was

detected, suggesting possible interactions. Co-immunoprecipitation experiments performed using cultured prostate epithelial cells, prostate cancer cells, and HEK-293 cells stably expressing TRPM8 further confirmed direct binding of the steroid hormone, testosterone, to the TRPM8 protein, suggesting that testosterone-induced TRPM8 could be an important regulator of Ca²⁺ homeostasis in prostate cells. In this view, TRPM8 would be an important channel to control cell cycling, including growth, proliferation, and apoptosis and down-regulation of plasma membrane TRPM8 activity could have an impact on cancer development.²⁸

1.3.2 TRPM8 and pain

The use of cooling to produce analgesia is described since Hippocrates and Galen.²⁹ Preparations containing menthol, which produces a cool sensation, are used topically to relieve neuralgia in traditional Chinese and European medicine.³⁰ Several clinical trials show beneficial effects of cooling on chronic back pain, dental pain, postoperative pain, and muscle injuries but no definitive mechanism has been established for cool-induced analgesia.³¹ All these data greatly promote the progress in exploring the relationship between temperature and pain.

TRPM8 seems the best candidate for being the mediator of cooling-induced analgesia. Mouse knockout studies have revealed that TRPM8 is required for cold sensation over a broad range of innocuous and noxious cold temperatures.³² A central spinal mechanism of analgesia is suggested, because cutaneous cooling can prevent pain produced by afferent stimulation. In addition several studies demonstrated marked analgesic effects of peripherally or centrally applied TRPM8 activators (such as icilin or menthol), or mild cooling of the skin, in a model of neuropathic pain. The channel response to agonists depends on their concentration, as low doses of menthol induce a sensation of cooling and analgesia in inflammatory and neuropathic pain models. Much higher doses of menthol induce a noxious cold sensation, although it is not clear if TRPM8 is specifically being targeted at such doses.^{29b}

An increased expression of these channels or an alteration in their functional properties could lead to the lower thresholds for cold pain and increased sensitivity to cold seen in neuropathic pain states.³³ Moreover several studies have

shown that levels of TRPM8 protein and RNA were both increased in rats with chronic neuropathic pain. In addition, inflammatory factors such as H⁺,³⁴ bradykinin and phospholipase can affect the activation of TRPM8.^{35,36} Several studies also showed that TRPM8 plays a role in amplifying pain sensation after injury, especially in models of neuropathic pain. Whereas hypersensitivity to cold is a common feature of individuals with neuropathies, these data suggest that patients suffering from cold hyperalgesia may respond best to TRPM8 antagonists.³⁷

1.3.3 TRPM8 in overactive bladder and painful bladder syndrome

TRPM8 is widely expressed in the urothelium and suburothelial sensory fiber and seems to be implicated in the bladder cooling reflex.^{38,39} The expression of TRPM8 is consistent with a role in the initiation of pain or the micturition reflex, with message being concentrated in the urothelium lining the bladder as well as in the dorsal root ganglia (DRG). Studies in a variety of animal models have shown that either cold or intravesical menthol induced micturition or increase bladder contraction frequency in a spontaneously contracting bladder.⁴⁰

Recent studies showed that the density of TRPM8 channels is elevated in bladder afferent nerve fibers of overactive bladder syndrome (OAB) patients, with an even higher density in patients with bladder pain. The positive correlation between the density of TRPM8 in the bladder mucosa and increased TRPM8 expression in patients with bladder pain, led to the suggestion that this channel was involved in the symptomatology and pathophysiology of these disorders.⁴¹ These observations suggest that a blocker of the TRPM8 channel could be effective for treatment of OAB and bladder pain.

1.4 TRPM8 modulation

1.4.1 TRPM8 activators

The activity of TRPM8 was shown to depend on a variety of stimuli.

Phosphatidylinositol 4,5-bisphosphate [PI(4,5)P₂] in cellular systems activates this channel through interactions with positively charged residues in the cytoplasmic tails.⁴² In addition, several studies have examined the role of phospholipase A₂ (PLA₂) in the activation of TRPM8. All PLA₂ enzymes hydrolyze the sn-2 ester of glycerophospholipids to release a free polyunsaturated fatty acid (PUFA) and a lysophospholipid (LPL). Two main groups of intracellular PLA₂ enzymes exist, cytosolic PLA₂ (cPLA₂) and calcium-insensitive PLA₂ (iPLA₂), also called group IV and group VI PLA₂, respectively. Although cPLA₂ is selective for phospholipids with arachidonic acid in the sn-2 position, this is not the case for iPLA₂, which releases other fatty acids as well. Recently has been reported that lysophospholipids, produced by PLA₂ activity, positively modulate TRPM8 and can act as endogenous agonists to activate the channel at normal physiological temperatures. In contrast, PUFAs such as arachidonic, eicosapentaenoic, and docosahexaenoic acid inhibit TRPM8. Although the two groups of PLA₂ products exert opposing modulatory effects on TRPM8, the net balance of equimolar concentrations of the PLA₂ products favors TRPM8 activation. These data introduce lysophospholipids as novel modulators of thermosensitive TRP channel activity.⁴³

TRPM8 can also be activated by menthol, the active ingredient of pepper mint, and by other cooling compounds as eucalyptol (the active ingredient in eucalyptus oil), the super-cooling AG-3-5 (also known as icilin), geraniol, hydroxycitronellal, linalool, PMD38, WS-3, and WS-23.⁴⁴ Of these AG-3-5 bears little structural resemblance to menthol and is more potent and effective than menthol in activating TRPM8.⁴⁵ Interestingly, the mechanism whereby AG-3-5 activates TRPM8 is different than that of menthol or cold. AG-3-5 requires a coincident rise in cytoplasmic calcium, either via permeation through the channel or by release from intracellular stores, in order to evoke TRPM8 currents, suggesting that the channel can be activated by multiple mechanisms.

In addition mutational studies identified a critical amino acid (Gly805): when mutated, it makes AG-3-5 unable of activating TRPM8.⁴⁶ This residue was located between the second and third transmembrane domains of the channel, a region known to be important for capsaicin sensitivity of TRPV1.⁴⁷

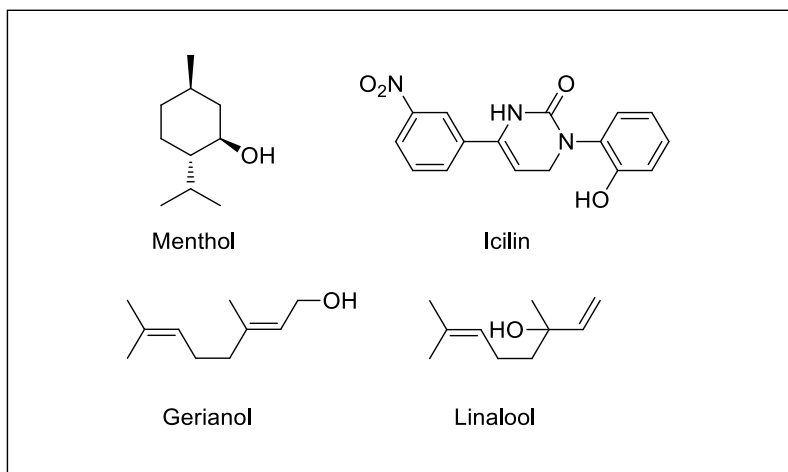


Figure 5. TRPM8 chemical activators.

1.4.2 TRPM8 inhibitors

Despite different positive modulators of TRPM8, a large class of inhibitors are subject to intense studies.

Endogenous antagonists comprise bradykinin, a proinflammatory agent, significantly downregulate TRPM8 in a PKC-dependent manner.^{48,49} Moreover several synthetic and natural antagonists have been identified, including BCTC (4-(3-Chloro-2-pyridinyl)-N-[4-(1,1-dimethylethyl)phenyl]-1 piperazinecarboxamide), thio-BCTC, CTPC ((2R)-4-C3-chloro-2-pyridinyl)-2-methyl-N-[4-(trifluoromethyl)phenyl]-1-piperazinecarboxamide), and capsazepine.⁵⁰ The antifungal medication clotrimazole has strong TRPM8 antagonistic activity, but also activates TRPV1 and TRPA1, actions consistent with the commonly reported side effects of irritation and burning.⁵¹ SKF96365, a non-specific blocker of several types of calcium channels, receptor-operated channels and inwardly rectifying potassium channels, also inhibits TRPM8 in vitro.⁵² Certain tryptamine derivatives that are ligands for 5-benzyloxytryptamine

receptors also act as TRPM8 antagonists.⁵³ Lastly, ethanol, at concentrations of 1–3%, inhibits TRPM8 channel function by disrupting interactions with the membrane phospholipid phosphatidylinositol 4,5-bisphosphate (PIP2), an obligate molecule for TRPM8 channel function.⁵⁴

Several structural classes of nanomolar TRPM8 antagonists have been reported, including substituted 4-benzyloxy-phenylmethanides (M8-B) benzyloxy-benzoic acid amides (AMTB), (1-phenylethyl-4-(benzyloxy)-3-methoxybenzyl(2-aminoethyl)carbamate (PBMC) and benzyloxy-phenylmethanureas.⁵⁰ Some of these compounds are patented for the treatment of urological disorders, although there are no data available on the in vivo efficacy of any of these compounds in animal models of these diseases. High affinity antagonists M8-B, AMTB and PBMC have been used as selective pharmacological probes of TRPM8 to explore the range of therapeutic applications resulting from blockade of this receptor, such as the regulation of deep body temperature, treatment of urological disorders and cold hypersensitivity associated with inflammatory and neuropathic conditions.⁵⁵

In vitro, PBMC is the most potent TRPM8 antagonist reported to date and inhibits channel activation to both chemical and thermal stimuli. Using calcium microfluorimetry and whole cell electrophysiology, PBMC was found to reduce TRPM8 activity in a dose-dependent manner and unlike other TRPM8 antagonists, any cross reactivity was observed with either TRPV1 or TRPA1.⁵⁶

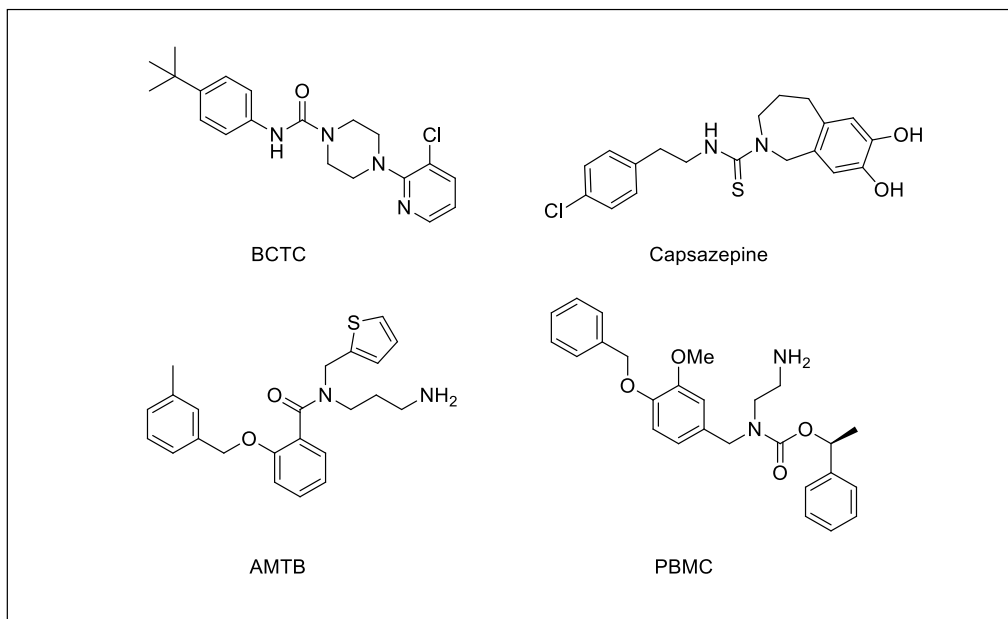


Figure 6. TRPM8 chemical inhibitors.

Indeed, many of these compounds also antagonize the heat-gated channel TRPV1. Thus, there is significant pharmacologically overlap between the two channels,⁵⁷ which suggests a conserved mechanism for ligand activation of the thermosensitive TRP proteins. These results complicate the search for selective agents for TRPM8 channels.⁴⁴

2.1 Tryptamine-based derivatives as TRPM8 channel modulators:

Background

Because of its above described role as cellular sensor, TRPM8 represents a good target for therapeutic intervention. Actually, most of current TRPM8 inhibitors showed also agonistic/antagonistic properties towards other receptors and have side effects that justify the need for new, more selective compounds.

The design and synthesis of new TRPM8 modulators is a central goal of my PhD programme because of their potential therapeutic applications in cancer and pain process.

Recently, some indole compounds have been identified as potent and selective TRPM8 antagonists. Voacangine (1), an iboga-type indole alkaloid, is found in the root bark of *Voacanga africana* Stapf ex Scott-Elliot (*Apocynaceae*) and it is characterized by the presence of an isoquinuclidine ring. This compound acts as modulators for TRPV1, TRPM8, and TRPA1. Voacangine showed TRPA1 agonistic and notable TRPM8 antagonistic activity.⁵⁸

Also 5-substituted tryptamines have been studied as potent TRPM8 blockers and a structure-activity study described some important determinants of TRPM8 activity. In detail, the phenyl ring and ethylamine side-chain were found to be important to the antagonist activity of 5-benzyloxytryptamine (Figure 7).⁵³

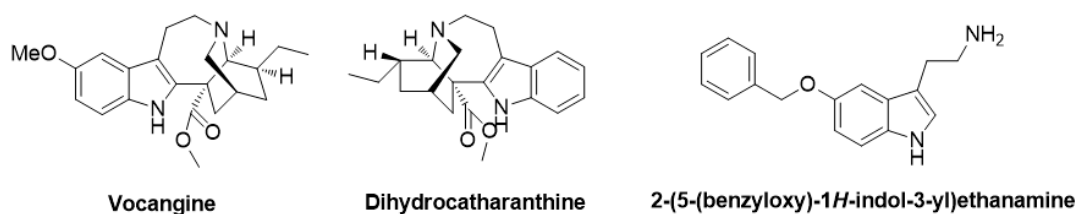


Figure 7. Indole-based TRPM8 modulators.

In addition, the most potent natural TRPM8 activator, icilin, is characterized by the presence of a central tetrahydropyrimidine-2-one ring and several other analogues, based on the tetrahydropyrimidine-2-one moiety, have been described and patented for their cooling activity.⁵⁹

The need for a heterocyclic ring to elicit efficient interactions with TRPM8 is also demonstrated by the isolation of the potent cooling agent α -ketoenamine from roast malt extract; however, these molecules are penalized by their instability to oxidation. Therefore, different heterocyclic moieties have been utilized as chemical scaffolds for the synthesis of new TRPM8 modulators; these include benzimidazole-based, as well as fused oxazole and thiazole.⁶⁰

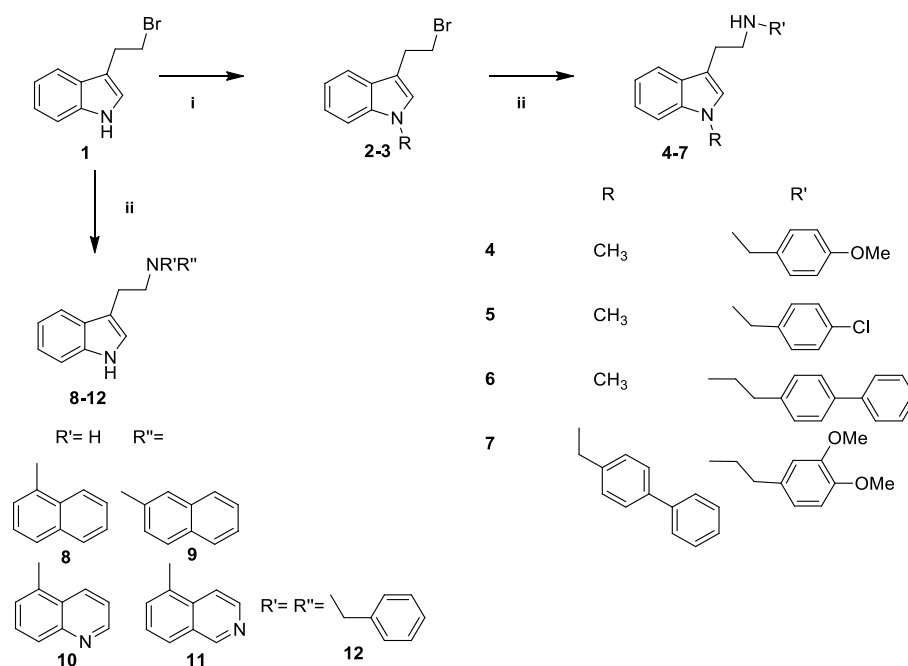
On the basis of these findings, we chose the tryptamine nucleus as template for the design of a small library of TRPM8 modulators and considered of interest to introduce different substituents on the side chain of the starting tryptamine and to derivatize the N-1 position of the indole scaffold.

Derivatives in this series, compared to the above cited tryptamine-based modulators, are modified at different positions and have a reduced scaffold complexity compared with ibogaine alkaloids.⁶¹

2.2 Synthesis of 1st series

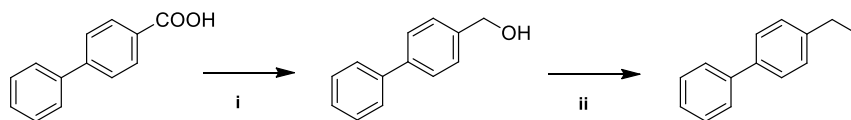
Derivatives **4–12** were prepared applying the synthetic route shown in Scheme 1. A subset of compounds (**4–7**) were prepared from the N-1 substituted intermediates **2** and **3**. Reaction of 3-(2-bromoethyl)-1H-indole (**1**) with methyl iodide or 4-phenylbenzyl iodide in DCM/DMF using NaH as a base led to derivatives **2** and **3** with 67% and 61% yields, respectively. The 4-phenylbenzyl iodide (**3a**) used in the formation of intermediate **3**, was previously prepared from the corresponding biphenyl-4-carboxylic acid as shown in Scheme 2. Nucleophilic displacement of the bromine atom of **1**, **2**, and **3** by different commercially available amines was performed in THF/TEA using palladium acetate as a catalyst. The final compounds **4–12** were obtained in 55–75% yield under microwave conditions.

Scheme 1. Synthesis of the N,2-substituted indolethanamine derivatives 4–12.



Reagents and conditions: i: RI, NaH in DCM/DMF, over night, rt; ii: R'NH₂ or R''NH₂, TEA, (CH₃COO)₂Pd in THF, MW, 20 min, 100°C.

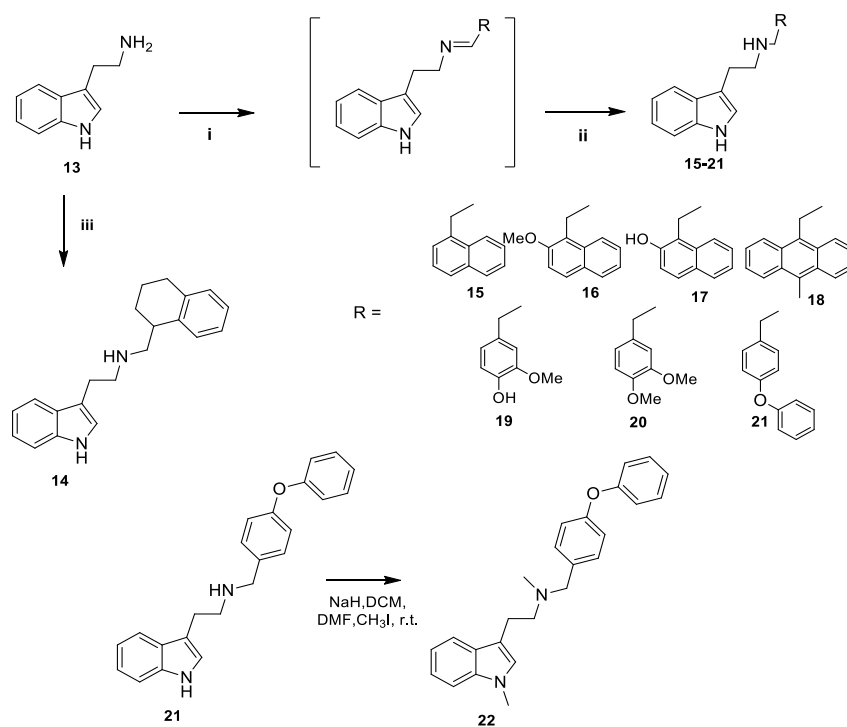
Scheme 2: Synthesis of intermediate 4-phenylbenzyl iodide (3a).



Reagents and conditions: i: LiAlH_4 in THF, 30 min., 0°C ; ii: triphenylphosphine, imidazole, I_2 in dry DCM, overnight, rt

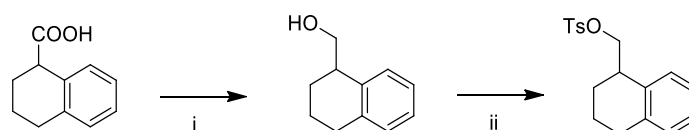
Derivatives **14–22** were prepared using an alternative synthetic route as shown in Scheme 3. Tryptamine (**13**) has been used as starting material. Compound **14** was obtained as racemic mixture by nucleophilic substitution reaction of the tosyl derivative of the (1,2,3,4-tetrahydronaphthalen-4-yl)methanol (**6a**) with tryptamine (**13**). The intermediate **6a** has been synthesized by reducing the 1,2,3,4-tetrahydronaphthalene-1-carboxylic acid with lithium aluminum hydride, followed by tosylation with 4-methylbenzene-1-sulfonyl chloride (Scheme 4). Reductive amination of different commercially available aldehydes with the tryptamine, using sodium triacetoxyborohydride as reductive agent, gave the final compounds **15–21** in 51–85% yields (Scheme 3). Finally, treatment of derivative **21** with methyl iodide using NaH as a base allowed us to obtain the dimethyl derivative **22** in 37% yield.

Scheme 3. Synthesis of the N,2-substituted indolethanamine derivatives 14–22.



Reagents and conditions: i: RCHO in DCM/CH₃COOH, 1.5 h, reflux; ii: Na(CH₃COO)₃BH, 3-5h; iii: 1,2,3,4-tetrahydronaphthalen-4-yl)methyl 4-methylbenzenesulfonate, TEA in THF, 30 min., 50 °C; (iv): CH₃I, NaH in DCM/DMF, 3 h, rt

Scheme 4: Synthesis of intermediate 1,2,3,4 tetrahydronaphthalen-4-yl)methyl 4-methylbenzenesulfonate (6a).



Reagents and conditions: i: LiAlH₄ in THF, 30 min., 0°C; ii: CITos, DMAP, TEA in DCM, 4h, rt

2.3 Activity and binding evaluation of the N-substituted tryptamines synthesized

2.3.1 Screening of the activity of the 1st series by Ca²⁺-Imaging experiments on TRPM8

The synthesized compounds were examined, in the Institute of Molecular and Cellular Biology of University Miguel Hernández of Elche, for their modulating activity on TRPM8 channels. The results obtained are summarized in Figure 8. All synthesized derivatives were tested at three different concentrations (0.5, 5, and 50 μM) by in vitro Ca²⁺ fluorometric assays experiments using Fluo4-NW in HEK293 cells stably expressing mouse TRPM8 channels. The results obtained are normalized to the effects prompted by 100 μM canonical agonist menthol⁶² or by 10 μM TRPM8 antagonist AMTB + 100 μM menthol,⁶³ whose effects were reported as +100% (activation) or -100% (inhibition), respectively.

Derivatives **4** and **5** showed agonist activity at high concentration (50 μM), being about 2-fold more effective than menthol. At the same concentration, the presence of the sterically hindered biphenyl ethyl group on the amine moiety (**6**) led to slight loss of efficacy in comparison to **4** and **5**, maintaining an efficacy similar to menthol. Interestingly, introduction of a sterically hindered group at N-1 indole position, such as a biphenyl methyl group, together with increased flexibility of the substituent on the amine moiety (**7** versus **4** or **5**), maintained agonistic efficacy.

The nonsubstituted N-1 indole derivatives (**8–21**) were quite productive. A direct linkage of the amine moiety with different bulky aromatic groups, such as naphthalene and quinolines, gives compounds **8–11** unable to act as TRPM8 modulators (Figure 8A and Figure 8B). By contrast, the tertiary amine obtained by derivatization of tryptamine with a benzyl moiety (**12**) proved to be an effective and potent antagonist. Introduction of a methylene spacer between the amine group and the bulky aryl moiety in **8** led to the potent agonist **15**, which was shown to be 3-fold more effective than menthol at 50 μM . Introduction of substituents at position 2 of the naphthalene ring, such as OMe (**16**) and OH (**17**), induced a shift from agonist to antagonistic activity for these derivatives at high

concentration (50 μM). A similar effect was observed when the bicyclic system modification involved changes in the electronic nature of the ring (**14**) or an increase in ring size (**18**). In addition, tryptamine benzyl derivatives **19** and **20** lost the agonistic activity shown by the methylated analogue **4**. Notably, compound **21** bearing a p-methoxybenzyl group showed significant agonist activity at 0.5 μM , with an efficacy similar to that of menthol. At 50 μM , the efficacy of derivative **21** was nearly 3-fold higher than that of menthol. Conversion of this compound to its N-methyl-2-(1-methyl-1H-indol-3-yl)derivative (**22**) shifted the agonistic activity to antagonism, with an efficacy comparable to that of derivative **12**, at all tested concentrations (Figure 8B).

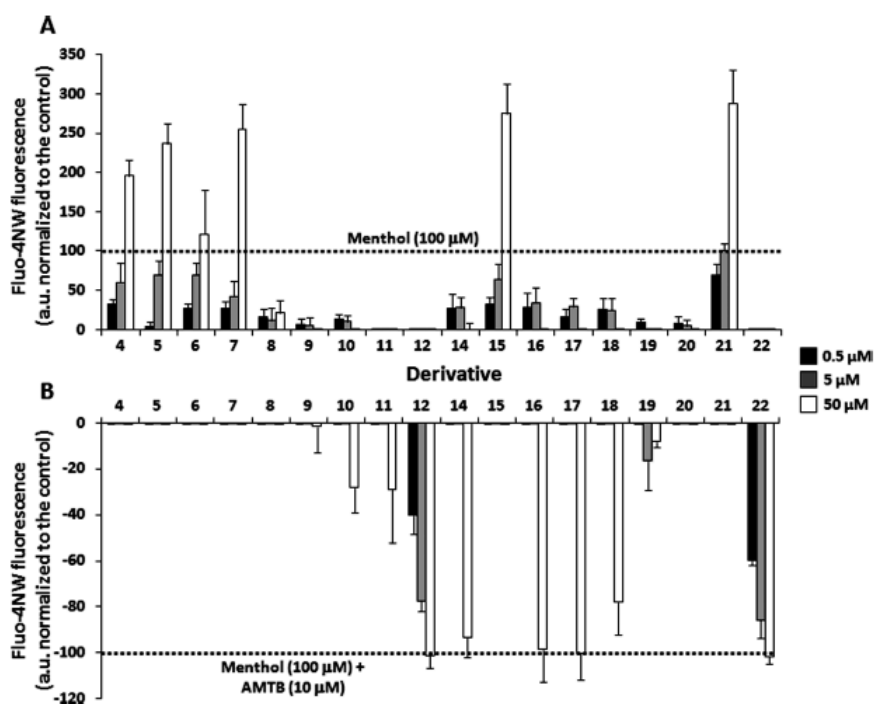


Figure 8. Efficacy of synthesized compounds as TRPM8 agonists (A) or antagonists (B) at three different increasing concentrations (0.5 μM , 5 μM , and 50 μM). Values are expressed as the mean \pm SEM of three independent measurements.

2.3.2 Screening of the activity of the 1st series by Ca²⁺-Imaging experiments on TRPA1 and TRPV1

We decided to evaluate the activity of the synthesized compounds on other members of TRP family, in detail TRPV1 and TRPA1, because their physiopathological pathways are deeply connected.^{64,65,66}

The most active derivatives, in detail two TRPM8 antagonists (**12**, **22**) and one agonist (**21**), were tested in calcium fluorometric experiments in SH-SY5Y cells stably expressing mouse TRPV1 channels and in IMR90 cells natively expressing mouse TRPA1 channels to investigate the ability to interfere with the activity of other TRP channels.

In these experiments, the canonical TRPV1 agonist (capsaicin, 10 μM) or antagonist (ruthenium red, 10 μM) as well as the canonical TRPA1 agonist (AITC, 500 μM) or antagonist (ruthenium red, 10 μM) were used as controls. The values obtained for the tested compounds were normalized to the effects exerted by canonical agonists or agonist + antagonist coexposure.

The performed Ca²⁺-imaging experiments showed a weak activity of compound **12** on TRPV1 only at the highest concentration (50 μM) and unremarkable activity on TRPA1 at all concentrations, suggesting a selective TRPM8 antagonism. The TRPM8 agonist **21** behaved, instead, as an antagonist on both TRPV1 and TRPA1 receptors, showing in both full antagonist ability at the highest concentrations (50 μM). Compound **22** appeared less selective, acting as an antagonist of both TRPV1 and TRPA1 channels with potency comparable to that on TRPM8 at all concentrations, and was therefore not further investigated. Whereas these results the most interesting synthesized derivatives are compounds **12** and **21** with agonist and antagonist activity, respectively (Figure 9).

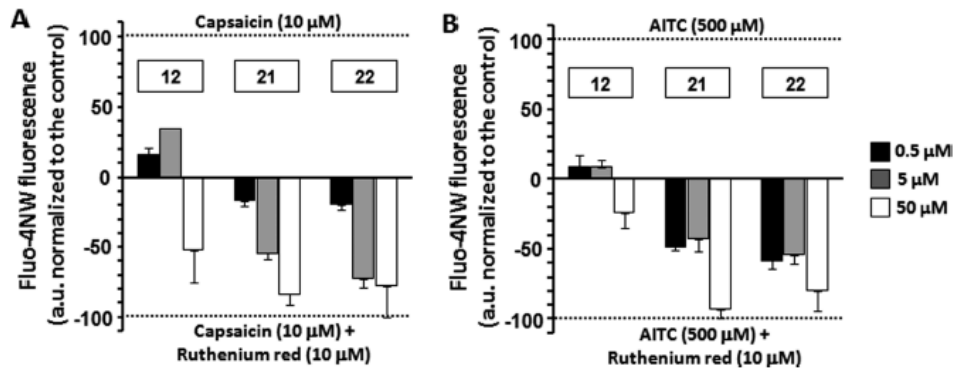


Figure 9. Efficacy of synthesized compounds at three different increasing concentrations (0.5 μM , 5 μM , and 50 μM) as modulators of TRPV1 (vs capsaicin and capsaicin + ruthenium red) (A) and TRPA1 (vs AITC and AITC + ruthenium red) (B). Values are expressed as the mean \pm SEM of three independent measurements.

2.3.3 Patch-Clamp Electrophysiology of the 1st series

To corroborate the activity of derivatives **21** and **12**, these compounds were tested in patch-clamp assays in the Department of Medicine and Health Science V. Tiberio, University of Molise.

The assays were performed in single HEK293 cells transiently expressing the rat TRPM8 isoform by patch-clamp recordings using a 100 ms voltage ramp ranging from -100 mV to +100 mV delivered every 4 s. Perfusion with 500 μ M menthol activated a large, strongly outwardly rectifying current ($I_{+80\text{mV}}/I_{-80\text{mV}}$ was 90 ± 25 ; $n = 39$) reversing at a potential near 0 mV (-1.3 ± 0.7 mV; $n = 10$) (Figure 10A and Figure 10B). No currents were activated when menthol was perfused in nontransfected cells (0 pA/pF at +80 mV; $n = 4$). The dose-response curve for menthol-evoked currents (Figure 10C) at +80 mV showed an EC_{50} of 75 ± 4 μ M, a value close to those reported for rat⁶⁷ and mouse isoforms.^{34,68}

Perfusion of derivative **21** (100 μ M) in rat TRPM8-transfected HEK-293 cells also triggered the appearance of large outwardly rectifying currents, reversing around 0 mV (-1.1 ± 0.3 mV; $n = 10$; Figure 10D and Figure 10E). By contrast, perfusion of derivative **12** (100 μ M) failed to activate TRPM8 currents. When compared to menthol, derivative **21** displayed a significantly higher potency (EC_{50} was 40 ± 4 μ M; $n = 3-10$) and a similar efficacy (current density at +80 mV was 134 ± 13 and 140 ± 7 for derivative **21** and menthol, respectively; $p > 0.05$) (Figure 10F).

To investigate possible antagonistic effects exerted by the new synthesized compounds, we investigated their ability to inhibit menthol-evoked responses. As previously reported, the canonical TRPM8 antagonist BCTC (3 μ M) produced a fast and complete inhibition of menthol-gated TRPM8 currents, which largely recovered after drug washout (Figure 11A and Figure 11B). Similarly, perfusion with the same concentration (3 μ M) of derivative **12** produced a complete inhibition of menthol-induced TRPM8 currents at +80 mV (Figure 11C and Figure 11D), with slower kinetics when compared to those of BCTC. TRPM8 block by derivative **12** appeared concentration-dependent, with an IC_{50} of 367 ± 24 nM ($n = 3-9$), a value slightly lower than that reported for BCTC (475 nM).⁶⁹

These effects were largely reversible upon drug washout (Figure 11C), although with much slower kinetics when compared to those of BCTC.

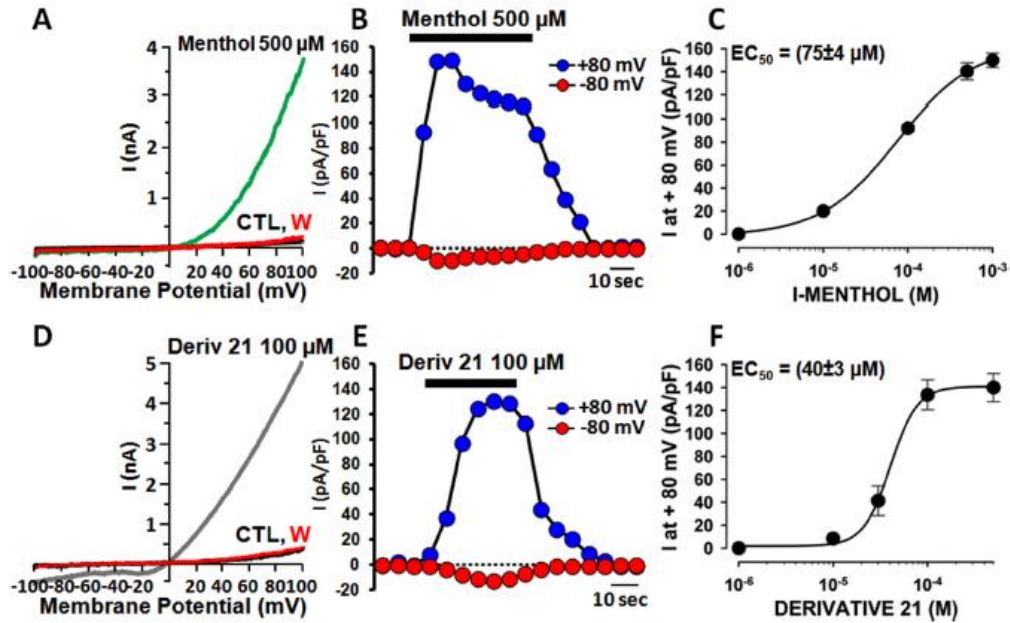


Figure 10. Menthol- and derivative 21-induced currents in HEK293 cells expressing TRPM8. (A, D) Representative traces of currents evoked by a 100 ms voltage ramp ranging from -100 mV to $+100$ mV applied every 4 s in control solution (CTL, black trace; A, D), during application of menthol (green trace; A) or derivative 21 (grey trace; D) or after washout (W, red trace; A, D). (B, E) Time-course of currents recorded at $+80$ mV (blue symbols) or -80 mV (red symbols) in single HEK293 cells transiently expressing TRPM8 upon exposure to menthol ($500 \mu\text{M}$; B) or derivative 21 ($100 \mu\text{M}$; E). The duration of compounds exposure is indicated by the bar on top of the traces. (C, F) Concentration–response curves for TRPM8 current activation by menthol (C) or derivative 21 (F). Peak current data were expressed as pA/pF (to facilitate comparison among cells of different size) and expressed as a function of agonist concentrations. The solid lines represent fits of the experimental data to the following binding isotherm: $y = \text{max}/(1 + x/\text{EC}_{50})^n$, where x is the drug concentration and n the Hill coefficient. The fitted values for n were 0.97 ± 0.05 or 3.0 ± 0.6 for menthol or derivative 21, respectively. Each point is the mean \pm SEM of 4–13 (for menthol) or 3–10 (for derivative 21) determinations, each obtained in different cells.

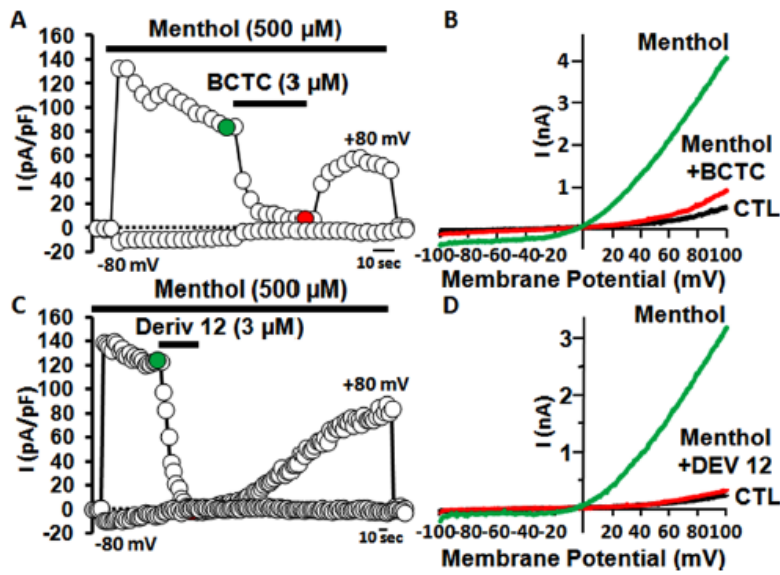


Figure 11. BCTC and derivative 12 block TRPM8-mediated responses evoked by menthol in TRPM8 expressing HEK293 cells. (A, C) Time-course of currents recorded at +80 mV or -80 mV in HEK293 cells transiently expressing TRPM8 upon application of 500 μM menthol (A, C), 500 μM menthol + 3 μM BCTC (A) or 500 μM menthol + 3 μM derivative 12 (C). (B, D) I-V curves obtained in HEK293 cells expressing TRPM8 and exposed to control solution (CTL, black trace; B, D), 500 μM menthol (green trace; B, D), 500 μM menthol + 3 μM BCTC (red trace; B), or 500 μM menthol + 3 μM derivative 12 (red trace; D). Traces shown in parts B and D correspond to the currents measured at the time points shown in colors (green or red circles) in parts A and C.

2.3.4 Molecular modeling studies

To study the exact binding mode and to better rationalize the reasons behind the activity of our N-substituted tryptamines, molecular docking studies were carried on derivatives **21** and **12**, which are the most potent TRPM8 agonist and antagonist, respectively. To investigate the binding characteristics of newly synthesized TRPM8 modulators with particular attention to the difference between agonist and antagonist binding which might be indicative of the residues involved in TRPM8 gating, we ran a series of molecular dynamic simulations using a homology model of a rat TRPM8 subunit. The homology model is based on the experimentally solved structures of TRPV1 (PDB code 3J5P).⁷¹ Notably, human, rat, and mouse TRPM8 amino acid sequences are highly similar within the modeled regions; the percent of overall identity/similarity is 93.8%/97.4% (human versus mouse), 93.8%/97.3% (human versus rat), and 98.6%/99.5% (mouse versus rat). More importantly, some of the critical residues involved in drug binding (namely, Leu697, Ile710, Tyr754, Leu843, Glu1004, and Arg1008) are strictly conserved among the three species. Overall, these data strongly suggest a high level of structural similarity in the binding sites for the described modulators among TRPM8 receptors belonging to humans, rats, and mice. By SiteMap⁷⁰ calculations on the whole monomer the best site identified was BP1. It has a volume of 791 Å³ and a site score of 1.093 (the cutoff value generally used to distinguish between drug-binding and nondrug-binding sites is 0.80) and is located between S1, S2, S3, and S4 helices, while at the bottom it is delimited by residues 990–1010. Recently Taberner et al. reported the central role of S6-TRP box linker (amino acids 980–992 in rat TRPM8) in the gating mechanism of TRPM8 channel and showed that mutations in the 986–990 region had a deep impact on channel gating by voltage and menthol.⁷¹ The proximity of the binding site to the 980–992 region suggests that the binding of a molecule to BP1 might influence the conformation of this linker region in the TRP domain and, as a result, the pore opening.

Molecular docking simulations have been performed to predict the binding mode into BP1 of the most potent antagonist (**12**) and agonist (**21**) in our series. The best docked models were then submitted to molecular dynamics simulations to

analyze protein–ligand contacts and protein conformational rearrangements at the level of BP1 and of the 980–992 region. BP1–12 and BP1–21 complexes are stabilized by similar interactions, such as hydrophobic contacts with Leu843, Ile701, Leu697, π – π stacking with Tyr754, and electrostatic interactions with the Glu1004 side chain. Apart from these similar interactions, the antagonist and the agonist also show different interactions that could be responsible for different conformational rearrangements of the 980–992 region. In particular, **21** makes a hydrogen bond with the phenoxy group of Tyr754 by its amino linker and a second hydrogen bond, with the backbone of Arg1008, provided by the indole NH. The different interaction of **12** or **21** to TRPM8 possibly brings differences in the conformation of BP1, regarding in particular Arg1008. Upon **21** binding Arg1008 side chain appears projected outside BP1 (Figure 12A), with the ligand indole ring claiming its space and hydrogen-binding to Arg1008 backbone. In the case of **12** binding, Arg1008 is instead pointing toward the BP1 cavity, keeping its interaction with Glu1004 (Figure 12B). Moreover, compound **12** establishes a wider hydrogen bonding network, interacting even with Gln1003 and Glu662, possibly stabilizing the TRP domain helix which might be responsible for its antagonistic nature. We used the predicted bioactive conformations of **12** and **21** to summarize the most stable interactions involved in the binding of these ligands as representative antagonists and agonists of this tryptamine-based series (Figure 12). The pharmacophore model for tryptamine-based agonists accounts for the interaction with Ile837, Leu806, Ile701 (H1), Leu697, Leu843, Ile844 (H2), Glu1004 (D2/P1), Arg1008 (D3), Tyr754 (D1/R1), and Leu757, and Met758 (R1). On the other hand, the antagonist model accounts for the interaction with Ile701, Leu751, Leu697, Leu843 (R1), Glu1004 (P1/D1), Val800 (H1), Arg1008 (R2), and Tyr754 (R1/R2). The two pharmacophore models might help to understand which chemical features are required to endow a ligand with agonist or antagonist capabilities. Despite binding to the same site, the two models present in fact substantial differences that may cause the observed differences induced in TRPM8 conformation.

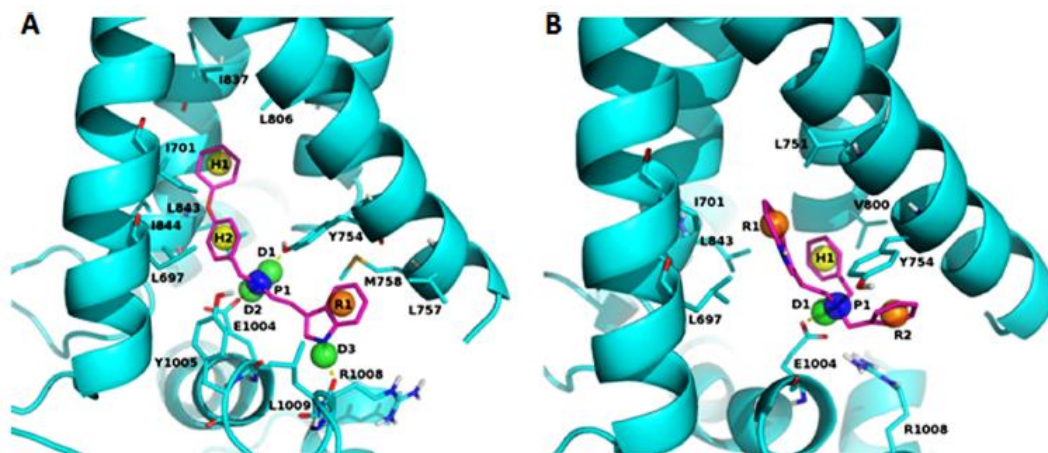


Figure 12. Pharmacophore models for tryptamine-based TRPM8 agonists (A) and antagonists (B). Chemical features are depicted as spheres and color-coded as follows: yellow, H = hydrophobic; blue, P = positive charge; green, D = HB donor; orange, R = aromatic ring. 21 and 12 are represented as references in panels A and B, respectively.

3.1 Tetrahydro- β -carboline and tetrahydroisoquinoline-based TRPM8 modulators (series III, IV, V): Background and design

The aim of my second year of PhD was to identify new potent and selective TRPM8 modulators. Based on the structural requirements of our previous series (**12**) and taking into account the tetrahydroisoquinoline derivatives described in literature.⁷² (series I and II) as potent TRPM8 antagonists, we developed two new series of derivatives using the tetrahydro- β -carboline (TH β C, series III and IV) and tetrahydroisoquinoline (TIQ, series V) scaffolds (Figure 13). These templates could be considered as the conformationally rigid analogues of triptamine and dopamine, respectively.

Pictet–Spengler reaction, which involves the condensation of β -arylethylamine with an aldehyde or its synthetic equivalent, is one of the most convenient methods to obtain tetrahydro- β -carboline and tetrahydroisoquinoline derivatives. In this synthetic strategy, the stereogenic C-1 center is generated during the ring closure in a one-pot process.⁷³ This condensation also occurs with aminoacids such as tryptophan and 3,4-dihydroxyphenylalanine (Dopa), chosen as starting materials, because of the easy derivatization procedure of the carboxylic functional group. This feature may be exploited to synthesize the corresponding hydantoin-fused tetrahydro- β -carboline or tetrahydroisoquinoline scaffold as shown in Figure 13.

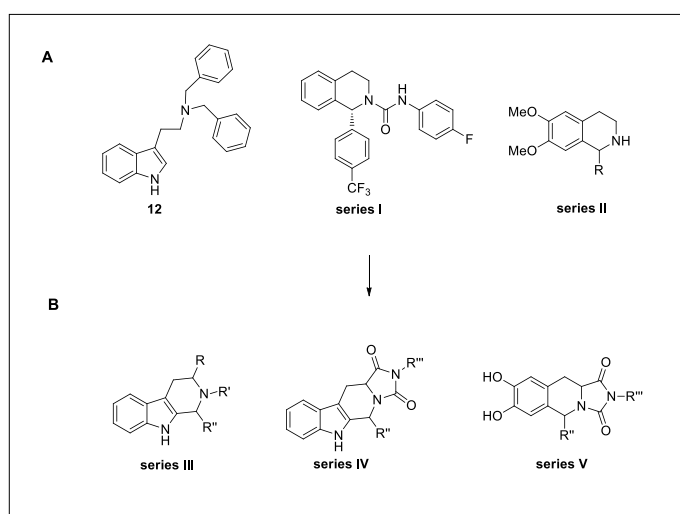
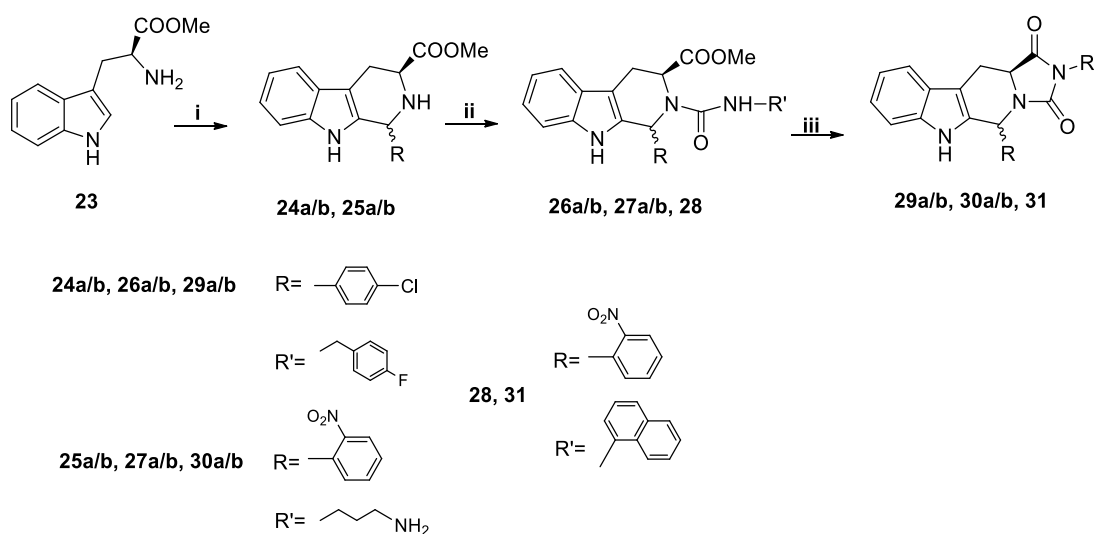


Figure 13. TRPM8 identified antagonists (A) and new designed modifications (B).

3.2 Synthesis of series III-V

The tetrahydro- β -carboline nucleus was obtained by a Pictet-Spengler condensation starting from L-Trp-OCH₃ (**23**) and differently substituted aromatic aldehydes, in methanol, in the presence of trifluoroacetic acid as catalyst and using microwave irradiation (Scheme 5). Using these reaction conditions means exploiting the power of the pseudo three-component reactions to obtain the 1,2,3,4-tetrahydro- β -carboline-1,3-disubstituted as a mixture of diastereoisomers (**24a/b** and **25a/b**) in a short time with a very high yield (87%). Compounds thus obtained were then easily separated by flash chromatography and the single diastereoisomers were reacted with triphosgene and an alkyl or aryl amine leading to the formation of ureidic intermediates **26a/b**, **27a/b** and **28**. Cyclization of **26a/b**, **27a/b** and **28** in MeOH and TEA furnished the final hydantoin-fused tetrahydrobetacarboline derivatives **29a/b**, **30a/b** and **31**.

Scheme 5. Synthesis of the derivatives 29a/b, 30a/b and 31.

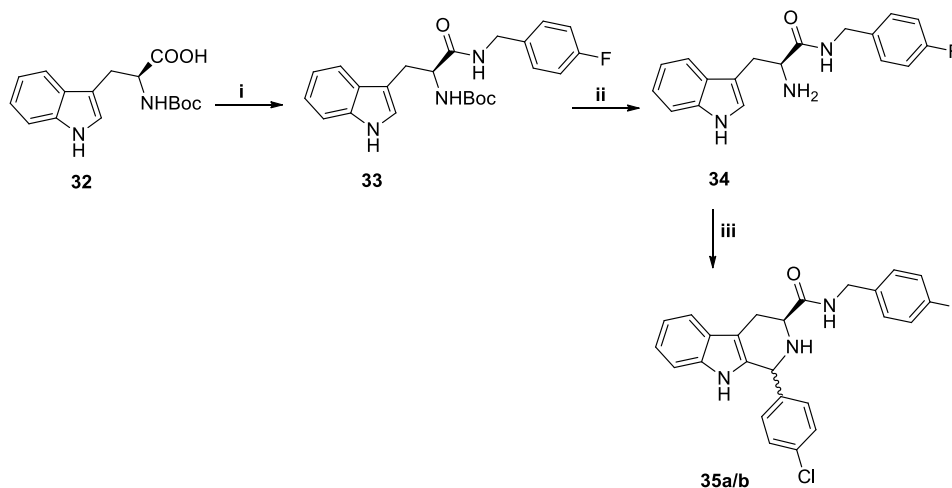


Reagents and conditions: i: MeOH, TFA, RCHO, 30', MW, 110°C; ii: DCM, TEA, CCl₃COCCl₃, R'NH₂, 10', rt; iii: MeOH/TEA, 10', reflux.

The tetrahydro- β -carboline derivatives **35a/b** were obtained using an alternative synthetic pathway, as shown in Scheme 6. Coupling of N α -Boc-L-tryptophan (**32**) with 4-fluorobenzylamine, using HOBt, HBTU and Dipea as base, gave the intermediate

33. The cleavage of Boc protecting group in acid conditions, led to the formation of **34**. Final condensation of **34** with 4-chlorobenzaldehyde via Pictet-Spengler reaction, provided **35a/b**, as a diasterosomeric mixture.

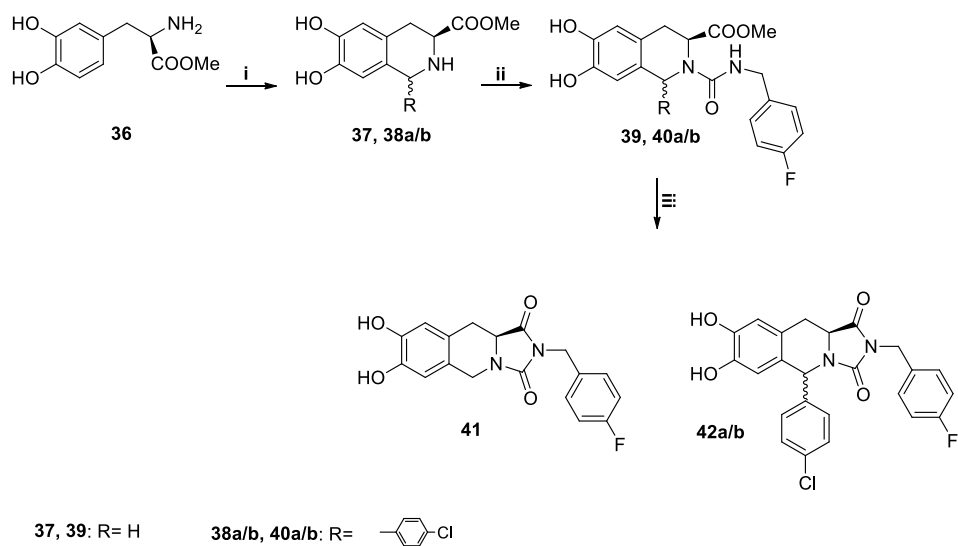
Scheme 6. Synthesis of the derivatives 35a/b.



Reagents and conditions: i: DCM/DMF, HOBt, HBTU, DIPEA, 4-fluorobenzylamine, 12 h, rt; ii: DCM/TFA 3/1, TIS, 2h, rt; iii: MeOH, TFA, 4-chlorobenzaldehyde, 30', MW, 110°C.

Tetrahydroisoquinoline derivatives **41** and **42a/b** were obtained using the synthetic strategy previously described for the derivatives **29a/b**, **30a/b** and **31** (Scheme 7). In this case, Pictet-Spengler reaction of L-Dopa-OMe (**36**) with formaldehyde or 4-chlorobenzaldehyde yield the intermediate **37** or **38a/b** as a mixture of diastereoisomers, respectively. Reaction of isoquinoline-based compounds with triphosgene and 4-fluorobenzylamine, using TEA as base, led to the formation of derivatives **39** and **40a/b**. The final cyclization in methanol and TEA, at reflux temperature, provided the final hydantoin-fused tetrahydroisoquinolines **41** and **42a/b**.

Scheme 7. Synthesis of the derivatives 41, 42a/b.



Reagents and conditions: i: MeOH, TFA, RCHO, 30', MW, 110°C; ii: DCM, TEA, CCl₃OCOCCl₃, 4-fluorobenzylamine, 10', rt; iii: MeOH/TEA, 10', reflux.

3.3 Activity evaluation of series III-V

3.3.1 Screening of the activity of series III-V by Ca^{2+} -Imaging experiments on TRPM8

The tetrahydro- β -carbolines **29a/b**, **30a/b**, **31**, **35a/b** and the tetrahydroisoquinolines **41**, **42a/b** were tested for their modulating activity on TRPM8 channels at the Institute of Molecular and Cellular Biology of University Miguel Hernández of Elche.

At 50 μ M, compound **30a** showed higher agonist activity than menthol. At the same concentration, the trans diastereoisomer **30b** completely lost efficacy. The introduction of a sterically hindered group at N-hydantoin nucleus (**31**), as well as the presence of a substituent at C-1 tetrahydroisoquinoline scaffold (**42a/b**) led to ineffective derivatives. Compounds **29a/b**, **35a**, and, particularly, the trans diastereoisomer **35b** and the unsubstituted hydantoin-fused tetrahydroisoquinoline **41** showed antagonistic activity at the tested concentration (Figure 14).

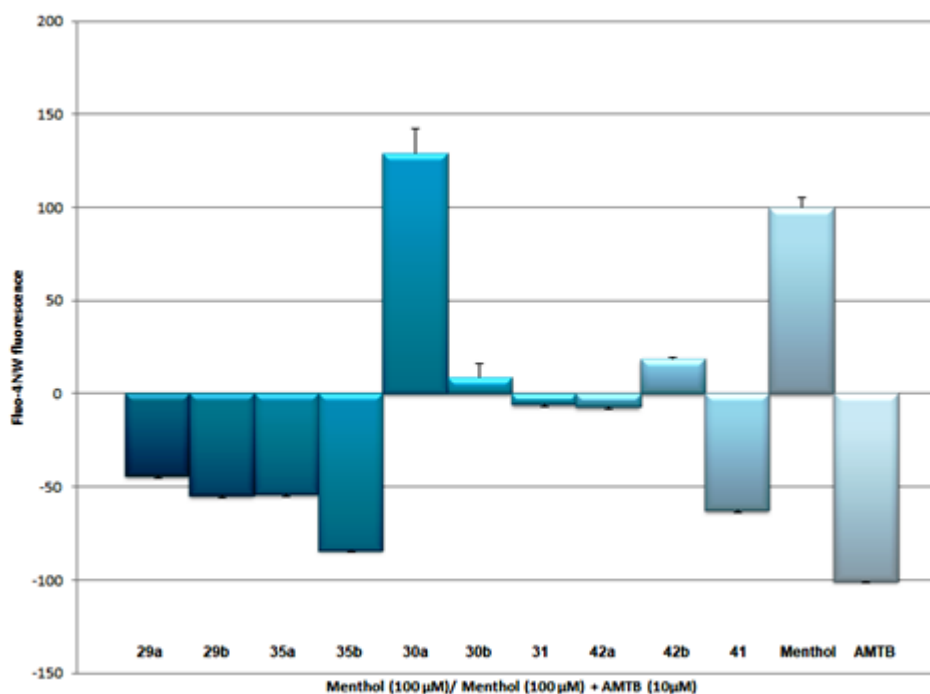


Figure 14. Efficacy of synthesized compounds as TRPM8 agonists or antagonists at the concentration of 50 μ M. Values are expressed as the mean \pm SEM of three independent measurements.

3.3.2 Patch-Clamp Electrophysiology of series III-V

To provide evidence of the activity of derivatives **35b** and **41**, the compounds were tested in single HEK293 cells transiently expressing the rat TRPM8 isoform by patch-clamp recordings, using a 100 ms voltage ramp ranging from -100 mV to $+100$ mV delivered every 4 s. To test possible antagonistic effects exerted by the newly synthesized compounds, we investigated their ability to inhibit menthol-evoked responses and compared the results with the activity of the canonical TRPM8 antagonist BCTC (Figure 15A). Perfusion with 50 μ M concentration of derivative **35b** and 100 μ M concentration of **41** produced a complete inhibition of menthol-induced TRPM8 currents at $+80$ mV (Figure 15B and Figure 15C). Derivatives **35b** and **41** showed an IC_{50} of 10.7 ± 0.6 μ M and 30.3 ± 0.7 μ M, respectively, values higher than that reported for BCTC (475 nM) and for derivative **12** (367 nM).

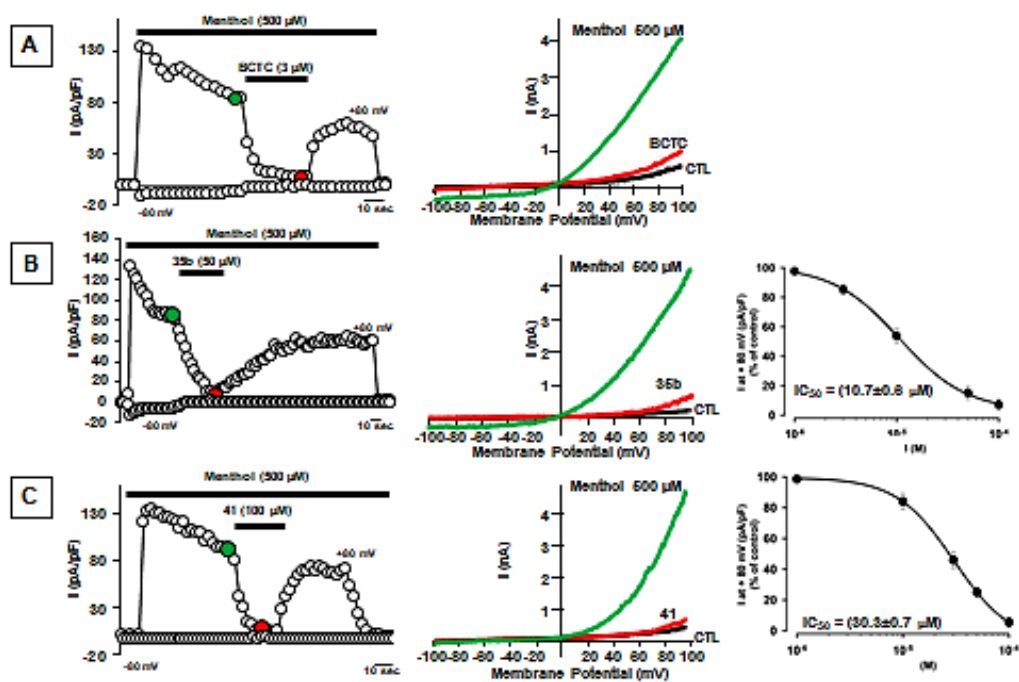


Figure 15. BCTC, derivatives **35b** and **41** block TRPM8-mediated responses evoked by menthol in TRPM8 expressing HEK293 cells (A, C). Time-course of currents recorded at $+80$ mV or -80 mV in HEK293 cells transiently expressing TRPM8 upon application of 500 μ M menthol + 3 μ M BCTC (A) or 500 μ M menthol + 50 μ M derivative **35b** (B) or 500 μ M menthol + 100 μ M derivative **41** (C).

4.1 Tetrahydro- β -carboline and tetrahydroisoquinoline-based TRPM8 modulators (series III, IV, V, and VI): Background and design

The pharmacological results obtained from the TH β C/TIC series provided us some interesting data about the structural requirements important for TRPM8 modulation. With regards to antagonistic effect of derivatives **35b** and **41** and bearing in mind the potent and selective activity of compound **12**, we decided to deepen the study of the structure-activity relationships of the series III, IV and V. Thus, we have modified the nature of substituents at C-1 and N-2 in series III, at C-1 and N-hydantoin in series IV and V. In addition, we modified the nature and dimension of cycle by introducing a diketopiperazine (series VI) or diaza-bridged moieties.

Hence, we designed and synthesized new potential TRPM8 antagonists as depicted in Figure 16.

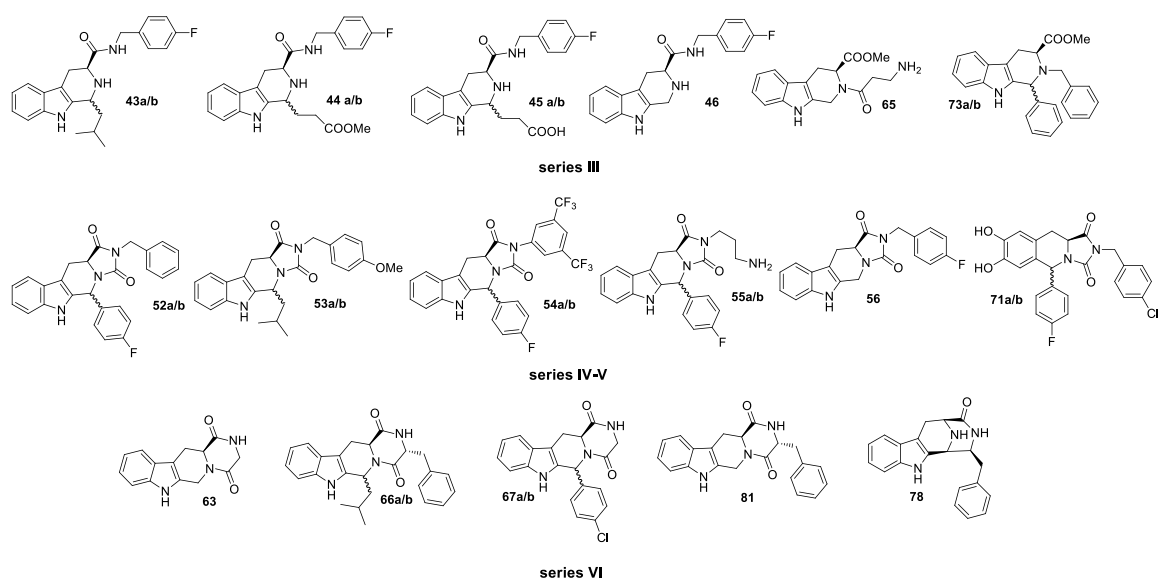
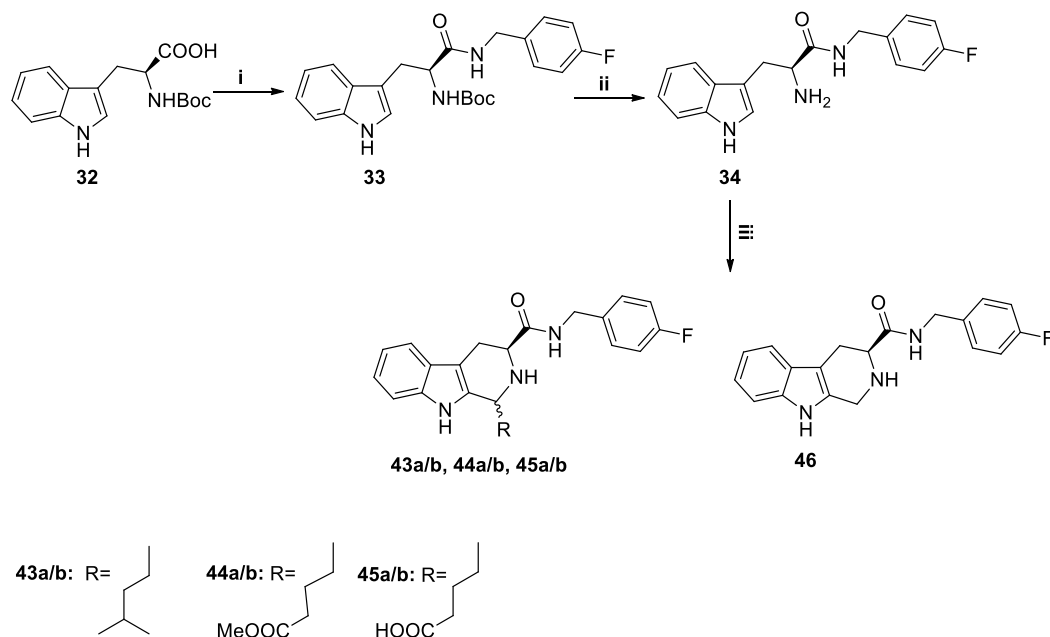


Figure 16. New potential TRPM8 antagonists designed.

4.2 Synthesis of series III- VI

Derivatives **43-45a/b** and **46** were prepared using the synthetic route shown in Scheme 8, starting from N α -Boc-L-tryptophan (**32**). Reaction with 4-fluorobenzylamine gave the amide intermediate **33**. Deprotection by trifluoroacetic acid in dichloromethane provided the intermediate **34**, which was subsequently reacted with formaldehyde or isovaleraldehyde or methyl 5-oxopentanoate or 5-oxopentanoic acid to form derivative **46** and diastereoisomeric mixtures of tetrahydrobetacarbolines **43-45a/b**.

Scheme 8. Synthesis of derivatives 43a/b-46.

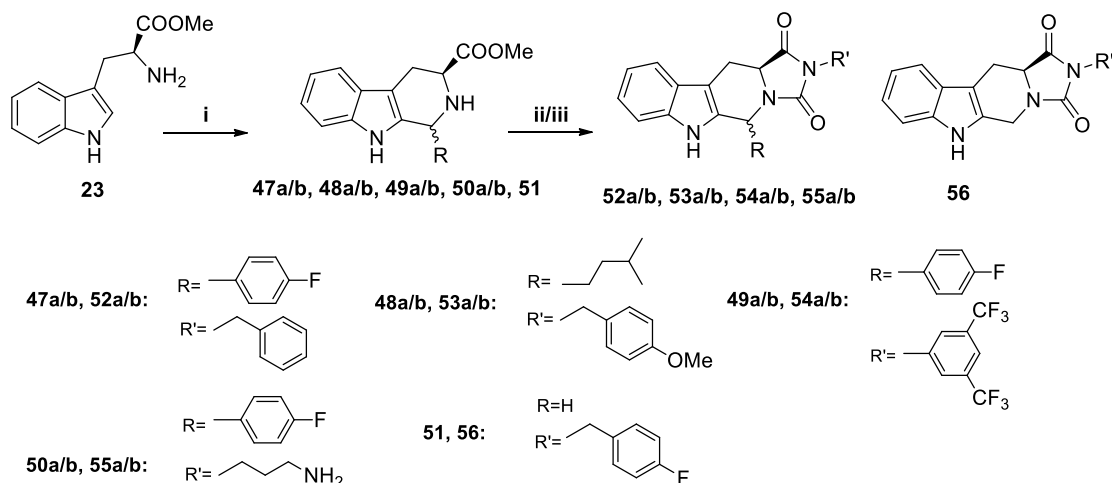


Reagents and conditions: i: DCM/DMF, HOBt, HBTU, DIPEA, 4-fluorobenzylamine, 12 h, rt; ii: DCM/TFA 3/1, TIS, 2h, rt; iii: MeOH, TFA, RCHO or CH₂O, 30', MW, 110°C.

Derivatives **52-55a/b** and **56** were prepared from L-Trp-OMe applying the synthetic route shown in Scheme 9. The reaction between **23** and different aromatic and aliphatic aldehydes in methanol containing trifluoroacetic acid, yielded in short time the mixtures of diastereoisomers of 1,3-disubstituted-1,2,3,4-tetrahydro- β -carbolines **47-51a/b** and the enantiomeric derivative **51**. Ureas were

made by coupling the tetrahydrobetacarboline intermediates with triphosgene and an alkyl or aryl amine. The spontaneous cyclization of intermediate ureas furnished the final hydantoin-fused tetrahydrobetacarboline derivatives **52-55a/b** and **56**.

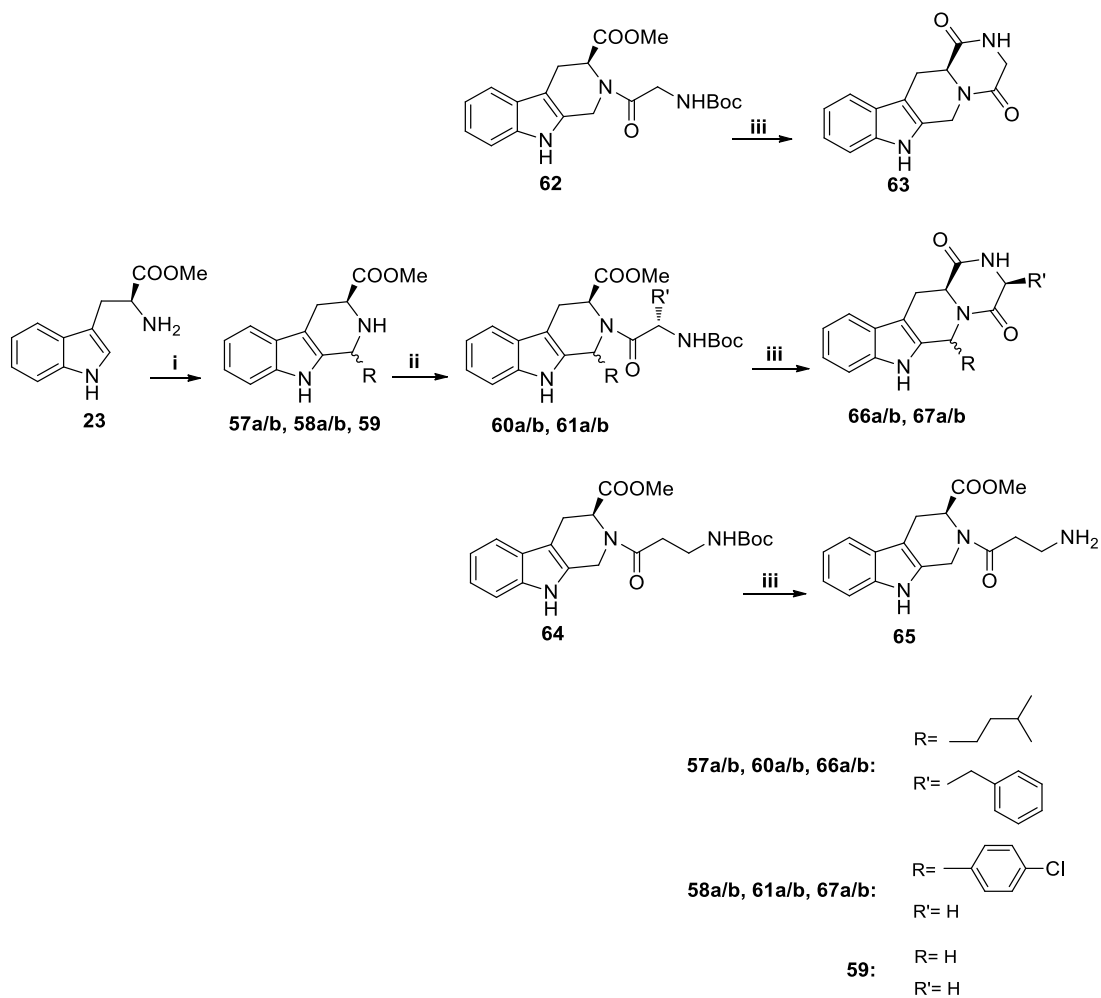
Scheme 9. Synthesis of derivatives **52a/b-56**.



Reagents and conditions: i: MeOH, TFA, RCHO or CH₂O, 30', MW, 110°C; ii: DCM, TEA, CCl₃COCCl₃, R'NH₂, 10', rt.
iii: MeOH/tiTEA, 10', reflux.

Tetrahydrobetacarboline derivatives **63** and **65-67a/b** were prepared as shown in Scheme 10. Starting with L-tryptophan methyl ester (**23**), reaction with isovaleraldehyde or 4-chlorobenzaldehyde or formaldehyde gave and the diastereoisomeric mixtures **57-58a/b**, and intermediate **59**. Treatment of **57-58a/b** with Boc-L-phenylalanine or Boc-L-glycine under coupling conditions gave intermediates **60-61a/b**. Intermediate **59** underwent the same reaction using Boc-L-glycine and Boc-beta-alanine, furnishing compounds **62** and **64**. The removal of the protecting group using a mixture of DCM and trifluoroacetic acid provided the final diketopiperazine-fused tetrahydrobetacarbolines **63**, **66-67a/b** and the (S)-methyl 2-(3-aminopropanoyl)-2,3,4,9-tetrahydro-1H-pyrido[3,4-b]indole-3-carboxylate **65**.

Scheme 10. Synthesis of derivatives 63, 65-67a/b.



Reagents and conditions: i: MeOH, TFA, RCHO or CH₂O, 30', MW, 110°C; ii: DCM/DMF, L-aminoacids, PyBOP, DIPEA, 12h, rt; iii: DCM/TFA 3/1, TIS, 2h, rt.

All the synthesized compounds were characterized by ROESY experiments to assign the absolute configuration. The ROESY and ^1H NMR spectra of derivatives 67a/b are shown (Figure 19, 21).

The configuration at C-6 asymmetric center of 67a was assigned as S on the basis of an NOE effect between H-6 and H-12a observed in the 2D ROESY spectra, indicating a cis disposition between these protons (Figure 19). The R configuration assigned to chiral centre 6 of 67b is justified by the absence of correlation between H-6 and H-12a (Figure 21). The absolute configuration of 67a/b as 6S,12aS and 6R,12aS, respectively, was determined by hypothesizing the retention of configuration at C-12a.

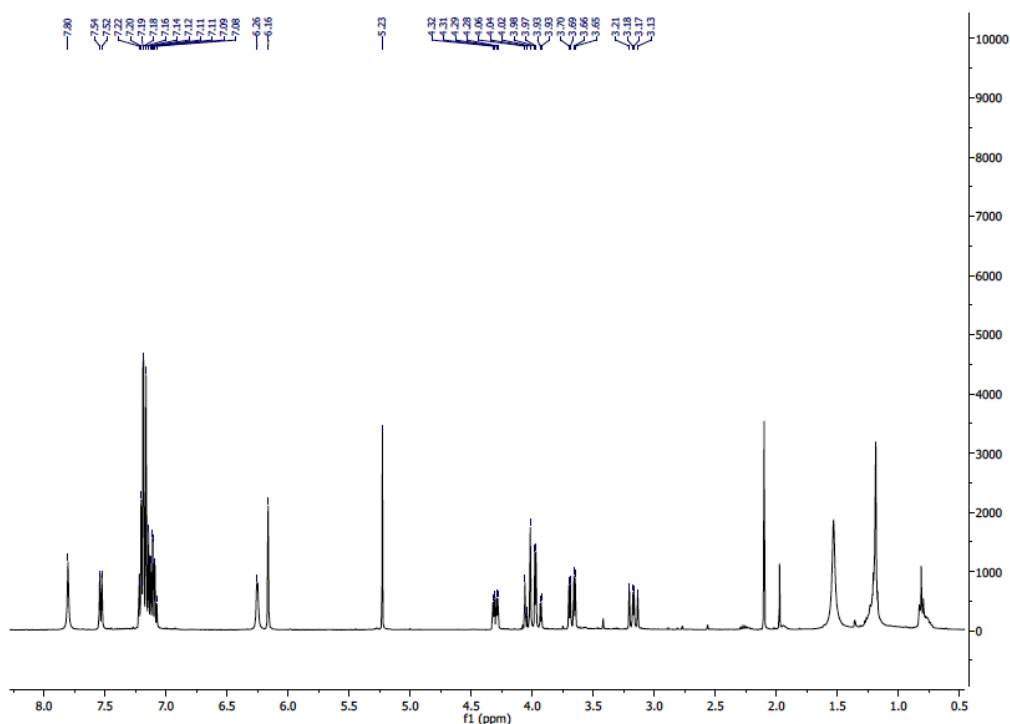


Figure 18. ^1H NMR spectrum of compound 67a.

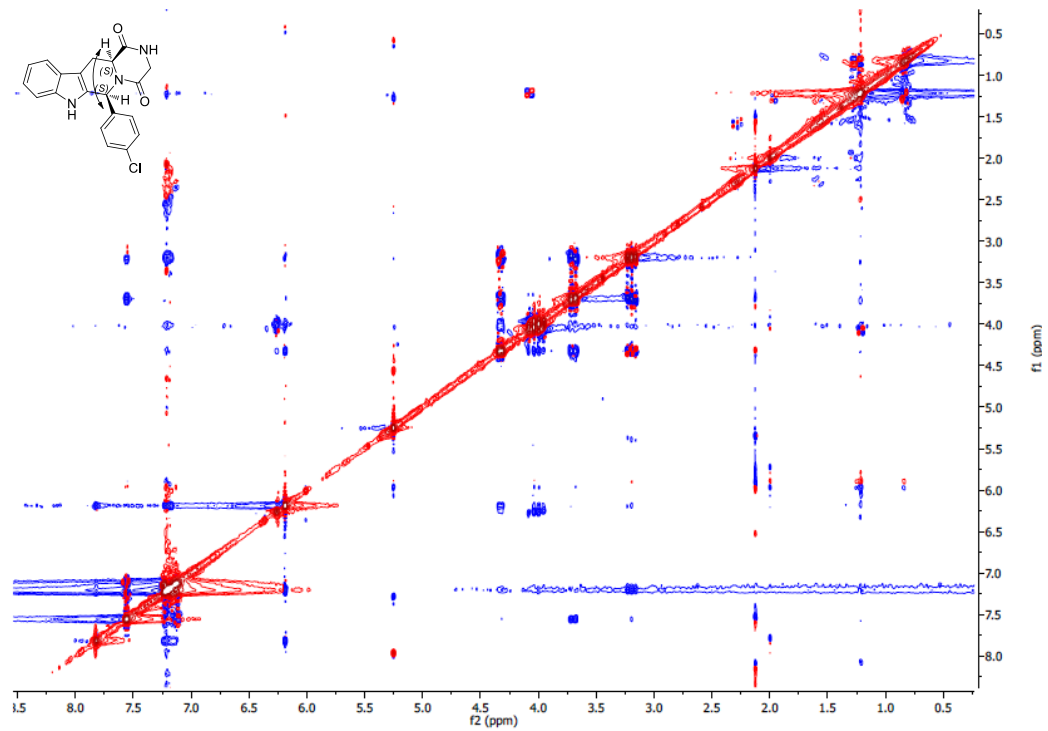


Figure 19. ROESY NMR spectrum of compound 67a.

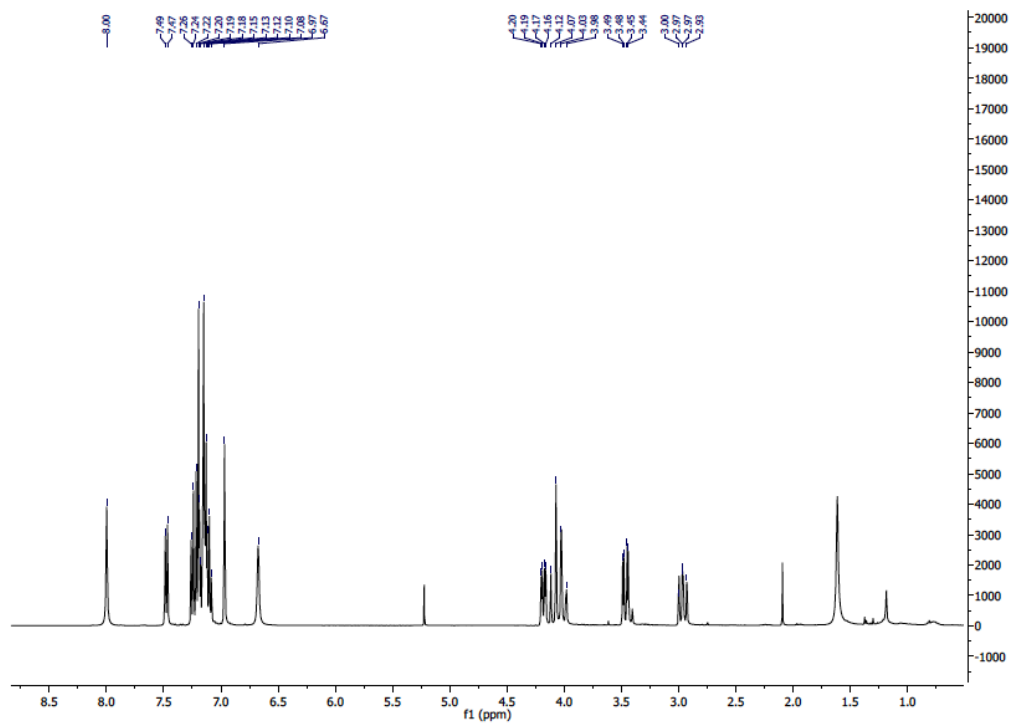


Figure 20. ^1H NMR spectrum of compound 67b.

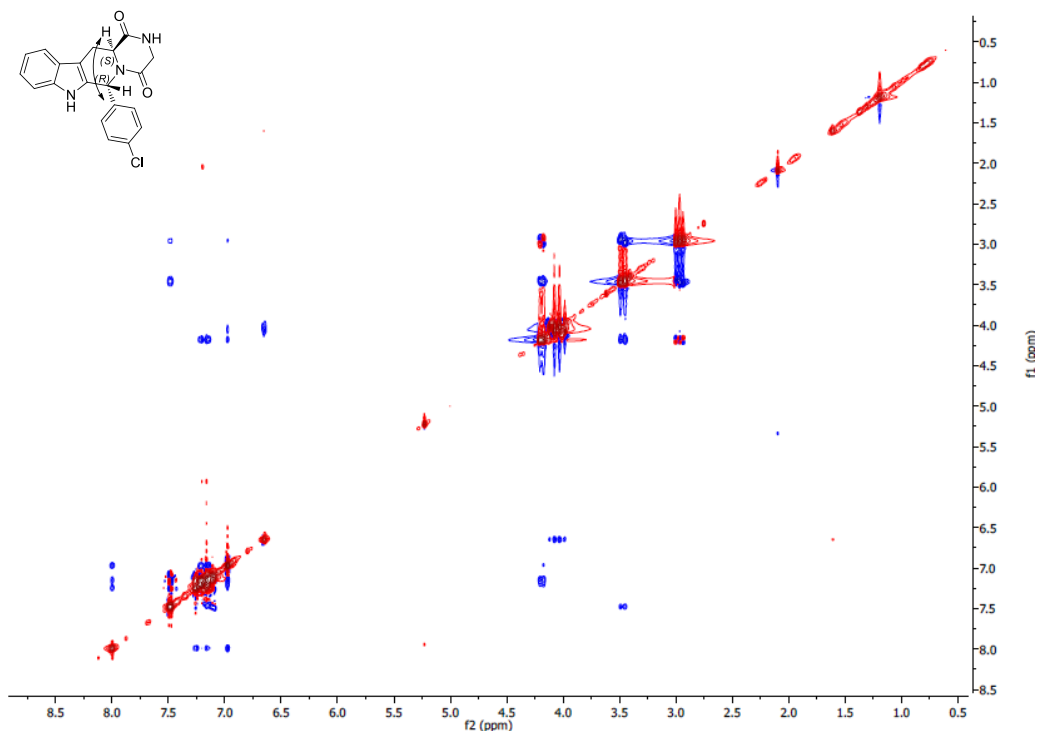
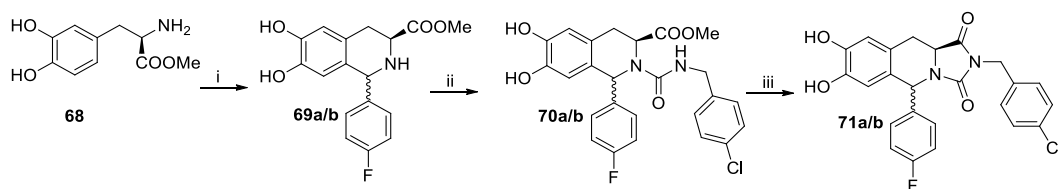


Figure 21. ROESY NMR spectrum of compound 67b.

Tetrahydroisoquinoline derivatives **71a/b** were prepared as shown in Scheme 11. Starting from L-Dopa methyl ester (**68**), reaction with 4-fluorobenzaldehyde gave the diastereoisomeric mixture **69a/b**. Treatment with triphosgene and 4-chlorobenzylamine and the subsequent cyclization provided the final hydantoin-fused tetrahydroisoquinolines.

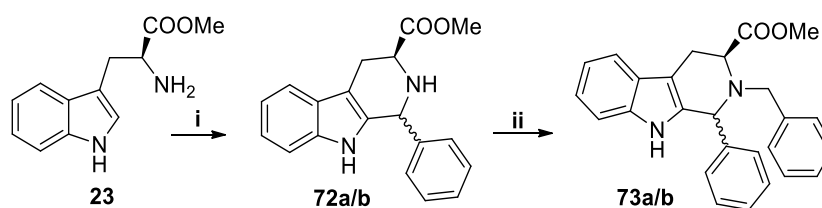
Scheme 11. Synthesis of derivatives 71a/b.



Reagents and conditions: i: MeOH, TFA, RCHO or CH₂O, 30', MW, 110°C; ii: DCM; TEA, CCl₃COCCl₃, 4-chlorobenzylamine, 10', rt; iii: MeOH/TEA, 30', reflux.

Derivatives **73a/b** were synthesized as shown in Scheme 12. The Pictet-Spengler reaction between L-tryptophan methyl ester and benzaldehyde furnished intermediates **72a/b** as diastereoisomeric mixture which was separated by flash chromatography. Then the nucleophilic displacement of bromine atom of benzyl bromide by the isolated diastereoisomers led to the final compounds **73a/b**.

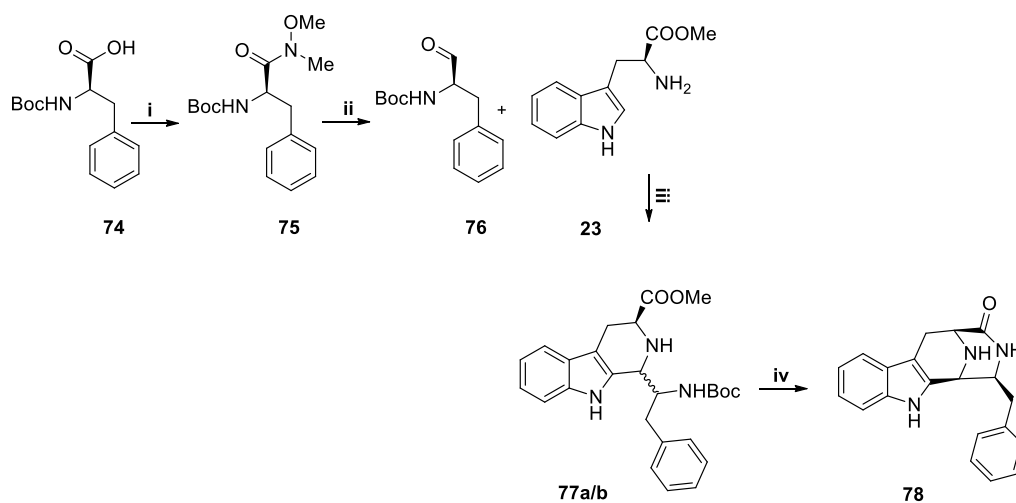
Scheme 12. Synthesis of derivatives 73a/b.



Reagents and conditions: i: MeOH, TFA, benzaldehyde, 30', MW, 110°C;
ii: DCM, NaH, benzyl bromide, 30', MW.

Compound **78** was synthesized using an alternative synthetic route as shown in Scheme 13. The first step involved the Weinreb amidation of Boc-L-phenylalanine and N,O-dimethylhydroxylamine; the subsequent treatment of this species with an excess of lithium aluminum hydride led to the aldehyde **76**, which was used to perform a Pictet-Spengler reaction using L-tryptophan methyl ester. The obtained diastereoisomeric mixture **77a/b** was separated by flash chromatography; the final deprotection of the isolated intermediates using a mixture DCM/TFA led to the indole-fused bicycle **78** as single diastereoisomer (1*S*,2*S*,5*S*). The cyclization of the derivative with configuration 1*R*,2*S*,5*S* was not observed, as previously described by my research group.⁷⁴

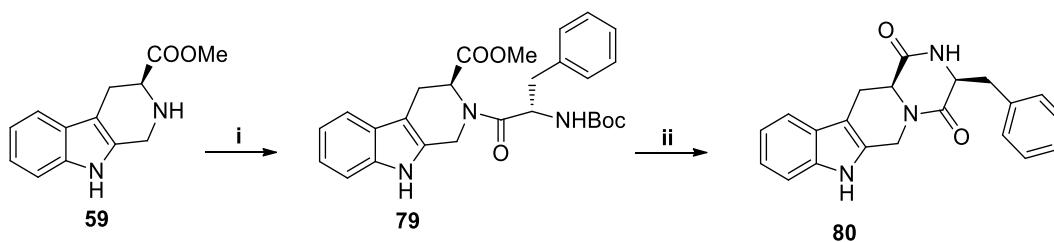
Scheme 13. Synthesis of derivative 78.



Reagents and conditions: i: DCM/DMF, N,O-dimethylhydroxylamine, HOBT, HBTU, DIPEA, 12h, rt; ii: THF dry, LiAlH₄ (1M in THF), N₂, 10', 0°C; iii: MeOH, TFA, N-Boc-L-phenylalaninal, 30', MW, 110°C; iv: DCM/TFA 3/1, TIS, 2h, rt.

Derivative **80** was synthesized according to Scheme 14. Intermediate **59**, synthesized as previously described, was used as starting material and coupled with Boc-L-phenylalanine to obtain **79**. Deprotection by trifluoroacetic acid in dichloromethane provided the derivative **80**.

Scheme 14. Synthesis of derivative 80.



Reagents and conditions: i: DCM/DMF, Boc-L-Phe-OH, PyBOP, DIPEA, 12h, rt; ii: DCM/TFA 3/1, TIS, 2h, rt.

4.3 Activity evaluation of the series III-VI

All the synthesized derivatives are current in the process of biological assays to test their activity on TRPM8 channels.

5.1 Conclusions

In this chapter, we report the synthesis and pharmacological evaluation of a small library of derivatives based on the tryptamine scaffold designed as potential TRPM8 modulators. Two of the synthesized derivatives, compounds 12 and 21 were shown to be efficient and potent TRPM8 antagonist and agonist, respectively. In detail, 12 showed a potency higher than that one reported for the wellknown TRPM8 antagonist BCTC. Meanwhile the agonist 21 showed a potency and efficacy significantly higher than menthol. In addition, compound 12 showed unremarkable activity on TRPV1 and TRPA1 at different concentrations. Computational studies allowed us to hypothesize a binding site and two pharmacophore prototypes for this series of tryptamine-based TRPM8 modulators. Moreover we designed and synthesized new potential modulators, using as scaffold tetrahydrobetacarboline and tetrahydroisoquiniline nucleus. The preliminary biological evaluation of this new class of compound didn't lead to an activity increase. Further studies to investigate the potential activity of the new series of TRPM8 modulators are in progress.

Experimental section

6.1 Chemistry

Reagents, starting materials, and solvents were purchased from Sigma-Aldrich (Milan, Italy) and used as received. Reactions were carried out with magnetic stirring in round-bottomed flasks unless otherwise noted. Moisture-sensitive reactions were conducted in oven-dried glassware under a positive pressure of dry nitrogen, using predried, freshly distilled solvents. Microwave assisted reactions were performed in a Biotage Initiator+ reactor. Analytical thin layer chromatography (TLC) was performed on precoated glass silica gel plates 60 (F254, 0.25 mm, VWR International). Purifications were performed by flash column chromatography on silica gel (230–400 mesh, Merck Millipore). NMR spectra were recorded on Varian Mercury-400 apparatus. ^1H NMR and ^{13}C NMR spectra were recorded with a Varian-400 spectrometer, operating at 400 and 100 MHz, respectively. Chemical shifts are reported in δ values (ppm) relative to internal Me_4Si , and J values are reported in hertz (Hz). The following abbreviations are used to describe peaks: s (singlet), d (doublet), dd (double double), t (triplet), q (quadruplet), and m (multiplet). ESI-MS experiments were performed on an Applied Biosystem API 2000 triple-quadrupole spectrometer. Combustion microanalyses were performed on a Carlo Erba CNH 1106 analyzer, and results were within 0.4% of calculated values and confirmed >95% purity for the final products. Analytical RP-HPLC was performed on a Phenomenex Synergi Fusion RP-80A (75 mm \times 4.6 mm, 4 μm), with a flow rate of 1 mL/min, using a tunable UV detector at 254 nm. Mixtures of CH_3CN and 0.05% TFA in H_2O were used as mobile phase.

General Procedure for the Synthesis of Derivatives 2 and 3.

3-(2-Bromoethyl)indole (**1**, 1.0 equiv) was dissolved in a mixture of anhydrous DCM/DMF (2/1 v/v) under magnetic stirring, and the temperature was set to 0 $^\circ\text{C}$. To this solution, an amount of 1.5 equiv of NaH was added portionwise and the mixture was allowed to react for 30 min. Then, an amount of 1.5 equiv of alkyl iodide [methyl iodide or 4-[phenyl]iodomethylbenzene (**3a**)] in DCM was added

dropwise and the reaction was warmed to room temperature and maintained under stirring for further 12 h. Then, reaction was quenched by 10% aqueous solution of citric acid and washed with brine. Organic layer was separated, dried over anhydrous Na₂SO₄, filtered, and evaporated in vacuo. Crude products were purified by column chromatography using n-hexane/ethyl acetate (4:1 v:v) as mobile phase.

3-(2-Bromoethyl)-1-methyl-1H-indole (2).

Yield 67%. ¹H NMR (400 MHz, CDCl₃) δ 3.39–3.46 (m, 4H, CH₂); 3.79 (s, 3H, CH₃); 6.97 (s, 1H); 7.20 (t, 1H, J = 7.6 Hz); 7.28 (d, 1H, J = 8.0 Hz); 7.34 (t, 1H, J = 8.0 Hz); 7.62 (d, 1H, J = 8.0 Hz). ESIMS m/z calcd for C₁₁H₁₂BrN, 237.02; found 238.11[(M + H)⁺].

Synthesis of 1-(Iodomethyl)-4-phenylbenzene (3a).

To 1 equiv of biphenyl-4-carboxylic acid (**1a**) dissolved in dry THF was added portionwise LiAlH₄ (3.0 equiv), under stirring at room temperature. After 2 h the solution was washed three times with HCl 2 N and then water and the organic layer was dried over anhydrous Na₂SO₄, filtered, and concentrated. The resultant 4-biphenylmethanol (**2a**) was purified by flash chromatography using ethyl acetate as solvent and was obtained as oil.

Yield 89%. ¹H NMR (400 MHz, CDCl₃) δ 2.98 (bs, 1H, OH); 4.70 (s, 2H, CH₂); 7.33–7.43 (m, 5H, aryl); 7.59–7.61 (m, 4H, aryl).

Then, treatment of **2a** with triphenylphosphine and I₂ in dry DCM according to the procedure previously described²⁷ gave the title compound.

Yield 65%. ¹H NMR (400 MHz, CDCl₃) δ 4.53 (s, 2H, CH₂); 7.15 (d, 2H, J = 8.0 Hz); 7.24 (d, 2H, J = 8.0 Hz); 7.43–7.55 (m, 5H).

1-(Biphenyl-4-ylmethyl)-3-(2-bromoethyl)-1H-indole (3).

Prepared from intermediate **3a** and 3-(2-bromoethyl)indole as described above. Yield 61%. ¹H NMR (400 MHz, CD₃OD) δ 3.27 (t, 1H, J = 7.4 Hz, CH₂); 3.38–3.46 (m, 2H, CH₂); 3.81 (t, 1H, J = 7.6 Hz, CH₂); 5.35 (s, 2H, CH₂); 7.07

(s, 1H); 7.14–7.61 (m, 13H). ESIMS m/z calcd for $C_{23}H_{20}BrN$, 391.08; found 392.13[(M + H)⁺].

General Procedure for the Synthesis of Derivatives 4–12.

One equivalent of 3-(2-bromoethyl)indole (**1**) or intermediate **2** or **3** was dissolved in THF and 1.5 equiv of the proper amine, 1.5 equiv of TEA, 1.5 equiv of NaI, and 0.3 equiv of $(CH_3COO)_2Pd$ were added to this solution (**Scheme 1**). The reaction was conducted under μW , at 100 °C, for 20 min. The resulting mixture was filtered through Celite, dried in vacuo, and reconstituted in DCM. The organic phase was washed with water (3 × 50 mL), dried over anhydrous Na_2SO_4 , filtered, concentrated, and purified by column chromatography using DCM/MeOH as mobile phase.

N-(4-Methoxybenzyl)-2-(1-methyl-1H-indol-3-yl)ethanamine (4).

Synthesized starting from **3** and 4-methoxybenzylamine, yield 71%. ¹H NMR (400 MHz, $CDCl_3$) δ 2.92 (t, 2H, $J = 7.6$ Hz, CH_2); 3.19 (t, 2H, $J = 7.6$ Hz, CH_2); 3.49 (s, 6H, 2 CH_3); 3.72 (s, 2H, CH_2); 6.81 (s, 1H); 7.07–7.15 (m, 3H); 7.20 (t, 1H, $J = 6.8$ Hz); 7.24–7.30 (m, 3H); 7.52 (d, 1H, $J = 8.0$ Hz). ¹³C NMR (100 MHz, $CDCl_3$) δ 22.7, 41.6, 50.8, 57.1, 109.1, 110.0, 112.4, 118.6, 118.8, 121.4, 121.9, 124.2, 126.4, 128.0, 128.3, 135.3, 199.8. ESIMS m/z calcd for $C_{19}H_{22}N_2O$, 294.17; found 295.20 [(M + H)⁺].

N-(4-Chlorobenzyl)-2-(1-methyl-1H-indol-3-yl)ethanamine (5).

Synthesized starting from **3** and 4-chlorobenzylamine, yield 69%. ¹H NMR (400 MHz, $CDCl_3$) δ 2.93–3.00 (m, 4H, 2 CH_2); 3.74 (s, 3H, CH_3); 3.77 (s, 2H, CH_2); 6.87 (s, 1H); 7.10 (t, 1H, $J = 8.0$ Hz); 7.20–7.30 (m, 6H); 7.58 (d, 1H, $J = 8.0$ Hz). ¹³C NMR (100 MHz, $CDCl_3$) δ 25.57, 32.56, 49.40, 53.06, 109.2, 110.0, 112.3, 118.7, 118.9, 121.6, 126.7, 127.8, 128.4, 129.4, 132.5, 137.1, 138.7. ESIMS m/z calcd for $C_{18}H_{19}ClN_2$, 298.12; found 299.17 [(M + H)⁺].

2-([1,1'-Biphenyl]-4-yl)-N-(2-(1-methyl-1H-indol-3-yl)ethyl)-ethanamine (6).

Synthesized starting from **3** and 2-(4-biphenyl)-ethylamine, yield 65%. ¹H NMR (400 MHz, CD₃OD) δ 3.03 (t, 2H, J = 8.8 Hz, CH₂); 3.17 (t, 2H, J = 8.6 Hz, CH₂); 3.32–3.37 (m, 4H, CH₂); 3.76 (s, 3H, CH₃); 7.06–7.11 (m, 2H); 7.20 (t, 1H, J = 7.2 Hz); 7.31–7.44 (m, 6H); 7.56–7.60 (m, 5H). ¹³C NMR (100 MHz, CD₃OD) δ 22.0, 31.7, 48.4, 109.4, 118.0, 119.0, 121.8, 126.7, 127.3, 127.5, 128.7, 129.1, 135.5. ESIMS m/z calcd for C₂₅H₂₆N₂, 354.21; found 355.26 [(M + H)⁺].

2-(1-([1,1'-Biphenyl]-4-ylmethyl)-1H-indol-3-yl)-N-(3,4-dimethoxyphenethyl)ethanamine (7).

Synthesized starting from **3** and 3,4-dimethoxyphenethylamine, yield 75%. ¹H NMR (400 MHz, CD₃OD) δ 2.91 (t, 2H, J = 7.2 Hz, CH₂); 3.17–3.26 (m, 4H, CH₂); 3.34 (t, 2H, J = 7.4 Hz, CH₂); 3.77 (s, 3H, OCH₃); 3.79 (s, 3H, OCH₃); 5.39 (s, 2H, CH₂); 6.83–6.87 (m, 2H); 7.09 (t, 1H, J = 8.0 Hz); 7.11–7.24 (m, 5H); 7.37–7.41 (m, 4H); 7.50–7.55 (m, 4H); 7.62 (d, 1H, J = 8.0 Hz). ¹³C NMR (100 MHz, CD₃OD) δ 22.1, 31.7, 48.8, 49.2, 55.2, 109.2, 110.1, 112.1, 112.3, 118.3, 119.3, 120.9, 112.0, 126.7, 126.9, 127.0, 127.2, 127.4, 127.7, 128.7, 129.0, 137.3, 140.7, 148.6 149.6. ESIMS m/z calcd for C₃₃H₃₄N₂O₂, 490.26; found 491.31 [(M + H)⁺].

N-[2-(1H-Indol-3-yl)ethyl]naphthalen-1-amine (8).

Synthesized starting from **1** and 1-naphthalenamine, yield 55%. ¹H NMR (400 MHz, CDCl₃) δ 3.26 (t, 2H, J = 8.0 Hz, CH₂); 3.64 (t, 2H, J = 8.2 Hz, CH₂); 6.70 (d, 1H, J = 7.8 Hz); 7.06 (s, 1H); 7.20 (t, 1H, J = 7.2 Hz); 7.25–7.27 (m, 2H); 7.37–7.43 (m, 4H); 7.66 (d, 1H, J = 7.6 Hz); 7.72 (d, 1H, J = 8.0 Hz); 7.80 (d, 1H, J = 8.2 Hz); 7.98 (s, 1H, NH). ¹³C NMR (100 MHz, CDCl₃) δ 25.1; 44.3; 104.7, 111.5; 113.6; 117.5, 119.0, 119.8, 120.1, 122.3; 122.5; 123.7; 124.8, 125.9, 126.9; 127.6; 128.9; 133.4; 136.7, 143.7. ESI-MS m/z calcd for C₂₀H₁₈N₂, 286.15; found 287.20 [(M + H)⁺].

N-[2-(1H-Indol-3-yl)ethyl]naphthalen-2-amine (9).

Synthesized starting from **1** and 2-naphthalenamine, yield 58%. ¹H NMR (400 MHz, CDCl₃) δ 3.16 (t, 2H, J = 7.8 Hz CH₂); 3.58 (t, 2H, J = 8.0 Hz, CH₂); 6.81–6.85 (m, 2H); 7.08 (s, 1H); 7.12–7.24 (m, 4H); 7.33–7.40 (m, 3H); 7.59 (d, 1H, J = 8.4 Hz); 7.64 (d, 1H, J = 8.2 Hz); 8.07 (s, 1H, NH). ¹³C NMR (100 MHz, CDCl₃) δ 25.1; 44.1; 104.8, 111.4, 118.4, 119.0, 119.7 122.1, 122.3; 122.4; 123.0; 126.1; 126.5; 126.8; 127.4; 127.8; 129.1; 133.7; 136.5; 146.0. ESI-MS m/z calcd for C₂₀H₁₈N₂, 286.15; found 287.17 [(M + H)⁺]

2-(1H-Indol-3-yl)-N-(quinolin-5-ylmethyl)ethanamine (10).

Synthesized starting from **1** and 5-aminoquinoline, yield 63%. ¹H NMR (400 MHz, CDCl₃) δ 3.26 (t, 2H, J = 8.0 Hz, CH₂); 3.62 (t, 2H, J = 8.2 Hz, CH₂); 6.82 (d, 1H, J = 7.6 Hz); 7.12–7.48 (m, 7H); 7.69 (d, 1H, J = 7.8 Hz); 8.15 (s, 1H, NH); 8.37 (d, 1H, J = 4.0 Hz); 9.13 (d, 1H, J = 4.0 Hz). ¹³C NMR (100 MHz, CDCl₃) δ 24.9; 44.1; 107.9; 111.6; 113.0; 113.6, 116.2; 118.9; 119.4; 119.8, 122.3; 122.6; 127.4; 128.4; 136.5; 138.7; 141.9; 146.6, 153.0. ESI-MS m/z calcd for C₁₉H₁₇N₃, 287.14; found 288.26 [(M + H)⁺].

2-(1H-Indol-3-yl)-N-(isoquinolin-5-ylmethyl)ethanamine (11).

Synthesized starting from **1** and 5-aminoisoquinoline, yield 67%. ¹H NMR (400 MHz, CDCl₃) δ 3.23 (t, 2H, J = 6.4 Hz, CH₂); 3.61 (t, 2H, J = 6.2 Hz, CH₂); 7.82 (d, 1H, J = 8.0 Hz); 7.15–7.54 (m, 7H); 7.71 (d, 1H, J = 8.0 Hz); 8.11 (s, 1H, NH); 8.39 (d, 1H, J = 7.2 Hz); 9.17 (s, 1H). ¹³C NMR (100 MHz, CDCl₃) δ 25.9; 49.9; 111.4; 114.9; 116.9, 119.0, 119.5, 122.3, 122.4, 127.0; 127.3; 127.5; 127.7; 130.1; 134.7; 134.9; 135.4; 136.6; 143.3; 153.2. ESIMS m/z calcd for C₁₉H₁₇N₃ 287.14; found 288.24 [(M + H)⁺].

N,N-Dibenzyl-2-(1H-indol-3-yl)ethanamine (12).

Synthesized starting from **1** and dibenzylamine, yield 73%. ¹H NMR (400 MHz, CDCl₃) δ 2.84 (t, 2H, J = 5.6 Hz, CH₂); 3.01 (t, 2H, J = 6.0 Hz, CH₂); 3.73 (s, 4H, 2CH₂); 6.90 (s, 1H); 7.06 (t, 1H, J = 8.2 Hz, aryl); 7.18 (t, 1H, J = 8.0 Hz); 7.26 (t, 2H, J = 8.4 Hz); 7.32–7.35 (m, 5H); 7.40–7.43 (m, 5H); 7.85 (s, 1H, NH). ¹³C

NMR (100 MHz, CDCl₃) δ 23.3; 54.1; 58.5; 111.2; 114.8; 119.1, 119.3, 121.6, 122.0 127.0; 127.8; 128.4; 129.0; 136.4; 140.1. ESI-MS *m/z* calcd for C₂₄H₂₄N₂, 340.19 found 341.27 [(M + H)⁺].

Synthesis of N-[(1,2,3,4-Tetrahydronaphthalen-1-yl)methyl]-2-(1H-indol-3-yl)ethanamine. (14) (1,2,3,4-Tetrahydronaphthalen-1-yl)methyl 4-Methylbenzenesulfonate (6a).

(1,2,3,4-Tetrahydronaphthalen-1-yl)methanol (**5a**) was synthesized by reduction of 1,2,3,4-tetrahydronaphthalenecarboxylic acid (**4a**) following the procedure described for intermediate **2a**. Yield 95%. ¹H NMR (400 MHz, CDCl₃) δ 1.80–1.89 (m, 2H, CH₂); 2.02–2.11 (m, 2H, CH₂); 2.79–2.90 (m, 3H, CH₂ and CH); 3.90–3.96 (m, 2H, CH₂O); 7.12–7.23 (m, 4H).

Then, to a solution of **5a** in DCM was added Cl-Tos (2.0 equiv), TEA (2.0 equiv), and DMAP (0.7 equiv). After 2 h at room temperature, the solution was washed with brine. The organic layer was dried over anhydrous Na₂SO₄, filtered, concentrated, and purified with flash chromatography in n-hexane/ethyl acetate 30:20.

The title compound **6a** was obtained in 61% yield. ¹H NMR (400 MHz, CDCl₃) δ 1.67–1.73 (m, 2H, CH₂); 1.85–1.91 (m, 2H, CH₂); 2.48 (s, 3H, CH₃); 2.68–2.74 (m, 2H, CH₂); 3.18 (t, 1H, J = 8.0 Hz, CH); 4.07 (t, 1H, J = 7.8 Hz, CH₂O); 4.21–4.26 (m, 1H, CH₂O); 7.05–7.13 (m, 4H); 7.36 (d, 2H, J = 8.0 Hz, tosyl); 7.86 (d, 2H, J = 8.0 Hz, tosyl).

N-[(1,2,3,4-Tetrahydronaphthalen-1-yl)methyl]-2-(1H-indol-3-yl)ethanamine (14).

A 10 mL sealable flask, equipped with a stir bar, was charged with 1 equiv of tosylate **6a** and 2.6 equiv of tryptamine dissolved in THF. The flask was sealed, heated to 60–70 °C, and allowed to stir at that temperature overnight.

The resulting slurry was cooled to room temperature, added to DCM, and washed with brine. The organic layer solvents was dried over Na₂SO₄, filtered, and evaporated under vacuum. The resulting mixture was separated by silica gel chromatography using DCM/MeOH 9/1 as eluent.

Yield 69%. ^1H NMR (400 MHz, CDCl_3) δ 1.68–1.71 (m, 2H, CH_2); 1.82–1.85 (m, 2H, CH_2); 2.65–2.68 (m, 2H, CH_2); 3.02–3.05 (m, 2H, CH_2); 3.25–3.29 (m, 5H, CH and 2 CH_2); 6.96 (d, 1H, $J = 8.0$ Hz); 7.00–7.14 (m, 5H); 7.21 (t, 1H, $J = 8.4$ Hz); 7.36 (d, 1H, $J = 8.2$ Hz); 7.62 (d, 1H, $J = 8.4$ Hz); 8.08 (s, 1H, NH); ^{13}C NMR (100 MHz, CDCl_3) δ 19.2; 22.8; 26.1; 29.3; 36.0; 49.1; 54.1; 111.6; 113.0; 118.8, 120.0, 122.9, 123.1, 126.2, 126.8, 127.5, 128.7, 129.8; 136.0; 136.9, 143.7. ESIMS m/z calcd for $\text{C}_{21}\text{H}_{24}\text{N}_2$, 304.19; found 305.43 [(M + H) $^+$].

General Procedure for the Synthesis of Derivatives 15–22.

Tryptamine (1.0 equiv) was dissolved in a solution of DCM/ CH_3COOH (5:1 v/v) at room temperature. To this solution an amount of 2.0 equiv of the proper aldehyde was added and the mixture was warmed to reflux for 1.5 h. Then, an amount of 1.8 equiv of sodium triacetoxyborohydride was added portionwise and the mixture was allowed to reflux for further 3–5 h. After cooling to room temperature, NaOH 1 N was added. The organic phase was separated and extracted one more time with the alkaline solution. Then it was dried over Na_2SO_4 , filtered, and concentrated in vacuo. The crude products were purified by column chromatography using mixtures of DCM/MeOH as eluent.

2-(1H-Indol-3-yl)-N-(naphthalen-1-ylmethyl)ethanamine (15).

Synthesized starting from **13** and 1-naphthaldehyde, yield 75%. ^1H NMR (400 MHz, CDCl_3) δ 3.05 (t, 2H, $J = 6.8$ Hz, CH_2); 3.13 (t, 2H, $J = 6.8$ Hz, CH_2); 4.27 (s, 2H, CH_2); 6.97 (s, 1H); 7.20 (t, 1H, $J = 7.2$ Hz); 7.33–7.48 (m, 4H); 7.64 (d, 1H, $J = 7.8$ Hz); 7.74 (d, 1H, $J = 8.2$ Hz); 7.84 (d, 1H, $J = 7.8$ Hz); 8.00 (d, 2H, $J = 4.0$ Hz). ^{13}C NMR (100 MHz, CDCl_3) δ 25.7, 49.8, 51.4, 111.1, 113.9, 118.9, 119.3, 121.9, 122.0, 123.5, 125.4, 125.5, 125.9, 126.0, 127.4, 127.7, 128.7, 131.7, 133.8, 135.7. ESIMS m/z calcd for $\text{C}_{21}\text{H}_{20}\text{N}_2$, 300.16; found 301.18 [(M + H) $^+$].

2-(1H-Indol-3-yl)-N-[(2-methoxynaphthalen-1-yl)methyl]-ethanamine (16).

Synthesized starting from **13** and 2-methoxy-1-naphthaldehyde, yield 63%. ^1H NMR (400 MHz, CDCl_3) δ 3.05–3.09 (m, 4H, CH_2); 3.61 (s, 3H, CH_3); 4.35 (s, 2H, CH_2); 7.01–7.19 (m, 3H); 7.28–7.44 (m, 6H); 7.76 (d, 1H, $J = 7.8$ Hz); 7.90

(d, 1H, J = 7.0 Hz); 8.14 (s, 1H, NH). ¹³C NMR (100 MHz, CDCl₃) δ 25.1; 42.6; 48.1; 56.0; 94.6, 111.4; 112.7; 119.0, 119.6, 122.3, 122.7, 122.9; 123.6; 127.3; 128.8; 129.9; 130.7; 131.7; 136.5, 142.8. ESIMS m/z calcd for C₂₁H₂₀N₂O 330.17; found 331.21 [(M + H)⁺].

1-[(2-(1H-Indol-3-yl)ethyl)amino]methyl]naphthalen-2-ol (17).

Synthesized starting from **13** and 2-hydroxy-1-naphthaldehyde, yield 51%. ¹H NMR (400 MHz, CDCl₃) δ 3.05–3.09 (m, 4H, 2CH₂); 4.41 (s, 2H, CH₂); 7.07–7.14 (m, 3H); 7.20 (t, 1H, J = 7.0 Hz); 7.26–7.42 (m, 3H); 7.60 (d, 1H, J = 8.0 Hz); 7.65 (d, 1H, J = 8.0 Hz); 7.73 (d, 2H, J = 8.0 Hz); 8.08 (s, 1H, NH). ¹³C NMR (100 MHz, CDCl₃) δ 25.2; 47.4; 48.7; 111.4; 111.5; 112.8; 113.0; 118.9, 119.6, 119.7, 121.1, 122.5; 122.6; 126.6; 127.5; 128.6; 129.0; 129.3; 131.9; 137.4, 142.7. ESIMS m/z calcd for C₂₁H₂₀N₂O, 316.16; found 317.40 [(M + H)⁺].

2-(1H-Indol-3-yl)-N-[(10-methylanthracen-9-yl)methyl]-ethanamine (18).

Synthesized starting from **13** and 10-methyl-9-anthracenecarbaldehyde, yield 58%. ¹H NMR (400 MHz, CDCl₃) δ 3.04–3.07 (m, 4H, 2CH₂); 3.26 (t, 2H, J = 6.4 Hz, CH₂); 3.48 (s, 3H, CH₃); 6.92 (s, 1H); 7.10 (t, 1H, J = 8.0 Hz); 7.20 (t, 1H, J = 8.0 Hz); 7.32 (d, 1H, J = 8.0 Hz); 7.39 (t, 2H, J = 7.8 Hz); 7.46 (t, 2H, J = 8.0 Hz, aryl); 7.56 (d, 1H, J = 8.0 Hz); 7.95 (s, 1H, NH); 8.19 (d, 2H, J = 8.0 Hz); 8.29 (d, 2H, J = 8.0 Hz). ¹³C NMR (100 MHz, CDCl₃) δ 17.1; 25.5; 45.6; 49.7; 111.4; 111.5; 112.2; 113.0; 119.7, 122.2, 122.4, 124.6; 125.0; 125.7; 125.9; 136.5; 142.7. ESIMS m/z calcd for C₂₆H₂₄N₂, 364.19 found 365.48 [(M + H)⁺].

5[(2-(1H-Indol-3-yl)ethylamino)methyl]-2-methoxyphenol (19).

Synthesized starting from **13** and vanillin, yield 58%. ¹H NMR (400 MHz, CD₃OD) δ 2.84 (t, 2H, CH₂, J = 7.4 Hz); 2.92 (t, 2H, CH₂, J = 7.4 Hz); 3.59 (s, 2H, CH₂); 3.67 (s, 3H, CH₃); 6.61 (d, 1H, J = 8.0 Hz); 6.71 (s, 1H); 6.73 (d, 1H, J = 8.0 Hz); 6.94–6.98 (m, 2H); 7.05 (t, 1H, J = 8.0 Hz); 7.31 (d, 1H, J = 8.0 Hz); 7.48 (d, 1H, J = 8.0 Hz). ¹³C NMR (100 MHz, CD₃OD) δ 24.7, 48.6, 52.8, 55.1, 111.2, 111.8, 112.1, 115.0, 118.2, 121.2, 121.3, 122.4, 122.5, 127.4, 130.1, 137.0, 145.9, 147.9. ESIMS m/z calcd for C₁₈H₂₀N₂O₂, 296.15; found 297.16 [(M + H)⁺].

N-(3,4-Dimethoxybenzyl)-2-(1H-indol-3-yl)ethanamine (20).

Synthesized starting from **13** and 3,4-dimethoxybenzaldehyde, yield 72%. ¹H NMR (400 MHz, CDCl₃) δ 3.01–3.15 (m, 4H, 2CH₂); 3.80 (s, 2H, CH₂); 3.82 (s, 6H, 2CH₃); 6.75 (d, 1H, J = 8.0 Hz); 6.81 (d, 1H, J = 8.0 Hz); 6.88 (s, 1H); 7.03 (s, 1H); 7.10 (t, 1H, J = 4.0 Hz); 7.18 (t, 1H, J = 4.0 Hz); 7.35 (d, 1H, J = 8.0 Hz); 7.58 (d, 1H, J = 8.0 Hz); 8.10 (s, 1H, NH). ¹³C NMR (100 MHz, CDCl₃) δ 25.4; 49.0; 53.5; 56.0; 111.0, 111.4; 111.5; 112.7; 119.0, 119.5, 120.8, 122.3; 122.4; 127.4; 130.1; 137.0; 145.9, 147.9. ESIMS m/z calcd for C₁₉H₂₂N₂O₂, 310.17; found 311.25 [(M + H)⁺].

2-(1H-Indol-3-yl)-N-(4-phenoxybenzyl)ethanamine (21).

Synthesized starting from **13** and 4-phenoxybenzaldehyde, yield 83%. ¹H NMR (400 MHz, CD₃OD) δ 3.12 (t, 2H, CH₂, J = 8.8 Hz); 3.24 (t, 2H, CH₂, J = 8.4 Hz); 4.08 (s, 2H, CH₂); 6.95–7.05 (m, 5H); 7.10–7.18 (m, 3H); 7.31–7.42 (m, 5H); 7.53 (d, 1H, J = 8.0 Hz). ¹³C NMR (100 MHz, CD₃OD) δ 24.5; 50.7; 52.7; 111.4; 113.4; 119.8; 120.6; 120.9, 121.3, 123.6, 124.9; 125.9; 128.8; 129.0; 131.9; 133.4; 139.2; 158.8, 160.8. ESIMS m/z calcd for C₂₃H₂₂N₂O, 342.17; found 343.25 [(M + H)⁺].

N-Methyl-2-(1-methyl-1H-indol-3-yl)-N-(4-phenoxybenzyl)-ethanamine (22).

Compound **21** (1 equiv) was dissolved in a mixture of anhydrous DCM/DMF (2/1 v/v) under magnetic stirring, and the temperature was set to 0 °C. To this solution, an amount of 3 equiv of NaH was added portionwise, and the mixture was allowed to react for 30 min. Then, an amount of 3 equiv of methyl iodide in dry DCM was added dropwise and the reaction was warmed to room temperature and maintained under stirring for further 12 h. Then, reaction was quenched by 10% aqueous solution of citric acid and washed with brine. Organic layer was separated, dried over anhydrous Na₂SO₄, filtered, and evaporated in vacuo. Crude product was purified by column chromatography using DCM/MeOH (9:1 v:v) as mobile phase.

Yield 55%. ^1H NMR (400 MHz, CDCl_3) δ 3.14–3.18 (m, 5H, CH_3 and CH_2); 3.78 (s, 3H, CH_3); 3.84 (t, 2H, $J = 8.0$ Hz, CH_2); 4.99 (s, 2H, CH_2); 6.95 (d, 2H, $J = 8.0$ Hz); 7.05 (d, 2H, $J = 8.0$ Hz); 7.17 (t, 1H, $J = 7.6$ Hz); 7.18–7.24 (m, 4H); 7.35 (t, 2H, $J = 8.0$ Hz); 7.59 (d, 3H, $J = 8.0$ Hz). ^{13}C NMR (100 MHz, CDCl_3) δ 19.3, 32.8, 49.7, 63.7, 67.0, 109.5, 118.2, 118.4, 119.3, 119.9, 120.7, 121.9, 124.5, 126.9, 128.2, 130.0, 134.8, 136.8, 155.4, 159.9. ESIMS m/z calcd for $\text{C}_{25}\text{H}_{26}\text{N}_2\text{O}$, 370.49; found 371.55 $[(\text{M} + \text{H})^+]$.

General procedure for the synthesis of derivatives **29a/b**, **30a/b**, **31**

p-Cl benzaldehyde or *o*- NO_2 benzaldehyde (1.5 eq) was added to a solution of L-Trp-OMe (**23**) dissolved in methanol and TFA (1.5eq). The reaction mixture was heated to 110 °C for 30 min in a microwave reactor (Scheme 1). The combined organic layer was concentrated, diluted with dichloromethane and washed with water (3 x 20 mL). The combined organic layer was dried over anhydrous sodium sulfate, filtered, concentrated and purified by flash chromatography in *n*-hexane/ethyl acetate (40:10 ratio) to separate the diastereomeric mixture (yield 87%). To a solution of **24** and **25** as singles diastereoisomers dissolved in DCM, 0.4 eq of triphosgene, 1.2 eq of TEA and 1.2 eq of proper amine were added. The reaction was mixed at room temperature for 20 minutes. Then the solution was washed with water (3 x 20 mL). The combined organic layer was dried over anhydrous sodium sulfate, filtered, concentrated and purified by flash chromatography in 30:20 *n*-hexane/ethyl acetate (yield: 65%). Final compounds **29a/b**, **30a/b**, **31** were obtained by refluxing intermediates **26a/b**, **27a/b** and **28** in MeOH/TEA for 10 minutes. The crude was concentrated in vacuo, washed with water (3 X 20 mL), dried over anhydrous sodium sulfate, filtered, concentrated and purified by flash chromatography in 75:25 *n*-hexane/ethyl acetate. For compounds **29a/b** ethyl acetate was used as mobile phase. The final compounds are obtained as two diastereoisomers; the TRANS isomer **41** was obtained in such small quantities that it can not be characterized.

(1S,3S)5-(4-chlorophenyl)-2(4-fluorobenzyl)-5,6,11,11a-tetrahydro-1H-imidazo[1',5':1,6]pyrido[3,4-b]indole-1,3(2H)-dione (29a).

Overall yield 46%. ¹H NMR (400 MHz, CDCl₃) δ 2.83 (t, 1H, *J* = 7.6 Hz, H-11'); 3.47 (dd, 1H, *J*' = 5.6, *J*" = 15.6 Hz, H-11"); 4.28 (dd, 1H, *J*' = 5.2, *J*" = 10.8 Hz, H-11a); 4.58 (d, 1H, CH_{2a}, *J* = 14.4 Hz); 4.68 (d, 1H, CH_{2b}, *J* = 14.4 Hz); 6.24 (s, 1H, H-5); 6.97 (t, 2H, *J* = 8.0 Hz aryl); 7.17-7.31 (m, 7H, aryl); 7.37 (t, 2H, *J* = 8.0 Hz aryl); 7.54 (d, 1H, *J* = 8.0 Hz, aryl); 7.86 (s, 1H, NH). ¹³C NMR (100 MHz, CDCl₃) δ 23.5, 41.9, 51.6, 53.4, 108.5, 111.5, 115.7, 115.9, 118.7, 120.5, 123.3, 126.2, 129.6, 129.8, 130.7, 130.8, 132.0, 135.2, 136.8, 137.6, 154.7, 163.9, 172.4. HR-MS *m/z* calcd for C₂₆H₂₀ClFN₃O₂ [(M + H)]⁺: 460,1223; found 460,1236.

(1R,3S)5-(4-chlorophenyl)-2(4-fluorobenzyl)-5,6,11,11a-tetrahydro-1H-imidazo[1',5':1,6]pyrido[3,4-b]indole-1,3(2H)-dione (29b).

Overall yield 32%. ¹H NMR (400 MHz, CDCl₃) δ 3.05 (t, 1H, *J* = 7.6 Hz, H-11'); 3.47 (dd, 1H, *J*' = 6.0 Hz, *J*" = 11.6 Hz, H-11"); 4.36 (dd, 1H, *J*' = 5.4, *J*" = 11.2 Hz, H-11a); 4.51 (d, 1H, *J* = 14.0 Hz CH_{2a}); 4.68 (d, 1H, *J* = 14.0 Hz, CH_{2b}); 5.78 (s, 1H, H-5); 6.98 (t, 2H, *J* = 7.6 Hz, aryl); 7.18-7.31 (m, 6H, aryl); 7.38 (t, 2H, *J* = 7.6 Hz, aryl); 7.58 (d, 2H, *J* = 8.0 Hz, aryl). ¹³C NMR (100 MHz, CDCl₃) δ 24.7, 52.4, 52.8, 54.4, 109.7, 111.1, 116.5, 117.2, 118.4, 119.1, 121.0, 127.5, 128.8, 129.8, 130.3, 131.1, 132.4, 134.9, 137.2, 137.8, 152.2, 164.4, 173.5. HR-MS *m/z* calcd for C₂₆H₂₀ClFN₃O₂ [(M + H)]⁺: 460,1223; found 460,1239.

(1S,3S)2-(3-aminopropyl)-5-(2-nitrophenyl)-5,6,11,11a-tetrahydro-1H-imidazo[1',5':1,6]pyrido[3,4-b]indole-1,3(2H)-dione (30a).

Overall yield 66%. ¹H NMR (400 MHz, CDCl₃) δ: 1.70-1.72 (m, 2H, CH₂); 3.04-3.13 (m, H, H-11' and CH₂); 3.48-3.58 (m, 3H, H-11" and CH₂); 4.46 (d, 1H, *J* = 12.0 Hz, H-11a); 6.48 (s, 1H, H-5); 7.16-7.32 (m, 4H, aryl); 7.40 (t, 1H, *J* = 8.0 Hz, aryl); 7.47 (t, 1H, *J* = 8.0 Hz, aryl); 7.57 (d, 1H, *J* = 8.0 Hz, aryl); 7.92 (d, 1H, *J* = 8.0 Hz, aryl); 8.51 (s, 1H, NH). ¹³C NMR (100 MHz, CDCl₃) δ 22.6, 29.9, 36.0; 37.3, 50.4, 58.3, 107.6, 111.6, 118.7, 120.5, 126.3, 128.7, 129.0, 130.5,

134.1, 134.7, 135.3, 137.1, 155.8, 173.5. HR-MS m/z calcd for $C_{22}H_{22}N_5O_4$ [(M + H)]⁺: 420,1666; found 420,1684.

(1R,3S)-2-(3-aminopropyl)-5(2-nitrophenyl)-5,6,11,11a-tetrahydro-1H-imidazo[1',5':1,6]pyrido[3,4-b]indole-1,3(2H)-dione (30b).

Overall yield 31%. ¹H NMR (400 MHz, CDCl₃) δ: 1.73 (t, 2H, J = 8.0 Hz, CH₂); 2.66-2.69 (m, 3H, H-11' and CH₂); 2.90 (t, 1H, J = 12.0 Hz, H-11''); 3.57-3.64 (m, 2H, CH₂); 4.56 (dd, 1H, J' = 5.4, J'' = 11.2 Hz, H-11a); 6.81 (s, 1H, H-5); 7.15-7.35 (m, 5H, aryl); 7.49 (t, 1H, J = 8.0 Hz, aryl); 7.55 (t, 1H, J = 8.0 Hz, aryl); 7.93 (d, 1H, J = 8.0 Hz, aryl); 8.42 (s, 1H, NH). ¹³C NMR (100 MHz, CDCl₃) δ 23.3, 31.5, 36.4, 38.9, 47.5, 55.2, 107.4, 111.6, 118.7, 120.5, 123.4, 124.9, 126.1, 129.4, 129.6, 130.0, 133.9, 134.0, 135.1, 136.9, 155.6, 172.9. HR-MS m/z calcd for $C_{22}H_{22}N_5O_4$ [(M + H)]⁺: 420,1666; found 420,2851.

2-(naphthalen-1-yl)-5(2-nitrophenyl)-5,6,11,11a-tetrahydro-1H-imidazo[1',5':1,6]pyrido[3,4-b]indole-1,3(2H)-dione (31).

Overall yield 31%. ¹H NMR (400 MHz, CDCl₃) δ: 3.37 (t, 1H, J = 11.6 Hz, H-11'); 3.76 (t, 1H, J = 14.8 Hz, H-11''); 4.73 (dd, 1H, J' = 4.4, J'' = 11.6 Hz, H-11a); 6.64 (s, 1H, H-5); 7.19-7.26 (m, 4H, aryl); 7.32-7.45 (m, 4H, aryl); 7.65 (d, 2H, J = 8.0 Hz, aryl); 7.86-7.92 (m, 5H, aryl); 8.58 (s, 1H, NH). ¹³C NMR (100 MHz, CDCl₃) δ 23.4, 50.8, 58.6, 104.3, 111.7, 118.8, 120.6, 122.3, 123.5, 124.7, 125.4, 126.7, 127.1, 127.5, 128.7, 129.1, 130.3, 133.9, 134.2, 134.8, 136.4, 142.3, 150.2, 153.7, 171.5. HR-MS m/z calcd for $C_{29}H_{21}N_4O_4$ [(M + H)]⁺: 489,1557; found 489,1563.

General procedure for the synthesis of derivatives 35a/b.

To a solution of N α -Boc-L-Tryptophan (**32**), dissolved in DCM/DMF (ratio 9:1), 1.2 eq of HOBt, 1.2 eq of HBTU and 2.4 eq of Dipea at room temperature were added. After 30 min 1.2 eq of 4-fluorobenzylamine were added and the reaction was mixed at room temperature over night. Then the crude was washed with water (3 x 20 mL), 10% aqueous solution of citric acid (3 X 20 mL) and saturated aqueous solution of sodium bicarbonate (3 x 20 mL). The combined organic layer

was dried over anhydrous sodium sulfate, filtered, concentrated and purified by flash chromatography in 30:20 n-hexane/ethyl acetate. The removal of the protecting group, using a solution of DCM/TFA in ratio 3:1 (9:3 mL), led to intermediate **34** after treatment with saturated aqueous solution of sodium bicarbonate (3 x 20 mL). Final compounds **35a/b** were obtained performing a Pictet-Spengler reaction. To a solution of derivative **34** dissolved in methanol and 1.5 eq of TFA, p-Cl benzaldehyde (1.5 eq) was added. The reaction mixture was heated to 110 °C for 30 min in a microwave reactor. Then the solution was washed with water (3 x 20 mL). The combined organic layer was dried over anhydrous sodium sulfate, filtered, concentrated and purified by flash chromatography using ethyl acetate as mobile phase to separate the diastereoisomeric mixture.

(1S,3S)1-(4-chlorophenyl)-N-(4-fluorobenzyl)-2,3,4,9-tetrahydro-1H-pyrido[3,4-b]indole-3-carboxamide (35a).

Overall yield 66%. ¹H NMR (400 MHz, CDCl₃) δ 2.88 (t, 1H, *J* = 11.6 Hz, H-11'); 3.43 (dd, 1H, *J*' = 4.0, *J*' = 16.2 Hz, H-11''); 3.81 (dd, 1H, *J*' = 3.6, *J*' = 11.4 Hz, H-11a); 4.41 (dd, 1H, *J*' = 4.0, *J*' = 12.0 Hz, CH_{2a}); 4.48 (dd, 1H, *J*' = 4.0, *J*' = 12.0 Hz, CH_{2b}); 5.20 (s, 1H, H-5); 7.01 (t, 2H, *J* = 8.0 Hz, aryl); 7.13-7.22 (m, 7H, aryl); 7.35 (d, 2H, *J* = 8.0 Hz, aryl); 7.57 (d, 1H, *J* = 7.8 Hz, aryl). ¹³C NMR (100 MHz, CDCl₃) δ 24.8, 42.7; 52.6, 54.0, 110.9, 111.1, 115.8, 118.8, 120.0, 122.7, 127.2, 129.0, 129.7, 130.1, 132.6, 134.2, 136.4, 139.8, 163.9, 172.8. HR-MS *m/z* calcd for C₂₅H₂₂ClFN₃O [(M + H)]⁺: 434,1430; found 434,1472.

(1R,3S)1-(4-chlorophenyl)-N-(4-fluorobenzyl)-2,3,4,9-tetrahydro-1H-pyrido[3,4-b]indole-3-carboxamide (35b).

Overall yield 54%. ¹H NMR (400 MHz, CDCl₃) δ 2.93 (dd, 1H, *J*' = 10.0, *J*'' = 16.0 Hz, H-11'); 3.34 (dd, 1H, *J*' = 4.8, *J*'' = 16.0 Hz, H-11''); 3.61 (dd, 1H, *J*' = 5.2, *J*'' = 10.0 Hz, H-11a); 4.41 (dd, 1H, *J*' = 5.6, *J*' = 15.0 Hz, CH_{2a}); 4.48 (dd, 1H, *J*' = 5.6, *J*' = 15.0 Hz, CH_{2b}); 5.21 (s, 1H, H-5); 7.00 (t, 2H, *J* = 8.0 Hz, aryl); 7.12-7.28 (m, 9H, aryl); 7.58 (d, 1H, *J* = 8.0 Hz, aryl); 7.79 (s, 1H, NH). ¹³C NMR (100 MHz, CDCl₃) δ 25.7, 42.7; 52.6, 55.0, 110.9, 111.1, 115.5, 115.8, 118.7,

120.1, 122.6, 127.3, 128.8, 129.9, 129.5, 129.6, 129.8, 130.1, 132.6, 134.3, 136.5, 139.8, 164.1, 172.9. HR-MS m/z calcd for $C_{25}H_{22}ClFN_3O [(M + H)]^+$: 434,1430; found 434,1442.

General procedure for the synthesis derivatives 41, 42a/b.

Intermediates **37** and **38a/b** were obtained adding *p*-chlorobenzaldehyde or formaldehyde (1.5 eq) to a solution of L-Dopa methyl ester (1 eq) dissolved in methanol and TFA (1.5eq) and heating the reaction mixture to 110 °C for 30 min in a microwave reactor. Then the solution was concentrated in vacuo, diluted with DCM (10 mL) and washed with water (3 x 20 mL). The combined organic layer was dried over anhydrous sodium sulfate, filtered, concentrated and purified by flash chromatography in n-hexane/ethyl acetate 50:50 to separate the diastereoisomeric mixture of **38a/b** (yield 82%), while compound **37** was obtained without further purification steps. To a solution of obtained tetrahydroisoquinolines dissolved in DCM, 0.4 eq of triphosgene, 1.2 eq of TEA and 1.2 eq of 4-fluorobenzylamine were added. The reaction was mixed at room temperature for 20 minutes. Then the combined organic layer was washed with water (3 x 20 mL), dried over anhydrous sodium sulfate, filtered, concentrated and purified by flash chromatography in 50:50 n-hexane/ethyl acetate. Intermediates **39**, **40a/b** were refluxed in MeOH/TEA for 10 minutes. The solvent was removed in vacuo and the crude was diluted with DCM, washed with water, dried over anhydrous sodium sulfate, filtered, concentrated and purified by flash chromatography in 75:25 n-hexane/ethyl acetate to obtain derivatives **42a/b**. The purification of compound **41** was allowed using ethyl acetate as mobile phase.

2-(4-fluorobenzyl)-7,8-dihydroxy-10,10a-dihydroimidazo[1,5-b]isoquinoline-1,3(2H,5H)-dione (41).

Overall yield 52%. 1H NMR (400 MHz, $CDCl_3$) δ 2.70 (t, 1H, $J = 11.6$ Hz, H-10'); 3.13 (dd, 1H, $J' = 2.8$, $J'' = 14.0$ Hz, H-10''); 4.06 (dd, 1H, $J' = 4.4$, $J'' = 10.8$ Hz, H-10a); 4.27 (d, 1H, $J = 16.0$ Hz, CH_{2a}); 4.71 (s, 2H, H-5); 4.82 (d, 1H, $J = 16.0$ Hz, CH_{2b}); 6.71 (s, 1H, aryl); 6.73 (s, 1H, aryl); 7.01-7.07 (m, 2H, aryl); 7.44-7.50 (m, 2H, aryl). ^{13}C NMR (100 MHz, $CDCl_3$) δ 28.5, 40.3; 47.8, 55.9, 113.1, 116.2, 118.6, 126.9, 127.4, 129.4, 130.7, 133.5, 140.8, 142.4, 145.7, 155.1,

173.7. HR-MS m/z calcd for $C_{18}H_{16}FN_2O_4$ $[(M + H)]^+$: 343,1089; found 343,1105.

(1S,3S)5-(4-chlorophenyl)-2-(4-fluorobenzyl)-7,8-dihydroxy-10,10a-dihydroimidazo[1,5b] isoquinoline-1,3 (2H,5H)-dione (42a).

Overall yield 50%. 1H NMR (400 MHz, $CDCl_3$) δ 2.72 (t, 1H, $J = 10.8$ Hz, H-10'); 3.11 (dd, 1H, $J' = 4.0$, $J'' = 12.2$ Hz, H-10''); 4.10 (dd, 1H, $J' = 5.2$, $J'' = 11.6$ Hz, H-10a); 4.53, (d, 1H, $J = 16.0$ Hz, CH_{2a}); 4.61 (d, 1H, $J=16.0$ Hz, CH_{2b}); 6.00 (s, 1H, H-5); 6.39 (s, 1H, aryl); 6.67 (s, 1H, aryl); 6.93-6.99 (m, 2H, aryl); 7.13 (d, 2H, $J = 8.0$ Hz, aryl); 7.24 (d, 2H, $J = 8.0$ Hz, aryl); 7.31-7.36 (m, 2H, aryl). ^{13}C NMR (100 MHz, $CDCl_3$) δ 29.6, 41.5; 52.9, 55.0, 115.8, 116.0, 116.7, 117.4, 123.7, 125.4, 129.2, 130.1, 131.2, 131.7, 134.8, 140.2, 143.4, 144.0, 154.8, 172.9. HR-MS m/z calcd for $C_{24}H_{19}ClFN_2O_4$ $[(M + H)]^+$: 453,1012; found 453,1016.

(1R,3S)5-(4-chlorophenyl)-2-(4-fluorobenzyl)-7,8-dihydroxy-10,10a-dihydroimidazo[1,5b] isoquinoline-1,3 (2H,5H)-dione (42b).

Overall yield 35%. 1H NMR (400 MHz, $CDCl_3$) δ 2.74 (t, 1H, $J = 10.8$ Hz, H-10'); 3.12 (dd, 1H, $J' = 4.4$, $J'' = 11.4$ Hz, H-10''); 4.11 (dd, 1H, $J' = 5.2$, $J'' = 11.6$ Hz, H-10a); 4.54, (d, 1H, $J = 14.4$ Hz, CH_{2a}); 4.62 (d, 1H, $J=14.4$ Hz, CH_{2b}); 6.02 (s, 1H, H-5); 6.39 (s, 1H, aryl); 6.69 (s, 1H, aryl); 6.94-7.00 (m, 2H, aryl); 7.16 (d, 2H, $J = 8.0$ Hz, aryl); 7.26 (d, 2H, $J = 8.0$ Hz, aryl); 7.30-7.37 (m, 2H, aryl). ^{13}C NMR (100 MHz, $CDCl_3$) δ 30.1, 41.9, 52.7, 54.3, 115.0, 115.4, 115.7, 115.9, 123.9, 125.5, 129.2, 129.9, 130.8, 131.9, 134.3, 140.4, 143.3, 143.9, 154.8, 172.7. HR-MS m/z calcd for $C_{24}H_{19}ClFN_2O_4$ $[(M + H)]^+$: 453,1012; found 453,1097.

General procedure for the synthesis of derivatives 43a/b-46.

To a solution of $N\alpha$ -Boc-L-Tryptophan (**32**), dissolved in DCM/DMF (ratio 9:1), 1.2 eq of HOBt, 1.2 eq of HBTU and 2.4 eq of Dipea at room temperature were added. After 30 min 1.2 eq of 4-fluorobenzylamine were added and the reaction was mixed at room temperature over night. Than the crude was washed with water

(3 x 20 mL), 10% aqueous solution of citric acid (3 X 20 mL) and saturated aqueous solution of sodium bicarbonate (3 x 20 mL). The combined organic layer was dried over anhydrous sodium sulfate, filtered, concentrated and purified by flash chromatography in 30:20 n-hexane/ethyl acetate. The removal of the protecting group, using a solution of DCM/TFA in ratio 3:1 (9:3 mL), led to intermediate **34** after treatment with saturated aqueous solution of sodium bicarbonate (3 x 20 mL). Final compounds **43-45a/b** and **46** were obtained performing a Pictet-Spengler reaction. To a solution of derivative **34** dissolved in methanol and 1.5 eq of TFA, formaldehyde, isovaleraldehyde, methyl 5-oxopentanoate or 5-oxopentanoic acid (1.5 eq) was added. The reaction mixture was heated to 110 °C for 30 min in a microwave reactor. Then the solution was washed with water (3 x 20 mL). The combined organic layer was dried over anhydrous sodium sulfate, filtered, concentrated and purified by flash chromatography using ethyl acetate as mobile phase to separate the diastereomeric mixture.

(1S,3S)-N-(4-fluorobenzyl)-1-isobutyl-2,3,4,9-tetrahydro-1H-pyrido[3,4-b]indole-3-carboxamide (43a).

Overall yield 61%. ¹H NMR (400 MHz, CDCl₃) δ: 0.92 (d, 3H, *J* = 8.0, CH₃); 0.96 (d, 3H, *J* = 8.0, CH₃); 1.41-1.48 (m, 1H, CH_{2a}); 1.61-1.67 (m, 1H, CH_{2b}); 1.91-1.99 (m, 1H, CH); 2.66 (dd, 1H, *J'*=4.2, *J''*= 12.6 Hz, H-4'); 3.29 (dd, 1H, *J'* = 4.2, *J''*= 15.6 Hz, H-4''); 3.52 (dd, 1H, *J'*=4.0, *J''*=8.4 Hz, H-3); 4.08 (dd, 1H, *J'* = 4.4, *J''*= 12.2 Hz, H-1); 4.42 (d, 2H, *J'* = 4.2, Hz, CH₂); 6.97 (t, 2H, *J* = 8.0 Hz, aryl); 7.01-7.10 (m, 2H, aryl); 7.21-7.26 (m, 2H, aryl); 7.38 (t, 1H, *J* = 8.0 Hz, aryl); 7.43 (d, 1H, *J* = 8.0 Hz, aryl); 7.75 (s, 1H, NH). ¹³C NMR (100 MHz, CDCl₃) δ 21.9, 23.8, 25.5, 30.9, 42.4, 44.2, 51.9, 57.9, 109.0, 110.8, 115.4, 115.6, 118.2, 119.7, 121.9, 127.4, 129.4, 134.3, 135.9, 136.5, 163.4, 172.9. HR-MS *m/z* calcd for C₂₃H₂₇FN₃O [(M + H)]⁺: 380.2133; found 380.2142.

(1R,3S)-N-(4-fluorobenzyl)-1-isobutyl-2,3,4,9-tetrahydro-1H-pyrido[3,4-b]indole-3-carboxamide (43b).

Overall yield 49%. ¹H NMR (400 MHz, CDCl₃) δ: 0.90 (d, 3H, *J* = 8.0, CH₃); 0.93 (d, 3H, *J* = 8.0, CH₃); 1.40-1.48 (m, 1H, CH_{2a}); 1.59-1.69 (m, 1H, CH_{2b});

1.83-1.91 (m, 1H, CH); 2.77 (dd, 1H, J' =11.6, J'' = 16.0 Hz, H-4'); 3.21 (dd, 1H, $J' = 4.4$, $J'' = 15.6$ Hz, H-4''); 3.71 (dd, 1H, $J' = 4.0$, $J'' = 8.4$ Hz, H-3); 4.05 (dd, 1H, $J' = 4.4$, $J'' = 12.2$ Hz, H-1); 4.36 (dd, 1H, $J' = 7.8$, $J'' = 15.6$ Hz, CH_{2a}); 4.43 (dd, 1H, $J' = 7.8$, $J'' = 15.6$ Hz, CH_{2a}); 6.95 (t, 2H, $J = 8.0$ Hz, aryl); 7.02-7.11 (m, 2H, aryl); 7.08-7.24 (m, 2H, aryl); 7.39 (t, 1H, $J = 8.0$ Hz, aryl); 7.45 (d, 1H, $J = 8.0$ Hz, aryl); 7.62 (s, 1H, NH). ¹³C NMR (100 MHz, CDCl₃) δ 22.0, 23.5, 24.6, 25.1, 42.5, 43.8, 49.5, 52.7, 108.3, 110.6, 115.4, 115.6, 118.3, 119.6, 121.2, 129.4, 135.9, 136.4, 172.9. HR-MS m/z calcd for C₂₃H₂₇FN₃O [(M + H)]⁺: 380.2133; found 380.2139.

methyl 3-((1R,3S)-3-((4-fluorobenzyl)carbamoyl)-2,3,4,9-tetrahydro-1H-pyrido[3,4-b]indol-1-yl)propanoate (44a).

Overall yield 55%. ¹H NMR (400 MHz, CDCl₃) δ: 1.98-2.14 (m, 2H, CH₂); 2.49-2.69 (m, 2H, CH₂); 2.80 (dd, 1H, $J' = 15.6$, $J'' = 19.8$ Hz, H-4'); 3.30 (dd, 1H, $J' = 4.6$, $J'' = 19.4$ Hz, H-4''); 3.67 (s, 3H, CH₃); 3.73 (dd, 1H, $J' = 8.0$, $J'' = 16.0$ Hz, H-3); 4.06 (dd, 1H, $J' = 4.4$, $J'' = 12.2$ Hz, H-1); 4.45 (dd, 1H, $J' = 7.8$, $J'' = 18.8$ Hz, CH_{2a}); 4.54 (dd, 1H, $J' = 7.8$, $J'' = 18.8$ Hz, CH_{2a}); 7.05 (t, 2H, $J = 8.0$ Hz, aryl); 7.10-7.18 (m, 2H, aryl); 7.21-7.39 (m, 3H, aryl); 7.53 (d, 1H, $J = 8.0$ Hz, aryl); 8.21 (s, 1H, NH). ¹³C NMR (100 MHz, CDCl₃) δ 24.7, 29.6, 31.3, 43.0, 51.3, 51.8, 52.6, 108.7, 110.8, 115.4, 118.4, 119.6, 122.1, 127.1, 129.5, 135.2, 136.0, 163.4, 172.7, 174.4. HR-MS m/z calcd for C₂₃H₂₅FN₃O₃ [(M + H)]⁺: 410.1874; found 410.1888.

methyl 3-((1S,3S)-3-((4-fluorobenzyl)carbamoyl)-2,3,4,9-tetrahydro-1H-pyrido[3,4-b]indol-1-yl)propanoate (44b).

Overall yield 48%. ¹H NMR (400 MHz, CDCl₃) δ: 1.80-1.90 (m, 1H, CH₂); 2.23-2.31 (m, 1H, CH₂); 2.29-2.54 (m, 2H, CH₂); 2.64-2.72 (m, 1H, H-4'); 3.25 (dd, 1H, $J' = 4.8$, $J'' = 12.0$ Hz, H-4''); 3.53-3.58 (m, 4H, CH₃ and H-3); 4.12 (dd, 1H, $J' = 4.2$, $J'' = 8.6$ Hz, H-1); 4.41 (d, 2H, $J = 7.8$ Hz, CH₂); 6.97 (t, 2H, $J = 8.0$ Hz, aryl); 7.04 (t, 1H, $J = 8.0$ Hz, aryl); 7.10 (t, 1H, $J = 8.0$ Hz, aryl); 7.21-7.27 (m, 3H, aryl); 7.43 (d, 1H, $J = 8.0$ Hz, aryl); 8.00 (s, 1H, NH). ¹³C NMR (100 MHz, CDCl₃) δ 25.4, 29.2, 30.3, 42.5, 51.8, 53.5, 57.8, 109.5, 111.0, 115.5, 115.7,

118.4, 119.8, 122.2, 127.2, 129.5, 129.6, 134.2, 136.1, 161.0, 163.4, 172.5, 174.2.
HR-MS m/z calcd for C₂₃H₂₅FN₃O₃ [(M + H)]⁺: 410.1874; found 410.1879.

3-((1R,3S)-3-((4-fluorobenzyl)carbamoyl)-2,3,4,9-tetrahydro-1H-pyrido[3,4-b]indol-1-yl)propanoic acid (45a).

Overall yield 42%. ¹H NMR (400 MHz, CD₃OD) δ: 2.03-2.06 (m, 1H, CH₂); 2.12-2.15 (m, 1H, CH₂); 2.47 (t, 2H, J = 8.0 Hz, CH₂); 2.90 (dd, 1H, J' = 8.6, J'' = 12.4 Hz, H-4'); 3.10 (dd, 1H, J' = 4.4, J'' = 11.6 Hz, H-4''); 3.90 (dd, 1H, J' = 4.0, J'' = 8.0 Hz, H-3); 4.20 (dd, 1H, J' = 4.4, J'' = 8.2 Hz, H-1); 4.45 (s, 2H, CH_{2a}); 6.96-7.09 (m, 4H, aryl); 7.29-7.35 (m, 3H, aryl); 7.42 (d, 1H, J = 8.0 Hz, aryl). ¹³C NMR (100 MHz, CD₃OD) δ: 24.4, 31.0, 34.8, 41.8, 51.2, 52.5, 106.1, 110.4, 114.6, 114.8, 117.1, 118.2, 120.7, 126.9, 128.9, 129.0, 134.7, 135.6, 136.5, 163.2, 174.1. HR-MS m/z calcd for C₂₂H₂₃FN₃O₃ [(M + H)]⁺: 396.1718; found 396.1725.

3-((1S,3S)-3-((4-fluorobenzyl)carbamoyl)-2,3,4,9-tetrahydro-1H-pyrido[3,4-b]indol-1-yl)propanoic acid (45b).

Overall yield 33%. ¹H NMR (400 MHz, CD₃OD) δ: 1.92-2.02 (m, 1H, CH₂); 2.38-2.40 (m, 3H, CH₂); 2.74-2.77 (m, 1H, H-4'); 3.09 (dd, 1H, J' = 4.4, J'' = 11.6 Hz, H-4''); 3.61 (dd, 1H, J' = 4.0, J'' = 12.6 Hz, H-3); 4.18 (dd, 1H, J' = 4.2, J'' = 8.4 Hz, H-1); 4.47 (s, 2H, CH_{2a}); 6.98 (t, 1H, J = 8.0 Hz, aryl); 7.04-7.10 (m, 3H, aryl); 7.31 (d, 1H, J = 8.0 Hz, aryl); 7.38-7.45 (m, 3H, aryl). ¹³C NMR (100 MHz, CD₃OD) δ 25.6, 30.8, 33.7, 41.8, 53.0, 57.7, 107.1, 110.6, 114.6, 114.8, 117.0, 118.3, 120.6, 127.1, 129.1, 134.7, 135.7, 136.6, 160.8, 163.3, 174.6, 181.2. HR-MS m/z calcd for C₂₂H₂₃FN₃O₃ [(M + H)]⁺: 396.1718; found 396.1729.

(S)-N-(4-fluorobenzyl)-2,3,4,9-tetrahydro-1H-pyrido[3,4-b]indole-3-carboxamide (46).

Overall yield 55%. ¹H NMR (400 MHz, CDCl₃) δ 2.68 (dd, 1H, J' = 8.0, J'' = 16.0 Hz, H-4'); 2.90 (dd, 1H, J' = 4.6, J'' = 16.0 Hz, H-4''); 3.47-3.52 (m, 1H, H-3); 3.95 (s, 2H, H-1); 4.32 (d, 2H, J' = 4.2, Hz, CH₂); 6.94 (t, 1H, J = 8.0 Hz, aryl); 6.99 (t, 1H, J = 8.0 Hz, aryl); 7.14 (t, 2H, J = 8.0 Hz, aryl); 7.26-7.39 (m, 3H,

aryl); 8.46 (t, 1H, $J = 8.0$ Hz, aryl); 10.38 (s, 1H, NH). ^{13}C NMR (100 MHz, CDCl_3) δ 25.2, 41.7, 42.4, 57.0, 106.9, 111.6, 113.1, 115.3, 115.5, 117.7, 118.8, 120.8, 125.9, 129.8, 134.3, 135.0, 136.2, 173.2. HR-MS m/z calcd for $\text{C}_{19}\text{H}_{19}\text{FN}_3\text{O}$ $[(\text{M} + \text{H})]^+$: 324.1507; found 324.1516.

General procedure for the synthesis derivatives 52a/b-56.

p-fluorobenzaldehyde, isovaleraldehyde or formaldehyde (1.5 eq) was added to a solution of L-Trp-OMe (**23**) dissolved in methanol and TFA (1.5eq). The reaction mixture was heated to 110 °C for 30 min in a microwave reactor (Scheme 1). The combined organic layer was concentrated, diluted with dichloromethane and washed with water (3 x 20 mL). The combined organic layer was dried over anhydrous sodium sulfate, filtered, concentrated and purified by flash chromatography in n-hexane/ethyl acetate (3:2 ratio) to separate the diastereoisomeric mixture. To a solution of **47-50a/b** as singles diastereoisomers, and **51** dissolved in DCM, 0.4 eq of triphosgene, 1.2 eq of TEA and 1.2 eq of proper amine were added. The reaction was mixed at room temperature for 20 minutes. Then the solution was washed with water (3 x 20 mL). The combined organic layer was dried over anhydrous sodium sulfate, filtered, concentrated and purified by flash chromatography in 30:20 n-hexane/ethyl acetate. Final compounds **52-55a/b** and **56** were obtained by refluxing urea intermediates in MeOH/TEA for 10 minutes. The crude was concentrated in vacuo, washed with water (3 X 20 mL), dried over anhydrous sodium sulfate, filtered, concentrated and purified by flash chromatography in 80:20 n-hexane/ethyl acetate. For compound **56** n-hexane/ethyl acetate (70:30 ratio) was used as mobile phase. The final derivatives **52-55a/b** were obtained as two diastereoisomers.

(5S,11aS)-2-benzyl-5-(4-fluorophenyl)-5,6,11,11a-tetrahydro-1H-imidazo[1',5':1,6]pyrido[3,4-b]indole-1,3(2H)-dione (52a).

Overall yield 66%. $[\alpha]_{\text{D}}^{25}$: -124.615 ± 0.162 . ^1H NMR (400 MHz, CDCl_3) δ : 2.80 (dd, 1H, $J' = 15.4$, $J'' = 19.6$ Hz, H-11'); 3.45 (dd, 1H, $J' = 8.4$, $J'' = 19.8$ Hz, H-11''); 4.30 (dd, 1H, $J' = 8.0$, $J'' = 16.4$ Hz, H-11a); 4.63 (d, 1H, $J = 20.0$ Hz, CH_2); 4.75 (d, 1H, $J = 20.0$ Hz, CH_2); 6.30 (s, 1H, H-5); 7.06 (t, 2H, $J = 8.0$ Hz,

aryl); 7.17-7.35 (m, 8H, aryl); 7.41-7.44 (m, 2H, aryl); 7.54 (d, 1H, $J = 8.0$ Hz, aryl); 7.75 (s, 1NH). ^{13}C NMR (100 MHz, CDCl_3) δ 23.4, 42.4, 51.3, 53.2, 108.3, 111.2, 116.0, 118.5, 120.3, 123.1, 128.0, 128.7, 130.1, 134.9, 136.0, 136.6, 154.6, 161.7, 164.2, 172.3. HR-MS m/z calcd for $\text{C}_{26}\text{H}_{20}\text{FN}_3\text{O}_2$ $[(\text{M} + \text{H})]^+$: 425.1540; found 425.1549.

(5R,11aS)-2-benzyl-5-(4-fluorophenyl)-5,6,11,11a-tetrahydro-1H-imidazo[1',5':1,6]pyrido[3,4-b]indole-1,3(2H)-dione (52b).

Overall yield 52%. $[\alpha]_{\text{D}}^{25}$: -53.529 ± 0.182 ($c = 0.10$, MeOH). ^1H NMR (400 MHz, CDCl_3) δ 2.87 (dd, 1H, $J' = 15.4$, $J'' = 19.6$ Hz, H-11'); 3.65 (dd, 1H, $J' = 8.4$, $J'' = 19.8$ Hz, H-11''); 4.42 (dd, 1H, $J' = 8.0$, $J'' = 16.4$ Hz, H-11a); 4.73 (d, 1H, $J = 20.0$ Hz, CH_2); 4.75 (d, 1H, $J = 20.0$ Hz, CH_2); 6.30 (s, 1H, H-5); 7.16 (t, 2H, $J = 8.0$ Hz, aryl); 7.17-7.45 (m, 8H, aryl); 7.41-7.48 (m, 2H, aryl); 7.54 (d, 1H, $J = 8.0$ Hz, aryl); 7.77 (s, 1NH). ^{13}C NMR (100 MHz, CDCl_3) δ 23.4, 42.4, 51.3, 53.2, 108.3, 111.2, 116.0, 118.5, 120.3, 123.1, 128.0, 128.7, 130.1, 134.9, 136.0, 136.6, 154.6, 161.7, 164.2, 172.3. HR-MS m/z calcd for $\text{C}_{26}\text{H}_{20}\text{FN}_3\text{O}_2$ $[(\text{M} + \text{H})]^+$: 425.1540; found 425.1552.

(5S,11aS)-5-isobutyl-2-(4-methoxybenzyl)-5,6,11,11a-tetrahydro-1H-imidazo[1',5':1,6]pyrido[3,4-b]indole-1,3(2H)-dione (53a).

Overall yield 63%. $[\alpha]_{\text{D}}^{25}$: -98.563 ± 0.158 ($c = 0.10$, MeOH). ^1H NMR (400 MHz, CDCl_3) δ 0.98 (d, 3H, $J = 8.8$ Hz, CH_3); 1.17 (d, 3H, $J = 8.8$ Hz, CH_3); 1.64-1.74 (m, 2H, CH_2); 1.78-1.86 (m, 1H, CH); 2.75 (dd, 1H, $J' = 8.2$, $J'' = 11.4$ Hz, H-11'); 3.36 (dd, 1H, $J' = 4.8$, $J'' = 12.6$ Hz, H-11''); 3.79 (s, 3H, CH_3); 4.31 (dd, 1H, $J' = 4.0$, $J'' = 8.0$ Hz, H-11a); 4.63 (d, 1H, $J = 16.0$ Hz, CH_2); 4.75 (d, 1H, $J = 16.0$ Hz, CH_2); 5.30-5.34 (m, 1H, H-5); 6.86 (d, 2H, $J = 8.0$ Hz, aryl); 7.15 (t, 1H, $J = 8.0$ Hz, aryl); 7.22 (t, 1H, $J = 8.0$ Hz, aryl); 7.28-7.39 (m, 3H, aryl); 7.47 (d, 1H, $J = 8.0$ Hz, aryl); 7.88 (s, 1NH). ^{13}C NMR (100 MHz, CDCl_3) δ 22.2, 23.5, 23.6, 25.0, 41.8, 45.8, 46.9, 52.9, 55.2, 105.7, 111.0, 114.1, 118.2, 120.1, 122.6, 126.3, 128.5, 130.0, 133.1, 136.2, 155.3, 159.3, 172.9. HR-MS m/z calcd for $\text{C}_{25}\text{H}_{28}\text{N}_3\text{O}_3$ $[(\text{M} + \text{H})]^+$: 418.2125; found 418.2132.

(5R,11aS)-5-isobutyl-2-(4-methoxybenzyl)-5,6,11,11a-tetrahydro-1H-imidazo[1',5':1,6]pyrido[3,4-b]indole-1,3(2H)-dione (53b).

Overall yield 52%. $[\alpha]_D^{25}$: -42.360 ± 0.179 ($c = 0.10$, MeOH). ^1H NMR (400 MHz, CDCl_3) δ 1.08 (d, 3H, $J = 8.8$ Hz, CH_3); 1.23 (d, 3H, $J = 8.8$ Hz, CH_3); 1.65-1.78 (m, 2H, CH_2); 1.81-1.88 (m, 1H, CH); 2.77 (dd, 1H, $J' = 8.2$, $J'' = 11.4$ Hz, H-11'); 3.38 (dd, 1H, $J' = 4.8$, $J'' = 12.6$ Hz, H-11''); 3.81 (s, 3H, CH_3); 4.33 (dd, 1H, $J' = 4.0$, $J'' = 8.0$ Hz, H-11a); 4.74 (d, 1H, $J = 16.0$ Hz, CH_2); 4.77 (d, 1H, $J = 16.0$ Hz, CH_2); 5.36-5.44 (m, 1H, H-5); 6.86 (d, 2H, $J = 8.0$ Hz, aryl); 7.15 (t, 1H, $J = 8.0$ Hz, aryl); 7.22 (t, 1H, $J = 8.0$ Hz, aryl); 7.32-7.39 (m, 3H, aryl); 7.47 (d, 1H, $J = 8.0$ Hz, aryl); 7.92 (s, 1NH). ^{13}C NMR (100 MHz, CDCl_3) δ 22.2, 23.5, 23.6, 25.0, 41.8, 45.8, 46.9, 52.9, 55.2, 105.7, 111.0, 114.1, 118.2, 120.1, 122.6, 126.3, 128.5, 130.0, 133.1, 136.2, 155.3, 159.3, 172.9. HR-MS m/z calcd for $\text{C}_{25}\text{H}_{28}\text{N}_3\text{O}_3$ $[(M + H)]^+$: 418.2125; found 418.2139.

(5S,11aS)-5-(4-chlorophenyl)-2-(3-(trifluoromethyl)phenyl)-5,6,11,11a-tetrahydro-1H-imidazo[1',5':1,6]pyrido[3,4-b]indole-1,3(2H)-dione (54a).

Overall yield 37% $[\alpha]_D^{25}$: -1.000 ± 0.001 ($c = 0.10$, MeOH). ^1H NMR (400 MHz, CDCl_3) δ 3.12 (dd, 1H, $J' = 8.4$, $J'' = 12.0$ Hz, H-11'); 3.58 (dd, 1H, $J' = 4.6$, $J'' = 12.2$ Hz, H-11''); 4.52 (dd, 1H, $J' = 4.4$, $J'' = 10.2$ Hz, H-11a); 5.85 (s, 1H, H-5); 6.97 (t, 2H, $J = 8.0$ Hz, aryl); 7.10-7.21 (m, 4H, aryl); 7.24-7.30 (m, 2H, aryl); 7.45-7.59 (m, 3H, aryl); 7.68 (s, 1H, aryl). ^{13}C NMR (100 MHz, CDCl_3) δ 22.7, 56.4, 57.9, 107.2, 110.0, 111.3, 116.0, 116.2, 118.6, 120.5, 122.8, 123.2, 124.7, 126.1, 129.1, 129.5, 129.8, 132.0, 132.8, 133.9, 136.8, 153.2, 161.6, 164.0, 169.9. HR-MS m/z calcd for $\text{C}_{26}\text{H}_{18}\text{ClF}_3\text{N}_3\text{O}_2$ $[(M + H)]^+$: 496.1034; found 496.1042.

(5R,11aS)-5-(4-chlorophenyl)-2-(3-(trifluoromethyl)phenyl)-5,6,11,11a-tetrahydro-1H-imidazo[1',5':1,6]pyrido[3,4-b]indole-1,3(2H)-dione (54b).

Overall yield 25% $[\alpha]_D^{25}$: -166.0 ± 0.1 ($c = 0.10$, MeOH). ^1H NMR (400 MHz, CDCl_3) δ 3.00 (dd, 1H, $J' = 12.2$, $J'' = 16.0$ Hz, H-11'); 3.54 (dd, 1H, $J' = 4.2$, $J'' = 12.2$ Hz, H-11''); 4.41 (dd, 1H, $J' = 8.6$, $J'' = 12.4$ Hz, H-11a); 6.32 (s, 1H, H-5); 7.12-7.30 (m, 7H, aryl); 7.49-7.60 (m, 3H, $J = 8.0$ Hz, aryl); 7.62 (d, 1H, $J = 8.0$ Hz, aryl); 7.69 (s, 1H, aryl); 7.71 (s, 1NH). ^{13}C NMR (100 MHz, CDCl_3) δ 23.6,

51.7, 53.1, 108.4, 111.3, 118.6, 120.5, 122.8, 123.3, 124.8, 126.0, 129.0, 129.5, 129.8, 132.1, 135.3, 136.7, 137.0, 153.2, 170.9. HR-MS m/z calcd for $C_{26}H_{18}ClF_3N_3O_2 [(M + H)]^+$: 496.1034; found 496.1048.

(5S,11aS)-2-(3-aminopropyl)-5-(4-fluorophenyl)-5,6,11,11a-tetrahydro-1H-imidazo[1',5':1,6]pyrido[3,4-b]indole-1,3(2H)-dione (55a).

Overall yield 52%. $[\alpha]_D^{25}$: -107.83 ± 0.21 ($c = 0.10$, MeOH). 1H NMR (400 MHz, CD_3OD) δ 1.71-1.80 (m, 2H, CH_2); 2.61 (t, 2H, $J = 8.0$ Hz, CH_2) 2.80 (dd, 1H, $J' = 12.0$, $J'' = 16.0$ Hz, H-11'); 3.43 (dd, 1H, $J' = 8.2$, $J'' = 20.2$ Hz, H-11''); t, 2H, $J = 8.0$ Hz, CH_2) 4.46 (dd, 1H, $J' = 8.4$, $J'' = 16.2$ Hz, H-11a); 6.30 (s, 1H, H-5); 7.03-7.15 (m, 4H, aryl); 7.26 (d, 1H, $J = 8.0$ Hz, aryl); 7.29-7.39 (m, 2H, aryl); 7.52 (d, 1H, $J = 8.0$ Hz, aryl). ^{13}C NMR (100 MHz, CD_3OD) δ 22.6, 30.7, 35.5, 38.0, 51.4, 53.2, 106.6, 110.9, 115.3, 117.7, 119.0, 121.8, 126.0, 129.8, 129.9, 130.3, 135.9, 137.2, 155.1, 161.5, 163.9, 173.6. HR-MS m/z calcd for $C_{22}H_{22}FN_4O_2 [(M + H)]^+$: 393.1721; found 393.1729.

(5R,11aS)-2-(3-aminopropyl)-5-(4-fluorophenyl)-5,6,11,11a-tetrahydro-1H-imidazo[1',5':1,6]pyrido[3,4-b]indole-1,3(2H)-dione (55b).

Overall yield 44%. $[\alpha]_D^{25}$: -37.500 ± 0.075 ($c = 0.10$, MeOH). 1H NMR (400 MHz, CD_3OD) δ 1.73-1.82 (m, 2H, CH_2); 2.66 (t, 2H, $J = 8.0$ Hz, CH_2) 2.82 (dd, 1H, $J' = 12.0$, $J'' = 16.0$ Hz, H-11'); 3.45 (dd, 1H, $J' = 8.2$, $J'' = 20.2$ Hz, H-11''); t, 2H, $J = 8.0$ Hz, CH_2) 4.47 (dd, 1H, $J' = 8.4$, $J'' = 16.2$ Hz, H-11a); 6.33 (s, 1H, H-5); 7.06-7.17 (m, 4H, aryl); 7.26 (d, 1H, $J = 8.0$ Hz, aryl); 7.29-7.39 (m, 2H, aryl); 7.53 (d, 1H, $J = 8.0$ Hz, aryl). ^{13}C NMR (100 MHz, CD_3OD) δ 22.6, 30.7, 35.5, 38.0, 51.4, 53.2, 106.6, 110.9, 115.3, 117.7, 119.0, 121.8, 126.0, 129.8, 129.9, 130.3, 135.9, 137.2, 155.1, 161.5, 163.9, 173.6. HR-MS m/z calcd for $C_{22}H_{22}FN_4O_2 [(M + H)]^+$: 393.1721; found 393.1733.

(S)-2-(4-fluorobenzyl)-5,6,11,11a-tetrahydro-1H-imidazo[1',5':1,6]pyrido[3,4-b]indole-1,3(2H)-dione (56).

Overall yield 55%. ¹H NMR (400 MHz, CDCl₃) δ 2.80 (dd, 1H, *J*' = 12.0, *J*'' = 16.0 Hz, H-11'); 3.40 (dd, 1H, *J*'=8.2, *J*''=16.4 Hz, H-11''); 4.25 (dd, 1H, *J*' =8.2, *J*'' = 12.4 Hz, H-11a); 4.39 (d, 1H, *J* = 12.0, Hz, H-5'); 4.73 (s, 2H, CH₂); 5.10 (d, 1H, *J* = 12.0, Hz, H-5''); 7.02 (t, 2H, *J* = 8.0 Hz, aryl); 7.16 (t, 1H, *J* = 8.0 Hz, aryl); 7.21 (t, 1H, *J* = 8.0 Hz, aryl); 7.34 (d, 1H, *J* = 8.0 Hz, aryl); 7.43-7.46 (m, 2H, aryl); 7.50 (d, 1H, *J* = 8.0 Hz, aryl); 8.15 (s, 1H, NH). ¹³C NMR (100 MHz, CDCl₃) δ 23.1, 37.8, 41.7, 55.3, 106.2, 111.0, 115.5, 115.7, 120.1, 122.6, 130.5, 136.5, 155.1, 161.3, 163.7, 172.5. HR-MS *m/z* calcd for C₂₀H₁₇FN₃O₂ [(M + H)]⁺: 350.1299; found 350.1307.

General procedure for the synthesis of derivatives 63, 65 and 66-67a/b.

p-chlorobenzaldehyde, isovaleraldehyde or formaldehyde (1.5 eq) was added to a solution of L-Trp-OMe (**23**) dissolved in methanol and TFA (1.5eq). The reaction mixture was heated to 110 °C for 30 min in a microwave reactor (scheme 1). The crude was concentrated, diluted with dichloromethane and washed with water (3 x 20 mL). The combined organic layer was dried over anhydrous sodium sulfate, filtered, concentrated and purified by flash chromatography in *n*-hexane/ethyl acetate (70:30 ratio) to separate the diastereoisomeric mixtures of **57-58a/b**, while intermediate **59** was obtained with no further purification. To 1 mmol of the isolated intermediate dissolved in DCM/DMF (10/1) 1.2 eq of PyBOP and 2.4 eq of Dipea at room temperature were added. After 30 min 1.2 eq of the proper L-aminoacids were added and the reaction was mixed at room temperature over night. Then the crude was washed with water (3 x 20 mL), 10% aqueous solution of citric acid (3 X 20 mL) and saturated aqueous solution of sodium bicarbonate (3 x 20 mL). The combined organic layer was dried over anhydrous sodium sulfate, filtered, concentrated and purified by flash chromatography in 40:10 *n*-hexane/ethyl acetate, providing intermediates **60-61a/b**, **62** and **64**. The removal of the protecting group, using a solution of DCM/TFA in ratio 3:1 (9:3 mL) and treatment with saturated aqueous solution of sodium bicarbonate (3 x 20 mL) led to final derivatives **63**, **65** and **66-67a/b**.

(3R,12aS)-3-benzyl-2,3,12,12a-tetrahydropyrazino[1',2':1,6]pyrido[3,4-b]indole-1,4(6H,7H)-dione (63).

Overall yield 65%. ¹H NMR (CDCl₃, 400 MHz) : δ: 2.79 (dd, 1H, H-12', *J*' = 12.0, *J*'' = 16.0 Hz); 3.03 (dd, 1H, CH₂ benzyl, *J*' = 8.0, *J*'' = 12.0 Hz); 3.32 (d, 1H, CH₂ benzyl, *J* = 4.0 Hz); 3.40 (dd, 1H, H-12', *J*' = 4.0, *J*'' = 24.0 Hz); 3.67 (dd, 1H, H-12a, *J*' = 4.0, *J*'' = 8.0 Hz); 4.02 (dd, 1H, H-6', *J*' = 4.0, *J*'' = 16.0 Hz); 4.32 (dd, 1H, H-3, *J*' = 4.0, *J*'' = 8.0 Hz); 5.49 (d, 1H, H-6'', *J* = 16.0 Hz); 7.04 (t, 1H, aryl, *J* = 8.0 Hz); 7.12 (t, 1H, aryl, *J* = 8.0 Hz); 7.16-7.24 (m, 6H, aryl); 7.37 (d, 1H, aryl, *J* = 8.0 Hz); 7.82 (s, 1NH); ¹³C NMR (CDCl₃, 100 MHz) δ: 28.0, 41.4, 42.1, 56.8, 56.9, 108.4, 112.0, 119.3, 121.0, 123.4, 127.3, 128.7, 129.2, 130.2, 130.77, 136.1, 137.3, 163.9, 166.1.

HR-MS *m/z* calcd for C₂₁H₂₀N₃O₂ [(M + H)]⁺: 346.1550; found 346.1558.

(S)-methyl 2-(3-aminopropanoyl)-2,3,4,9-tetrahydro-1H-pyrido[3,4-b]indole-3-carboxylate (65).

58% yield. ¹H NMR (CD₃OD, 400 MHz) : δ: (A) 2.54-2.65 (m, 2H, CH₂); 2.86-2.91 (m, 2H, CH₂); 3.01 (dd, 1H, H-6', *J*' = 8.0 and *J*'' = 16.0 Hz); 3.42 (d, 1H, H-6'', *J* = 16.0 Hz); 3.52 (s, 3H, CH₃); 4.24 (d, 1H, H-2', *J* = 16.0 Hz); 5.04 (d, 1H, H-2'', *J* = 16.0 Hz); 5.16 (d, 1H, H-5, *J* = 4.0 Hz); 6.90 (t, 1H, aryl, *J* = 8.0 Hz); 6.97 (d, 1H, aryl, *J* = 8.0 Hz); 7.18 (t, 1H, aryl, *J* = 8.0 Hz); 7.31 (d, 1H, aryl, *J* = 8.0 Hz); ¹³C NMR (CD₃OD, 100 MHz) δ: 22.8, 35.4, 36.8, 38.3, 51.0, 54.8, 104.9, 110.0, 116.8, 118.0, 120.6, 126.4, 128.5, 137.2, 171.4, 173.5.

¹H NMR (CD₃OD, 400 MHz): δ: (B) 2.54-2.65 (m, 2H, CH₂); 2.86-2.91 (m, 3H, CH₂ and H-6'); 3.36 (d, 1H, H-6'', *J* = 16.0 Hz); 3.50 (s, 3H, CH₃); 4.63 (d, 1H, H-2', *J* = 16.0 Hz); 4.81 (d, 1H, H-2'', *J* = 16.0 Hz); 5.74 (d, 1H, H-5, *J* = 4.0 Hz); 6.90 (t, 1H, aryl, *J* = 8.0 Hz); 6.97 (d, 1H, aryl, *J* = 8.0 Hz); 7.18 (t, 1H, aryl, *J* = 8.0 Hz); 7.31 (d, 1H, aryl, *J* = 8.0 Hz); ¹³C NMR (CD₃OD, 100 MHz) (A + B) δ: 21.8, 35.4, 36.8, 40.8, 51.0, 50.5, 104.9, 110.0, 116.8, 118.0, 120.6, 137.2, 128.5, 126.4, 171.4, 173.5.

HR-MS *m/z* calcd for C₁₆H₂₀N₃O₃, [(M+H)]⁺: 302.1499; found 302.1503.

(3S,6S,12aS)-3-benzyl-6-isobutyl-2,3,12,12a-tetrahydropyrazino[1',2':1,6]pyrido[3,4-b]indole-1,4(6H,7H)-dione (66a).

Overall yield 53%. ¹H NMR (400 MHz, CDCl₃) δ 0.78 (d, 3H, *J* = 8.2 Hz, CH₃); 1.01 (d, 3H, *J* = 8.2 Hz, CH₃); 1.47-1.55 (m, 2H, CH₂); 1.74-1.76 (m, 1H, CH); 2.80 (dd, 1H, *J*' = 11.6, *J*'' = 15.8 Hz, H-12'); 2.94 (dd, 1H, *J*' = 12.0, *J*'' = 16.0 Hz, CH₂); 3.51 (dd, 1H, *J*' = 4.0, *J*'' = 16.0 Hz, CH₂); 3.64 (dd, 1H, *J*' = 4.0, *J*'' = 12.0 Hz, H-12''); 3.98 (dd, 1H, *J*' = 4.0, *J*'' = 11.6 Hz, H-3); 4.14 (dd, 1H, *J*' = 4.6, *J*'' = 11.4 Hz, H-12a); 5.45 (dd, 1H, *J*' = 4.4, *J*'' = 8.8 Hz, H-6); 5.67 (s, 1NH); 7.07-7.16 (m, 2H, aryl); 7.19 (d, 2H, *J* = 8.0 Hz, aryl); 7.25 (d, 1H, *J* = 8.0 Hz, aryl); 7.31 (t, 3H, *J* = 8.0 Hz, aryl); 7.50 (d, 1H, *J* = 8.0 Hz, aryl); 7.95 (s, 1NH). ¹³C NMR (100 MHz, CDCl₃) δ 21.7, 22.1, 23.8, 30.9, 37.2, 45.9, 51.2, 55.0, 56.1, 107.0, 111.2, 118.2, 120.2, 122.2, 126.1, 127.7, 129.1, 129.4, 134.3, 135.8, 168.2, 169.1 HR-MS *m/z* calcd for C₂₅H₂₈N₃O₂ [(M + H)]⁺: 402.2176; found 402.2190.

(3S,6R,12aS)-3-benzyl-6-isobutyl-2,3,12,12a-tetrahydropyrazino[1',2':1,6]pyrido[3,4-b]indole-1,4(6H,7H)-dione (66b).

Overall yield 42%. ¹H NMR (400 MHz, CD₃OD) δ 1.02 (d, 3H, *J* = 8.2 Hz, CH₃); 1.14 (d, 3H, *J* = 8.2 Hz, CH₃); 1.60-1.80 (m, 4H, H-12', CH and CH₂); 3.11 (dd, 1H, *J*' = 4.6, *J*'' = 11.6 Hz, H-12''); 3.18 (d, 2H, *J* = 4.8 Hz, CH₂); 4.30 (dd, 1H, *J*' = 8.0, *J*'' = 12.0 Hz, H-3); 4.43-4.46 (m, 1H, H-12a); 5.98-6.00 (m, 1H, H-6); 6.26 (s, 1NH); 7.12-7.24 (m, 7H, aryl); 7.36 (t, 2H, *J* = 8.0 Hz, aryl); 7.84 (s, 1NH). ¹³C NMR (100 MHz, CD₃OD) δ 22.4, 23.2, 25.2, 27.2, 41.7, 43.6, 47.8, 52.3, 56.9, 106.6, 110.8, 118.2, 119.9, 122.3, 126.4, 127.5, 129.0, 129.8, 132.7, 135.0, 135.9, 164.2, 167.5 HR-MS *m/z* calcd for C₂₅H₂₈N₃O₂ [(M + H)]⁺: 402.2176; found 402.2189.

(6S,12aS)-6-(4-chlorophenyl)-2,3,12,12a-tetrahydropyrazino[1',2':1,6]pyrido[3,4-b]indole-1,4(6H,7H)-dione (67a).

Overall yield 66%. $[\alpha]_D^{25}$: -79 ± 0.01 . $^1\text{H NMR}$ (CDCl_3 , 400 MHz): δ : 3.26 (dd, 1H, H-12', $J' = 12.0$, $J'' = 4.0$ Hz); 3.77 (dd, 1H, H-12'', $J' = 4.0$, $J'' = 16.0$ Hz); 4.06 (dd, 2H, H-3' and H-3'', $J' = 20.0$, $J'' = 36$ Hz); 4.40 (dd, 1H, H-12a, $J' = 4.0$, $J'' = 12$ Hz); 6.22 (s, 1NH, H-2); 6.26 (s, 1H, aryl); 7.16-7.32 (m, 7H, aryl); 7.63 (d, 1H, aryl, $J = 8.0$ Hz); 7.92 (s, 1NH). $^{13}\text{C NMR}$ (CDCl_3 , 100 MHz) δ : 23.4, 45.3, 55.8, 56.3, 109.6, 111.3, 118.6, 120.3, 122.8, 126.2, 128.6, 128.9, 132.2, 133.7, 136.6, 139.8, 167.1, 168.5.

HR-MS m/z calcd for $\text{C}_{20}\text{H}_{17}\text{ClN}_3\text{O}_2$ [(M + H)]⁺: 366.1004; found 366.1009.

(6R,12aS)-6-(4-chlorophenyl)-2,3,12,12a-tetrahydropyrazino[1',2':1,6]pyrido[3,4-b]indole-1,4(6H,7H)-dione (67b).

Overall yield 59%. $[\alpha]_D^{25}$: -244 ± 0.2 . $^1\text{H NMR}$ (CDCl_3 , 400 MHz): δ : 2.96 (dd, 1H, H-12', $J' = 12.0$, $J'' = 4.0$ Hz); 3.46 (dd, 1H, H-12'', $J' = 4.0$, $J'' = 16.0$ Hz); 4.05 (dd, 2H, H-3' and H-3'', $J' = 16.0$, $J'' = 36$ Hz); 4.18 (dd, 1H, H-12a, $J' = 4.0$, $J'' = 12$ Hz); 6.67 (s, 1NH, aryl); 6.97 (s, 1H, aryl); 7.08-7.26 (m, 7H, aryl); 7.48 (d, 1H, aryl, $J = 8.0$ Hz); 8.00 (s, 1NH). $^{13}\text{C NMR}$ (CDCl_3 , 100 MHz) δ : 22.7, 44.8, 51.5, 52.3, 109.1, 111.2, 118.5, 120.3, 123.0, 126.2, 129.1, 129.2, 130.1, 134.9, 136.4, 136.7, 161.8, 167.5.

HR-MS m/z calcd for $\text{C}_{20}\text{H}_{17}\text{ClN}_3\text{O}_2$, 366.1004; found 366.1011.

General procedure for the synthesis derivatives 71a/b.

Intermediates **69a/b** were obtained adding 4-fluorobenzaldehyde (1.5 eq) to a solution of L-Dopa methyl ester (1 eq) dissolved in methanol and TFA (1.5eq) and heating the reaction mixture to 110 °C for 30 min in a microwave reactor. Then the solution was concentrated in vacuo, diluted with DCM (10 mL) and washed with water (3 x 20 mL). The combined organic layer was dried over anhydrous sodium sulfate, filtered, concentrated and purified by flash

chromatography in n-hexane/ethyl acetate 50:50 to separate the diastereoisomeric mixture. To a solution of isolated tetrahydroisoquinolines dissolved in DCM, 0.4 eq of triphosgene, 1.2 eq of TEA and 1.2 eq of 4-chlorobenzylamine were added. The reaction was mixed at room temperature for 20 minutes. Then the combined organic layer was washed with water (3 x 20 mL), dried over anhydrous sodium sulfate, filtered, concentrated and purified by flash chromatography in 60:40 n-hexane/ethyl acetate. Intermediates **70a/b** were refluxed in MeOH/TEA for 10 minutes. The solvent was removed in vacuo and the crude was diluted with DCM, washed with water, dried over anhydrous sodium sulfate, filtered, concentrated and purified by flash chromatography in 75:25 n-hexane/ethyl acetate to obtain derivatives **71a/b**.

(5S,10aS)-2-(4-chlorobenzyl)-5-(4-fluorophenyl)-7,8-dihydroxy-10,10a-dihydroimidazo[1,5-b]isoquinoline-1,3(2H,5H)-dione (71a).

Overall yield 45%. $[\alpha]_{\text{D}}^{25}$: -148.20 ± 0.35 (c = 0.10, MeOH). ^1H NMR (400 MHz, CDCl_3) δ : 2.70 (dd, 1H, $J' = 12.2$, $J'' = 16.6$ Hz, H-10'); 3.10 (dd, 1H, $J' = 4.2$, $J'' = 16.6$ Hz, H-11"); 4.06 (dd, 1H, $J' = 4.0$, $J'' = 12.0$ Hz, H-10a); 4.48 (d, 1H, $J = 16.0$ Hz, CH_2); 4.56 (d, 1H, $J = 16.0$ Hz, CH_2); 5.99 (s, 1H, H-5); 6.36 (s, 1H, aryl); 6.65 (s, 1H, aryl); 6.93 (t, 2H, $J = 8.0$ Hz, aryl); 7.13-7.25 (m, 8H, aryl). ^{13}C NMR (100 MHz, CDCl_3) δ : 30.0, 41.7, 52.4, 54.0, 115.0, 115.3, 115.6, 115.9, 124.0, 125.9, 128.9, 129.9, 134.4, 142.9, 143.7, 172.6. HR-MS m/z calcd for $\text{C}_{24}\text{H}_{18}\text{ClFN}_2\text{O}_4$ [(M + H)]⁺: 452.0939; found 452.0944.

(5R,10aS)-2-(4-chlorobenzyl)-5-(4-fluorophenyl)-7,8-dihydroxy-10,10a-dihydroimidazo[1,5-b]isoquinoline-1,3(2H,5H)-dione (71b).

Overall yield 34%. $[\alpha]_{\text{D}}^{25}$: -102.36 ± 0.24 (c = 0.10, MeOH). ^1H NMR (400 MHz, CDCl_3) δ : 2.73 (dd, 1H, $J' = 12.2$, $J'' = 16.6$ Hz, H-10'); 3.12 (dd, 1H, $J' = 4.2$, $J'' = 16.6$ Hz, H-11"); 4.10 (dd, 1H, $J' = 4.0$, $J'' = 12.0$ Hz, H-10a); 4.50 (d, 1H, $J = 16.0$ Hz, CH_2); 4.58 (d, 1H, $J = 16.0$ Hz, CH_2); 6.02 (s, 1H, H-5); 6.39 (s, 1H,

aryl); 6.67 (s, 1H, aryl); 6.95 (t, 2H, $J = 8.0$ Hz, aryl); 7.15-7.27 (m, 8H, aryl). ^{13}C NMR (100 MHz, CDCl_3) δ : 30.0, 41.7, 52.4, 54.0, 115.0, 115.3, 115.6, 115.9, 124.0, 125.9, 128.9, 129.9, 134.4, 142.9, 143.7, 172.6. HR-MS m/z calcd for $\text{C}_{24}\text{H}_{18}\text{ClFN}_2\text{O}_4$ $[(\text{M} + \text{H})]^+$: 452.0939; found 452.0948.

General procedure for the synthesis derivatives 73a/b.

Benzaldehyde (1.5 eq) was added to a solution of L-Trp-OMe (**23**) dissolved in methanol and TFA (1.5eq). The reaction mixture was heated to 110 °C for 30 min in a microwave reactor. The combined organic layer was concentrated, diluted with dichloromethane and washed with water (3 x 20 mL). The combined organic layer was dried over anhydrous sodium sulfate, filtered, concentrated and purified by flash chromatography in n-hexane/ethyl acetate (30:20 ratio) to separate the diastereomeric mixture. The isolated tetrahydrobetacarbolines were dissolved in dichloromethane, then 1.2 eq of NaH and 1.2 eq of benzyl bromide were added. The reaction mixtures were heated to 120 °C for 30 min in a microwave reactor. The obtained crudes were washed with water (3 X 20 mL), dried over anhydrous sodium sulfate, filtered, concentrated and purified by flash chromatography in n-hexane/ethyl acetate (45:5 ratio).

(1S,3S)-methyl 2-benzyl-1-phenyl-2,3,4,9-tetrahydro-1H-pyrido[3,4-b]indole-3-carboxylate (73a).

Overall yield 58%. $[\alpha]_{\text{D}}^{25}$: 135.18 ± 0.25 ($c = 0.10$, MeOH) ^1H NMR (400 MHz, CDCl_3) δ : (dd, 1H, $J' = 4.4$, $J'' = 15.6$ Hz, H-4'); 3.31 (s, 3H, CH_3); dd, 1H, $J' = 7.8$, $J'' = 15.6$ Hz, H-4'') 87 (t, 1H, $J = 8.0$ Hz, H-3); 3.92 δ d, 1H, $J = 16.0$ Hz, CH_2) 4.08 (d, 1H, $J = 16.0$ Hz, CH_2) 4.97 (s, 1H, H-1); 7.11-7.23 (m, 2H, aryl); 7.24-7.37 (m, 11H, aryl); 7.55 (d, 1H, $J = 8.0$ Hz, aryl). ^{13}C NMR (100 MHz, CDCl_3) δ 22.7, 51.4 57.2, 61.0, 61.8, 107.2, 110.8, 118.4, 119.5, 121.8, 126.8, 127.1, 128.0, 128.5, 129.3, 133.2, 136.4, 138.2, 140.2, 173.5. HR-MS m/z calcd for $\text{C}_{26}\text{H}_{25}\text{N}_2\text{O}_2$ $[(\text{M} + \text{H})]^+$: 397.1911; found 397.1920.

(1R,3S)-methyl 2-benzyl-1-phenyl-2,3,4,9-tetrahydro-1H-pyrido[3,4-b]indole-3-carboxylate (73b).

Overall yield 55%. $[\alpha]_D^{25}$: -101.16 ± 0.17 ($c = 0.10$, MeOH). ^1H NMR (400 MHz, CDCl_3) δ (d, 2H, $J = 4.8$, H-4' and H-4''); 3.55 (s, 3H, CH_3); δd , 2H, $J = 11.8$, CH_2) δ 81-3.88 (m, 1H, H-3); 5.39 (s, 1H, H-1); 6.99-7.03 (m, 2H, aryl); 7.04 (d, 1H, $J = 8.0$ Hz, aryl); 7.10-7.29 (m, 6H, aryl); 7.38 (d, 2H, $J = 8.0$ Hz, aryl); 7.42 (d, 2H, $J = 8.0$ Hz, aryl); 7.44 (d, 1H, $J = 8.0$ Hz, aryl). ^{13}C NMR (100 MHz, CDCl_3) δ 24.5, 51.4, 54.4, 56.1, 60.9, 106.4, 110.8, 118.2, 119.3, 121.6, 127.0, 127.1, 128.1, 128.3, 128.6, 128.8, 128.9, 135.0, 136.5, 139.4, 142.2, 173.5. HR-MS m/z calcd for $\text{C}_{26}\text{H}_{25}\text{N}_2\text{O}_2$ $[(\text{M} + \text{H})]^+$: 397.1911; found 397.1918.

Synthesis of derivative 78.

To a solution of, Boc-L-Phe-OH (1 mmol) dissolved in DCM/DMF (10/1) 1.2 eq of HOBt, 1.2 eq of HBTU and 2.4 eq of Dipea at room temperature were added. After 30 min 1.2 eq of N,O-dimethylhydroxylamine were added and the reaction was mixed at room temperature over night. Then the crude was washed with water (3 x 20 mL), 10% aqueous solution of citric acid (3 X 20 mL) and saturated aqueous solution of sodium bicarbonate (3 x 20 mL). The combined organic layer was dried over anhydrous sodium sulfate, filtered, concentrated and purified by flash chromatography in 40:10 n-hexane/ethyl acetate.

The N-methoxy-N-methylcarbamoyl derivative (1 mmol; 88 % yield) was dissolved in dry THF and mixed at 0°C under nitrogen atmosphere. Then 2.5 eq of LiAlH_4 (1 M in THF) were added and the reaction was mixed at 0°C for 6 minutes. The crude was washed with 10% aqueous solution of citric acid (3 X 20 mL), the combined organic layer was dried over anhydrous sodium sulfate, filtered and concentrated. No further purification was performed. The obtained intermediate (1.5 eq) was added to a solution of L-Trp-OMe dissolved in MeOH and TFA (1.5 eq). The reaction mixture was heated to 110°C for 30 min in a microwave reactor. Then the crude was concentrated, diluted with dichloromethane and washed with water (3 x 20 mL). The combined organic layer was dried over anhydrous sodium sulfate, filtered, concentrated and purified by

flash chromatography in n-hexane/ethyl acetate (30:20 ratio) to separate the diastereoisomeric mixture. The removal of the protecting group using a mixture DCM/TFA 3/1 provided the indole-fused bicycle **78** as single diastereoisomer.

(1S,2S,5S)-2-benzyl-2,3,5,6-tetrahydro-1H-1,5-epiminoazocino[4,5-b]indol-4(11H)-one (78).

Overall yield 35%. ¹H NMR (400 MHz, CD₃OD) δ: dd, 1H, *J*' = 12.0, *J*'' = 16.0 Hz, CH₂); δ: d, 1H, *J* = 12.0 Hz, H-6') δ: 20 (dd, 1H, *J*' = 4.6, *J*'' = 16.2 Hz, H-6''); 3.28-3.37 (m, 1H, CH₂); δ: d, 1H, *J* = 8.0 Hz, H-5) δ: 4.28 (dd, 1H, *J*' = 4.4, *J*'' = 8.6 Hz, H-2); 4.41 δ: d, 1H, *J* = 4.4 Hz, H-1) δ: 7.04 (t, 1H, *J* = 8.0 Hz, aryl); 7.15 (t, 1H, *J* = 8.0 Hz, aryl); 7.26-7.31 (m, 3H, aryl); 7.35-7.39 (m, 3H, aryl); 7.47 (d, 1H, *J* = 8.0 Hz, aryl). ¹³C NMR (100 MHz, CD₃OD) δ 26.0, 38.3, 49.2, 52.6, 59.0, 107.2, 110.8, 117.4, 118.7, 121.4, 126.2, 126.6, 126.8, 128.8, 129.6, 136.6, 174.5, 183.6. HR-MS *m/z* calcd for C₂₀H₁₉N₃O [(M + H)]⁺: 318.1601; found 318.1619.

Synthesis of derivative 80.

Intermediate **59**, synthesized as previously described, was added to a solution of Boc-L-Phe-OH (1 mmol) dissolved in DCM/DMF (10/1), HOBt (1.2 eq), HBTU (1.2 eq) and Dipea (2.4 eq) and the reaction was mixed at room temperature over night. Then the crude was washed with water (3 x 20 mL), 10% aqueous solution of citric acid (3 X 20 mL) and saturated aqueous solution of sodium bicarbonate (3 x 20 mL). The combined organic layer was dried over anhydrous sodium sulfate, filtered, concentrated and purified by flash chromatography in 30:20 n-hexane/ethyl acetate. The removal of the protecting group using a mixture of DCM and trifluoroacetic acid provided the final diketopiperazine-fused tetrahydrobetacarboline **80**.

(3S,12aS)-3-benzyl-2,3,12,12a-tetrahydropyrazino[1',2':1,6]pyrido[3,4-b]indole-1,4(6H,7H)-dione (80).

Overall yield 31%. ¹H NMR (CDCl₃, 400 MHz) : δ: 2.79 (dd, 1H, H-12', *J*' = 12.0, *J*'' = 16.0 Hz); 3.03 (dd, 1H, CH₂ benzyl, *J*' = 8.0, *J*'' = 12.0 Hz); 3.32 (d, 1H, CH₂ benzyl, *J* = 4.0 Hz); 3.40 (dd, 1H, H-12', *J*' = 4.0, *J*'' = 24.0 Hz); 3.67 (dd, 1H, H-12a, *J*' = 4.0, *J*'' = 8.0 Hz); 4.02 (dd, 1H, H-6', *J*' = 4.0, *J*'' = 16.0 Hz); 4.32 (dd, 1H, H-3, *J*' = 4.0, *J*'' = 8.0 Hz); 5.49 (d, 1H, H-6'', *J* = 16.0 Hz); 7.04 (t, 1H, aryl, *J* = 8.0 Hz); 7.12 (t, 1H, aryl, *J* = 8.0 Hz); 7.16-7.24 (m, 6H, aryl); 7.37 (d, 1H, aryl, *J* = 8.0 Hz); 7.82 (s, 1NH); ¹³C NMR (CDCl₃, 100 MHz) δ: 28.0, 41.4, 42.1, 56.8, 56.9, 108.4, 112.0, 119.3, 121.0, 123.4, 127.3, 128.7, 129.2, 130.2, 130.77, 136.1, 137.3, 163.9, 166.1.

HR-MS *m/z* calcd for C₂₁H₂₀N₃O₂ [(M + H)]⁺: 346.1550; found 346.1558.

6.2 Pharmacology and molecular modeling

Cell Culture and Transfections

For fluorescence assays, cells stably expressing TRP channels (SH-SY5Y for TRPV1, HEK for TRPM8, and IMR90 for TRPA1) were cultured in a monolayer at 37 °C in a humidified atmosphere of 5% CO₂ in Earle's minimum essential medium with Earle's salts supplemented with 10% fetal calf serum, 1% nonessential amino acids, 2 mM L-glutamine, 100 µg of streptomycin/mL, 100 U penicillin/mL, and the correspondent antibiotic for each stable cell line (0.4 µg/mL puromycin for Sh-SY5Y and 400 µg/mL G418 for HEK-CR1).

For electrophysiological experiments, HEK293 cells were grown in 100 mm plastic Petri dishes in Dulbecco's modified Eagle medium containing 10% fetal bovine serum, penicillin (100 U/mL), and streptomycin (100 U/mL) in a humidified atmosphere at 37 °C with 5% CO₂. The cells were seeded on glass coverslips (Carolina Biological Supply Company, Burlington, NC) and transfected the next day with 3.6 µg of rat TRPM8 receptor cDNA (a gift from Dr. Felix Viana, Alicante Institute of Neuroscience, Elche, Spain) using Lipofectamine 2000 (Invitrogen, Milan, Italy). A plasmid encoding for the Enhanced Green Fluorescent Protein (Clontech, Palo Alto, CA) was used as a transfection marker. Total cDNA in the transfection mixture was kept constant at 4 µg.

Fluorescence Assays

For fluorescence assays, the cells were seeded in 96-well plates (Corning Incorporated, Corning, NY) at a cell density of 40 000 cells 2 days before treatment. On the day of treatment the medium was replaced with 100 µL of the dye loading solution Fluo-4 NW supplemented with probenecid 2.5 mM. Then the tested molecules dissolved in DMSO were added at the desired concentrations and the plates were incubated in darkness at 37 °C in a humidified atmosphere of 5% CO₂ for 60 min. The fluorescence was measured using instrument settings appropriate for excitation at 485 nm and emission at 535 nm (POLARstar Omega BMG LABtech). A baseline recording of four cycles was recorded prior to

stimulation with the agonist (10 μ M capsaicin for TRPV1, 100 μ M menthol for TRPM8, and 100 μ M AITC for TRPA1). Each antagonist (10 μ M ruthenium red for TRPV1 and TRPA1, 10 μ M AMTB for TRPM8) was added to the medium containing the corresponding agonist to induce channel blockade. The changes in fluorescence intensity were recorded during 15 cycles more. The higher concentration of DMSO used in the experiment was added to the control wells. The cells' fluorescence was measured before and after the addition of various concentrations of test compounds ($\lambda_{EX} = 488$ nm, $\lambda_{EM} = 516$ nm). The fluorescence values obtained are normalized to that prompted by the corresponding agonist (for channel activating compounds) or upon agonist + antagonist coexposure (for channel blocker compounds).

Whole-Cell Electrophysiology

Macroscopic currents from transiently transfected HEK293 cells were recorded at room temperature 1 day after transfection, with an Axopatch 200B amplifier (Molecular Devices, Union City, CA) using the whole-cell configuration of the patch-clamp technique, with glass micropipettes of 3–5 M Ω resistance. The extracellular solution contained the following (mM): 138 NaCl, 5.4 KCl, 2 CaCl₂, 1 MgCl₂, 10 glucose, and 10 HEPES, pH 7.4 with NaOH. The pipet (intracellular) solution contained the following (mM): 140 CsCl, 1 EGTA, 10 HEPES, and 5 Mg-ATP, pH 7.3–7.4 with CsOH. The pCLAMP software (version 10.2; Molecular Devices) was used for data acquisition and analysis. Linear cell capacitance (C) was determined by integrating the area under the whole-cell capacity transients, evoked by short (5–10 ms) pulses from –80 to –75 mV with the whole-cell capacitance compensation circuit of the Axopatch 200B turned off. Data were acquired at 5 kHz and filtered at 1–5 kHz with the four-pole low-pass Bessel filter of the amplifier. No corrections were made for liquid junction potentials. Currents were evoked by consecutive voltage ramps from –100 to +100 mV in 100 ms, delivered every 4 s. Current densities (expressed in pA/pF) were calculated at +80 mV or –80 mV and divided by C.

Chemical Modulators

l-Menthol and BCTC were purchased from Applichem Panreac (Barcelona, Spain) and Tocris Bioscience (Bristol, U.K.), respectively. AITC, capsaicin, and ruthenium red were purchased from Sigma-Aldrich (St. Louis, MO, USA). These compounds were dissolved in DMSO (final concentration, $\leq 1\%$). In each experiment, the same volume of solvent used for tested drugs was added to the control solution. Fast solution exchanges (< 1 s) were achieved by means of a cFlow 8 flow controller attached to a cF-8VS eight-valve switching apparatus, as previously described⁷⁵.

Molecular Modeling, Protein and Ligands Preparations

The TRPM8 homology model was prepared using the Protein Preparation^{76,77} utility in order to obtain satisfactory starting structures for the following studies. This utility is meant to ensure chemical correctness and to optimize protein structures for further analysis. In particular, Epik⁷⁸ was then used to predict ionization and tautomeric states for the ligands using a pH of 7 ± 1 . Successively, optimization of the hydrogen-bonding network was obtained by reorienting hydroxyl and thiol groups, amide groups of Asn and Gln, and His rings. The ionization and tautomeric states of His, Asp, Glu, Arg, and Lys were adjusted to match a pH of 7.4. The structure was finally submitted to a restrained minimization (OPLS2005 force field) that was stopped when rmsd of heavy atoms reached 0.30 Å.

Ligands were sketched using the Maestro,⁷⁹ interface and 3D coordinates were generated using LigPrep.⁸⁰ Ionization/tautomeric states were predicted for a pH range of 7 ± 1 using Epik⁷⁸. The most populated ionization state for each ligand was retained.

In order to investigate the potential usefulness of the described TRPM8 rat homology model also for the results obtained in other species, pairwise alignments were performed among the rat, human, and mouse TRPM8 sequences using Clustal Omega.

SiteMap Calculations

All TRPM8 atoms were considered in the identification the top ranking potential binding sites. Each site was required to have at least five site points and was cropped at 4 Å from the nearest site point. The definition of hydrophobicity was set to “restrictive”.

Molecular Docking

Docking of 12 and 21 was performed using Glide SP44–46 and XP47 in a stepwise manner. The docking spaces were defined as a 50 Å³ cubic box, while the diameter midpoint of docked ligands was required to remain within a smaller, nested 30 Å³ cubic box centered on the centroid of BP1 site points. Receptor OH and SH groups were set free to rotate. Two docking grids were used for SP and XP docking, differing for the scaling of vdW radii for nonpolar receptor atoms only. For SP a coefficient of 0.85 was used, while no scaling was used for XP. At most 10 poses for each ligand were retrieved from the SP docking, discarding as duplicates poses that showed both rms deviation less than 1.5 Å and maximum atomic displacement less than 2.0 Å. These poses were then refined, rescored, and minimized using Glide XP. The best scoring XP pose for each ligand was then retained for the MD simulations.

Molecular Dynamics Simulation

MD simulations of TRPM8/12 and TRPM8/21 complexes were set and run using Desmond MD system⁸¹. The simulated environment was built using the system builder utility, with the structures being neutralized by Cl⁻ ions. The small 903–924 fragment was removed. With the exception of the 954–1016 fragment, which was unconstrained, the protein backbone was constrained by a 1 kcal/mol force. Octanol was used as explicit solvent. Before performing the simulations, a series of minimizations and short MD simulations were carried out to relax the model system by means of a relaxation protocol consisting of six stages: (i) minimization with the solute restrained; (ii) minimization without restraints; (iii) simulation (12 ps) in the NVT ensemble using a Berendsen thermostat (10 K)

with non-hydrogen solute atoms restrained; (iv) simulation (12 ps) in the NPT ensemble using a Berendsen thermostat (10 K) and a Berendsen barostat (1 atm) with non-hydrogen solute atoms restrained; (v) simulation (24 ps) in the NPT ensemble using a Berendsen thermostat (300 K) and a Berendsen barostat (1 atm) with non-hydrogen solute atoms restrained; (vi) unrestrained simulation (24 ps) in the NPT ensemble using a Berendsen thermostat (300 K) and a Berendsen barostat (1 atm). At this point, 12 ns long MD simulations were carried out at a temperature of 300 K in the NPT ensemble using a Nose–Hoover chain thermostat and a Martyna–Tobias–Klein barostat (1.013 25 bar). Trajectory analyses were performed using the Desmond simulation event analysis tool for the rmsd calculations, Desmond Simulation Interaction diagram tool for the ligand interaction analysis, and Schrodinger clustering of conformers script for the bound conformation analysis.

Pharmacophore Modeling

Docking/MD predicted bound conformations were used to manually build the pharmacophore models summarizing the chemical feature of tryptamine based agonists and antagonists. Models were built using the software Phase. Features and their coordinates were automatically detected using the ligand-based option of Phase and were then edited in freestyle modes according to the ligand–protein interaction detected by the Simulation. Interaction diagram tool. In particular, H1 and H2 features were previously detected as aromatic features but were changed to hydrophobic since during the MD trajectories they interacted with nonaromatic hydrophobic residues only. For the same reason, the R3 feature of the antagonist model was changed to H1. After the model generation, a refinement phase was used to evaluate the fitness of the tryptamine based agonists and antagonists on the two models.

Statistical Analysis

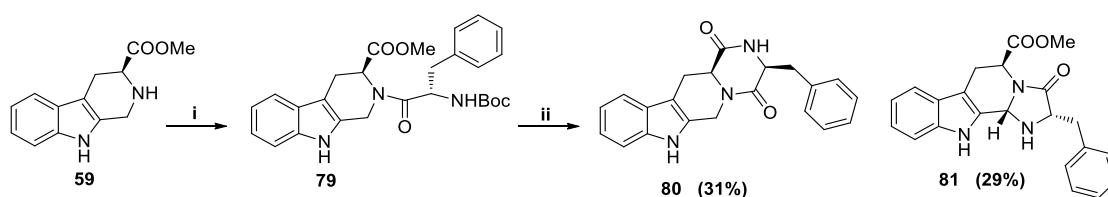
Data are expressed as the mean \pm SEM. Statistically significant differences were evaluated with the Student t test or with ANOVA followed by the Student–Newman–Keuls test, with the threshold set at $p < 0.05$.

CHAPTER II:
**Ring fused cyclic amins from TH β C-based
dipeptide compounds**

1. Background

While synthesizing compound **80** (Chapter I, paragraph 4.2), we found that the reduced yields in the desired product were due to the simultaneous formation of a side product. In order to rationalize this unprecedented reaction pathway, this side product was isolated and characterized by NMR spectroscopy leading to the identification of the aminoacetal derivative **81** (Scheme 1), as suggested by its ^1H NMR spectra showing both the methyl ester signal ($\delta= 3.60$) and a singlet at 5.84 ppm, compatible with the aminoacetal CH proton (Figure 1).

Scheme 1. Cyclization of **79** leading to 2,5-diketopiperazine **80** and aminoacetal derivative **81**.



Reagents and conditions: i: DCM/DMF, 1.2eq Boc-L-Phe-OH, 1.2eq PyBOP, 2.4eq DIPEA, 12h, rt; ii: DCM/TFA 3/1, TIS, 2h, rt.

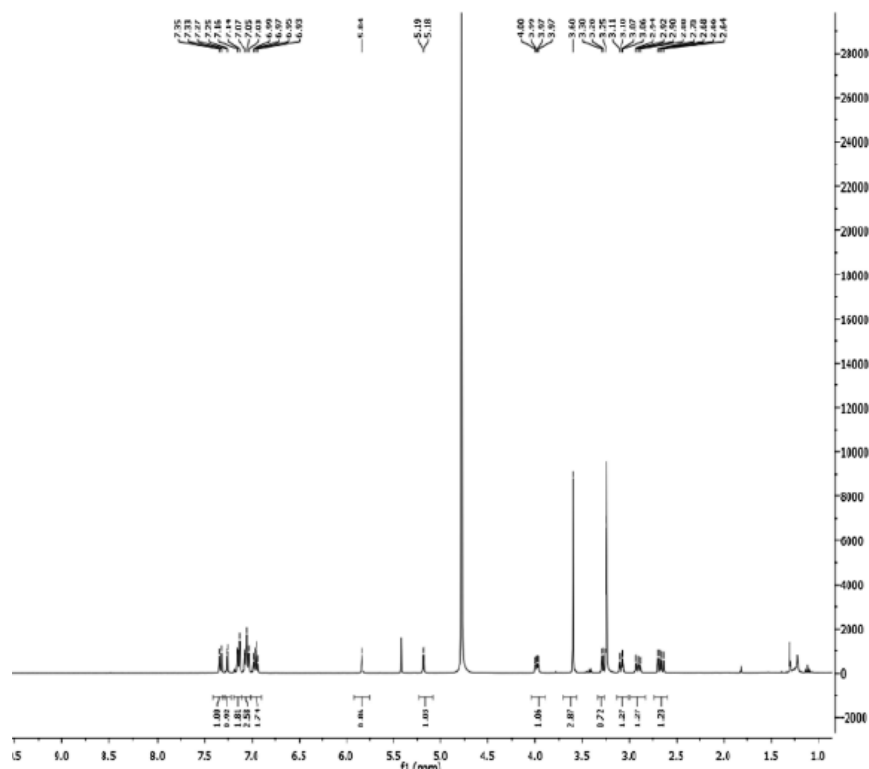


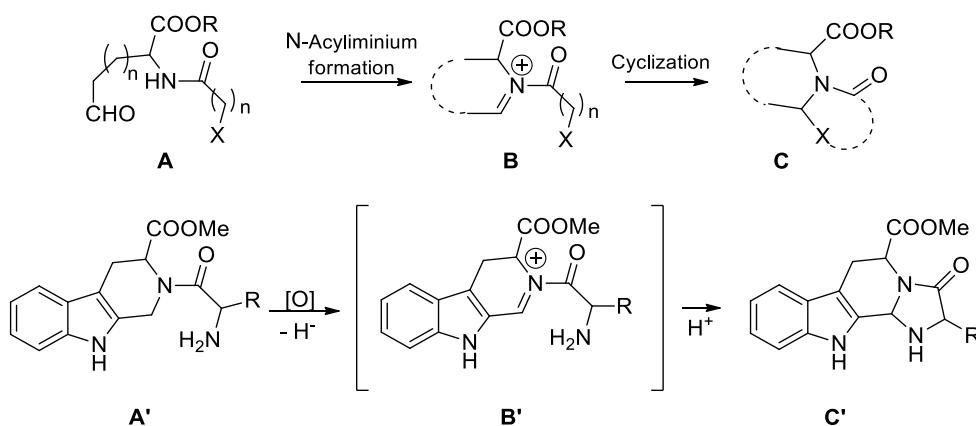
Figure 1. ^1H NMR of derivative 81.

Aminoacetal derivatives of tetrahydrobetacarbolines are endowed with potential pharmacological activities.⁸² This structural motif finds applications in medicinal chemistry due to various valuable biological activities such as anti-cancer, anti-microbial and anti-malarial. In addition many alkaloids contain the aminoacetal moiety.⁸³ This is the reason why the central goals of this part of my PhD programme were the full characterization of this new chemical entity and the design and optimization of an efficient method for the preparation of ring-fused aminals by a mild functionalization of nitrogen heterocycles, extending the structural diversity of indole-based chemotypes.

2. Chemistry and computational studies

N-Acyliminium ions are powerful reactive species for the formation of carbon–carbon and carbon–heteroatom bonds. Strategies relying on intramolecular reactions of N-acyliminium intermediates have been employed for the construction of structurally diverse scaffolds, ranging from simple bicyclic skeletons to complex polycyclic systems and natural-product-like compounds.⁸⁴ Based on the evidence that the formation of tetrahydro- β -carbolines occurs through the Pictet–Spengler reaction,^{73, 85} we envisaged that the regeneration of the latent N-acyliminium ion (B') in type A' dipeptides could provide access to the corresponding aminoacetal derivatives (C') via α -functionalization of the amine (Scheme 2).⁸⁶

Scheme 2. N-acyliminium ion-mediated cyclization reaction (A-C), and its application to dipeptides (A'-C').



Structure and relative stereochemistry of **81** were determined by analysis of 1D and 2D NMR data, including COSY, qDEPT, HSQC, HMBC, and ROESY. The configuration at C-11b asymmetric center was assigned as *S* on the basis of an NOE effect between H-2 and H-11b observed in the 2D ROESY spectra, indicating a *cis* disposition between these protons. The absolute configuration of **81** as 2*S*,5*S*,11*bS* was determined by hypothesizing the retention of configuration at C-2 and C-5 (Figure 2).

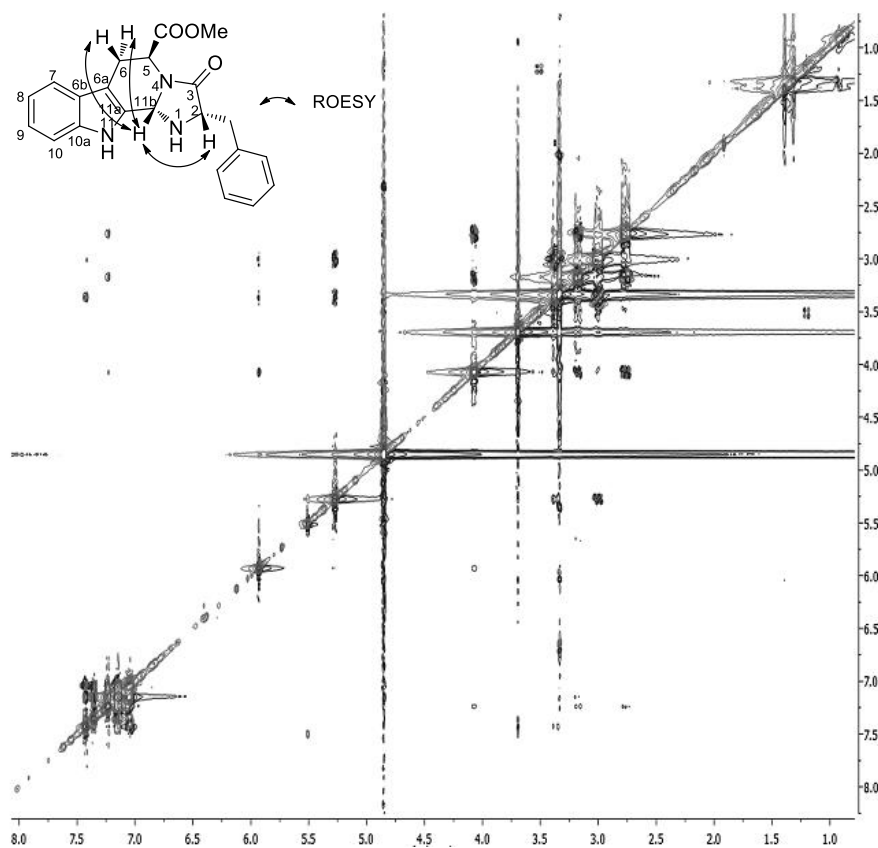


Figure 2. ROESY NMR spectrum and NOE correlations related to compound **81**.

The proposed stereochemical behavior of the reported reaction was corroborated by the comparison of the experimental $^{13}\text{C}/^1\text{H}$ NMR chemical shifts and the corresponding calculated values at the density functional theory level (DFT). NMR parameters were predicted at the density functional theory level for **81** and the other hypothetical diastereoisomer **81'**, specifically differ from **81** for the R configuration at C-11b in order to confirm the proposed stereochemical assignment. The comparison between experimental and calculated $^{13}\text{C}/^1\text{H}$ chemical shift data clearly confirmed the good accordance for **81** ($^{13}\text{C}/^1\text{H}$ mean absolute errors, MAEs = 1.88/0.29 ppm, respectively), while higher $^{13}\text{C}/^1\text{H}$ MAEs (2.29/0.46 ppm, respectively) were found for **81'** (Figure 3).⁸⁷

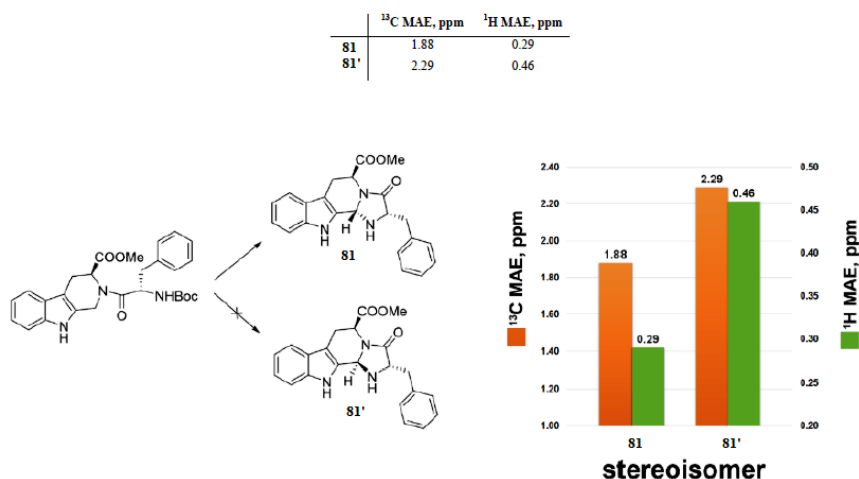


Figure 3. ¹³C (orange bars) and ¹H (green bars) mean absolute errors (MAE) histograms related to compounds **81/81'**.

To find suitable reaction conditions for the formation of **81**, we investigated the influence of both redox and acid mediums on the cyclization of **79**. Initially, we decided to explore the use of a weak oxidant agent as promoter of the H-abstraction of C-H adjacent to nitrogen in acid medium.^{86a, 88} Treatment of **79** with 0.2 equiv of TEMPO in 3/1 DCM/TFA led to the enantiomerically pure (2*S*,5*S*,11*bS*)-methyl 2-benzyl-3-oxo-(2,3,5,6,11,11*b*)-hexahydro-1*H*-imidazo[1',2':1,2]pyrido[3,4-*b*]indole-5-carboxylate (**81**) and to the 2,5-diketopiperazine **80** in 48% and 20% yield, respectively. Use of O₂ (Table 1, entry 2) or perbenzoic acid (1 equiv, entry 3) exclusively afforded the aminoacetal in 82–85% isolated yield. Treatment of **79** with perbenzoic acid in a MeOH/37% HCl solution leads to **81** with lower yields (Table 1, entry 4). The lack of an oxidizing agent (Table 1, entry 5) also favors the nucleophilic attack of amine on the carbonyl group and formation of **80**, which was obtained with 31% yield. Inorganic oxidizing agents were less effective in promoting cyclization to **81** (Table 1, entries 6–10).

Table 1. Optimization of cyclization reaction of **79**^a.

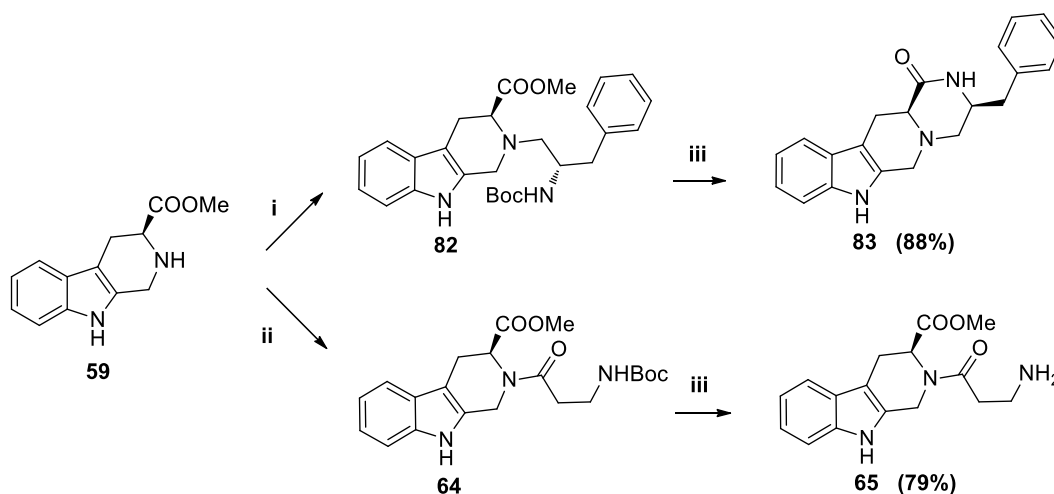
entry	solvent/acid ^a	redox cond.	yields (%)	
			80	81
1	3/1 DCM/TFA	TEMPO (0.2 eq)	20	48
2	3/1 MeOH/TFA	O ₂	-	85
3	3/1 DCM/TFA	Perbenzoyc acid (1eq)	-	82
4	MeOH/37%HCl	Perbenzoyc acid (1eq)	-	65
5	3/1 DCM/TFA	-	31	29
6	1/1/2 MeOH/H ₂ O/TFA	Oxone	19	27
7	1/1/2 MeOH/H ₂ O/TFA	KMnO ₄	26	19
8	1/1/2 MeOH/H ₂ O/TFA	K ₂ Cr ₂ O ₇	18	14
9	1/1/2 MeOH/H ₂ O/TFA	HIO ₄	30	22
10	1/1/2 MeOH/H ₂ O/TFA	FeCl ₃	12	15

^aReactions were performed for 2 h on a 1.0 mmol scale. b“- = no redox reagents used.

In order to verify the importance of the amide group in the mechanism of aminocetal formation via N-acyliminium generation, we performed the reaction using the Boc-Phe-Tpi(OMe)-reduced analogue **82** (Scheme 3) in the optimized conditions (Table 1, entry 3); using **82** as starting material we observed the cyclization to the corresponding hexahydropyrazino[1',2':1,6]-pyrido[3,4-b]indole-4-one (**83**) in 88% yield.⁸⁹ According to the literature, the protonation of the tertiary amine of intermediate **82** could cause ring opening and formation of a carbocation intermediate,^{85a,90} incompatible with the formation of the corresponding aminal derivatives.

Additionally intramolecular cyclization of 2-(3-Boc-aminopropanoyl)-Tpi-OMe intermediate **64** did not occur, while the linear compound **65** was isolated in 79% yield (Scheme 3).

Scheme 3. Cyclization of reduced and N-aminopropanoyl Tpi intermediates **64** and **82**.



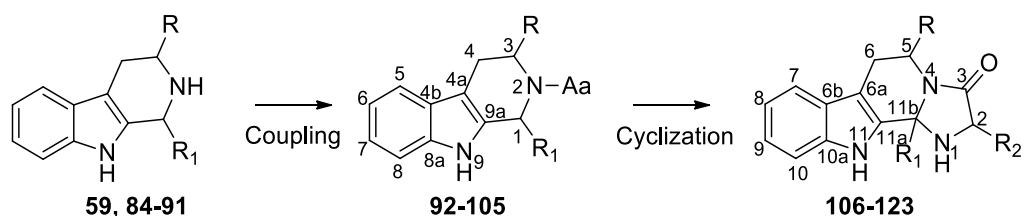
Reagents and conditions: i: MeOH dry, Boc-L-Phe-H, N₂, 12 h, then NaBH₄, 3h, rt; ii: DCM/DMF, Boc-β-Ala-OH, PyBOP, DIPEA, 12h, rt; iii: DCM/TFA 1/1, 1eq perbenzoic acid, TIS, 2h, rt.

Various other Tpi derivatives and amino acids were used for the preparation of functionalized polycyclic indole derivatives (Table 2). Cyclization of L- or D-N-acyl-Tpi using 1 equiv of perbenzoic acid gave the corresponding (2S,5S 11bS) (**106–108**) or (2R,5S,11bS) (**109**) derivatives in high yields (Table 2, entries 1–4). Reactions of intermediates containing different N-protecting groups (Table 2, entries 5 and 6) led to N-protected aminals **110** and **111** in lower yields, perhaps due to the steric hindrance of the reactive nitrogen. When D-Tpi-OMe (entry 7), Tpi (entry 8), Tpi-NHCH₂CH₃ (entry 9), or tryptamine (entry 10) were used as starting compounds, no significant differences in the corresponding yields of **112** (2S,5R,11bR), **113** (2S,5S,11bS), **114** (2S,5S,11bS), or **115** (2S,11bS) aminoacetal were evidenced in comparison with Tpi-OMe.

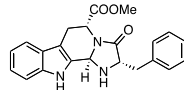
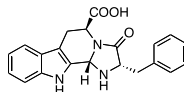
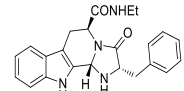
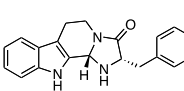
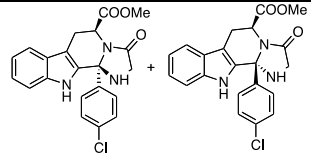
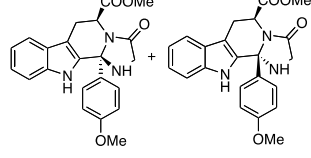
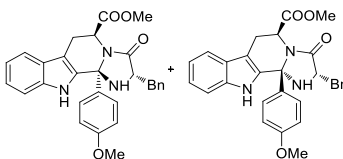
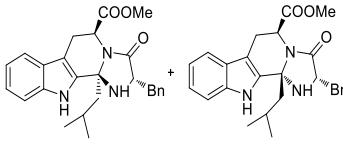
Interestingly, the total stereoselectivity observed in the cyclization reaction using an intermediate not substituted at the C-1 position (**106–115**) was completely lost with substituted intermediates at C-1. Cyclization of the 1-(S or R)-substituted tetrahydro-β-carboline glycyl or phenylalanil derivatives to the corresponding aminals resulted in the formation of a mixture of (5S,11bS) and (5S,11bR) diastereoisomers (Table 2, entries 11–13, **116/117**, **118/119**, and **120/121** in a 1:1 ratio; entry 14, **122/123** in a 3:2 ratio), as strongly confirmed by the comparison of

experimental and calculated $^{13}\text{C}/^1\text{H}$ chemical shift data and by the analysis of the most energetically favored conformers of **116** and **117**. Furthermore, the absence of the stereoselectivity in the formation of the products (**116** and **117**) was investigated through the analysis of the energy diagrams, again confirming that the cyclization is kinetically and thermodynamically driven. The reported data indicate the steric hindrance at C-11 on the final products as a key factor in determining the stereoselectivity of the cyclization reaction, as confirmed by the smaller difference of the energies of the species at the transition state for the formation of **116** and **117**.

Table 2. Synthesis of aminoacetal derivatives 106-123.



Entry/ Starting compound	R (conf. C_3)	R_1 (conf. C_1)	Aa (dipeptides number)	Products	Number (yield %)
1/59	COOMe (<i>S</i>)	H	Boc-Gly (92)		106 (70)
2/59	COOMe (<i>S</i>)	H	Boc-Ala (93)		107 (79)
3/59	COOMe (<i>S</i>)	H	Boc-Pro (94)		108 (72)
4/59	COOMe (<i>S</i>)	H	Boc- <i>D</i> -Phe (95)		109 (81)
5/59	COOMe (<i>S</i>)	H	Z-Leu (96)		110 (40)
6/59	COOMe (<i>S</i>)	H	Fmoc-Phe (97)		111 (25)

7/84	COOMe (<i>R</i>)	H	Boc-Phe (98)		112 (65)
8/85	COOH (<i>S</i>)	H	Boc-Phe (99)		113 (69)
9/86	CONHEtyl (<i>S</i>)	H	Boc-Phe (100)		114 (57)
10/87	H	H	Boc-Phe (101)		115 (39)
11/88	COOMe (<i>S</i>)	(4-Cl)- phenyl(<i>S,R</i>)	Boc-Gly (102)		116, 117 (25, 26)
12/89	COOMe (<i>S</i>)	(4-OMe)- phenyl(<i>S, R</i>)	Boc-Gly (103)		118, 119 (37, 37)
13/90	COOMe (<i>S</i>)	(4-OMe)- phenyl(<i>S,R</i>)	Boc-Phe (104)		120, 121 (29, 32)
14/91	COOMe (<i>S</i>)	isobutyl(<i>S,R</i>)	Boc-Phe (105)		122, 123 (33, 24)

3. Conclusions

An efficient method for the preparation of ring-fused ainals by a mild functionalization of nitrogen heterocycles, extending the structural diversity of indole-based chemotypes, has been described. Some of the reported compounds could be useful for preparing analogues of biologically active natural and synthetic products. The observed stereoselectivity has been rationalized by means of DFT calculations, providing useful information for future investigations about the quantitative prediction of the products. Studies aimed at increasing the scope of this cyclization are ongoing. Moreover, the synthesized compounds are attractive templates for drug discovery. Several cyclic ainals have been proposed as antitumor agents^{82d, 82h-j} and PDE5 inhibitors.⁹¹ Moreover, cyclic ainals are involved in Transient Receptor Potential (TRP) channel modulations.⁹² Preliminary *in silico* assays on synthesized compounds are ongoing, using a previously described model.⁹³ Finally, computational investigation of the molecular docking models between **81** and microsomal prostaglandin E₂ synthase-1 (mPGES-1) highlighted the presence of several key interactions that could be responsible of the inhibitory activity towards of the reported compounds with the investigated target suggesting further studies for assessing their use as new anti-inflammatory/anticancer agents (Figure 4).⁹⁴

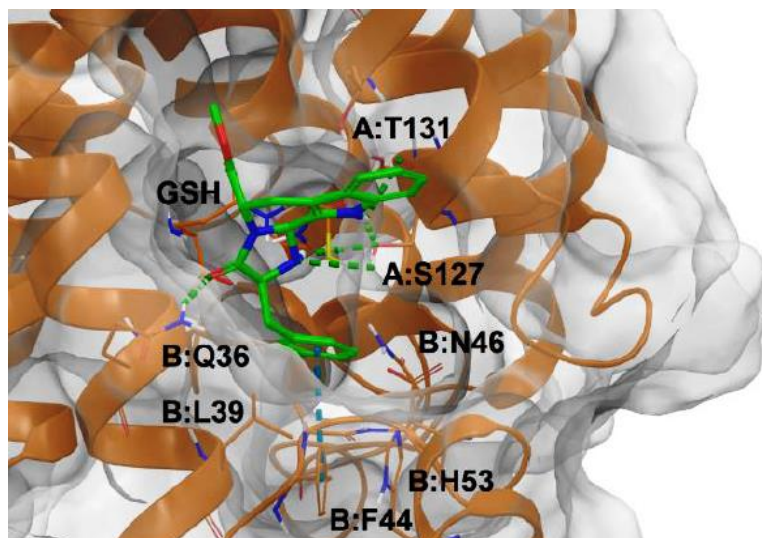


Figure 4. 3D docking model of the interaction between **81** and mPGES-1 target. Specifically, **81** establishes a wide set of interaction with the receptor counterpart, making contacts with key residues in the ligand binding site (LBD). In details, **81** establishes: a) hydrogen bonds with A:Ser127, A:Thr131, B:Gln36 (represented with dotted green lines); b) edge to face interactions with B:Phe44; c) polar contacts with B:Asn46, B:His53, glutathione (GSH); d) hydrophobic contacts with B:Leu39.

Experimental section

4.1 Chemistry

Reagents, starting materials, and solvents were purchased from Sigma-Aldrich (Milan, Italy) and used as received. Reactions were carried out with magnetic stirring in round-bottomed flasks unless otherwise noted. Purifications were conducted on the Biotage Isolera One flash purification system, using prepacked KP-sil columns, (Biotage, Uppsala, Sweden). Microwave-assisted closed vessel reactions were performed in a Biotage Initiator+ reactor using 10–20 mL vials and an external temperature sensor. Analytical TLC was performed on precoated glass silica gel plates 60 (F254, 0.25 mm, VWR International). 1D and 2D NMR spectra were recorded on a Bruker Avance (400 MHz) spectrometer, at room temperature. Spectra were referenced to residual chloroform (7.24 ppm, ^1H ; 77.23 ppm, ^{13}C) or methanol (3.31 ppm, ^1H ; 49.15 ppm, ^{13}C). Chemical shifts are reported in δ values (ppm) relative to internal Me_4Si , and J values are reported in hertz (Hz). The following abbreviations are used to describe peaks: s (singlet), d (doublet), dd (double doublet), t (triplet), q (quartet), and m (multiplet). HR-MS experiments were performed using an LTQ-Orbitrap-XL-ETD mass spectrometer (Thermo Scientific, Bremen, Germany) using electrospray ionization. Optical rotations were measured on an Atago Polax 2-L polarimeter at a concentration of 0.1 g/100 mL.

General Procedure for the Synthesis of Derivatives 59 and 84–91.

Compounds **59**, and **84–91** were obtained by microwave-assisted Pictet–Spengler reactions, starting from tryptophan derivatives or tryptamine and differently substituted aldehydes, according to the procedure previously described.⁹⁵ NMR and mass spectra are in accordance with literature data.

General Procedure for the Synthesis of Derivatives 79, 64, 92–99, and 101–103.

To a solution of the corresponding tetrahydro- β -carboline (4 mmol) in dichloromethane (25 mL) were successively added different N-protected amino

acids (4.4 mmol), PyBop (4.8 mmol), and DIPEA (8.8 mmol). Stirring was continued at room temperature for 12 h. Afterward, the reaction mixture was diluted with dichloromethane (20 mL), and the resulting solution was washed successively with 10% citric acid (2 × 25 mL), 10% NaHCO₃ (2 × 25 mL), and water (2 × 25 mL), dried over Na₂SO₄, and evaporated to dryness. Flash chromatography of the residues, using different eluent systems, yielded, in each case, the corresponding N-protected aminoacyl derivatives **64**, **79**, **90–97**, and **99–101** as rotamer mixtures.

(S)-methyl 2-((S)-2-((tert-butoxycarbonyl)amino)-3-phenylpropanoyl)-2,3,4,9-tetrahydro-1H-pyrido[3,4-b]indole-3-carboxylate (79).

68% yield. ¹H NMR (CDCl₃, 400 MHz): (**A**) δ: 1.45 (s, 9H, Boc); 2.70-2.78 (m, 1H, CH₂a); 2.97 (dd, 1H, H-4b, *J*' = 8.0, *J*'' = 12.0 Hz); 3.08-3.15 (m, 1H, CH₂b); 3.34 (d, 1H, H4a, *J* = 12.0 Hz); 3.61 (s, 3H, CH₃); 4.73 (d, 1H, H1a, *J* = 16.0 Hz); 4.97-5.13 (m, 2H, H-1b and H-2'); 5.48 (d, 1H, NHBoc, *J* = 8.0 Hz); 5.87 (d, 1H, H-3, *J* = 8.0 Hz); 7.12 (t, 1H, H-7, *J* = 8.0 Hz); 7.18 (t, 1H, H-6, *J* = 8.0 Hz); 7.23-7.32 (m, 6H, H-8 and aryl); 7.45 (d, 1H, H-5, *J* = 8.0 Hz); 8.48 (s, 1H, NH); (**B**) δ: 1.43 (s, 9H, Boc); 2.41 (dd, 1H, CH₂a, *J*' = 8.0, *J*'' = 16.0 Hz); 3.23 (dd, 1H, H-4b, *J*' = 4.0, *J*'' = 16.0 Hz); 3.08-3.15 (m, 1H, CH₂b); 3.28 (d, 1H, H4a, *J* = 12.0 Hz); 3.60 (s, 3H, CH₃); 4.53 (d, 1H, H1a, *J* = 16.0 Hz); 4.97-5.13 (m, 3H, H-3, H-1b and H-2'); 5.48 (d, 1H, NHBoc, *J* = 8.0 Hz); 7.12 (t, 1H, H-7, *J* = 8.0 Hz); 7.18 (t, 1H, H-6, *J* = 8.0 Hz); 7.23-7.32 (m, 6H, H-8 and aryl); 7.45 (d, 1H, H-5, *J* = 8.0 Hz); 8.45 (s, 1H, NH); ¹³C NMR (CDCl₃, 100 MHz) (**A** + **B**) δ: 22.5; 22.7; 23.4; 28.3; 31.6; 38.7; 39.0; 40.3; 41.4; 51.1; 52.3; 52.5; 52.8; 53.3; 80.1; 105.2; 106.6; 111.0; 118.0; 118.2; 119.6; 121.9; 122.1; 126.5; 126.9; 127.1; 127.7; 128.4; 128.7; 128.9; 129.4; 129.6; 136.1; 136.5; 155.0; 155.5; 170.6; 171.3; 172.2; 172.6. HR-MS *m/z*: calcd for C₂₇H₃₂N₃O₅, [(M+H)⁺]: 478.2336; found 478.2329.

(S)-methyl 2-(3-((tert-butoxycarbonyl)amino)propanoyl)-2,3,4,9-tetrahydro-1H-pyrido[3,4-b]indole-3-carboxylate (64).

71% yield. ¹H NMR (CDCl₃, 400 MHz) : (A) δ: 1.46 (s, 9H, Boc); 2.66-2.75 (m, 2H, H-2'); 3.05-3.18 (m, 1H, H-4a); 3.46-3.57 (m, 3H, H-4b and H-3'); 3.64 (s, 3H, CH₃); 4.80 (dd, 2H, H-1, *J*' = 16.0, *J*" = 16.8 Hz); 5.32 (d, 1H, NHBoc, *J* = 8.0 Hz); 5.93 (d, 1H, H-3, *J* = 4.0 Hz); 7.15 (t, 1H, H-7, *J* = 8.0 Hz); 7.21 (t, 1H, H-6, *J* = 8.0 Hz); 7.35 (d, 1H, H-8, *J* = 8.0 Hz); 7.53 (d, 1H, H-5, *J* = 8.0 Hz); 7.95 (s, 1NH); (B) δ: 1.60 (s, 9H, Boc); 2.55-2.62 (m, 1H, H-2'a); 3.05-3.18 (m, 2H, H-4a and H-2'b); 3.46-3.57 (m, 3H, H-4b and H-3'); 3.66 (s, 3H, CH₃); 4.44 (d, 1H, H-1a, *J* = 16.0 Hz); 4.98 (d, 1H, H-3, *J* = 4.0 Hz); 5.27 (d, 1H, H-1b, *J* = 16.0 Hz); 5.32 (d, 1H, NHBoc, *J* = 8.0 Hz); 7.15 (t, 1H, H-7, *J* = 8.0 Hz); 7.21 (t, 1H, H-6, *J* = 8.0 Hz); 7.35 (d, 1H, H-8, *J* = 8.0 Hz); 7.53 (d, 1H, H-5, *J* = 8.0 Hz); 8.00 (s, 1NH); ¹³C NMR (CDCl₃, 100 MHz) (A + B) δ: 22.9; 23.9; 28.4; 34.0; 34.2; 36.2; 39.0; 41.4; 50.6; 52.5; 52.8; 54.8; 79.6; 110.9; 118.09; 118.3; 118.6; 119.5; 119.8; 122.1; 122.3; 126.6; 128.1; 136.5; 170.8; 171.4. HR-MS *m/z* calcd for C₂₁H₂₈N₃O₅, 402.2023; [(M+H)⁺]:402.2022.

(S)-methyl 2-(2-((tert-butoxycarbonyl)amino)acetyl)-2,3,4,9-tetrahydro-1H-pyrido[3,4-b]indole-3-carboxylate (92).

72% yield. ¹H NMR (CDCl₃, 400 MHz): (A) δ: 1.50 (s, 9H, Boc); 3.10-3.16 (m, 1H, H-4a); 3.48 (d, 1H, H-4b, *J* = 16.0 Hz); 3.62 (s, 3H, CH₃); 4.12 (dd, 1H, H-2'a, *J*' = 4.0, *J*" = 8.0 Hz); 4.23-4.26 (m, 1H, H-2'b); 4.65 (d, 1H, H-1a, *J* = 12.0 Hz); 4.76 (d, 1H, H-1b, *J* = 12.0 Hz); 5.59 (d, 1H, NHBoc, *J* = 8.0 Hz); 5.86 (d, 1H, H-3, *J* = 4.0 Hz); 7.12-7.23 (m, 2H, H-6 and H-7); 7.28-7.37 (m, 1H, H-8); 7.50-7.53 (m, 1H, H-5); 8.42 (s, 1H, NH); (B) δ: 1.51 (s, 9H, Boc); 3.10-3.16 (m, 1H, H-4a); 3.50 (d, 1H, H-4b, *J* = 16.0 Hz); 3.65 (s, 3H, CH₃); 4.20 (dd, 1H, H-2'a, *J*' = 4.0, *J*" = 8.0 Hz); 4.23-4.26 (m, 1H, H-2'b); 4.51 (d, 1H, H-1a, *J* = 12.0 Hz); 4.78 (d, 1H, H-3, *J* = 4.0 Hz); 5.23 (d, 1H, H-1b, *J* = 12.0 Hz); 5.57 (d, 1H, NHBoc, *J* = 8.0 Hz); 7.12-7.23 (m, 2H, H-6 and H-7); 7.28-7.37 (d, 1H, H-8); 7.50-7.53 (d, 1H, H-5); 8.42 (s, 1H, NH); ¹³C NMR (CDCl₃, 100 MHz) (A + B) δ: 22.8; 23.8; 28.4; 28.4; 39.5; 40.5; 43.0; 51.2; 52.6; 52.9; 54.1; 80.1; 105.0; 106.7;

111.01; 111.06; 118.0; 118.2; 119.64; 119.75; 122.1; 122.3; 126.5; 127.5; 128.8; 136.5; 155.8; 169.2; 170.4; 171.3. HR-MS m/z : calcd for $C_{20}H_{26}N_3O_5$, $[(M+H)^+]$: 388.1867; found 388.1864.

(S)-methyl 2-((S)-2-((tert-butoxycarbonyl)amino)propanoyl)-2,3,4,9-tetrahydro-1H-pyrido[3,4-b]indole-3-carboxylate (93).

69% yield. 1H NMR ($CDCl_3$, 400 MHz): (**A**) δ : 1.42-1.50 (m, 12H, Boc and CH_3); 2.85 (dd, 1H, H-4a, $J' = 4.0$ and $J'' = 16.0$ Hz); 3.36 (d, 1H, H-4b, $J = 16.0$ Hz); 3.65 (s, 3H, CH_3); 4.81-4.91 (m, 2H, H1a and H-2'); 5.00 (d, 1H, H-1b, $J = 16.0$ Hz); 5.58 (d, 1H, NHBoc, $J = 8.0$ Hz); 5.89 (d, 1H, H-3, $J = 4.0$ Hz); 7.12-7.18 (m, 2H, H-6 and H-7); 7.21 (d, 1H, H-8, $J = 8.0$ Hz); 7.49 (d, 1H, H-5, $J = 8.0$ Hz); 8.17 (s, 1H, NH); (**B**) δ : 1.42-1.50 (m, 12H, Boc and CH_3); 3.18 (dd, 1H, H-4a, $J' = 8.0$ and $J'' = 16.0$ Hz); 3.57 (d, 1H, H-4b, $J = 16.0$ Hz); 3.63 (s, 3H, CH_3); 4.54 (d, 1H, H1a, $J = 16.0$ Hz); 4.71-4.74 (m, 1H, H-2'); 5.11 (d, 1H, H-3, $J = 4.0$ Hz); 5.20 (d, 1H, H-1b, $J = 16.0$ Hz); 5.56 (d, 1H, NHBoc, $J = 8.0$ Hz); 7.12-7.18 (m, 2H, H-6 and H-7); 7.23 (d, 1H, H-8, $J = 8.0$ Hz); 7.51 (d, 1H, H-5, $J = 8.0$ Hz); 8.16 (s, 1H, NH); ^{13}C NMR ($CDCl_3$, 100 MHz) (**A + B**) δ : 18.6; 19.7; 22.5; 24.1; 28.4; 39.7; 41.3; 47.0; 51.1; 52.5; 52.84; 54.87; 80.0; 110.9; 118.2; 119.7; 122.2; 126.5; 127.6; 136.4; 136.5; 155.3; 171.3; 173.5. HR-MS m/z : calcd for $C_{21}H_{28}N_3O_5$, $[(M+H)^+]$: 402.2023; found 402.2019.

(S)-methyl-2-((S)-1-(tert-butoxycarbonyl)pyrrolidine-2-carbonyl)-2,3,4,9-tetrahydro-1H-pyrido[3,4-b]indole-3-carboxylate (94).

63% yield. 1H NMR ($CDCl_3$, 400 MHz): (**A**) δ : 1.43 (s, 9H, Boc); 1.79-1.87 (m, 3H, $CH_2 \gamma$ and H-4a); 1.98-2.11 (m, 2H, $CH_2 \beta$); 2.84 (d, 1H, H-4b, $J = 16.0$ Hz); 3.46 (s, 3H, CH_3); 3.50-3.64 (m, 2H, $CH_2 \delta$); 4.60 (δ , 1H, H1a $J = 16.0$ Hz); 4.80-4.87 (m, 2H, H-1b, and H-2'); 5.49 (d, 1H, H-3, $J = 8.0$ Hz); 6.97-7.10 (m, 2H, H-6 and H-7); 7.23-7.30 (m, 1H, H-8); 7.46 (d, 1H, H-5, $J = 8.0$ Hz); 8.08 (s, 1H, NH); (**B**) δ : 1.43 (s, 9H, Boc); 1.67-1.75 (m, 2H, $CH_2 \gamma$); 2.12-2.20 (m, 2H, $CH_2 \beta$); 2.96 (dd, 1H, H-4a, $J' = 4.0$, $J'' = 16.0$ Hz); 3.40-3.56 (m, 6H, CH_3 H-4b, $CH_2 \delta$); 4.44 (δ , 1H, H1a $J = 16.0$ Hz); 4.70 (m, 1H, H-2'); 4.93 (δ , 1H, H1b $J = 16.0$ Hz); 5.87 (d, 1H, H-3, $J = 8.0$ Hz); 6.97-7.10 (m, 2H, H-6 and H-7); 7.23-

7.30 (m, 1H, H-8); 7.40 (d, 1H, H-5, $J = 8.0$ Hz); 8.33 (s, 1H, NH); ^{13}C NMR (CDCl_3 , 100 MHz) (**A + B**) δ : 21.2; 22.8; 23.5; 24.0; 28.3; 28.4; 29.0; 30.0; 41.1; 41.3; 46.3; 46.6; 46.9; 50.9; 51.1; 52.2; 52.4; 52.7; 57.1; 57.4; 79.8; 80.2; 106.2; 108.4; 111.1; 117.9; 118.2; 119.0; 119.7; 121.7; 122.2; 126.4; 127.2; 128.1; 129.1; 136.8; 171.9; 173.0. HR-MS m/z : calcd for $\text{C}_{23}\text{H}_{30}\text{N}_3\text{O}_5$, $[(\text{M}+\text{H})^+]$: 428.2180; found 428.2184.

(S)-methyl 2-((R)-2-((tert-butoxycarbonyl)amino)-3-phenylpropanoyl)-2,3,4,9-tetrahydro-1H-pyrido[3,4-b]indole-3-carboxylate (95).

65% yield. ^1H NMR (CDCl_3 , 400 MHz): (**A**) δ : 1.50 (s, 9H, Boc); 2.94-3.05 (m, 3H, H-4a and CH_2); 3.42 (d, 1H, H-4b, $J = 12.0$ Hz); 3.60 (s, 3H, CH_3); 4.37 (d, 1H, H1a, $J = 16.0$ Hz); 4.69 (d, 1H, H-1b, $J = 16.0$ Hz); 4.98-5.02 (m, 1H, H-2'); 5.61 (d, 1H, NHBoc, $J = 8.0$ Hz); 5.86 (d, 1H, H-3, $J = 4.0$ Hz); 7.01 (t, 1H, H-7, $J = 8.0$ Hz); 7.11-7.21 (m, 4H, H-6 and aryl); 7.24-7.32 (m, 3H, H-8 and aryl); 7.50 (d, 1H, H-5, $J = 8.0$ Hz); 7.96 (s, 1H, NH); (**B**) δ : 1.48 (s, 9H, Boc); 2.94-3.05 (m, 2H, CH_2); 3.16-3.21 (m, 1H, H-4a); 3.51 (d, 1H, H-4b, $J = 12.0$ Hz); 3.58 (s, 3H, CH_3); 4.51 (d, 1H, H1a, $J = 16.0$ Hz); 4.98-5.02 (m, 1H, H-2'); 5.35 (t, 1H, H-3, $J = 4.0$ Hz); 5.38 (d, 1H, H-1b, $J = 16.0$ Hz); 5.61 (d, 1H, NHBoc, $J = 8.0$ Hz); 6.86 (t, 1H, H-7, $J = 8.0$ Hz); 7.11-7.21 (m, 4H, H-6 and aryl); 7.24-7.32 (m, 3H, H-8 and aryl); 7.50 (d, 1H, H-5, $J = 8.0$ Hz); 8.57 (s, 1H, NH); ^{13}C NMR (CDCl_3 , 100 MHz) (**A + B**) δ : 22.9; 24.4; 28.3; 28.4; 38.7; 39.4; 40.7; 41.2; 51.1; 51.9; 52.3; 52.5; 52.8; 55.0; 80.0; 105.3; 106.4; 110.9; 111.0; 118.04; 118.08; 119.51; 119.54; 121.91; 122.05; 126.5; 126.7; 126.8; 127.9; 128.2; 128.5; 129.1; 129.5; 135.8; 136.4; 155.1; 170.6; 170.10; 171.7; 172.2. HR-MS m/z : calcd for $\text{C}_{27}\text{H}_{32}\text{N}_3\text{O}_5$, $[(\text{M}^+\text{H})^+]$: 478.2336; found 478.2325.

(S)-methyl 2-((S)-2-(((benzyloxy)carbonyl)amino)-4-methylpentanoyl)-2,3,4,9-tetrahydro-1H-pyrido[3,4-b]indole-3-carboxylate (96).

60% yield. ^1H NMR (CDCl_3 , 400 MHz): (**A**) δ : 1.00 (d, 3H, CH_3 , $J = 8.0$ Hz); 1.07 (d, 3H, CH_3 , $J = 8.0$ Hz); 1.57-1.71 (m, 2H, CH_2); 1.84-1.87 (m, 1H, CH); 2.70 (dd, 1H, H-4a, $J' = 4.0$, $J'' = 16.0$ Hz); 3.25 (d, 1H, H-4b, $J = 16.0$ Hz); 3.60 (s, 3H, CH_3); 4.85 (d, 1H, H1a, $J = 12.0$ Hz); 4.96 (t, 1H, H-2', $J = 12.0$ Hz);

5.05-5.18 (m, 3H, H-1b and CH₂ benzyl); 5.77 (d, 1NH, *J* = 12.0 Hz); 5.87 (d, 1H, H-3, *J* = 4.0 Hz); 7.11-7.20 (m, 2H, H-6 and H-7); 7.24 (d, 1H, H-8, *J* = 8.0 Hz); 7.29-7.38 (m, 5H, aryl); 7.44 (d, 1H, H-5, *J* = 8.0 Hz); 8.56 (s, 1H, NH); (**B**) δ: 1.00 (d, 3H, CH₃, *J* = 8.0 Hz); 1.07 (d, 3H, CH₃, *J* = 8.0 Hz); 1.57-1.71 (m, 2H, CH₂); 1.84-1.87 (m, 1H, CH); 3.18 (dd, 1H, H-4a, *J*' = 4.0, *J*'' = 16.0 Hz); 3.59-3.65 (m, 4H, H-4b and CH₃); 4.52 (d, 1H, H1a, *J* = 16.0 Hz); 4.84-4.87 (m, 1H, H-2'); 5.05-5.18 (m, 3H, H-1b and CH₂ benzyl); 5.21 (d, 1H, H-3, *J* = 4.0 Hz); 5.77 (d, 1NH, *J* = 12.0 Hz); 7.11-7.20 (m, 2H, H-6 and H-7); 7.24 (d, 1H, H-8, *J* = 8.0 Hz); 7.29-7.38 (m, 5H, aryl); 7.52 (d, 1H, H-5, *J* = 8.0 Hz); 8.37 (s, 1H, NH); ¹³C NMR (CDCl₃, 100 MHz) (**A** + **B**) δ: 21.9; 22.3; 22.4; 23.19; 23.26; 24.0; 24.7; 39.9; 41.3; 41.8; 43.1; 49.9; 50.1; 51.1; 52.5; 52.8; 55.0; 60.4; 67.00; 67.16; 105.1; 106.6; 111.0; 118.03; 118.15; 119.51; 119.63; 122.02; 122.09; 126.5; 127.6; 127.97; 128.02; 128.14; 128.19; 128.5; 129.2; 136.1; 136.6; 156.3; 156.6; 170.5; 171.4; 173.32. HR-MS *m/z*: calcd for C₂₇H₃₂N₃O₅, [(M⁺H)⁺]: 478.2336; found 478.2328.

(S)-methyl 2-((S)-2-(((9H-fluoren-9-yl)methoxy)carbonyl)amino)-3-phenylpropanoyl)-2,3,4,9-tetrahydro-1H-pyrido[3,4-b]indole-3-carboxylate (97).

61% yield. ¹H NMR (CDCl₃, 400 MHz): (**A**) δ: 2.98 (dd, 1H, H-4a, *J*' = 4.0, *J*'' = 16.0 Hz); 3.27-3.34 (m, 2H, CH₂a,b); 3.45 (d, 1H, H-4b, *J* = 16.0 Hz); 3.63 (s, 3H, CH₃); 4.17-4.24 (m, 1H, CHFmoc); 4.38-4.47 (m, 2H, CH₂Fmoc); 4.77 (d, 1H, H1a, *J* = 12.0 Hz); 5.02-5.14 (m, 1H, H-1b); 5.19 (q, 1H, H-2'); 5.96 (d, 2H, H-3 and NHFmoc, *J* = 8.0 Hz); 7.11-7.50 (m, 15H, H-6, H-7, H-8 and aryl); 7.61 (t, 1H, aryl, *J* = 8.0 Hz); 7.78 (d, 1H, H-5, *J* = 8.0 Hz); 8.29 (s, 1H, NH); (**B**) δ: 2.40 (dd, 1H, H-4a, *J*' = 4.0, *J*'' = 16.0 Hz); 3.07 (dd, 1H, CH₂a, *J*' = 8.0, *J*'' = 16.0 Hz); 3.15-3.19 (m, 1H, CH₂b); 3.27-3.34 (m, 1H, H-4b); 3.56 (s, 3H, CH₃); 4.17-4.24 (m, 1H, CHFmoc); 4.30 (q, 2H, CH₂Fmoc); 4.53 (d, 1H, H1a, *J* = 12.0 Hz); 4.93 (d, 1H, H-3, *J* = 4.0 Hz); 5.02-5.14 (m, 2H, H-1b and H-2'); 5.87 (d, 1H, NHFmoc, *J* = 8.0 Hz); 7.11-7.50 (m, 15H, H-6, H-7, H-8 and aryl); 7.56 (t, 1H, aryl, *J* = 8.0 Hz); 7.80 (d, 1H, H-5, *J* = 8.0 Hz); 8.23 (s, 1H, NH); ¹³C NMR (CDCl₃, 100 MHz) (**A** + **B**) δ: 22.7; 23.3; 31.6; 38.6; 40.0; 40.2; 41.5; 47.05;

47.08; 50.8; 51.3; 52.5; 52.67; 52.72; 52.86; 55.4; 65.9; 67.2, 105.2; 106.8; 110.96; 110.99; 118.06; 118.22; 119.62; 119.71; 120.00; 122.04; 122.26; 125.09; 125.14; 125.21; 126.5; 127.08; 127.12; 127.27; 127.7; 128.5; 128.8; 129.4; 129.7; 135.8; 136.5; 141.3; 143.9; 155.6; 155.9; 170.5; 171.2; 171.8; 172.3. HR-MS m/z : calcd for $C_{37}H_{34}N_3O_5$, $[(M+H)^+]$: 600.2493; found 600.2499.

(R)-methyl 2-((S)-2-((tert-butoxycarbonyl)amino)-3-phenylpropanoyl)-2,3,4,9-tetrahydro-1H-pyrido[3,4-b]indole-3-carboxylate (98).

66% yield. 1H NMR ($CDCl_3$, 400 MHz): (**A**) δ : 1.50 (s, 9H, Boc); 2.94-3.05 (m, 3H, H-4a and CH_2); 3.42 (d, 1H, H-4b, $J = 12.0$ Hz); 3.60 (s, 3H, CH_3); 4.37 (d, 1H, H1a, $J = 16.0$ Hz); 4.69 (d, 1H, H-1b, $J = 16.0$ Hz); 4.98-5.02 (m, 1H, H-2'); 5.61 (d, 1H, NHBoc, $J = 8.0$ Hz); 5.86 (d, 1H, H-3, $J = 4.0$ Hz); 7.01 (t, 1H, H-7, $J = 8.0$ Hz); 7.11-7.21 (m, 4H, H-6 and aryl); 7.24-7.32 (m, 3H, H-8 and aryl); 7.50 (d, 1H, H-5, $J = 8.0$ Hz); 7.96 (s, 1H, NH); (**B**) δ : 1.48 (s, 9H, Boc); 2.94-3.05 (m, 2H, CH_2); 3.16-3.21 (m, 1H, H-4a); 3.51 (d, 1H, H-4b, $J = 12.0$ Hz); 3.58 (s, 3H, CH_3); 4.51 (d, 1H, H1a, $J = 16.0$ Hz); 4.98-5.02 (m, 1H, H-2'); 5.35 (t, 1H, H-3, $J = 4.0$ Hz); 5.38 (d, 1H, H-1b, $J = 16.0$ Hz); 5.61 (d, 1H, NHBoc, $J = 8.0$ Hz); 6.86 (t, 1H, H-7, $J = 8.0$ Hz); 7.11-7.21 (m, 4H, H-6 and aryl); 7.24-7.32 (m, 3H, H-8 and aryl); 7.50 (d, 1H, H-5, $J = 8.0$ Hz); 8.57 (s, 1H, NH); ^{13}C NMR ($CDCl_3$, 100 MHz) (**A + B**) δ : 22.9; 24.4; 28.29; 28.42; 38.7; 39.4; 40.7; 41.2; 51.1; 51.8; 52.3; 52.5; 52.8; 55.0; 80.0; 105.3; 106.4; 110.9; 111.0; 118.04; 118.08; 119.51; 119.54; 121.91; 122.05; 126.5; 126.73; 126.83; 127.9; 128.2; 128.5; 129.1; 129.5; 135.8; 136.4; 155.2; 170.6; 171.0; 171.7; 172.21. HR-MS m/z : calcd for $C_{27}H_{32}N_3O_5$, $[(M+H)^+]$: 478.2336; found 478.2325.

(S)-2-((S)-2-((tert-butoxycarbonyl)amino)-3-phenylpropanoyl)-2,3,4,9-tetrahydro-1H-pyrido[3,4-b]indole-3-carboxylic acid (99).

63% yield. 1H NMR ($CDCl_3$, 400 MHz): (**A**) δ : 1.36 (s, 9H, Boc); 2.80-2.88 (m, 2H, H-4a and CH_2a); 3.06-3.15 (m, 1H, CH_2b); 3.29-3.41 (m, 1H, H-4b); 4.62 (d, 1H, H-1a, $J = 12.0$ Hz); 4.96-5.08 (m, 2H, H1b and H-2'); 5.56 (d, 1H, NHBoc, $J = 8.0$ Hz); 5.87 (d, 1H, H-3, $J = 4.0$ Hz); 7.06-7.29 (m, 8H, H-6, H-7, H-8 and

aryl); 7.46 (d, 1H, H-5, $J = 8.0$ Hz); 8.49 (s, 1H, NH); (**B**) δ : 1.23 (s, 9H, Boc); 2.37-2.44 (m, 1H, CH_2a); 2.94-3.03 (m, 1H, H-4a); 3.06-3.15 (m, 1H, H-4b); 3.29-3.41 (m, 1H, CH_2b); 4.40 (d, 1H, H-1a, $J = 12.0$ Hz); 4.96-5.08 (m, 3H, H-1b, H-3 and H-2'); 5.63 (d, 1H, NHBoc, $J = 8.0$ Hz); 7.06-7.29 (m, 8H, H-6, H-7, H-8 and aryl); 7.40 (d, 1H, H-5, $J = 8.0$ Hz); 8.19 (s, 1H, NH); ^{13}C NMR ($CDCl_3$, 100 MHz) (**A** + **B**) δ : 22.6; 23.2; 28.3; 28.3; 29.7; 38.4; 39.8; 40.1; 41.4; 51.2; 53.4; 55.3; 60.5; 80.5; 105.3; 106.5; 111.03; 111.09; 118.02; 118.12; 119.47; 119.53; 121.8; 122.1; 126.5; 126.8; 127.1; 127.9; 128.25; 128.35; 128.58; 128.64; 129.1; 129.37; 129.46; 129.7; 135.8; 136.36; 136.53; 155.37; 155.55; 172.3; 172.9; 174.0; 175.2; 176.38. HR-MS m/z : calcd for $C_{26}H_{29}N_3O_5$, $[(M+H)^+]$: 464.2180; found 464.2185.

Synthesis of tert-butyl ((S)-1-((S)-3-(ethylcarbamoyl)-3,4-dihydro-1H-pyrido[3,4-b]indol-2(9H)-yl)-1-oxo-3-phenylpropan-2-yl)carbamate (100).

Acid intermediate **99** (2 mmol) was dissolved in 10 mL of DCM/DMF (7:3 v:v) and ethylamine hydrochloride (2.4 mmol), PyBop (2.4 mmol) and DIPEA (4.4 mmol) were successively added. Stirring was continued at room temperature for 12 h. Afterward, the reaction mixture was concentrated *in vacuo*, diluted with dichloromethane (20 mL), and washed successively with 10% citric acid (2 x 25 mL), 10% $NaHCO_3$ (2 x 25 mL), and water (2 x 25 mL), dried over Na_2SO_4 and evaporated to dryness. Flash chromatography of the residues with ethyl acetate yielded **100** as rotamers mixture.

59% yield. 1H NMR ($CDCl_3$, 400 MHz): (**A**) δ : 1.10 (t, 3H, CH_3 , $J = 8.0$ Hz); 1.46 (s, 9H, Boc); 1.66 (dd, 1H, H-4a, $J' = 8.0$, $J'' = 16.0$ Hz); 2.97-3.11 (m, 2H, H-3'a and H-3'b); 3.15-3.28 (m, 2H, CH_2); 3.32 (d, 1H, H-4b, $J = 16.0$ Hz); 4.09 (d, 1H, H-1a, $J = 20.0$ Hz); 4.78 (d, 1H, H-3, $J = 8.0$ Hz); 4.84 (q, 1H, H-2'); 5.45 (d, 1H, H-1b, $J = 16.0$ Hz); 5.60 (d, 1H, NHBoc, $J = 8.0$ Hz); 7.04-7.23 (m, 8H, H-6, H-7, H-8 and aryl); 7.40 (d, 1H, H-5, $J = 8.0$ Hz); 7.53 (t, 1H, NH, $J = 8.0$ Hz); 8.64 (s, 1NH). (**B**) δ : 0.97 (t, 3H, CH_3 , $J = 8.0$ Hz); 1.46 (s, 9H, Boc); 2.89 (dd, 1H, H-4a, $J' = 8.0$, $J'' = 16.0$ Hz); 2.97-3.11 (m, 2H, H-3'a and H-3'b); 3.15-3.28 (m, 2H, CH_2); 3.37 (d, 1H, H-4b, $J = 16.0$ Hz); 4.50 (d, 1H, H-1a, $J = 16.0$ Hz); 5.07 (d, 1H, H-1b, $J = 16.0$ Hz); 5.13 (q, 1H, H-2'); 5.57 (d, 1H, NHBoc, $J = 8.0$ Hz); 5.70

(d, 1H, H-3, $J = 8.0$ Hz); 7.04-7.23 (m, 8H, H-6, H-7, H-8 and aryl); 7.46 (d, 1H, H-5, $J = 8.0$ Hz); 7.53 (t, 1H, NH, $J = 8.0$ Hz); 8.85 (s, 1NH). ^{13}C NMR (CDCl_3 , 100 MHz) (**A + B**) δ : 14.4; 14.7; 21.4; 22.1; 28.31; 28.38; 34.6; 35.0; 38.63; 38.80; 39.4; 41.7; 52.4; 56.1; 65.9; 80.2; 80.7; 106.5; 110.8; 111.0; 118.09; 118.16; 119.1; 119.3; 121.5; 121.8; 126.6; 127.1; 127.4; 127.90; 127.97; 128.47; 128.58; 129.0; 129.2; 129.5; 135.4; 136.5; 155.3; 156.2; 168.3; 169.5; 172.4; 172.6. HR-MS m/z : calcd for $\text{C}_{28}\text{H}_{35}\text{N}_4\text{O}_4$, $[(\text{M}+\text{H})^+]$: 491.2653; found 491.2658.

(S)-tert-butyl (1-(3,4-dihydro-1H-pyrido[3,4-b]indol-2(9H)-yl)-1-oxo-3-phenylpropan-2-yl)carbamate (101).

67% yield. ^1H NMR (CDCl_3 , 400 MHz) : (**A**) δ : 1.44 (s, 9H, Boc); 2.72-2.80 (m, 2H, H-4a,b); 2.95-3.12 (m, 2H, CH_2 a,b); 3.64-3.71 (m, 1H, H-3a); 3.95-4.01 (m, 1H, H-3b); 4.68 (d, 1H, H-1a, $J = 16.0$ Hz); 4.85 (d, 1H, H-1b, $J = 16.0$ Hz); 5.04 (q, 1H, H-2'); 5.44 (d, 1H, NHBoc, $J = 8.0$ Hz); 7.07-7.35 (m, 8H, H-6, H-7, H-8 and aryl); 7.43 (d, 1H, H-5, $J = 8.0$ Hz); 7.94 (s, 1H, NH); (**B**) δ : 1.60 (s, 9H, Boc); 2.39-2.46 (m, 2H, H-4a,b); 2.95-3.12 (m, 2H, CH_2 a,b); 3.42-3.49 (m, 1H, H-3a); 3.79-3.85 (m, 1H, H-3b); 4.53 (d, 1H, H-1a, $J = 16.0$ Hz); 4.85 (d, 1H, H-1b, $J = 16.0$ Hz); 4.90 (q, 1H, H-2'); 5.55 (d, 1H, NHBoc, $J = 8.0$ Hz); 6.97 (t, 1H, H-7, $J = 8.0$ Hz); 7.07-7.35 (m, 7H, H-6, H-8 and aryl); 7.47 (d, 1H, H-5, $J = 8.0$ Hz); 7.75 (s, 1H, NH); ^{13}C NMR (CDCl_3 , 100 MHz) (**A + B**) δ : 20.8; 21.7; 28.4; 40.4; 40.70; 40.75; 43.2; 43.8; 51.7; 52.1; 79.6; 110.1; 118.0; 119.7; 120.1; 122.0; 127.0; 128.3; 128.5; 129.25; 129.43; 136.1; 136.3; 171.0; 171.4. HR-MS m/z calcd for $\text{C}_{25}\text{H}_{30}\text{N}_3\text{O}_3$, $[(\text{M}+\text{H})^+]$: 420.2282; found 420.2285.

(1S, 3S)-methyl 2-(2-((tert-butoxycarbonyl)amino)acetyl)-1-(4-chlorophenyl)-2,3,4,9-tetrahydro-1H-pyrido[3,4-b]indole-3-carboxylate (102a).

52% yield. ^1H NMR (CDCl_3 , 400 MHz) : (**A**) δ : 1.49 (s, 9H, Boc); 2.97 (dd, 1H, H-4a, $J' = 8.0$, $J'' = 16.0$ Hz); 3.64 (d, 1H, H-4b, $J = 16.0$ Hz); 3.80 (s, 3H, CH_3); 4.10 (d, 1H, H-2'a, $J'' = 12.0$ Hz); 4.24 (d, 1H, H-2'b, $J'' = 12.0$ Hz); 4.65 (d, 1H, H-3, $J = 8.0$ Hz); 5.28 (s, 1H, NH-Boc); 6.81 (s, 1H, H-1); 7.18-7.32 (m, 7H, H-6, H-7, H-8 and aryl); 7.55 (d, 1H, H-5, $J = 8.0$ Hz); 8.03 (s, 1H, NH-9). (**B**) δ : 1.58 (s, 9H, Boc); 2.55 (dd, 1H, H-4a, $J' = 8.0$, $J'' = 16.0$ Hz); 3.25-3.30 (m, 1H, H-

4b); 3.72 (s, 3H, CH_3); 4.14 (d, 1H, H-2'a, $J'' = 12.0$ Hz); 4.21 (d, 1H, H-2'b, $J'' = 12.0$ Hz); 4.48 (d, 1H, H-3, $J = 8.0$ Hz); 5.33 (s, 1H, NH-Boc); 6.83 (s, 1H, H-1); 7.18-7.32 (m, 7H, H-6, H-7, H-8 and aryl); 7.59 (d, 1H, H-5, $J = 8.0$ Hz); 8.03 (s, 1H, NH-9). ^{13}C NMR ($CDCl_3$, 100 MHz) (**A + B**) δ : 22.1; 22.2; 28.55; 28.63; 43.1; 52.7; 53.2; 58.1, 58.7; 62.1; 80.0; 106.5; 111.2; 113.6; 118.0; 119.2; 121.6; 126.4; 130.2; 130.8; 136.8; 139.3; 157.5; 168.0; 170.4. HR-MS m/z : calcd for $C_{26}H_{29}ClN_3O_5$, $[(M+H)^+]$: 498.1790, 500.1761; found 498.1783, 500.1765.

(1R, 3S)-methyl 2-(2-((tert-butoxycarbonyl)amino)acetyl)-1-(4-chlorophenyl)-2,3,4,9-tetrahydro-1H-pyrido[3,4-b]indole-3-carboxylate (102b).

62% yield. 1H NMR (CD_3OD , 400 MHz) : (**A**) δ : 1.39 (s, 9H, Boc); 3.14 (dd, 1H, H-4a, $J' = 8.0$, $J'' = 16.0$ Hz); 3.72-3.75 (m, 4H, CH_3 and H-4b); 3.99 (d, 1H, H-2'a, $J = 16.0$ Hz); 4.10 (d, 1H, H-2'b, $J = 16.0$ Hz); 5.02-5.06 (m, 1H, H-3); 5.59 (s, 1H, NH-Boc); 6.08 (s, 1H, H-1); 7.11-7.28 (m, 7H, H-6, H-7, H-8 and aryl); 7.49 (d, 1H, H-5, $J = 8.0$ Hz); 8.04 (s, 1H, NH-9). (**B**) δ : 1.41 (s, 9H, Boc); 3.07 (dd, 1H, H-4a, $J' = 8.0$, $J'' = 16.0$ Hz); 3.72-3.75 (m, 4H, CH_3 and H-4b); 4.03 (d, 1H, H-2'a, $J = 16.0$ Hz); 4.25 (d, 1H, H-2'b, $J = 16.0$ Hz); 5.02-5.06 (m, 1H, H-3); 5.66 (s, 1H, NH-Boc); 6.21 (s, 1H, H-1); 7.11-7.28 (m, 7H, H-6, H-7, H-8 and aryl); 7.54 (d, 1H, H-5, $J = 8.0$ Hz); 8.10 (s, 1H, NH-9). ^{13}C NMR ($CDCl_3$, 100 MHz) (**A + B**) δ : 23.4; 23.6; 28.33; 28.39; 43.1; 52.4; 56.0; 57.2; 80.1; 107.1; 110.6; 114.2; 118.5; 119.1; 121.8; 127.5; 128.9; 130.0; 136.4; 138.9; 155.1; 170.3; 172.1. HR-MS m/z : calcd for $C_{26}H_{29}ClN_3O_5$, $[(M+H)^+]$: 498.1790, 500.1761; found 498.1797, 500.1770.

(1S, 3S)-methyl 2-(2-((tert-butoxycarbonyl)amino)acetyl)-1-(4-methoxyphenyl)-2,3,4,9-tetrahydro-1H-pyrido[3,4-b]indole-3-carboxylate (103a).

54% yield. 1H NMR ($CDCl_3$, 400 MHz) : δ : 1.46 (s, 9H, Boc); 3.05 (dd, 1H, H-4a, $J' = 8.0$, $J'' = 16.0$ Hz); 3.10 (s, 3H, OCH_3); 3.68 (d, 1H, H-4b, $J = 16.0$ Hz); 3.78 (s, 3H, CH_3); 4.12 (d, 1H, H-2'a, $J'' = 12.0$ Hz); 4.25 (d, 1H, H-2'b, $J'' = 12.0$ Hz); 4.73 (d, 1H, H-3, $J = 8.0$ Hz); 5.63 (s, 1H, NH-Boc); 6.79 (d, 2H, aryl, $J = 8.0$ Hz); 6.94 (s, 1H, H-1); 7.16-7.24 (m, 4H, H-6, H-7 and aryl); 7.29 (d, 1H,

H-8, $J = 8.0$ Hz); 7.62 (d, 1H, H-5, $J = 8.0$ Hz); 7.80 (s, 1H, NH-9). ^{13}C NMR (CDCl_3 , 100 MHz) δ : 21.6; 28.4; 43.1; 51.6; 51.9; 52.3; 55.3; 79.8; 107.5; 111.0; 113.5; 118.6; 119.8; 122.5; 126.4; 129.9; 130.8; 136.4; 155.7; 159.4; 168.7; 170.0. HR-MS m/z : calcd for $\text{C}_{27}\text{H}_{32}\text{N}_3\text{O}_6$, $[(\text{M}+\text{H})^+]$: 494.2286; found 494.2288.

(1R,3S)-methyl 2-(2-((tert-butoxycarbonyl)amino)acetyl)-1-(4-methoxyphenyl)-2,3,4,9-tetrahydro-1H-pyrido[3,4-b]indole-3-carboxylate (103b).

65% yield. ^1H NMR (CDCl_3 , 400 MHz) : (A) δ : 1.43 (s, 9H, Boc); 3.26 (dd, 1H, H-4a, $J' = 8.0$, $J'' = 16.0$ Hz); 3.65-3.70 (m, 4H, OCH_3 and H-4b); 3.78 (s, 3H, CH_3); 4.08-4.16 (m, 1H, H-2'a and H-2'b); 5.10-5.14 (m, 1H, H-3); 5.48 (s, 1H, NH-Boc); 5.96 (s, 1H, H-1); 6.84 (d, 2H, aryl, $J = 8.0$ Hz); 7.11-7.19 (m, 2H, H-6, and H-7); 7.23-7.27 (m, 3H, H-8 and aryl); 7.54 (d, 1H, H-5, $J = 8.0$ Hz); 7.86 (s, 1H, NH-9). (B) δ : 1.43 (s, 9H, Boc); 3.26 (dd, 1H, H-4a, $J' = 8.0$, $J'' = 16.0$ Hz); 3.65-3.70 (m, 4H, OCH_3 and H-4b); 3.78 (s, 3H, CH_3); 4.08-4.16 (m, 1H, H-2'a and H-2'b); 4.94-4.97 (m, 1H, H-3); 5.48 (s, 1H, NH-Boc); 6.08 (s, 1H, H-1); 6.84 (d, 2H, aryl, $J = 8.0$ Hz); 7.11-7.19 (m, 2H, H-6, and H-7); 7.23-7.27 (m, 3H, H-8 and aryl); 7.54 (d, 1H, H-5, $J = 8.0$ Hz); 7.86 (s, 1H, NH-9). ^{13}C NMR (CDCl_3 , 100 MHz) (A + B) δ : 22.5; 28.3; 43.9; 50.9; 52.4; 55.3; 56.8; 79.6; 108.5; 111.1; 114.8; 118.4; 119.9; 122.5; 126.3; 127.9; 136.7; 155.6; 171.2; 171.5. HR-MS m/z : calcd for $\text{C}_{27}\text{H}_{32}\text{N}_3\text{O}_6$, $[(\text{M}+\text{H})^+]$: 494.2286; found 494.2272.

General procedure for the synthesis of derivatives 104 and 105.

A solution of N-Boc-L-Phe-OH (8.0 mmol), 2-chloro-1-methylpyridinium iodide (Mukaiyama reagent, 8.0 mmol) and triethylamine (8.0 mmol) in dichloromethane (50 mL) was refluxed for 15 min. Then (1S,3S)/(1R,3S)-methyl 1-(4-methoxyphenyl)-2,3,4,9-tetrahydro-1H-pyrido[3,4-b]indole-3-carboxylate (4 mmol) or (1S,3S)/(1R,3S)-methyl 1-isobutyl-2,3,4,9-tetrahydro-1H-pyrido[3,4-b]indole-3-carboxylate (4 mmol) was added. Stirring was continued for 24 h. Afterward, the reaction mixture was diluted with dichloromethane (20 mL), and the resulting solution was washed successively with 10% citric acid (2 x 25 mL), 10% NaHCO_3 (2 x 25 mL), and water (2 x 25 mL), dried over Na_2SO_4 and

evaporated to dryness. Flash chromatography of the residues, using n-hexane/ethyl acetate 2/1 v/v as eluent, yielded, the corresponding N-protected phenylalanil derivatives **104a**, **104b** or **105a**, **105b** as diastereoisomeric mixtures.

(1S,3S)-methyl-2-((S)-2-((tert-butoxycarbonyl)amino)-3-phenylpropanoyl)-1-(4-methoxyphenyl)-2,3,4,9-tetrahydro-1H-pyrido[3,4-b]indole-3-carboxylate (104a).

36% yield. ^1H NMR (CDCl_3 , 400 MHz) : (A) δ : 1.35 (s, 9H, Boc); 2.10-2.18 (m, 1H, H-4a); 2.87-3.03 (m, 5H, CH_2a benzyl, CH_2b benzyl and OCH_3); 3.34 (d, 1H, H-4b, $J = 16.0$ Hz); 3.65 (s, 3H, CH_3); 4.63-4.67 (m, 1H, H-3); 4.92-4.95 (m, 1H, H-2'); 5.45 (d, 1H, NH-Boc, $J = 8.0$ Hz); 6.76 (s, 1H, H-1); 6.65 (d, 2H, aryl, $J = 8.0$ Hz); 6.81 (d, 1H, aryl, $J = 8.0$ Hz); 6.90-7.24 (m, 9H, H-6, H-7, H-8 and aryl); 7.44 (d, 1H, H-5, $J = 8.0$ Hz); 7.79 (s, 1H, NH-9). (B) δ : 1.34 (s, 9H, Boc); 2.67 (dd, 1H, CH_2a benzyl, $J' = 8.0$, $J'' = 12.0$ Hz); 2.87-3.03 (m, 4H, CH_2b benzyl and OCH_3); 3.17 (d, 1H, H-4b, $J = 16.0$ Hz); 3.44 (dd, 1H, H-4a, $J' = 4.0$, $J'' = 12.0$ Hz); 3.68 (s, 3H, CH_3); 4.63-4.67 (m, 1H, H-3); 5.02-5.06 (m, 1H, H-2'); 5.58 (d, 1H, NH-Boc, $J = 8.0$ Hz); 6.51 (s, 1H, H-1); 6.70 (d, 2H, aryl, $J = 8.0$ Hz); 6.88 (d, 1H, aryl, $J = 8.0$ Hz); 6.90-7.24 (m, 9H, H-6, H-7, H-8 and aryl); 7.44 (d, 1H, H-5, $J = 8.0$ Hz); 7.69 (s, 1H, NH-9).. ^{13}C NMR (CDCl_3 , 100 MHz) (A + B) δ : 28.1; 28.3; 29.7; 31.4; 40.5; 41.7; 51.7; 52.1; 55.2; 52.4; 55.7; 57.7; 79.7; 80.1; 107.5; 113.4; 114.2; 118.4; 118.56; 119.7; 122.3; 126.4; 127.0; 127.3; 128.0; 128.24; 128.36; 128.; 128.89; 129.1; 129.42; 129.58; 129.61; 130.0; 130.3; 130.9; 131.3; 136.0; 136.7; 154.8; 159.2; 170.12; 172.15; 172.27; 173.0. HR-MS m/z : calcd for $\text{C}_{34}\text{H}_{38}\text{N}_3\text{O}_6$, $[(\text{M}+\text{H})^+]$: 584.2755; found 584.2760.

(1R,3S)-methyl 2-((S)-2-((tert-butoxycarbonyl)amino)-3-phenylpropanoyl)-1-(4-methoxyphenyl)-2,3,4,9-tetrahydro-1H-pyrido[3,4-b]indole-3-carboxylate (104b).

28% yield. ^1H NMR (CDCl_3 , 400 MHz) : (A) δ : 1.42 (s, 9H, Boc); 2.77 (dd, 1H, H-4a, $J' = 4.0$, $J'' = 12.0$ Hz); 2.97-3.07 (m, 1H, H- CH_2a benzyl and CH_2b benzyl); 3.25-3.33 (m, 1H, H-4b); 3.58 (s, 3H, OCH_3); 3.79 (s, 3H, CH_3); 4.81 (d, 1H, H-2', $J = 4.0$ Hz); 4.85-4.91 (m, 1H, H-3); 5.44 (t, 1H, NH-Boc, $J = 8.0$ Hz);

6.03 (s, 1H, H-1); 6.74 (d, 1H, aryl, $J = 8.0$ Hz); 6.79-6.85 (m, 2H, aryl); 7.01 (d, 2H, aryl); 7.07-7.32 (m, 7H, H-6, H-7, H-8 and aryl); 7.54 (d, 1H, H-5, $J = 8.0$ Hz); 7.75 (s, 1H, NH-9). (**B**) δ : 1.46 (s, 9H, Boc); 2.84-2.92 (m, 2H, CH_2a benzyl and H-4a); 2.97-3.07 (m, 1H, CH_2b benzyl); 3.44 (d, 1H, H-4b, $J = 16.0$ Hz); 3.70 (s, 3H, OCH_3); 3.77 (s, 3H, CH_3); 4.02 (d, 1H, H-3, $J = 8.0$ Hz); 5.12-5.17 (m, 1H, H-2'); 5.44 (t, 1H, NH-Boc, $J = 8.0$ Hz); 5.82 (s, 1H, H-1); 6.79-6.85 (m, 2H, aryl); 6.91 (d, 1H, aryl, $J = 8.0$ Hz); 7.01 (d, 2H, aryl); 7.07-7.32 (m, 7H, H-6, H-7, H-8 and aryl); 7.47 (d, 1H, H-5, $J = 8.0$ Hz); 7.75 (s, 1H, NH-9). ^{13}C NMR ($CDCl_3$, 100 MHz) (**A + B**) δ : 28.11; 28.20; 39.8; 40.7; 52.1; 52.3; 52.6; 53.0; 53.2; 53.4; 55.3; 56.6; 57.3; 61.2; 79.6; 80.0; 110.2; 111.0; 113.7; 114.1; 118.1; 118.4; 119.8; 122.1; 122.5; 126.1; 126.4; 128.0; 128.5; 128.9; 129.3; 129.7; 130.3; 131.0; 134.1; 134.3; 135.6; 136.4; 136.6; 158.7; 159.6; 171.5; 172.2; 174.3; 174.4. HR-MS m/z : calcd for $C_{34}H_{38}N_3O_6$, $[(M+H)^+]$: 584.2755; found 584.2764.

(1S,3S)-methyl 2-((S)-2-((tert-butoxycarbonyl)amino)-3-phenylpropanoyl)-1-isobutyl-2,3,4,9-tetrahydro-1H-pyrido[3,4-b]indole-3-carboxylate (105a).

29% yield. 1H NMR ($CDCl_3$, 400 MHz) : (**A**) δ : 0.95 (d, 3H, CH_3 , $J = 8.0$ Hz); 1.02 (d, 3H, CH_3 , $J = 8.0$ Hz); 1.33-1.43 (m, 11H, Boc and CH_2); 1.70-1.77 (m, 1H, CH); 2.06 (dd, 1H, H-4a, $J' = 8.0$, $J'' = 16.0$ Hz); 2.86-2.97 (m, 1H, CH_2a benzyl); 3.15-3.20 (m, 2H, H-4b and CH_2b benzyl); 3.57 (s, 3H, CH_3); 4.62 (d, 1H, H-3, $J = 8.0$ Hz); 4.88-4.98 (m, 1H, H-2'); 5.42 (d, 1H, NH-Boc, $J = 8.0$ Hz); 5.57 (t, 1H, H-1, $J = 8.0$ Hz); 7.01-7.12 (m, 3H, aryl and H-6); 7.17-7.26 (m, 5H, aryl, H-7 and H-8); 7.35 (d, 1H, H-5, $J = 8.0$ Hz); 7.70 (s, 1H, NH-9). (**B**) δ : 0.76 (d, 3H, CH_3 , $J = 8.0$ Hz); 0.80 (d, 3H, CH_3 , $J = 8.0$ Hz); 1.18-1.23 (m, 11H, Boc and CH_2); 1.53-1.60 (m, 1H, CH); 2.86-2.97 (m, 2H, CH_2a benzyl and H-4a); 3.15-3.20 (m, 1H, CH_2b benzyl); 3.26 (dd, 1H, H-4b, $J' = 8.0$, $J'' = 12.0$ Hz); 3.59 (s, 3H, CH_3); 4.88-4.98 (m, 2H, H-3 and NH-Boc); 5.33 (t, 1H, H-2', $J = 8.0$ Hz); 5.48 (t, 1H, H-1, $J = 8.0$ Hz); 7.01-7.12 (m, 3H, aryl and H-6); 7.17-7.26 (m, 5H, aryl, H-7 and H-8); 7.43 (d, 1H, H-5, $J = 8.0$ Hz); 7.99 (s, 1H, NH-9). ^{13}C NMR ($CDCl_3$, 100 MHz) (**A + B**) δ : 21.8; 22.1; 22.7; 23.47; 23.65; 24.8; 25.9; 28.18; 28.36; 40.6; 44.9; 45.5; 48.6; 51.1; 51.75; 51.83; 52.2; 52.4; 52.6; 53.5; 79.7;

80.1; 105.0; 110.7; 111.0; 118.1; 118.3; 119.68; 119.79; 122.1; 126.4; 126.8; 127.0; 128.4; 128.6; 129.4; 129.9; 132.9; 134.0; 136.0; 136.8; 154.8; 171.08; 172.25. HR-MS m/z : calcd for $C_{31}H_{40}N_3O_5$, $[(M+H)^+]$: 534.2962; found 534.2971.

(1R,3S)-methyl 2-((S)-2-((tert-butoxycarbonyl)amino)-3-phenylpropanoyl)-1-isobutyl-2,3,4,9-tetrahydro-1H-pyrido[3,4-b]indole-3-carboxylate (105b).

25% yield. 1H NMR ($CDCl_3$, 400 MHz) : (A) δ : 0.89 (d, 3H, CH_3 , $J = 8.0$ Hz); 1.05 (d, 3H, CH_3 , $J = 8.0$ Hz); 1.44-1.49 (m, 11H, Boc and CH_2); 1.81-1.86 (m, 1H, CH); 2.85-2.92 (m, 1H, CH_2a benzyl); 2.98-3.04 (m, 1H, H-4a); 3.12-3.23 (m, 2H, H-4b and CH_2b benzyl); 3.77 (s, 3H, CH_3); 4.17-4.21 (m, 1H, H-3); 4.57 (t, 1H, H-1, $J = 8.0$ Hz); 4.83-4.93 (m, 1H, H-2'); 5.34-5.42 (m, 1H, NH-Boc); 6.81 (t, 2H, aryl, $J = 8.0$ Hz), 7.01 (d, 2H, aryl, $J = 8.0$ Hz); 7.06-7.21 (m, 3H, aryl, H-7 and H-6); 7.26-7.34 (m, 1H, H-8); 7.48 (d, 1H, H-5, $J = 8.0$ Hz); 7.58 (s, 1H, NH-9). (B) δ : 0.83 (d, 3H, CH_3 , $J = 8.0$ Hz); 1.10 (d, 3H, CH_3 , $J = 8.0$ Hz); 1.26-1.31 (m, 11H, Boc and CH_2); 1.61-1.70 (m, 1H, CH); 2.48 (dd, 1H, H-4a, $J' = 8.0$, $J'' = 16.0$ Hz); 2.85-2.92 (m, 1H, CH_2a benzyl); 2.98-3.04 (m, 1H, CH_2b benzyl); 3.30 (d, 1H, H-4b, $J = 12.0$ Hz); 3.43 (s, 3H, CH_3); 4.37-4.40 (m, 1H, H-3); 4.69-4.77 (m, 1H, H-2'); 5.34-5.42 (m, 1H, H-1); 5.54 (d, 1H, NH-Boc, $J = 8.0$ Hz); 6.72 (t, 2H, aryl, $J = 8.0$ Hz), 7.06-7.21 (m, 3H, aryl, H-7 and H-6); 7.26-7.34 (m, 3H, H-8 and aryl); 7.43 (d, 1H, H-5, $J = 8.0$ Hz); 8.23 (s, 1H, NH-9). ^{13}C NMR ($CDCl_3$, 100 MHz) (A + B) δ : 22.1; 22.9; 23.0; 23.4; 25.1; 26.1; 29.1; 29.9; 41.6; 44.3; 46.1; 49.6; 50.9; 51.3; 52.0; 52.6; 53.3; 53.6; 80.1; 81.3; 107.0; 110.5; 111.1; 118.3; 120.4; 121.7; 122.7; 125.8; 126.1; 126.4; 128.1; 129.7; 130.0; 130.5; 133.4; 134.2; 136.7; 137.0; 155.1; 171.5; 172.8. HR-MS m/z : calcd for $C_{31}H_{40}N_3O_5$, $[(M+H)^+]$: 534.2962; found 534.2969.

Methods for the synthesis of (2S, 5S, 11bS)-methyl-2-benzyl-3-oxo-2,3,5,6,11,11b-hexahydro-1H-imidazo[1',2':1,2] pyrido[3,4-b]indole-5-carboxylate (81) and (3S,12aS)-3-benzyl-2,3,12,12a-tetrahydropyrazino[1',2':1,6] pyrido[3,4-b]indole-1,4(6H,7H)-dione (80).

Method A: Cyclization under redox (TEMPO) and acidic conditions (TFA)

Intermediate **79** (1.0 mmol) was dissolved in 20 mL of DCM/TFA (3:1 v:v, Table 1 entry 1). Triethylsilane (0.25 mmol) and (2,2,6,6-Tetramethylpiperidin-1-yl)oxyl (TEMPO) were added. Reactions were stirred at room temperature for 2 hours. Then, the solvent was evaporated *in vacuo*, the crude product was reconstituted in DCM (30 mL) and washed with water and 3M NaOH solution adjusting the pH to 7. The organic phase was washed with brine (2x 25 mL), dried over Na₂SO₄ and evaporated to dryness. Final compounds were isolated by flash-chromatography using ethyl acetate as solvent.

Method B: Cyclization under oxygen flush and acidic conditions (TFA)

Intermediate **79** (1.0 mmol) was dissolved in 20 mL of MeOH/TFA (3:1 v:v, Table 1 entry 2) and added with 0.25 mmol of triethylsilane. In a separate round-bottomed flask, hydrogen peroxide solution (12.5 ml, 30 % w/w in water) acidified with H₂SO₄ (0.15 mmol, 7.9 ml) was added dropwise with aqueous KMnO₄ (0.05 mol, 12.5 mL) for 20 minutes. The oxygen thus generated was bubbled in the solution containing intermediate **79** that was maintained under stirring at room temperature for 2 hours. The mixture was then subjected to the same work up procedure described for method A.

Method C: Cyclization under redox (Perbenzoic acid) and acidic conditions (TFA)

Intermediate **79** (1.0 mmol) was dissolved in 20 mL of DCM/TFA (3:1 v:v, Table 1 entry 3) Then 0.25 mmol of triethylsilane and 1.0 mmol of perbenzoic acid were added. Reactions were stirred at room temperature for 2 hours and treated as described for method A.

Method D: Cyclization under redox (Perbenzoic acid) and acidic conditions (37% HCl)

Intermediate **79** (1.0 mmol) was dissolved in 20 mL of aqueous HCl (37%)/MeOH (9.8:0.2 v:v, Table 1, entry 4). Then 0.25 mmol of triethylsilane and 1.0 mmol of perbenzoic acid were added. Reactions were stirred at room temperature for 2 hours and treated as described for method A.

Method E: Cyclization under acidic conditions

Intermediate **79** (1.0 mmol) was dissolved in a 20 mL volume consisting of DCM/TFA (3:1 v:v, Table 1 entry 5) and added with 0.25 mmol of triethylsilane. Reaction was stirred at room temperature for 2 hours and treated as described for method A.

Method F: Cyclization using inorganic oxidating reagents (oxone, $KMnO_4$, $K_2Cr_2O_7$, HIO_4 , $FeCl_3$)

Intermediate **79** (1.0 mmol) was dissolved in a 10 mL MeOH (Table 1 entry 6-10) and added with a solution of oxidating agent (2.0 mmol) in H_2O /TFA (1/2 v/v, 30 mL) and 0.25 mmol of triethylsilane. Reaction was stirred at room temperature for 2 hours and treated as described for method A.

(2S,5S,11bS)-methyl-2-benzyl-3-oxo-2,3,5,6,11,11b-hexahydro-1H-imidazo[1',2':1,2]pyrido[3,4-b]indole-5-carboxylate (81).

Obtained from intermediate **79** using methods A, B, C, D and E.

For the obtained yield see table 1. $[\alpha]_D^{25}$: 84.00 ± 0.08 (c = 0.10, MeOH). 1H NMR (CD_3OD , 400 MHz): δ : 2.68 (dd, 1H, CH_2' , $J' = 8.0$ and $J'' = 12.0$ Hz); 2.92 (dd, 1H, H-6', $J' = 8.0$, $J'' = 16.0$ Hz); 3.06 (dd, 1H, CH_2'' , $J' = 4.0$ and $J'' = 16.0$ Hz); 3.25-3.30 (m, 1H, H-6''); 3.60 (s, 3H, CH_3); 3.98 (dd, 1H, H-2, $J' = 4.0$, $J'' = 12.0$ Hz); 5.19 (d, 1H, H-5, $J = 8.0$ Hz); 5.84 (s, 1H, H-11b); 6.93-6.99 (m, 2H, H-8 and aryl); 7.03-7.07 (m, 3H, H-9 and aryl); 7.15 (d, 2H, aryl, $J = 8.0$ Hz); 7.26 (d, 1H, H-10, $J = 8.0$ Hz); 7.34 (d, 1H, H-7, $J = 8.0$ Hz); ^{13}C NMR (CD_3OD , 100 MHz) δ : 24.7 (C-6); 38.4 (CH_2); 52.4 (C-5); 53.3 (CH_3); 63.4 (C-2);

67.9 (C-11b); 107.1 (C-6a); 112.5 (C-10); 119.4 (C-7); 120.4 (C-8); 123.5 (C-9); 127.6 (aryl); 138.5 (C-10a); 129.3 (aryl); 130.55 (aryl), 131.9 (C-11a), 127.7 (C-6b), 139.1 (aryl), 172.4 (C=O); 176.0 (C-3). HR-MS m/z : calcd. for $C_{22}H_{22}N_3O_3$, $[(M+H)^+]$: 376.1656; found 376.1662.

(3*S*,12*aS*)-3-benzyl-2,3,12,12a-tetrahydropyrazino[1',2':1,6]pyrido[3,4-b]indole-1,4(6*H*,7*H*)-dione (80).

Obtained from intermediate **79** using method A and E.

For the obtained yield see table 1. $[\alpha]_D^{25}$: -68.000 ± 0.00108 ($c = 0.10$, MeOH). 1H NMR (CD_3OD , 400 MHz): δ : 0.80 (t, 1H, H-12', $J = 16$ Hz); 2.65 (dd, 1H, H-12'', $J' = 4.0$, $J'' = 16.0$ Hz); 2.90 (dd, 1H, CH_2 benzyl, $J' = 4.0$, $J'' = 12.0$ Hz); 3.27 (dd, 1H, CH_2 benzyl, $J' = 4.0$, $J'' = 16.0$ Hz); 3.98 (dd, 1H, H-12a, $J' = 4.0$, $J'' = 12.0$ Hz); 4.24 (d, 1H, H-6', $J = 16.0$ Hz); 4.40 (t, 1H, H-3, $J = 4.0$ Hz); 5.42 (d, 1H, H-6''); 6.89 (t, 1H, H-9, $J = 8.0$ Hz); 6.94-7.01 (m, 6H, H-10 and aryl); 7.10 (d, 1H, H-8, $J = 8.0$ Hz); 7.20 (d, 1H, H-11, $J = 8.0$ Hz); ^{13}C NMR (CD_3OD , 100 MHz) δ : 27.4 (C-12); 41.1 (CH_2 benzyl and C-6); 50.5 (C-12a); 57.6 (C-3); 107.3 (C-11b); 112.0 (C-11); 118.6 (C-10); 120.1 (C-9); 122.6 (C-8); 127.9 (C-6a); 128.5 (aryl); 129.4 (C-7a); 129.7, 131.6 (aryl); 136.5 (C-11a); 138.1 (aryl); 166.5 (C-4); 169.5 (C-1). HR-MS m/z : calcd. for $C_{21}H_{20}N_3O_2$, $[(M+H)^+]$: 346.1550; found 346.1556.

Synthesis of (S)-methyl 2-((S)-2-((tert-butoxycarbonyl)amino)-3-phenylpropyl)-2,3,4,9-tetrahydro-1*H*-pyrido[3,4-*b*]indole-3-carboxylate (82).

Derivative **82** was obtained by reductive amination reaction starting from **59** (4.0 mmol), which was reacted under reflux with Boc-L-Phenylalaninal (6.0 mmol) in ethanol (20 mL) for 3 hours. The reaction was then cooled to room temperature and $NaBH_4$ (12 mmol) was added portionwise. The mixture was allowed to react for 1 hour, then 10% citric acid was added portionwise till pH 7, ethanol was evaporated under vacuum and 25 mL of dichloromethane were added. The organic phase was washed twice with water (25 mL), dried over Na_2SO_4 and evaporated to dryness. The crude product was purified by flash chromatography using ethyl acetate/n-hexane 5/1 as eluent (43% yield).

¹H NMR (CDCl₃, 400 MHz): δ: 1.34 (s, 9H, Boc); 2.58 (dd, 1H, CH₂a, *J*' = 8.0, *J*'' = 12.0 Hz); 2.80-2.85 (m, 3H, H-4a, H-1'a and CH₂b); 3.03-3.06 (m, 2H, H-1'b and H-4b); 3.55 (s, 3H, CH₃); 3.77 (t, 1H, H-3, *J* = 8.0 Hz); 3.89-3.93 (m, 2H, H-1a and H-2'); 4.00 (d, 1H, H-1b, *J* = 16.0 Hz); 4.84-4.88 (m, 1H, NHBoc); 6.99-7.15 (m, 5H, H-6, H-7 and aryl); 7.17-7.24 (m, 3H, H-8 and aryl); 7.39 (d, 1H, H-5, *J* = 8.0 Hz); 7.68 (s, 1H, NH); ¹³C NMR (CDCl₃, 100 MHz) δ: 22.6; 23.6; 28.4; 31.6; 46.4; 50.9; 51.6; 60.8; 77.3; 110.7; 117.8; 199.4; 121.6; 126.3; 128.3; 129.6; 136.1; 137.9; 155.7; 173.1. HR-MS *m/z*: calcd for C₂₇H₃₄N₃O₄, [(M+H)⁺]: 464.2544; found 464.2551.

(3*S*,12*aS*)-3-benzyl-3,4,6,7,12,12*a*-hexahydropyrazino[1',2':1,6]pyrido[3,4-*b*]indol-1(2H)-one (83).

Obtained from intermediate **82** using method C.

88% yield. [α]_D²⁵: -82.0 ± 0.33 (c = 0.10, MeOH). ¹H NMR (CDCl₃, 400 MHz) : δ: 2.82 (dd, 1H, H-4', *J* = 12 Hz); 2.88-2.97 (m, 2H, H-4'' and H-12'); 3.01 (d, 2H, CH₂ benzyl, *J* = 8.0 Hz); 3.25 (dd, 1H, H-12a, *J*' = 4.0, *J*'' = 12.0 Hz); 3.40 (dd, 1H, H-12'', *J*' = 4.0, *J*'' = 16.0 Hz); 3.60-3.63 (m, 1H, H-3); 3.71 (d, 1H, H-6', *J* = 12.0 Hz); 3.96 (d, 1H, H-6'', *J* = 12.0 Hz); 5.93 (s, 1NH); 7.10 (t, 1H, H-10, *J* = 8.0 Hz); 7.13-7.18 (m, 3H, H-9 and aryl); 7.24 (t, 1H, aryl, *J* = 8.0 Hz); 7.29-7.33 (m, 3H, H-8 and aryl); 7.51 (d, 1H, H-11, *J* = 8.0 Hz); ¹³C NMR (CDCl₃, 100 MHz) δ: 25.0 (C-12); 42.1 (CH₂ benzyl); 52.0 (C-6); 53.0 (C-3); 53.6 (C-4); 62.0 (C-12a); 108.7 (C-11b); 110.9 (C-8); 118.5 (C-11); 120.1 (C-10); 122.1 (C-9); 124.5 (C-7a); 127.3; 129.1; 129.5 (aryl); 130.5 (C-6a); 136.3 (C-11a); 137.8 (aryl); 171.3 (C-1). HR-MS *m/z*: calcd for C₂₁H₂₂N₃O, [(M+H)⁺]: 332.1757; found 332.1750.

(*S*)-methyl 2-(3-aminopropanoyl)-2,3,4,9-tetrahydro-1H-pyrido[3,4-*b*]indole-3-carboxylate (65).

Obtained from intermediate **64** using method C.

79% yield. ¹H NMR (CD₃OD, 400 MHz) : δ: (A) 2.54-2.65 (m, 2H, CH₂); 2.86-2.91 (m, 2H, CH₂); 3.01 (dd, 1H, H-6', *J*' = 8.0 and *J*'' = 16.0 Hz); 3.42 (d, 1H, H-6'', *J* = 16.0 Hz); 3.52 (s, 3H, CH₃); 4.24 (d, 1H, H-2', *J* = 16.0 Hz); 5.04 (d,

1H, H-2'', $J = 16.0$ Hz); 5.16 (d, 1H, H-5, $J = 4.0$ Hz); 6.90 (t, 1H, H-8, $J = 8.0$ Hz); 6.97 (d, 1H, H-10, $J = 8.0$ Hz); 7.18 (t, 1H, H-9, $J = 8.0$ Hz); 7.31 (d, 1H, H-7, $J = 8.0$ Hz); ^{13}C NMR (CD_3OD , 100 MHz) δ : 22.8 (C-6); 35.4 (CH_2); 36.8 (CH_2); 38.3 (C-2); 51.0 (CH_3); 54.8 (C-5); 104.9 (C-6a); 110.0 (C-8); 116.8 (C-7); 118.0 (C-8); 120.6 (C-10), 126.4 (C-10a); 128.5 (C-11a), 137.2 (C-6b), 171.4, 173.5 (C=O).

^1H NMR (CD_3OD , 400 MHz) : δ : (B) 2.54-2.65 (m, 2H, CH_2); 2.86-2.91 (m, 3H, CH_2 and H-6'); 3.36 (d, 1H, H-6'', $J = 16.0$ Hz); 3.50 (s, 3H, CH_3); 4.63 (d, 1H, H-2', $J = 16.0$ Hz); 4.81 (d, 1H, H-2'', $J = 16.0$ Hz); 5.74 (d, 1H, H-5, $J = 4.0$ Hz); 6.90 (t, 1H, H-8, $J = 8.0$ Hz); 6.97 (d, 1H, H-10, $J = 8.0$ Hz); 7.18 (t, 1H, H-9, $J = 8.0$ Hz); 7.31 (d, 1H, H-7, $J = 8.0$ Hz); ^{13}C NMR (CD_3OD , 100 MHz) (A + B) δ : 21.8 (C-6); 35.4 (CH_2); 36.8 (CH_2); 40.8 (C-2); 51.0 (CH_3); 50.5 (C-5); 104.9 (C-6a); 110.0 (C-8); 116.8 (C-7); 118.0 (C-8); 120.6 (C-10), 137.2 (C-10a); 128.5 (C-11a), 126.4 (C-6b), 171.4, 173.5 (C=O).

HR-MS m/z calcd for $\text{C}_{16}\text{H}_{20}\text{N}_3\text{O}_3$, $[(\text{M}+\text{H})^+]$: 302.1499; found 302.1503.

(5S,11bS)-methyl-3-oxo-2,3,5,6,11,11b-hexahydro-1H-imidazo[1',2':1,2]pyrido[3,4-b]indole-5-carboxylate (106).

Obtained from intermediate **92** using method C.

70% yield. $[\alpha]_{\text{D}}^{25}$: 56.00 ± 0.030 ($c = 0.10$, MeOH). ^1H NMR (CDCl_3 , 400 MHz) : δ : 3.19 (dd, 1H, H-6', $J' = 4.0$ and $J'' = 16.0$ Hz); 3.39 (d, 1H, H-6'', $J = 16.0$ Hz); 3.52 (d, 1H, H-2', $J = 16.0$ Hz); 3.66 (d, 1H, H-2'', $J = 16.0$ Hz); 3.67 (s, 3H, CH_3); 5.28 (d, 1H, H-5, $J = 4.0$ Hz); 6.05 (s, 1H, H-11b); 7.13 (t, 1H, H-8, $J = 8.0$ Hz); 7.20 (t, 1H, H-9, $J = 8.0$ Hz); 7.35 (d, 1H, H-10, $J = 8.0$ Hz); 7.50 (d, 1H, H-7, $J = 8.0$ Hz); 8.32 (s, 1NH, H-11); ^{13}C NMR (CDCl_3 , 100 MHz) δ : 23.6 (C-6); 50.3 (C-2); 50.6 (C-5); 52.7 (CH_3); 68.3 (C-11b); 107.9 (C-6a); 111.4 (C-10); 118.9 (C-7); 120.2 (C-8); 136.6 (C-10a); 126.3 (C-9); 129.9 (C-11a), 126.3 (C-6b), 172.2 (C=O); 173.7 (C-3). HR-MS m/z : calcd. for $\text{C}_{15}\text{H}_{16}\text{N}_3\text{O}_3$, $[(\text{M}+\text{H})^+]$: 286.1186; found 286.1190.

(2*S*,5*S*,11*bS*)-methyl 2-methyl-3-oxo-2,3,5,6,11,11*b*-hexahydro-1*H*-imidazo[1',2':1,2]pyrido[3,4-*b*]indole-5-carboxylate (107).

Obtained from intermediate **93** using method C.

79% yield. $[\alpha]_D^{25}$: 125 ± 20 ($c = 0.10$, MeOH). $^1\text{H NMR}$ (CD_3OD , 400 MHz): δ : 1.33 (d, 3H, CH_3 , $J = 4.0$ Hz); 3.16 (dd, 1H, H-6', $J' = 8.0$ and $J'' = 16.0$ Hz); 3.46 (d, 1H, H-6'', $J = 16.0$ Hz); 3.70 (s, 3H, CH_3); 3.83 (q, 1H, H-2); 5.27 (d, 1H, H-5, $J = 8.0$ Hz); 5.94 (s, 1H, H-11*b*); 7.04 (t, 1H, H-8, $J = 8.0$ Hz); 7.16 (t, 1H, H-9, $J = 8.0$ Hz); 7.38 (d, 1H, H-10, $J = 8.0$ Hz); 7.48 (d, 1H, H-7, $J = 8.0$ Hz); $^{13}\text{C NMR}$ (CDCl_3 , 100 MHz) δ : 16.5 (CH_3); 24.1 (C-6); 50.6 (C-5); 52.9 (CH_3); 56.9 (C-2); 66.3 (C-11*b*); 107.6 (C-6*a*); 111.6 (C-10); 119.1 (C-7); 120.4 (C-8); 123.4 (C-9); 129.6 (C-11*a*), 126.5 (C-6*b*), 136.7 (C-10*a*); 171.2 (C=O); 175.1 (C-3). HR-MS m/z : calcd. for $\text{C}_{16}\text{H}_{18}\text{N}_3\text{O}_3$, $[(\text{M}+\text{H})^+]$: 300.1343; found 300.1347.

(3*aS*,6*S*,12*bS*)-methyl-4-oxo-2,3,3*a*,4,6,7,12,12*b*-octahydro-1*H*-pyrrolo[1'',2'':3',4']imidazo[1',2':1,2]pyrido [3,4-*b*]indole-6-carboxylate (108).

Obtained from intermediate **94** using method C.

72% yield. $[\alpha]_D^{25}$: 180.00 ± 0.36 ($c = 0.10$, MeOH). $^1\text{H NMR}$ (CDCl_3 , 400 MHz): δ : 1.71-1.79 (m, 2H, H-2' and H-2''); 2.13-2.26 (m, 3H, H-1', H-1'' and H-3'); 2.64-2.69 (m, 1H, H-3''); 3.11 (dd, 1H, H-7', $J' = 4.0$, $J'' = 12.0$ Hz); 3.47 (d, 1H, H-7'', $J = 16.0$ Hz); 3.64 (s, 3H, CH_3); 4.08 (dd, 1H, H-3*a*, $J' = 4.0$, $J'' = 8.0$ Hz); 5.22 (d, 1H, H-6, $J = 8.0$ Hz); 6.18 (s, 1H, H-12*b*); 7.14 (t, 1H, H-9, $J = 8.0$ Hz); 7.23 (t, 1H, H-10, $J = 8.0$ Hz); 7.35 (d, 1H, H-11, $J = 8.0$ Hz); 7.52 (d, 1H, H-8, $J = 8.0$ Hz); 8.83 (s, 1NH, H-12). $^{13}\text{C NMR}$ (CDCl_3 , 100 MHz) δ : 24.1 (C-7); 24.5 (C-2); 25.6 (C-1); 47.8 (C-3); 50.6 (C-6); 52.7 (CH_3); 66.3 (C-3*a*); 69.5 (C-12*b*); 108.8 (C-7*a*); 111.4 (C-11); 118.8 (C-8); 120.0 (C-9); 123.2 (C-10); 136.7 (C-11*a*); 127.1 (C-12*a*), 126.2 (C-7*b*), 170.9 (C=O); 174.5 (C-4). HR-MS m/z : calcd for $\text{C}_{18}\text{H}_{20}\text{N}_3\text{O}_3$, $[(\text{M}+\text{H})^+]$: 326.1499; found 326.1503.

(2R,5S,11bS)-methyl-2-benzyl-3-oxo-2,3,5,6,11,11b-hexahydro-1H-imidazo[1',2':1,2]pyrido[3,4-b]indole-5-carboxylate (109).

Obtained from intermediate **95** using method C.

81% yield. $[\alpha]_D^{25}$: 40.00 ± 0.01 ($c = 0.10$, MeOH). ^1H NMR (CDCl_3 , 400 MHz): δ : 3.01 (dd, 1H, CH_2' , $J' = 8.0$ and $J'' = 16.0$ Hz); 3.13 (dd, 1H, CH_2'' , $J' = 4.0$, $J'' = 16.0$ Hz); 3.19 (d, 1H, H-6', $J = 8.0$ Hz); 3.25 (d, 1H, H-6'', $J = 16.0$ Hz); 3.59 (s, 3H, CH_3); 3.69 (dd, 1H, H-2, $J' = 4.0$, $J'' = 8.0$ Hz); 5.25 (d, 1H, H-5, $J = 8.0$ Hz); 5.84 (s, 1H, H-11b); 7.05 (t, 1H, H-8, $J = 8.0$ Hz); 7.13 (t, 1H, H-9, $J = 8.0$ Hz); 7.19-7.30 (m, 6H, aryl and H-10); 7.42 (d, 1H, H-7, $J = 8.0$ Hz); 8.22 (s, 1NH, H-11); ^{13}C NMR (CDCl_3 , 100 MHz) δ : 23.4 (C-6); 36.4 (CH_2); 51.1 (C-5); 52.6 (CH_3); 61.3 (C-2); 66.6 (C-11b); 107.6 (C-6a); 111.3 (C-10); 118.7 (C-7); 120.0 (C-8); 123.0 (C-9); 123.2 (aryl); 136.3 (C-10a); 128.7 (aryl); 129.4 (aryl); 130.3 (C-11a), 126.4 (C-6b), 137.1 (aryl), 170.0 (C=O); 175.10 (C-3). HR-MS m/z : calcd for $\text{C}_{22}\text{H}_{22}\text{N}_3\text{O}_3$, $[(\text{M}+\text{H})^+]$: 376.1656; found 376.1660.

(2S,5S,11bR)-1-benzyl-5-methyl-2-isobutyl-3-oxo-2,3,5,6-tetrahydro-1H-imidazo[1',2':1,2]pyrido[3,4-b]indole-1,5(11H,11bH)-dicarboxylate (110).

Obtained from intermediate **96** using method C.

40% yield. $[\alpha]_D^{25}$: $+2.0 \pm 0.20$ ($c = 0.10$, MeOH). ^1H NMR (CDCl_3 , 400 MHz): δ : 0.63 (d, 3H, CH_3 , $J = 4.0$ Hz); 0.66 (d, 3H, CH_3 , $J = 4.0$ Hz); 1.51-1.60 (m, 2H, CH_2); 1.67-1.71 (m, 1H, CH); 3.16 (dd, 1H, H-6', $J' = 4.0$ and $J'' = 8.0$ Hz); 3.39 (d, 1H, H-6'', $J = 16.0$ Hz); 3.67 (s, 3H, CH_3); 4.37 (dd, 1H, H-2, $J' = 4.0$ and $J'' = 8.0$ Hz); 5.29 (q, 2H, CH_2); 5.48 (d, 1H, H-5, $J = 8.0$ Hz); 6.59 (s, 1H, H-11b); 7.09 (t, 1H, H-8, $J = 8.0$ Hz); 7.21 (t, 1H, H-9, $J = 8.0$ Hz); 7.35-7.38 (m, 6H, H-10 and aryl); 7.49 (d, 1H, H-7, $J = 8.0$ Hz); 9.19 (s, 1NH, H-11). ^{13}C NMR (CDCl_3 , 100 MHz) δ : 22.1 (CH_3); 23.2 (CH_3); 23.3 (C-6); 24.1 (CH); 40.9 (CH_2); 51.3 (C-5); 52.8 (CH_3); 57.9 (C-2); 66.4 (C-11b); 68.4 (CH_2); 106.5 (C-6a); 111.6 (C-10); 118.8 (C-7); 119.7 (C-9); 123.0 (C-8); 136.1 (C-10a); 128.3 (aryl); 128.7 (aryl); 130.0 (C-11a), 135.3 (aryl); 125.9 (C-6b), 156.3 (C=O); 170.4 (C-3); 170.4 (C=O). HR-MS m/z : calcd for $\text{C}_{27}\text{H}_{30}\text{N}_3\text{O}_5$, $[(\text{M}+\text{H})^+]$: 476.2180; found 476.2177.

(2*S*,5*S*,11*bR*)-1-((9*H*-fluoren-9-yl)methyl)-5-methyl-2-benzyl-3-oxo-2,3,5,6-tetrahydro-1*H*-imidazo [1',2':1,2]pyrido[3,4-*b*]indole-1,5(11*H*,11*bH*)-dicarboxylate (111).

Obtained from intermediate **97** using method C.

28% yield. $[\alpha]_D^{25}$: +207.00 ± 0.43 (c = 0.10, MeOH). ¹H NMR (CDCl₃, 400 MHz) : δ: 2.17-2.23 (m, 2H, CH₂' benzyl and H-6'); 2.68 (d, 1H, CH₂'' benzyl, *J*' = 16.0 Hz); 2.86 (d, 1H, H-6'', *J*'=16.0 Hz); 3.56 (s, 3H, CH₃); 4.19 (d, 1H, H-2, *J* = 8.0 Hz); 4.32 (t, 1H, CH Fmoc, *J* = 4.0 Hz); 4.80 (dd, 1H, CH₂ Fmoc, *J*' = 4.0, *J*'' = 12.0 Hz); 5.11-5.15 (m, 2H, CH₂ Fmoc and H-5); 6.27-6.35 (m, 3H, H-11*b* and aryl); 7.02 (t, 1H, H-9, *J* = 8.0 Hz); 7.14-7.19 (m, 2H, H-7 and H-8); 7.24-7.39 (m, 6H, H-10 and aryl); 7.62 (d, 2H, aryl, *J* = 8.0 Hz); 7.69-7.74 (m, 4H, aryl); 8.57 (s, 1*NH*, H-11). ¹³C NMR (CDCl₃, 100 MHz) δ: 22.9 (C-6); 35.3 (CH₂ benzyl); 47.5 (CH-Fmoc); 51.0 (C-5); 52.7 (CH₃); 60.5 (C-2); 65.9 (C-11*b*); 67.0 (CH₂ Fmoc); 106.2 (C-6*a*); 111.1 (C-10); 118.4 (C-7); 119.2 (C-9); 120.1 (aryl); 122.5 (C-8); 124.2 (aryl); 124.7 (aryl); 135.7 (C- 10*a*); 127.3 (aryl); 127.6 (aryl), 128.1 (aryl), 129.0 (C-11*a*); 129.5 (aryl); 133.9 (aryl), 126.1 (C-6*b*); 141.8 (aryl); 143.3 (aryl); 155.5 (C=O); 169.0 (C-3); 170.3 (C=O). HR-MS *m/z*: calcd for C₃₇H₃₂N₃O₅, [(*M*+*H*)⁺]: 598.2336; found 598.2336.

(2*S*,5*R*,11*bR*)-methyl-2-benzyl-3-oxo-2,3,5,6,11,11*b*-hexahydro-1*H*imidazo[1',2':1,2]pyrido[3,4-*b*]indole-5-carboxylate (112).

Obtained from intermediate **98** using method C.

65% yield. $[\alpha]_D^{25}$: -39.00 ± 0.00 (c = 0.10, MeOH). ¹H NMR, ¹³C NMR and mass spectra are as for derivative **109**.

(2*S*,5*S*,11*bS*)-2-benzyl-3-oxo-2,3,5,6,11,11*b*-hexahydro-1*H*-imidazo[1',2':1,2]pyrido[3,4-*b*]indole-5-carboxylic acid (113).

Obtained from intermediate **99** using method C.

69% yield. $[\alpha]_D^{25}$: -15.0 ± 0.7 (c = 0.10, MeOH). ¹H NMR (CD₃OD, 400 MHz) : δ: 2.66 (dd, 1H, CH₂, *J*' = 8.0 and *J*'' = 12.0 Hz); 2.86 (dd, 1H, H-6', *J*' = 8.0, *J*'' = 16.0 Hz); 3.10 (dd, 1H, CH₂, *J*' = 4.0 and *J*'' = 16.0 Hz); 3.40 (d, 1H, H-6'', *J* =

16.0 Hz); 3.98 (dd, 1H, H-2, $J' = 4.0$, $J'' = 8.0$ Hz); 4.96 (d, 1H, H-5, $J = 8.0$ Hz); 5.91 (s, 1H, H-11b); 6.91 (t, 1H, H-9, $J = 8.0$ Hz); 6.98-7.02 (m, 2H, H-8 and aryl); 7.07 (t, 2H, aryl, $J = 8.0$ Hz); 7.16 (d, 2H, aryl, $J = 8.0$ Hz); 7.21 (d, 1H, H-10, $J = 8.0$ Hz); 7.34 (d, 1H, H-7, $J = 8.0$ Hz); ^{13}C NMR (CD_3OD , 100 MHz) δ : 25.5 (C-6); 38.4 (CH_2); 49.2 (C-5); 63.8 (C-2); 68.2 (C-11b); 108.5 (C-6a); 112.5 (C-10); 119.6 (C-7); 120.3 (C-9); 123.3 (aryl); 127.8 (C-8); 138.6 (C-10a); 129.6 (aryl); 130.6 (aryl), 132.1 (C-11a), 128.3 (C-6b), 139.5 (aryl); 175.7 (C-3); 177.0 (C=O). HR-MS m/z : calcd. for $\text{C}_{21}\text{H}_{20}\text{N}_3\text{O}_3$, $[(\text{M}+\text{H})^+]$: 362.1499; found 362.1507.

(2*S*,5*S*,11*bS*)-2-benzyl-*N*-ethyl-3-oxo-2,3,5,6,11,11*b*-hexahydro-1*H*-imidazo[1',2':1,2]pyrido[3,4-*b*]indole-5-carboxamide (114).

Obtained from intermediate **100** using methods A (entry 3, table 1, 57% yield). $[\alpha]_{\text{D}}^{25}$: $+13.00 \pm 0.06$ ($c = 0.10$, MeOH). ^1H NMR (CDCl_3 , 400 MHz) : δ : 1.09 (t, 3H, CH_3 , $J = 8.0$ Hz); 2.69 (dd, 1H, CH_2 benzyl, $J' = 8.0$ and $J'' = 12.0$ Hz); 2.97 (dd, 1H, H-6', $J' = 8.0$, $J'' = 16.0$ Hz); 3.19-3.26 (m, 3H, CH_2 benzyl and CH_2); 3.42 (d, 1H, H-6'', $J = 16.0$ Hz); 3.98 (dd, 1H, H-2, $J' = 4.0$, $J'' = 8.0$ Hz); 5.08 (d, 1H, H-5, $J = 8.0$ Hz); 5.83 (s, 1H, H-11b); 5.86 (s, 1NH, H-1); 7.08-7.24 (m, 7H, H-8, H-9 and aryl); 7.30 (d, 1H, H-10, $J = 8.0$ Hz); 7.47 (d, 1H, H-7, $J = 8.0$ Hz); ^{13}C NMR (CDCl_3 , 100 MHz) δ : 15.0 (CH_3); 22.3 (C-6); 34.9 (CH_2); 37.5 (CH_2); 51.7 (C-5); 62.1 (C-2); 66.7 (C-11b); 108.0 (C-6a); 111.5 (C-10); 119.2 (C-7); 120.2 (C-8); 123.2 (C-9); 136.7 (C-10a); 127.2, 128.7; 129.3 (aryl); 129.7 (C-11a); 126.8 (C-6b), 137.2 (aryl); 169.3 (C=O); 174.9 (C-3).

HR-MS m/z : calcd for $\text{C}_{23}\text{H}_{25}\text{N}_4\text{O}_2$, $[(\text{M}+\text{H})^+]$: 389.1972; found 389.1975.

(2*S*,11*bS*)-2-benzyl-5,6,11,11*b*-tetrahydro-1*H*-imidazo[1',2':1,2]pyrido[3,4-*b*]indol-3(2*H*)-one (115).

Obtained from intermediate **101** using method C.

39% yield. $[\alpha]_{\text{D}}^{25}$: 29.0 ± 0.3 ($c = 0.10$, MeOH). ^1H NMR (CDCl_3 , 400 MHz) : δ : 2.69 (dd, 1H, CH_2 , $J' = 8.0$ and $J'' = 12.0$ Hz); 2.79-2.83 (m, 2H, H-6' and H-6''); 3.14-3.18 (m, 1H, H-5'); 3.26 (dd, 1H, CH_2 , $J' = 4.0$ and $J'' = 12.0$ Hz); 3.91 (dd, 1H, H-2, $J' = 4.0$ and $J'' = 8.0$ Hz); 4.46 (dd, 1H, H-5'', $J' = 8.0$, $J'' = 20.0$ Hz);

5.66 (s, 1H, H-11b); 7.08-7.22 (m, 7H, H-8, H-9 and aryl); 7.33 (d, 1H, H-10, $J = 8.0$ Hz); 7.47 (d, 1H, H-7, $J = 8.0$ Hz); 8.13 (s, 1NH, H-11). ^{13}C NMR (CDCl_3 , 100 MHz) δ : 21.2 (C-6); 37.6 (C-5); 38.2 (CH_2); 62.4 (C-2); 68.2 (C-11b); 110.2 (C-6a); 111.5 (C-10); 119.1 (C-7); 120.3 (C-8); 123.2 (C-9); 136.6 (C-10a); 127.0, 128.7 and 129.3 (aryl); 130.9 (C-11a), 126.8 (C-6b), 137.5 (aryl); 173.5 (C-3). HR-MS m/z : calcd. for $\text{C}_{20}\text{H}_{20}\text{N}_3\text{O}$, [(M+H) $^+$]: 318.1601; found 318.1603.

(5S,11bR)-methyl 11b-(4-chlorophenyl)-3-oxo-2,3,5,6,11,11b-hexahydro-1H-imidazo[1',2':1,2]pyrido [3,4-b]indole-5-carboxylate (116).

Obtained from intermediate **102a** or **102b** using method C.

25% yield. $[\alpha]_{\text{D}}^{25}$: -8.00 ± 0.08 ($c = 0.10$, MeOH). ^1H NMR (CDCl_3 , 400 MHz) δ : 2.93 (dd, 1H, H-6', $J' = 8.0$, $J'' = 16.0$ Hz); 3.16 (d, 1H, H-2', $J = 16.0$ Hz); 3.44- 3.48 (m, 1H, H-6''); 3.70 (d, 1H, H-2'', $J = 16.0$ Hz); 3.84 (s, 3H, CH_3); 3.93 (dd, 1H, H-5, $J' = 8.0$, $J'' = 12.0$ Hz); 7.15 (t, 1H, H-9, $J = 8.0$ Hz); 7.26 (t, 1H, H-8, $J = 8.0$ Hz); 7.36 (d, 2H, aryl, $J = 8.0$ Hz); 7.42 (d, 1H, H-10, $J = 8.0$ Hz); 7.51-7.54 (m, 3H, H-7 and aryl); 8.65 (s, 1NH, H-11); ^{13}C NMR (CDCl_3 , 100 MHz) δ : 21.7 (C-6); 48.9 (C-2); 52.6 (CH_3); 52.9 (C-5); 80.1 (C-11b); 111.5 (C-10), 111.9 (C-6a); 119.0 (C-7); 120.3 (C-9); 123.3 (C-8); 136.7 (C-10a); 128.3 (aryl); 129.3 (aryl), 132.3 (C-11a), 135.7 (aryl), 126.7 (C-6b), 138.7 (aryl), 169.7 (C=O); 176.8 (C-3). HR-MS m/z : calcd. for $\text{C}_{21}\text{H}_{19}\text{ClN}_3\text{O}_3$, 396.1109, 398.1080, [(M+H) $^+$]: found 396.1114, 398.1086.

(5S,11bS)-methyl 11b-(4-chlorophenyl)-3-oxo-2,3,5,6,11,11b-hexahydro-1H-imidazo[1',2':1,2]pyrido [3,4-b]indole-5-carboxylate (117).

Obtained from intermediate **102a** or **102b** using method C.

26% yield. $[\alpha]_{\text{D}}^{25}$: $+30.00 \pm 0.03$ ($c = 0.10$, MeOH). ^1H NMR (CDCl_3 , 400 MHz) δ : 3.17 (s, 3H, CH_3); 3.20 (dd, 1H, H-6', $J' = 8.0$, $J'' = 16.0$ Hz); 3.29 (dd, 1H, H-6'', $J' = 4.0$, $J'' = 16.0$ Hz); 3.46 (d, 1H, H-2', $J = 20.0$ Hz); 3.97 (d, 1H, H-2'', $J = 20.0$ Hz); 5.19 (dd, 1H, H-5, $J' = 4.0$, $J'' = 8.0$ Hz); 7.15-7.19 (m, 3H, H-9 and aryl); 7.24-7.28 (m, 3H, H-8 and aryl); 7.39 (d, 1H, H-10, $J = 8.0$ Hz); 7.56 (d, 1H, H-7, $J = 8.0$ Hz); ^{13}C NMR (CDCl_3 , 100 MHz) δ : 20.3 (C-6); 49.2 (C-2); 50.4 (C-5); 52.0 (CH_3); 78.7 (C-11b); 109.4 (C-6a); 111.5 (C-10); 119.1 (C-7);

120.3 (C-9); 123.2 (C-8); 136.1 (C-10a); 128.5 (aryl); 128.9 (aryl), 132.2 (C-11a), 135.3 (aryl), 126.6 (C-6b), 139.4 (aryl), 170.4 (C=O); 174.6 (C-3). HR-MS m/z : calcd. for $C_{21}H_{19}ClN_3O_3$, 396.1109, 398.1080, $[(M+H)^+]$: found 396.1112, 398.1074.

(5S,11bR)-methyl-11b-(4-methoxyphenyl)-3-oxo-2,3,5,6,11,11b-hexahydro-1H-imidazo[1',2':1,2]pyrido [3,4-b]indole-5-carboxylate (118).

Obtained from intermediate **103a** or **103b** using method C.

37% yield. $[\alpha]_D^{25}$: -89.0 ± 0.9 ($c = 0.10$, MeOH). 1H NMR (CD_3OD , 400 MHz) δ : 2.83 (dd, 1H, H-6', $J' = 4.0$, $J'' = 16.0$ Hz); 3.05 (d, 1H, H-2', $J = 16.0$ Hz); 3.24-3.29 (m, 1H, H-6''); 3.67 (d, 1H, H-2'', $J = 16.0$ Hz); 3.73 (s, 6H, OCH_3 and CH_3); 3.96 (dd, 1H, H-5, $J' = 4.0$, $J'' = 8.0$ Hz); 6.88 (d, 2H, aryl, $J = 8.0$ Hz); 6.98 (t, 1H, H-9, $J = 8.0$ Hz); 7.10 (t, 1H, H-8, $J = 8.0$ Hz); 7.34 (d, 1H, H-10, $J = 8.0$ Hz); 7.39-7.43 (m, 3H, aryl and H-7); ^{13}C NMR (DMSO, 100 MHz) δ : 21.3 (C-6); 48.3 (C-2); 51.9 (CH_3); 52.1 (C-5); 55.2 (OCH_3); 81.0 (C-11b); 108.8 (C-6a); 111.5 (C-10); 113.7 (aryl); 118.2 (C-7); 118.7 (C-9); 121.8 (C-8); 134.4 (C-10a); 128.4 (aryl); 132.5 (C-11a), 125.8 (C-6b), 136.4 (aryl), 159.5 (aryl), 169.7 (C=O); 177.0 (C-3). HR-MS m/z : calcd. for $C_{22}H_{22}N_3O_4$, $[(M+H)^+]$: 392.1605; found 392.1607.

(5S,11bS)-methyl-11b-(4-methoxyphenyl)-3-oxo-2,3,5,6,11,11b-hexahydro-1H-imidazo[1',2':1,2]pyrido[3,4-b]indole-5-carboxylate (119).

Obtained from intermediate **103a** or **103b** using method C.

37% yield. $[\alpha]_D^{25}$: $+42.0 \pm 0.35$ ($c = 0.10$, MeOH). 1H NMR ($CDCl_3$, 400 MHz) δ : 3.01 (s, 3H, CH_3); 3.05 (d, 1H, H-6', $J = 4.0$ Hz); 3.28 (d, 1H, H-6'', $J = 16.0$ Hz); 3.40 (d, 1H, H-2', $J = 12.0$ Hz); 3.69 (s, 3H, OCH_3); 3.99 (d, 1H, H-2'', $J = 12.0$ Hz); 5.16 (d, 1H, H-5, $J = 4.0$); 6.77 (d, 2H, aryl, $J = 8.0$ Hz); 7.00 (t, 1H, H-9, $J = 8.0$ Hz); 7.06 (d, 2H, aryl, $J = 8.0$ Hz); 7.09 (t, 1H, H-8, $J = 8.0$ Hz); 7.31 (d, 1H, H-10, $J = 8.0$ Hz); 7.47 (d, 1H, H-7, $J = 8.0$ Hz); ^{13}C NMR ($CDCl_3$, 100 MHz) δ : 21.5 (C-6); 50.5 (C-2); 51.4 (C-5); 52.6 (CH_3); 55.9 (OCH_3); 81.0 (C-11b); 108.9 (C-6a); 112.7 (C-10); 114.6 (aryl); 119.5 (C-7); 120.5 (C-9); 123.5 (C-8); 138.3 (C-10a); 130.4 (aryl); 134.2 (C-11a), 134.7 (aryl), 127.7 (C-6b),

161.6 (aryl), 172.0 (C=O); 176.8 (C-3). HR-MS m/z : calcd. for $C_{22}H_{22}N_3O_4$, $[(M+H)^+]$: 392.1605; found 392.1609.

(2S,5S,11bR)-methyl 2-benzyl-11b-(4-methoxyphenyl)-3-oxo-2,3,5,6,11,11b-hexahydro-1H-imidazo[1',2':1,2]pyrido[3,4-b]indole-5-carboxylate (120).

Obtained from intermediate **104a** or **104b** using method C.

29% yield. $[\alpha]_D^{25}$: -33.00 ± 0.01 ($c = 0.10$, MeOH). 1H NMR ($CDCl_3$, 400 MHz): δ : 2.93 (dd, 1H, H-6', $J' = 4.0$, $J'' = 16.0$ Hz); 3.00 (dd, 1H, CH_2a benzyl, $J' = 4.0$, $J'' = 12.0$ Hz); 3.42-3.53 (m, 2H, H-6'' and CH_2b benzyl); 3.48 (t, 1H, H-2, $J = 4.0$ Hz); 3.77 (s, 3H, OCH_3); 3.80 (dd, 1H, H-5, $J' = 4.0$, $J'' = 12.0$ Hz); 3.91 (s, 3H, CH_3); 6.67 (d, 2H, aryl, $J = 8.0$ Hz); 6.72 (d, 2H, aryl, $J = 8.0$ Hz); 7.18 (t, 1H, H-8, $J = 8.0$ Hz); 7.26-7.30 (m, 3H, H-9 and aryl); 7.42-7.44 (m, 3H, H-10 and aryl); 7.55 (d, 1H, H-7, $J = 8.0$ Hz); 8.51 (s, 1H, NH-11). ^{13}C NMR ($CDCl_3$, 100 MHz) δ : 21.8 (C-6); 35.3 (CH_2 benzyl); 52.4 (CH_3); 52.5 (C-5); 55.3 (OCH_3); 59.7 (C-2); 79.5 (C-11b); 111.3 (C-6a); 111.4 (C-10); 114.0 (aryl); 118.9 (C-7); 120.1 (C-9); 123.0 (C-8); 126.8 (C10a); 127.4, 128.2, 129.0; 130.1 (aryl); 135.7 (C-11a); 136.4 (C-6b); 160.2 (aryl); 169.8 (C=O); 177.4 (C-3). HR-MS m/z : calcd. for $C_{29}H_{28}N_3O_4$, $[(M+H)^+]$: 482.2074; found 482.2080.

(2S,5S,11bS)-methyl 2-benzyl-11b-(4-methoxyphenyl)-3-oxo-2,3,5,6,11,11b-hexahydro-1H-imidazo[1',2':1,2]pyrido[3,4-b]indole-5-carboxylate (121).

Obtained from intermediate **104a** or **104b** using method C.

32% yield. $[\alpha]_D^{25}$: 19.00 ± 0.09 ($c = 0.10$, MeOH). 1H NMR ($CDCl_3$, 400 MHz): δ : 2.38 (dd, 1H, CH_2a benzyl, $J' = 12.0$, $J'' = 16.0$ Hz); 2.92-3.03 (m, 5H, CH_2b benzyl, H-6' and CH_3); 3.26 (d, 1H, H-6'', $J = 16.0$ Hz); 3.67 (s, 3H, OCH_3); 4.35 (dd, 1H, H-2, $J' = 4.0$, $J'' = 8.0$ Hz); 5.15 (dd, 1H, H-5, $J' = 4.0$, $J'' = 8.0$ Hz); 6.68 (d, 2H, aryl, $J = 8.0$ Hz); 6.90-6.96 (m, 1H, aryl); 6.99-7.09 (m, 6H, aryl); 7.11 (t, 1H, H-8, $J = 8.0$ Hz); 7.21 (t, 1H, H-9, $J = 8.0$ Hz); 7.34 (d, 1H, H-10, $J = 8.0$ Hz); 7.47 (d, 1H, H-7, $J = 8.0$ Hz); 8.04 (s, 1H, NH-11). ^{13}C NMR ($CDCl_3$, 100 MHz) δ : 20.4 (C-6); 39.3 (CH_2 benzyl); 50.0 (C-5); 51.9 (CH_3); 55.3 (OCH_3); 61.1 (C-2); 77.4 (C-11b); 108.1 (C-6a); 111.3 (C-10); 113.4 (aryl); 119.0 (C-7); 120.0 (C-8); 127.8 (C-9); 126.4 (aryl); 126.8 (C10a); 128.1; 128.8; 129.3,

133.5 (aryl); 134.0 (C-11a); 136.2 (C-6b); 137.8 and 160.0 (aryl); 170.3 (C=O); 174.5 (C-3). HR-MS m/z : calcd. for $C_{29}H_{28}N_3O_4$, $[(M+H)^+]$: 482.2074; found 482.2083.

(2S,5S,11bR)-methyl 2-benzyl-11b-isobutyl-3-oxo-2,3,5,6,11,11b-hexahydro-1H-imidazo[1',2':1,2]pyrido[3,4-b]indole-5-carboxylate (122).

Obtained from intermediate **103a** or **103b** using method C.

33% yield. $[\alpha]_D^{25}$: -39.00 ± 1.00 ($c = 0.10$, MeOH). 1H NMR ($CDCl_3$, 400 MHz) : δ : 0.69 (d, 3H, CH_3 , $J = 8.0$ Hz); 0.73 (d, 3H, CH_3 , $J = 8.0$ Hz); 1.09-1.13 (m, 1H, CH); 1.64 (dd, 2H, CH_2 , $J' = 8.0$, $J'' = 16.0$ Hz); 2.92 (dt, 2H, H-6' and CH_2a benzyl, $J' = 4.0$, $J'' = 16.0$ Hz); 3.21 (dd, 1H, CH_2b benzyl, $J' = 8.0$, $J'' = 16.0$ Hz); 3.35-3.39 (m, 2H, H-2 and H6''); 3.83 (s, 3H, CH_3); 4.06 (dd, 1H, H-5, $J' = 4.0$, $J'' = 12.0$ Hz); 7.03 (t, 1H, H-9, $J = 8.0$ Hz); 7.12 (t, 1H, H-8, $J = 8.0$ Hz); 7.22-7.28 (m, 6H, H-10 and aryl); 7.41 (d, 1H, H-7, $J = 8.0$ Hz); 8.04 (s, 1H, NH-11). ^{13}C NMR ($CDCl_3$, 100 MHz) δ : 21.7 (C-6); 23.1 (CH); 23.4 (CH_3); 25.0 (CH_3); 35.1 (CH_2 benzyl); 45.7 (CH_2); 52.4 (CH_3); 53.3 (C-5); 58.7 (C-2); 78.5 (C-11b); 109.8 (C-6a); 111.4 (C-10); 118.8 (C-7); 120.0 (C-9); 122.9 (C-8); 126.8 (C10a); 127.4; 128.9; 129.8; 130.0 (aryl); 135.8 (C-11a); 136.2 (C-6b); 169.6 (C=O); 178.4 (C-3). HR-MS m/z : calcd. for $C_{26}H_{30}N_3O_3$, $[(M+H)^+]$: 432.2282; found 432.2287.

(2S,5S,11bS)-methyl 2-benzoyl-11b-isobutyl-3-oxo-2,3,5,6,11,11b-hexahydro-1H-imidazo[1',2':1,2]pyrido[3,4-b]indole-5-carboxylate (123).

Obtained from intermediate **105a** or **105b** using method C.

24% yield. $[\alpha]_D^{25}$: 26.00 ± 1.1 ($c = 0.10$, MeOH). 1H NMR ($CDCl_3$, 400 MHz) : δ : 0.75 (d, 3H, CH_3 , $J = 8.0$ Hz); 0.90 (d, 3H, CH_3 , $J = 8.0$ Hz); 1.19-1.23 (m, 1H, CH); 1.77 (t, 2H, CH_2 , $J = 12.0$ Hz); 2.45 (dd, 1H, CH_2a benzyl, $J' = 8.0$, $J'' = 12.0$ Hz); 3.06-3.13 (m, 2H, CH_2b benzyl and H-6'); 3.70 (s, 3H, CH_3); 4.04-4.09 (m, 1H, H-2); 5.13 (dd, 1H, H-5, $J' = 4.0$, $J'' = 8.0$ Hz); 7.03-7.17 (m, 7H, aryl, H-8 and H-9); 7.29 (d, 1H, H-10, $J = 8.0$ Hz); 7.43 (d, 1H, H-7, $J = 8.0$ Hz); 8.04 (s, 1H, NH-11). ^{13}C NMR ($CDCl_3$, 100 MHz) δ : 21.2 (C-6); 22.7 (CH); 24.2 (CH_3); 24.4 (CH_3); 37.9 (CH_2 benzyl); 48.8 (CH_2); 50.3 (C-5); 52.6 (CH_3); 60.3 (C-2);

76.7 (C-11b); 105.6 (C-6a); 111.3 (C-10); 118.7 (C-7); 120.1 (C-9); 122.6 (C-8);
126.3 (C10a); 126.6; 128.4; 129.0; (aryl); 134.9 (C-11a); 135.4 (C-6b); 136.5
(aryl); 171.3 (C=O); 178.8 (C-3). HR-MS *m/z*: calcd. for C₂₆H₃₀N₃O₃, [(M+H)⁺]:
432.2282; found 432.2293.

4.2 Computational details

Preparation of the chemical structures

The chemical structures of compounds **81**, **81'** were built with Maestro 10.5,⁹⁶ and optimized with MacroModel 11.1⁹⁶ with the OPLS force field⁹⁷ and the Polak-Ribier conjugate gradient algorithm (PRCG, maximum derivative less than 0.001 kcal/mol).

Molecular dynamics simulations

Molecular dynamics simulations were performed at 450 K, with a time step of 1.5 fs, an equilibration time of 0.5 ns, a simulation time of 100 ns, using MacroModel 11.1, and saving 2000 conformers for each compound.

DFT calculations

About compounds **81**, **81'** conformational search rounds were performed with MacroModel 11.1 at the empirical molecular mechanics (MM) level, with Monte Carlo Multiple Minimum (MCMM) method and Low mode Conformational Search (LMCS) method. Also, molecular dynamic simulations were performed at 450, 600, 700, 750 K, with a time step of 2.0 fs, an equilibration time of 0.1 ns, and a simulation time of 10 ns. All the produced conformers were then analyzed, and non-redundant conformers were selected by using the “Redundant Conformer Elimination” module of Macromodel 11.1.

QM calculations were performed using Gaussian 09 software package.⁹⁸ The obtained conformers were energy and geometry optimized at QM level by using the M062X functional and the 6-311+G(d,p) basis set. For the above mentioned compounds, the selected conformers were accounted for the subsequent computation of the ¹³C and ¹H NMR chemical shifts, using the MPW1PW91 functional and the 6-31G(d,p) basis set. The final ¹³C NMR and ¹H NMR spectra were built considering the influence of each conformer on the total Boltzmann distribution and taking into account the relative energies previously determined using M062X/6-311+G(d,p) functional/basis set. Calibrations of calculated ¹³C and ¹H chemical shifts were performed following the multi-standard approach

(MSTD).⁹⁹ In particular, sp^2 ^{13}C (excluding carbonyl carbons) and 1H chemical shift data were computed using benzene as reference compound, and the remaining $^{13}C/^1H$ data using tetramethylsilane as reference.

Experimental and calculated ^{13}C and 1H NMR chemical shifts were compared computing the $\Delta\delta$ parameter (compounds **81/81'**):

$$\Delta\delta = |\delta_{\text{exp}} - \delta_{\text{calc}}|$$

where, δ_{exp} (ppm) and δ_{calc} (ppm) are the $^{13}C/^1H$ experimental and calculated chemical shifts, respectively.

The mean absolute errors (MAEs) for the diastereoisomeric pairs **81/81'** were computed:

$$\text{MAE} = \sum(\Delta\delta)/n$$

defined as the summation through n of the absolute error values (difference of the absolute values between corresponding experimental and ^{13}C - 1H chemical shifts), normalized to the number of the chemical shifts considered (n).

The energy diagrams for the reactions leading to **81/81'** diastereoisomeric pairs were built computing the free energies (G) of the three main species involved: a) reactant (N-acyliminium ion); b) unstable chemical species at the transition state; c) product (aminoacetal derivatives species protonated at N1). In particular, for a) and c) steps, conformational searches were performed following the above reported workflow. Then, the produced conformers were optimized at the M062X/6-311+G(d,p) functional/basis set level of theory and, in order to reproduce the experimental environment, conformers showing intramolecular H-bonds were discarded. On the selected conformers, force constants and the resulting vibrational frequencies (*Freq* Gaussian keyword) were computed at the M062X/6-311+G(d,p) level of theory.

Furthermore, for each compound, a starting guess geometry model representing the transition state (step b) was built and optimized at the QM level (M062X/6-311+G(d,p) level of theory), using the Berny algorithm followed by vibrational frequency calculations (*TS*, *CalcAll*, *Freq* keywords for Gaussian calculations).

Analysis of the vibrational frequencies showed that the optimized structure was correctly associated to the transition state, since an imaginary frequency was detected and the vibration between C11b and N1 involved in the chemical bond leading to the formation of the aminoacetal species was correctly visualized.

Molecular docking

Docking calculations were performed using Glide software (version 7.0, Schrödinger package).¹⁰⁰ Glide docking experiments were performed using the crystal structure of mPGES-1 co-complexed with the potent inhibitor LVJ (PDB code: 4BPM), generating a receptor grid focused on the ligand binding site. Molecular docking calculations were performed using the XP (Extra Precision) Glide mode, sampling ligands as flexible. 20 maximum output structures were saved for the ligand; a post-docking optimization of the obtained docking outputs was performed, accounting 20 maximum number of poses. Docking results were analyzed with Maestro (version 10.5). Illustrations of the 3D models were generated using Maestro 10.5.^{100a}

CHAPTER III:
Indole-based derivatives as
varicella zoster virus (VZV) inhibitors

1.1 Introduction

The discovery and development of new antiviral drugs are of great interest for global human health, particularly as new pathogens emerge and old ones evolve to evade current therapeutic agents. Viruses are intracellular pathogens that have developed many strategies to evade host immune responses. Combating viral diseases with vaccines or antiviral drugs, or both, is a constant challenge. Even when successful strategies are discovered and employed, the high rate of genetic change exhibited by many viruses, particularly RNA viruses, often enables drug resistance or vaccine escape.¹⁰¹ Among the viruses which are able to develop resistance to drug treatment Varicella zoster virus infection is one of the worldwide distributed and virulent.

Varicella-zoster virus (VZV) is an ubiquitous human alphaherpesvirus, which causes varicella (chicken pox) and herpes zoster (shingles). Varicella results from primary VZV infection; it is a common childhood illness associated with fever and a generalized pruritic vesicular rash. Herpes zoster is a localized, painful, vesicular rash involving one or adjacent dermatomes and caused by VZV reactivation. The incidence of herpes zoster increases with age or immunosuppression.¹⁰²

1.2 Pathogenesis of Varicella-Zoster Virus

Humans are infected with varicella-zoster virus when the virus comes in contact with the mucosa of the upper respiratory tract or the conjunctiva. The virus disseminates throughout the bloodstream to the skin in mononuclear cells, causing the generalized rash of varicella.¹⁰³ The average incubation period for varicella is 14 days; almost all cases occur from 10 to 20 days after exposure. Other organs are infected, including the central nervous system. As is characteristic of the alphaherpesviruses, VZV establishes latency in cells of the dorsal root ganglia after primary infection.¹⁰⁴ When viral replication is reactivated, VZV reaches the skin via anterograde axonal transport to cause the symptoms of zoster, which is characterized by a vesicular rash in the dermatome. Both varicella and zoster skin lesions contain high concentrations of infectious virus and are thus responsible for transmission to susceptible individuals. It has been difficult to verify individual

steps in viral pathogenesis because VZV is a highly human-specific virus that has little or no capacity to infect other species.¹⁰⁵

1.3 Epidemiology of Varicella-Zoster Virus

Over 95% of immunocompetent individuals aged at least 50 years are seropositive for VZV and are, therefore, at risk of developing Herpes zoster (HZ).¹⁰⁶ VZV-specific cell-mediated immunity declines with age concomitantly with the rise in the incidence of HZ and its complications that occurs at about 50 years of age.¹⁰⁷ The estimated average overall incidence of HZ is about 3.4–4.82 per 1000 person per year which increases to more than 11 per 1000 person years in those aged at least 80 years. The overall incidences of medically attended HZ and HZ-related outpatient visits and hospitalizations were reported to increase with age.^{108,109} HZ-associated mortality is rare, with reported incidence in people aged at least 60 years.¹¹⁰

1.4 Treatment and resistance

In immunocompetent children, varicella zoster infections can cause severe morbidity and mortality, as well as in patients with impaired cell-mediated immune responses. In addition, complications of herpes zoster in immunocompetent hosts include post-herpetic neuralgia (PHN), a persistent pain syndrome, which is the most challenging complication particularly in older individuals.^{111,112} The dramatically improving of herpes zoster infections, especially in immunocompromised patients, led scientific research to develop safe and effective antiviral drugs. Vidarabine and interferon- α have been used in the treatment of severe VZV infection, but because their modest efficacy and substantial toxicity have been replaced by antiviral agents with enhanced in vitro activity, improved pharmacokinetic properties and safety profiles. Most of the approved compounds for the treatment of VZV infections are nucleoside analogues which require phosphorylation by the viral thymidine kinase. Three oral guanine-based antivirals are approved worldwide for the treatment of VZV-associated diseases: acyclovir, valacyclovir, and famciclovir.¹¹³ Acyclovir and its analogues are converted to their monophosphate by virus-encoded thymidine

kinase (TK). Cellular enzymes catalyze the subsequent diphosphorylation and triphosphorylation steps which yield high concentrations of the triphosphate derivative in VZV-infected cells. The triphosphate derivative inhibits viral DNA synthesis by competing with deoxyguanosine triphosphate as a substrate for viral DNA polymerase. Incorporation into viral DNA results in obligate chain termination since the molecule lacks the 3-hydroxyl group required for further DNA chain elongation. Viral DNA polymerase is tightly associated with the terminated DNA chain and is functionally inactivated.¹¹⁴ Among the nucleoside analogues that have been pursued for the treatment of VZV infections, one of the most potent inhibitors of in vitro VZV replication is brivudine. Brivudine is an analogue of thymidine and is incorporated into the viral DNA blocking the action of DNA polymerases.¹¹⁵

One of the limitations of the use of nucleoside derivatives is the emergence of single and multiple drug resistance linked to mutations in TK gene of VZV.¹¹⁶ Three distinct classes of acyclovir-resistant TK mutants have been identified: TK-negative (TKN), TK-partial (TKP), and TK-altered (TKA) mutants. TKN mutants lack TK activity, whereas TKP mutants express reduced levels of TK activity. TKA mutants phosphorylate thymidine but not acyclovir. Mutants with altered DNA polymerase have also been identified,¹¹⁷ although these are infrequently reported.¹¹⁸ A drug of choice for treatment of acyclovir-resistant VZV disease is foscarnet. It is a pyrophosphate analogue, which binds reversibly near the pyrophosphate-binding site of DNA polymerase without requiring further modification. After binding, the drug blocks the cleavage of the pyrophosphate moiety from deoxynucleotide triphosphates, halting DNA chain elongation.¹¹⁹ In addition, several small molecules have been identified and reported as potent and selective VZV inhibitors with different mechanisms of action. Some examples are the 4-oxo-dihydroquinoline and 4-oxo-dihydrothieno[2,3-b]pyridine derivatives as inhibitors of the viral DNA polymerases, the oxadiazolephenyl derivative (ASP2151) as a helicase-primase inhibitor,¹²⁰ and N- α -methylbenzyl-N'-arylthiourea derivatives that interfere with the function of the viral ORF54 protein, impairing morphogenesis of the capsid.¹²¹ Finally, a series of 4-

benzyloxy- γ -sultone derivatives has been also reported as non-selective VZV inhibitors with unknown mechanism of action.^{121a}

2.1 Background and design: 1st series

Given the difficulty of identifying initial hit compounds in this field, we considered of interest to use a privileged scaffold as effective starting point in the search for anti-VZV ligands.¹²² Indole scaffold is widely used in antiviral research. Examples of marketed indole-containing antiviral drugs include Arbidol and Delavirdine. Meanwhile, a number of indole derivatives are actively undergoing different phases of clinical evaluation, such as Ateviridine, GSK2248761 (IDX-12899), Golotimod, Panobinostat (LBH589), BILB 1941, BMS-791325, MK-8742 and Enfuvirtide.¹²³ With the aim to identify small molecules able to inhibit VZV replication we decided to explore the minimum structural requirements for anti-VZV activity starting from this scaffold. We synthesized a first series of derivatives based on substituted indoles (A, B) and tryptamines (C) (Figure 1).

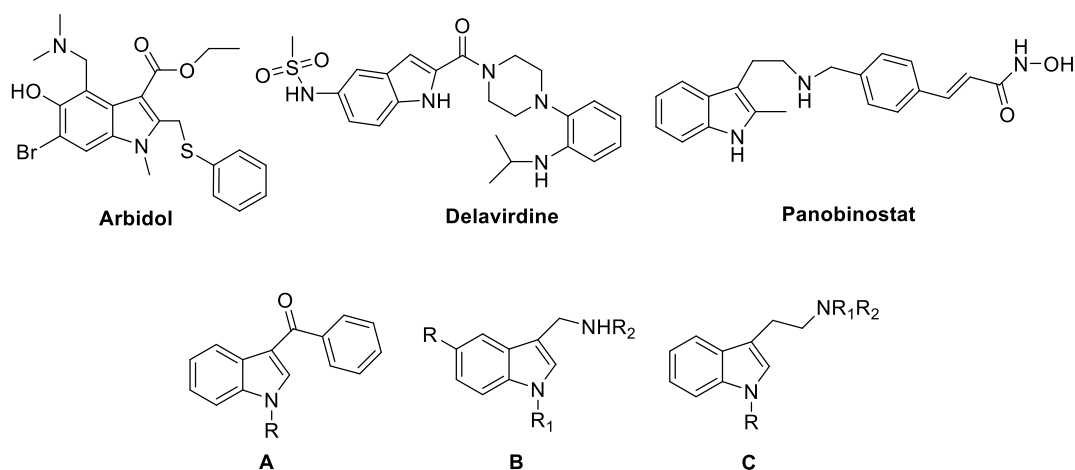
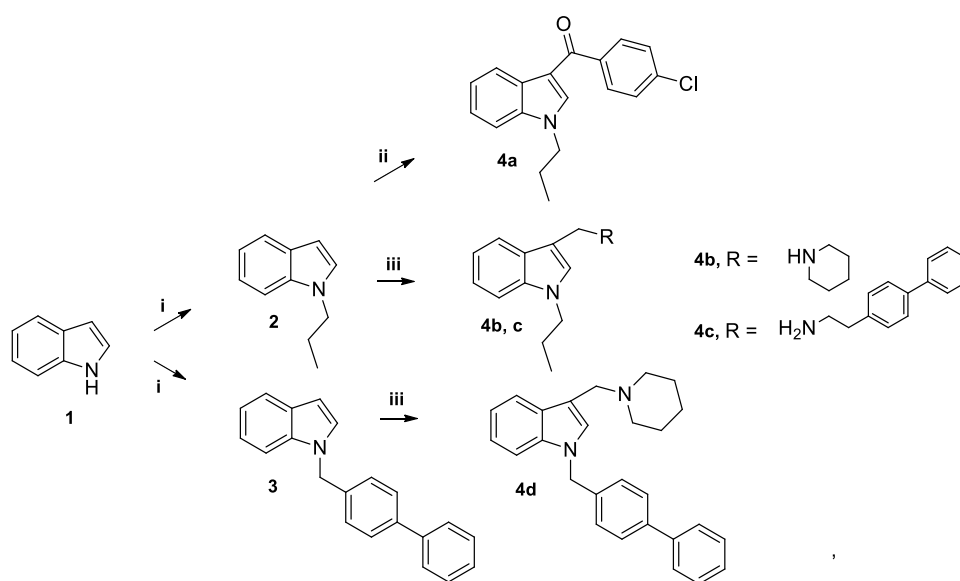


Figure 1. Indole-containing antiviral compounds. Structure of indole (A, B) and tryptamine (C) derivatives.

2.2 Synthesis of 1st series

Compounds **4a-d** were prepared starting from indole **1** according to Scheme 1. N-1 alkylation of **1** with propyl iodide or 4-phenylbenzyl iodide in DCM/DMF using NaH as base, gave the corresponding intermediates **2** and **3**, respectively. The 3-acyl derivative **4a** was obtained from **2** by Friedel-Crafts acylation, using 4-chlorobenzoyl chloride and AlCl₃ in acetonitrile (32% yield). Functionalization of **2** and **3** through a Mannich reaction, using formaldehyde and piperidine/or biphenyl ethyl amine, and TFA as catalyst, led to 3-methylamine derivatives **4b-d** (25-38% yield).

Scheme 1. Synthesis of derivatives 4a-d.

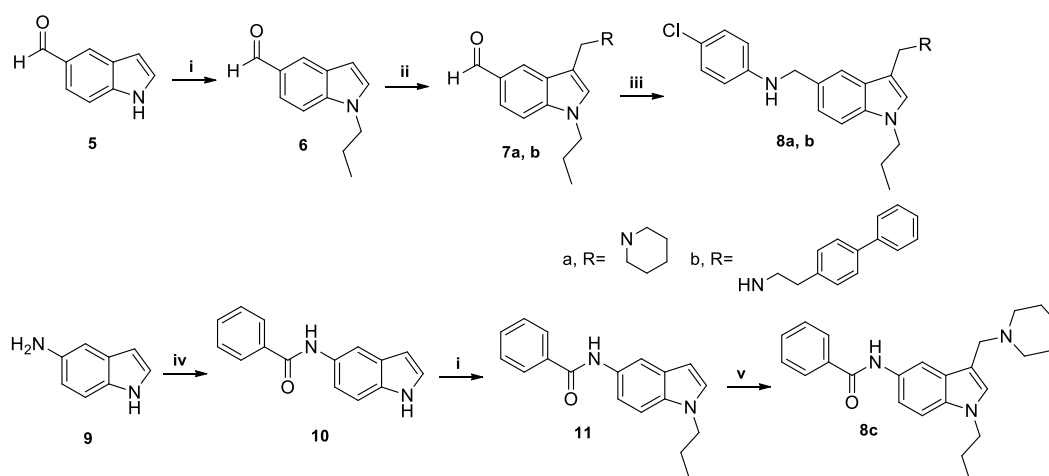


Reagents and conditions: i: DCM/DMF, NaH, n-propyl iodide or 4-phenylbenzyl iodide, 12h, rt; ii: CH₃CN dry, AlCl₃, 4-chlorobenzoyl chloride, 12h, rt; iii: DCM, CH₂O, 2eq TFA, RNH₂, 12h rt.

The 5-substituted indole derivatives (**8a-c**) were synthesized using the indole-5-carboxyaldehyde (**5**) and the 5-aminoindole (**9**) as starting material and following the two-synthetic strategy indicated in Scheme 2. **5** was first N-alkylated (**6**) and then subjected to a Mannich reaction to obtain the corresponding aldehydes **7a** and **7b**, as described above. Treatment of these intermediates with 4-chloroaniline and sodium triacetoxyborohydride in reductive amination conditions, led to final

products **8a** and **8b** in 24% and 30% yield, respectively. On the other hand, reaction of **9** with benzoic acid using HOBt/HBTU as coupling agents gave N-(1Hindol-5-yl)benzamide **10** in 63% yield. N-alkylation of **10** with n-propyl iodide followed by Mannich reaction with formaldehyde and piperidine afforded final compound **8c**.

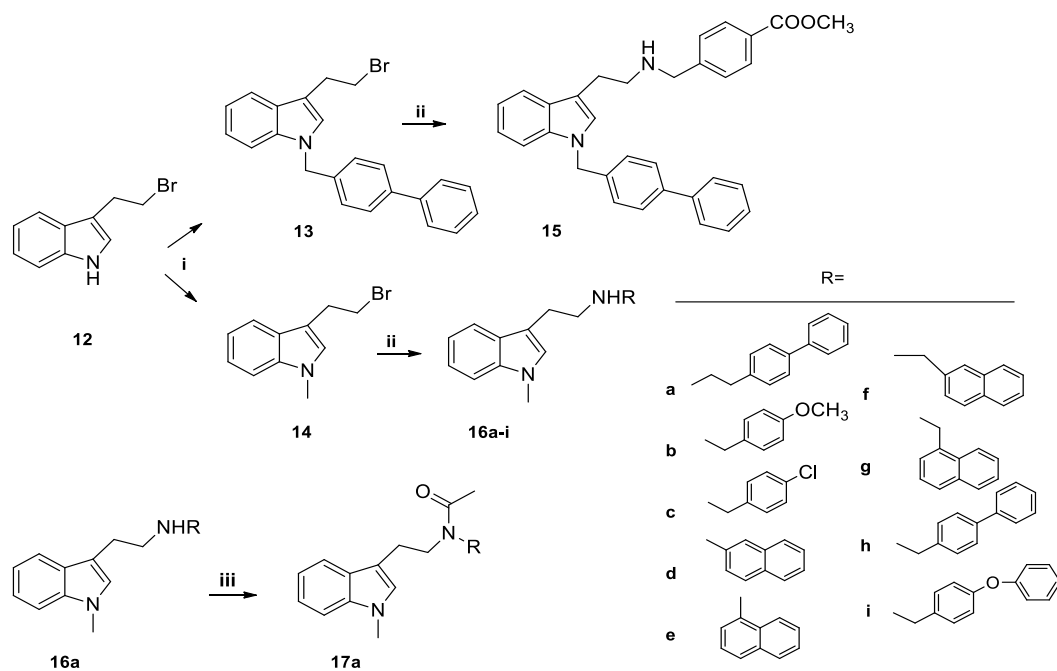
Scheme 2. Synthesis of derivatives 8a-c.



Reagents and conditions: i: DCM/DMF, NaH, n-propyl iodide, 12h, rt; ii: DCM, CH₂O, TFA, piperidine or biphenylethylamine, 12h, rt; iii: DCM/CH₃COOH, 4-chloroaniline, 1.5h, reflux, then Na(CH₃COO)₃BH, 3-5h, reflux; iv: DCM/DMF, HOBt, HBTU, DIPEA, benzoic acid, 12h, rt; v: DCM, CH₂O, TFA, piperidine, 12h, rt.

The tryptamine-based derivatives **15**, **16a-i** were prepared following Scheme 3. N-alkylation of 3-(2-bromoethyl)-1H-indole (**12**) with methyl iodide or 4-phenylbenzyl iodide led to derivatives **13** and **14** in 67% and 61% yield, respectively. Nucleophilic displacement of the bromine atom in these intermediates by different commercially available amines was performed under microwave conditions, using palladium acetate as catalyst, obtaining the compounds **15**, **16a-i** in 38-75% yield. Treatment of compound **16a** with acetyl chloride gave the corresponding acetyl derivative **17a**.

Scheme 3. Synthesis of derivatives 15-17.



Reagents and conditions: i: DCM/DMF, NaH, n-propyl iodide or 4-phenylbenzyl iodide, rt; ii: THF, NaI, R'NH₂, (CH₃COO)₂Pd, TEA, MW, 20', 100 °C; iii: ClCOCH₃, TEA, DCM, 30', rt.

Biological evaluation

3.1 Antiviral activity against Varicella zoster virus: 1st series

All the synthesized derivatives were examined in the Department of Microbiology and Immunology of the Rega Institute for Medical Research, for their ability to inhibit the replication of VZV in human embryonic lung (HEL) cells, and the results were compared to those obtained for the reference compounds acyclovir and brivudin (Table 1). The antiviral activity was expressed as EC₅₀, being the compound concentration required to reduce virus-plaque formation (VZV) by 50%.

As shown in Table 1, the N-propyl-3-acyl (**4a**) and N-propyl-3-piperidine methyl (**4b**) derivatives do not displayed antiviral or cytotoxic activities at 100 mM, while the substitution of piperidine at the 3-position by a biphenylethylamine group and of the propyl group at the N-1 indole by a biphenylmethyl moiety dramatically increased the cytotoxic activity of resultant compounds **4c** and **4d**, with CC₅₀ values of 1.7 and 6.9 mM, respectively. Compounds **8a-c**, derivatized at the C-5 indole position, proved less cytotoxic, but were also ineffective as inhibitors of VZV-induced plaque formation at similar concentrations. The most interesting results were obtained for the tryptamine derivatives. In this series, the presence of a methyl group at the N-indole position lead to weaker cytotoxicity (derivative **16a** versus **15**, CC₅₀ 20-41 versus 7.3 mM), while the acylation of the amine group (**17a**) also reduces cytotoxicity (CC₅₀ ≈ 31-39 mM) but with an inhibitory effect on the anti-VZV activity. Tryptamine derivative **17a** was indeed able to inhibit replication of TK β and TK-VZV strains with EC₅₀ values in the range of 1.7-3.6 mM (Table 1). The potency of **17a** against OKA strain (EC₅₀ ¼ 2.5-3.6 mM) was found comparable to that of the reference drug acyclovir (EC₅₀ ¼ 1.9-2.1 mM) but two orders of magnitude lower than that of brivudin (EC₅₀ ¼ 0.02-0.03 mM). However, the activity of this compound against thymidine kinase-deficient VZV strains, both 07-1 and YS-R, was maintained in the micromolar range with EC₅₀ ¼ 1.7e3.1 mM being, at least, one order of magnitude more active than acyclovir (EC₅₀ ¼ 33e103 mM) and brivudin (EC₅₀ ¼ 26e165 mM).

Table 1. Activity of compounds 4, 8, 15, 16 and 17a against varicella-zoster virus (VZV) in human embryonic lung (HEL) cells.

Comp.	R	R ₁	EC ₅₀ (μM) ^a			CC ₅₀ (μM) ^b
			TK ⁺		TK ⁻	
			OKA	07-1	YS-R	
4a	propyl	Phenylcarbonyl	>100	>100	nd	>100
4b	propyl	Piperidinemethyl	>100	>100	nd	>100
4c	propyl	Biphenylethylaminemethyl	>0.8	>0.8	nd	1.7
4d	biphenylmethyl	Piperidinemethyl	>4	>4	nd	6.9
8a	4-Ph-NHCH ₂	Piperidine	>4	>4	nd	15
8b	4-Ph-NHCH ₂	Biphenylethylamine	>4	>4	nd	9.7
8c	Ph-CO-NH	Piperidine	>20	>20	nd	31
15	biphenyl methyl	biphenyl ethyl	Nd	>4	>4	7.3
16^o	Methyl	biphenyl ethyl	>0.8	>4	nd	20
16b	Methyl	4-(OCH ₃)benzyl	>20	>20	nd	28
16c	Methyl	4-(Cl) benzyl	>4	>4	nd	22
16d	Methyl	2-naphtyl	>100	>100	nd	41
17a (1)^c			3.6	3.1	nd	31
17a (2)			2.5	1.7	2.1	39
Acyclovir (1)			2.1	26		224
Acyclovir (2)			1.9	165	nd	191
Brivudin (1)			0.019	33		300
Brivudin (2)			0.035	103	nd	160

^aEffective concentration required to reduce virus plaque formation by 50%. Virus input was 20 plaque forming units (PFU). ^bCytotoxic concentration required to reduced cell growth by 50%. ^cExperiment number.

3.2 Antiviral activity against other members of the *Herpesviridae* family: 1st series

As shown in Table 2 none of the synthesized compounds was found active either towards other members of *Herpesviridae* family, such as cytomegalovirus (HCMV, AD-169 strain and Davis strain) or against herpes simplex virus-1 (HSV-1; KOS and thymidine kinase-deficient acyclovir-resistant) (HSV-1/TK-KOS ACV^r strains) or against herpes simplex virus-2 (HSV-2; G strain). The derivatives were not active against other DNA viruses such as vaccinia virus, adenovirus-2 and feline herpesvirus. All these compounds also lacked inhibitory activity against a broad variety of RNA viruses, including HIV-1 and HIV-2, feline coronavirus, vesicular stomatitis virus, Coxsackie virus B4 and respiratory syncytial virus, para-influenza-3 virus, reovirus-1, Sindbis virus, Coxsackie virus B4, Punta Toro virus, influenza A virus (H1N1 and H3N2 subtypes) and influenza B virus.

Table 2. Activity of compounds 4, 8, 15, 16, and 17a against cytomegalovirus (HCMV), herpes simplex virus-1 (HSV-1) and herpes simplex virus-1 (HSV-2) in human embryonic lung (HEL) cell cultures.

Comp.	Antiviral activity EC ₅₀ (μM) ^a					Cytotoxicity (μM)
	HCMV		HSV-1		HSV-2	MMC ^b
	AD-169	Davis	(KOS)	TK KOS ACV ^r	(G)	
4a	Nd	>100	>100	>100	>100	>100
4b	>4	>4	>100	>100	>100	>100
4c	Nd	>0.16	>100	>100	>100	4
4d	Nd	>4	>20	>20	>20	20
8a	Nd	>4	>20	>20	>20	20
8b	Nd	>4	>4	>4	>4	20
8c	Nd	>20	>100	>100	>100	100
15	>4	>4	>100	>100	>100	20
16a	>4	>4	>100	>100	>100	>4
16b	>20	>20	>20	>20	>20	100
16c	>20	>20	>20	>20	>20	20
16d	76	100	>100	>100	>100	>100
17a	>4	>4	>100	>100	>100	20
Ganciclovir	3.1	2.1	0.09	100	0.03	>100
Cidofovir	0.38	0.51	0.4	1.2	0.7	>250
Acyclovir			0.08	112	0.2	>250
Brivudin			0.007	50	96	>250

^aEffective concentration required to reduce virus plaque formation by 50%. Virus input was 20 plaque-forming units (PFU). ^bMaximum cytotoxic concentration that cause a microscopically detectable alteration of morphology.

1.1 Background and design: 2nd and 3rd series

Starting from the previously obtained SAR results, we decided to further explore the structural requirements within the tryptamine series and to prepare two series of **17a** analogs featuring a) a modified aromatic moiety linking the acetamide group (series 2) and b) a modified acyl group (series 3). (Figure 2).

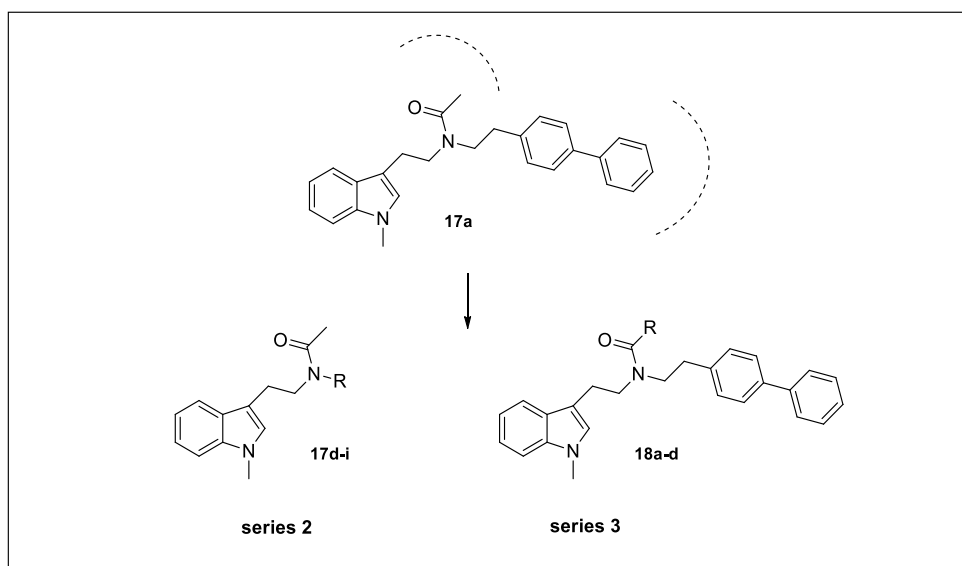
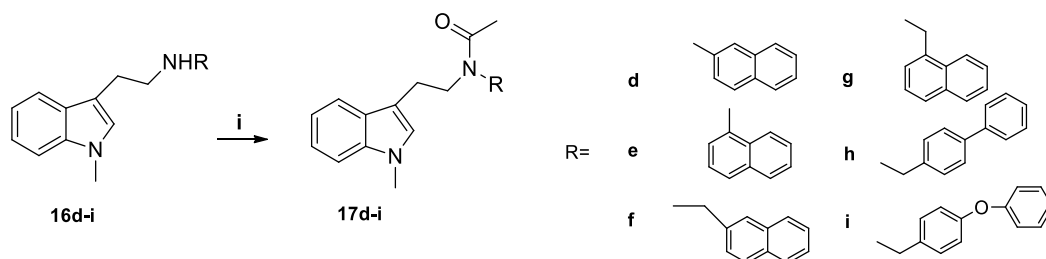


Figure 2. Synthesized compounds of series 2 and 3 starting from **17a**.

4.2 Synthesis of 2nd and 3rd series

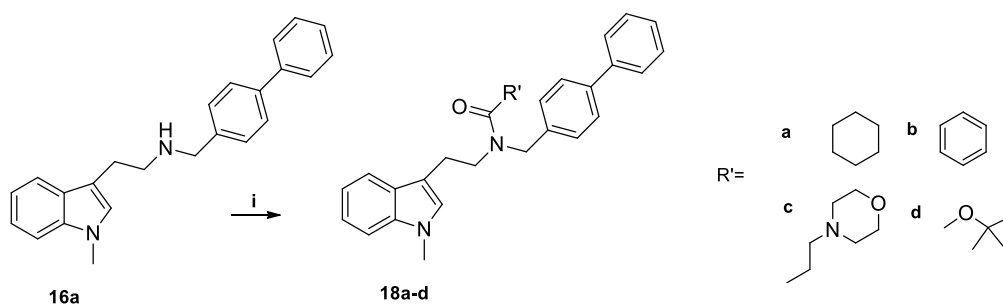
Derivatives **17d-i** were synthesized according to the synthetic route 4. Treatment of compounds **16d-i** with acetyl chloride gave the corresponding acetyl derivatives **17d-i** (42-58% yield).

Scheme 4. Synthesis of derivatives 17d-i.



Analogously, derivatives **18a-d** were prepared applying the synthetic route shown in Scheme 5. Treatment of **16a** with different aromatic and aliphatic acyl chlorides gave the corresponding acylated compounds **18a-c** (48-57% yield). The carbamoyl derivative **18d** was obtained in 58% yield by reaction of **16a** with di-tert-butyl dicarbonate in DCM/TEA.

Scheme 5. Synthesis of derivatives 18a-d.



Biological evaluation

5. Antiviral activity against Varicella zoster virus

The synthesized compounds were examined for their ability to inhibit the replication of VZV in human embryonic lung (HEL) cells. As shown in Table 3, substitution of biphenyl ethyl moiety by the more rigid naphthyl (compounds **17d**, **17e**) or their superior analog naphthylmethyl groups (**17f**, **17g**), as well as, the introduction of a biphenylmethyl or phenyloxybenzyl moieties (**17h**, **17i**) led to a complete loss of the antiviral activity. However, compounds containing 1-naphtyl (**17e**) or 1-naphtyl methyl (**17g**) groups or the inferior analog biphenylmethyl group (**17h**) were less cytotoxic. On the other hand, substitution of the acylmethyl group by bulkier alkyl groups such as cyclohexyl, morpholinethyl and tert-butyl groups (compound **18a**, **18c**, **18d**) led to an annihilation of antiviral activity. In this series of compounds, only the benzoyl derivative **18b** somewhat maintains the antiviral activity at an EC₅₀ of 20 μM, displaying also a reduced cytotoxic activity (MMC >100 μM).

Table 3. Activity of acyl analogs **17** and **18** against varicella-zoster virus (VZV) in human embryonic lung (HEL) cells.

Compounds	R	R ₁	EC ₅₀ (μM) ^a		MCC (μM) ^b
			TK+	TK-	
			OKA	07-1	
17a	Biphenylethyl	Methyl	2.6	2.0	35
17d	2-naphtyl		>4	>4	20
17e	1-naphtyl		>20	>20	100
17f	2-naphtylmethyl		>4	>4	20
17g	1-naphtylmethyl		>20	>20	100
17h	biphenylmethyl		>20	>20	100
17i	phenyloxybenzyl		>4	>4	20
18a		Cyclohexyl	>4	>4	20
18b		Phenyl	20	20	>100
18c		morpholinethyl	>4	>4	20
18d		t-butyl	>4	>4	20
Acyclovir			3.8	145	>440
Brivudin			0.026	143	>300

^aEffective concentration required to reduce virus plaque formation by 50%. Virus input was 20 plaque forming units (PFU). ^bMinimum cytotoxic concentration that causes a microscopically detectable alteration of cell morphology.

6. Conclusions

This work presents the results obtained in the searching for small-molecules able to inhibit VZV replication. In detail the research was based on the identification of a new family of non-nucleoside anti-VZV agents based upon the indole scaffold. The results obtained from the activity and cytotoxic assays shown that the substitution on the tryptamine moiety strongly influences the activity/toxicity of these derivatives. The N-biphenylethyl acetamide derivative **17a** displayed an interesting inhibition against VZV and was endowed with a selectivity of 10-20 (ratio CC_{50}/EC_{50}). The most interesting aspect is that compound **17a** showed similar activity against TK+ and TK- VZV strains, indicating a mechanism of action independent from the virus-encoded thymidine kinase. In addition tryptamine derivative **17a** was found to have a selective inhibitory activity against human varicella zoster virus (VZV) replication in vitro, being inactive against a variety of other DNA and RNA viruses. In order to identify the structural requirements for anti-VZV activity we performed a structure-activity relationship (SAR) study, which showed that the presence of a biphenyl ethyl moiety and the acetylation at the amino group of tryptamine are a prerequisite for anti-VZV activity. The possible mechanism of action of this novel class of compounds will be further investigated.

Experimental section

7.1 Chemistry

Reagents, starting materials, and solvents were purchased from Sigma-Aldrich (Milan, Italy) and used as received. Reactions were carried out with magnetic stirring in round-bottomed flasks unless otherwise noted. Moisture-sensitive reactions were conducted in oven-dried glassware under a positive pressure of dry nitrogen, using pre-dried, freshly distilled solvents. Microwave assisted reactions were performed in a Biotage Initiator + reactor. Analytical thin layer chromatography (TLC) was performed on pre-coated glass silica gel plates 60 (F254, 0.25 mm, VWR International). Purifications were performed by flash column chromatography on silica gel (230-400 mesh, Merck Millipore). NMR spectra were recorded on Varian Mercury-400 apparatus. ¹H NMR and ¹³C NMR spectra were recorded with a Varian-400 spectrometer, operating at 400 and 100 MHz, respectively. Chemical shifts are reported in δ values (ppm) relative to internal Me₄Si, and J values are reported in hertz (Hz). The following abbreviations are used to describe peaks: s (singlet), d (doublet), dd (double double), t (triplet), q (quadruplet) and m (multiplet). ESI-MS experiments were performed on an Applied Biosystem API 2000 triple-quadrupole spectrometer. Combustion microanalyses were performed on a Carlo Erba CNH 1106 analyzer, and were within 0.4% of calculated values and confirmed >95% purity for the final products.

General procedure for the synthesis of N-alkylated indole intermediates (2, 3, 6, 11, 13 and 14).

Indole (**1**, 1.0 eq) or 1H-indole-5-carbaldehyde (**5**, 1.0 eq), or N-(1H-indol-5-yl)benzamide (**10**, 1.0 eq), or 3-(2-Bromoethyl)indole (**13**, 1.0 eq.) were dissolved in a mixture of anhydrous DCM/DMF (2/1 v/v) under magnetic stirring and the temperature was set to 0° C. To this solution, 1.5 equivalents of NaH were added portionwise and the mixture was allowed to react for 30 min. Then, 1.5 equivalents of alkyl iodide [methyl iodide, or n-propyl iodide, or 4-(phenyl)iodomethylbenzene] in DCM were added dropwise and the reaction was

warmed to room temperature and maintained under stirring for further 12 h. The reaction was then quenched by a 10% aqueous solution of citric acid and washed with brine. The organic layer was separated, dried over anhydrous Na₂SO₄, filtered and evaporated in vacuo. Crude products were purified by column chromatography using n-hexane/ethyl acetate (4:1 v:v) as mobile phase. N-alkylated compounds were obtained in 75% yield (derivative **2**); 80% yield (derivatives **3** and **13**); 67% yield (derivative **6**); 55% yield (derivative **11**) and 50% yield (derivative **14**).

Synthesis of derivative 4a.

To a solution of 1-propyl-1H-indole (**2**) in dry CH₃CN was added aluminium trichloride (15 eq) and benzoyl chloride (10 eq), the reaction was stirred at room temperature overnight. The resulting mixture was dried in vacuo and reconstituted in DCM. The organic phase was washed with water (3 X 50 mL), dried over anhydrous Na₂SO₄, filtered, concentrated and purified by column chromatography using n-hexane/ethyl acetate (3/2) as mobile phase. Compound **4a** was obtained in 32% yield.

(4-chlorophenyl)(1-propyl-1H-indol-3-yl)methanone (4a).

Overall yield 32%. ¹H NMR (400 MHz, CDCl₃) δ; 0.88-0.94 (t, 3H, *J*=7.8 Hz, CH₃); 1.82-1.84 (m, 2H, CH₂); 4.12 (t, 2H, *J*=7.8 Hz, CH₂); 7.25-7.30 (m, 3H); 7.35 (d, 2H, *J*=8.0 Hz); 7.52 (s, 1H); 7.76 (d, 2H, *J*=8.0 Hz); 8.39 (d, 1H, *J*=5.2 Hz). ¹³C NMR (100 MHz, CDCl₃) δ 11.4, 22.7, 47.4, 109.6, 119.8, 119.9, 121.7, 126.5, 127.7, 128.9, 131.8, 137.4, 138.2, 181.2. ESIMS *m/z* calcd for C₁₈H₁₆ClNO [(M + H)⁺] 297.78; found, 297.09.

Synthesis of derivatives 4b-d.

A solution of formaldehyde (2 eq.), trifluoroacetic acid (2 eq.) and 2 equivalents of the proper amine (piperidine or bifenyloethylamine) was added portionwise to a solution of the intermediate **2** or **3** (1 eq.) in DCM. The mixture was stirred for 3 h at room temperature, then was washed with water (3 X 50 mL), dried over anhydrous Na₂SO₄, filtered, concentrated and purified by column chromatography

using DCM/MeOH (9:1 v/v) as mobile phase. Compounds **4b-d** were obtained in 25%-38% yield.

3-(piperidin-1-ylmethyl)-1-propyl-1H-indole (4b).

Overall yield 25% ¹H NMR (400 MHz, CDCl₃) δ; 0.88-0.94 (t, 3H, *J*=7.6 Hz, CH₃); 1.40-1.56 (m, 6H, CH₂); 1.88-1.82 (m, 2H, CH₂); 2.40-2.47 (m, 4H, CH₂); 3.68 (s, 2H, CH₂); 4.04 (t, 2H, *J*=7.6 Hz, CH₂); 7.18-7.12 (m, 2H); 7.28-7.22 (t, 1H, *J*=8.0 Hz); 7.34 (d, 1H, *J*=7.6 Hz); 7.68 (d, 1H, *J*=7.6 Hz). ¹³C NMR (100 MHz, CDCl₃) δ 11.9, 22.8, 24.5, 25.9, 47.2, 48.2, 50.8, 109.6, 119.8, 119.9, 121.7, 126.5, 127.7, 137.4. ESIMS *m/z* calcd for C₁₇H₂₄N₂ [(M + H)⁺] 256.39, found; 256.35.

2-([1,1'-biphenyl]-4-yl)-N-((1-propyl-1H-indol-3-yl)methyl)ethanamine (4c).

Overall yield 38% ¹H NMR (400 MHz, CDCl₃) δ; 0.90 (t, 3H, *J*=7.6 Hz, CH₃); 1.79-1.84 (m, 2H, CH₂); 2.91-2.95 (t, 2H, *J*=7.6 Hz, CH₂); 3.01-3.03 (t, 2H, *J*=7.8 Hz, CH₂); 3.98- 4.02 (t, 2H, *J*=7.8 Hz, CH₂); 4.31 (s, 2H, CH₂); 7.11-7.15 (m, 5H); 7.23 (s, 1H); 7.34 (t, 1H, *J*=7.2 Hz); 7.40-7.54 (m, 7H). ¹³C NMR (100 MHz, CDCl₃) δ 11.6, 22.9, 32.8, 47.3, 51.4, 109.1, 110.5, 118.7, 118.9, 121.4, 126.9, 127.5, 127.8, 127.9, 128.8, 129.5, 137.6, 139.5, 140.4. ES-MS *m/z* calcd for C₂₆H₂₈N₂ [(M + H)⁺] 368.23, found 368.51.

1-([1,1'-biphenyl]-4-ylmethyl)-3-(piperidin-1-ylmethyl)-1H-indole (4d).

Overall yield 29% ¹H NMR (400 MHz, CDCl₃) δ; 1.26-1.37 (m, 2H, CH₂); 1.50-1.58 (m, 4H, CH₂); 2.58-2.65 (m, 4H, CH₂); 3.83 (s, 2H, CH₂); 5.27 (s, 2H, CH₂); 7.07 (t, 1H, *J*=8.2 Hz); 7.10-7.15 (m, 4H); 7.23-7.26 (m, 2H); 7.28-7.33 (m, 2H); 7.34-7.37 (m, 4H); 7.62 (d, 1H, *J* = 8.0 Hz). ¹³C NMR (100 MHz, CDCl₃) δ 23.8, 25.1, 29.7, 49.9, 53.7, 109.9, 119.2, 119.6, 121.9, 127.0, 127.3, 127.4, 127.5, 128.8, 128.9, 129.0, 136.3, 136.5, 140.6, 140.7. ES-MS *m/z* calcd for C₂₇H₂₈N₂ [(M + H)⁺] 380.23, found 368.34.

Synthesis of derivatives **8a-b**.

The intermediate **7a** or **7b** (1.0 eq) was dissolved in a solution of DCM:CH₃COOH (5:1 v/v) at room temperature. To this solution 2.0 equivalents of 4-chloroaniline was added and the mixture was warmed to reflux for 1.5 h. Then, 1.8 equivalents of sodium triacetoxyborohydride were added portionwise and the mixture was allowed to reflux for further 3-5 h. After cooling to room temperature, NaOH 1 N was added. The organic phase was separated and extracted one more time with the alkaline solution. Then it was dried over Na₂SO₄, filtered and concentrated in vacuo. The crude products were purified by column chromatography using mixtures of DCM/MeOH as eluent giving desired compounds **8a** and **8b** in 24% and 30% yield, respectively.

4-chloro-N-((3-(piperidin-1-ylmethyl)-1-propyl-1H-indol-5-yl)methyl)aniline (8a).

Overall yield 24%. ¹H NMR (400 MHz, CDCl₃) δ; 0.92 (t, 3H, *J*=7.8 Hz, CH₃); 1.40-1.56 (m, 6H, CH₂); 1.82-1.88 (m, 2H, CH₂); 2.42 (s, 4H, CH₂); 3.68 (s, 2H, CH₂); 4.04 (t, 2H, *J*=7.6 Hz, CH₂); 4.36 (s, 2H, CH₂); 6.59 (d, 2H, *J*= 7.6 Hz); 7.04-7.08 (m, 2H); 7.19 (s, 1H); 7.26-7.30 (m, 2H); 7.65 (s, 1H). ¹³C NMR (100 MHz, CDCl₃) δ 12.2, 22.4, 24.8, 26.5, 47.8, 48.9, 50.3 51.1, 109.4, 119.7, 119.8, 121.5, 126.4, 127.4, 127.9, 129.9 137.8, 140.2. ES-MS *m/z* calcd for C₂₄H₃₀ClN₃ [(M + H)⁺] 395.21, found 395.28.

N-((3-(((2-([1,1'-biphenyl]-4-yl)ethyl)amino)methyl)-1-propyl-1H-indol-5-yl)methyl)-4-chloroaniline (8b).

Overall yield 30%. ¹H NMR (400 MHz, CDCl₃) δ; 0.90 (t, 3H, *J*=7.6 Hz, CH₃); 1.79-1.84 (m, 2H, CH₂); 2.91-2.95 (t, 2H, *J*=7.6 Hz, CH₂); 3.01-3.03 (t, 2H, *J*=7.8 Hz, CH₂); 3.71 (s, 2H, CH₂); 3.98-4.02 (t, 2H, *J*=7.6 Hz, CH₂); 4.31 (s, 2H, 5-CH₂); 6.57 (d, 2H, *J*=8.0 Hz); 7.31-7.56 (m, 14H); 7.61 (s, 1H). ¹³C NMR (100 MHz, CDCl₃) δ 11.5, 22.6, 32.2, 47.7, 50.5, 51.5, 109.6, 119.9, 119.5, 121.8, 126.1, 127.3, 127.0, 129.3 137.4, 140.6. ES-MS *m/z* calcd for C₃₃H₃₄ClN₃ [(M + H)⁺] 507.24, found 507.29.

Synthesis of derivative **8c**.

To a solution of 5-amino indole (**9**, 1.0 eq) in dichloromethane/DMF (20 mL/5 mL) were successively added benzoic acid (1.1 eq), HBTU (1.2 eq), HOBt (1.2 eq), and DIEA (2.4 eq), and stirring was continued at room temperature for 24 h. Afterward, the reaction mixture was diluted with dichloromethane (20 mL), and the resulting solution was washed successively with 10% citric acid (2 X 25 mL), 10% NaHCO₃ (2 X 25 mL), and water (2 X 25 mL), dried over Na₂SO₄, and evaporated to dryness. Intermediate **10** was obtained after flash chromatography using n-hexane/ethyl acetate 2/1 as ratio with 63% yield. Substitution with propyl group of indolic N1 was carried out using the same conditions described elsewhere, to give compound **11** with 44% yield. Mannich reaction performed on position 3 of intermediate **11** follows the procedure previously described yielded final compound **12** in 24% yield.

N-(3-(piperidin-1-ylmethyl)-1-propyl-1H-indol-5-yl)benzamide (8c).

Overall yield 24%. ¹H NMR (400 MHz, CDCl₃) δ; 0.94 (t, 3H, *J*=8.0 Hz, CH₃); 1.61-1.64 (m, 6H, CH₂); 1.87-1.89 (m, 2H, CH₂); 2.52 (s, 4H, CH₂); 3.73 (s, 2H, CH₂); 4.07 (t, 2H, *J*=8.0 Hz, CH₂); 7.13 (s, 1H); 7.30 (t, 2H, *J*=8.0 Hz); 7.44 (d, 1H, *J*=8.0 Hz); 7.50-7.56 (m, 2H); 7.93-7.98 (m, 3H). ¹³C NMR (100 MHz, CDCl₃) δ 11.5, 23.6, 24.2, 25.7, 48.1, 53.7, 54.2, 109.6, 111.8, 116.0, 127.0, 128.7, 128.8, 128.9, 129.7, 129.9, 131.5, 133.9, 135.4, 165.7. ES-MS *m/z* calcd for C₂₄H₂₉N₃O [(M + H)⁺] 375.23, found 375.51.

General procedure for the synthesis of derivatives **15 and **16a-i**.**

One equivalent of intermediate **14a** or **14b** was dissolved in THF and 1.5 eq of the proper amine, 1.5 eq of TEA, 1.5 eq of NaI and 0.3 eq of (CH₃COO)₂Pd were added to this solution. The reaction was conducted under mW, at 100° C, for 20 min. The resulting mixture was filtered through Celite, dried in vacuo and reconstituted in DCM. The organic phase was washed with water (3 X 50 mL), dried over anhydrous Na₂SO₄, filtered, concentrated and purified by column chromatography using DCM/MeOH (9:1 v/v) as mobile phase giving derivative **15** in 38% yield and compounds **16a-i** in 55-75% yield.

Methyl 4-(((2-(1-([1,1'-biphenyl]-4-ylmethyl)-1H-indol-3-yl)ethyl)amino)methyl)benzoate (15).

Overall yield 38%. ¹H NMR (400 MHz, CDCl₃) δ 2.88 (t, 2H, *J*=8.2 Hz, CH₂); 3.23 (t, 2H, *J*=8.0 Hz, CH₂); 3.68 (s, 3H, CH₃); 3.81 (s, 2H, CH₂); 5.30 (s, 2H, CH₂); 6.85 (s, 1H); 7.05-7.18 (m, 5H); 7.21-7.35 (m, 6H); 7.24-7.30 (m, 3H); 7.35-7.41 (m, 2H); 7.52 (d, 1H, *J* = 8.0 Hz). ¹³C NMR (100 MHz, CDCl₃) δ 22.7, 41.6, 48.7, 50.8, 57.1, 108.4, 110.9, 112.2, 119.0, 119.5, 121.8, 122.9, 123.3, 124.6, 125.8, 126.6, 128.0, 128.3, 128.4, 130.1, 135.8, 198.7. ESIMS *m/z* calcd for C₃₂H₃₀N₂O [(M + H)⁺] 474.23; found 474.30.

2-([1,1'-biphenyl]-4-yl)-N-(2-(1-methyl-1H-indol-3-yl)ethyl)ethanamine (16a).

Overall yield 75%. ¹H NMR (400 MHz, CDCl₃) δ 2.67 (t, 2H, *J*=7.6 Hz, CH₂); 2.99 (t, 2H, *J*=7.8 Hz, CH₂); 3.38-3.47 (m, 4H, CH₂); 3.73 (s, 3H, CH₃); 6.80 (s, 1H); 7.16-7.21 (m, 2H); 7.29-7.36 (m, 3H); 7.50 (t, 2H, *J*=8.0 Hz); 7.56-7.66 (m, 4H). ¹³C NMR (100 MHz, CDCl₃) δ 24.2, 32.3, 33.5, 46.2, 51.4, 109.3, 110.1, 117.7, 118.5, 121.2, 124.5, 126.1, 127.2, 127.6, 127.3, 128.2, 129.0, 137.5, 138.5, 140.1. ESIMS *m/z* calcd for C₂₅H₂₆N₂ [(M + H)⁺] 354.21; found 354.24.

N-(4-methoxybenzyl)-2-(1-methyl-1H-indol-3-yl)ethanamine (16b).

Overall yield 71%. ¹H NMR (400 MHz, CDCl₃) δ 2.92 (t, 2H, *J*=7.6 Hz, CH₂); 3.19 (t, 2H, *J*=7.6 Hz, CH₂); 3.49 (s, 6H, 2CH₃); 3.72 (s, 2H, CH₂); 6.81 (s, 1H); 7.07-7.15 (m, 3H); 7.20 (t, 1H, *J*= 6.8 Hz); 7.24-7.30 (m, 3H); 7.52 (d, 1H, *J*=8.0 Hz). ¹³C NMR (100 MHz, CDCl₃) δ 22.7, 41.6, 50.8, 57.1, 109.1, 110.0, 112.4, 118.6, 118.8, 121.4, 121.9, 124.2, 126.4, 128.0, 128.3, 135.3, 199.8. ESIMS *m/z* calcd for C₁₉H₂₂N₂O [(M + H)⁺] 294.39; found 295.60.

N-(4-chlorobenzyl)-2-(1-methyl-1H-indol-3-yl)ethanamine (16c).

Overall yield 69%. ¹H NMR (400 MHz, CDCl₃) δ 2.93-3.00 (m, 4H, 2CH₂); 3.74 (s, 3H, CH₃); 3.77 (s, 2H, CH₂); 6.87 (s, 1H); 7.10 (t, 1H, *J*=8.0 Hz); 7.20-7.30 (m, 6H); 7.58 (d, 1H, *J*=8.0 Hz). ¹³C NMR (100 MHz, CDCl₃) δ 25.57, 32.56, 49.40, 53.06, 109.2, 110.0, 112.3, 118.7, 118.9, 121.6, 126.7, 127.8, 128.4, 129.4,

132.5, 137.1, 138.7. ESIMS m/z calcd for $C_{18}H_{19}ClN_2 [(M + H)^+]$ 299.12; found 299.17.

General procedure for the synthesis of derivative 17a.

One equivalent of intermediate **16a** was dissolved in DCM, then 1.5 eq of acetyl chloride and 1.5 eq of TEA were added to the solution. The reaction was conducted for 20 min at room temperature. The organic phase was washed with water (3 X 50 mL), dried over anhydrous Na_2SO_4 , filtered, concentrated and purified by column chromatography using n-hexane/ethyl acetate (2:1 v/v) as mobile phase. Final derivative **17a** was obtained in 42% yield.

N-(2-([1,1'-biphenyl]-4-yl)ethyl)-N-(2-(1-methyl-1H-indol-3-yl)ethyl)acetamide (17a).

Overall yield 55%. (A/B (A) 1H NMR (400 MHz, $CDCl_3$) δ 2.01 (s, 3H, CH_3); 2.85 (t, 2H, $J=7.6$ Hz, CH_2); 3.07 (t, 2H, $J=7.4$ Hz, CH_2); 3.43-3.50 (m, 4H, CH_2); 3.77 (s, 3H, CH_3); 6.84 (s, 1H); 7.14-7.19 (m, 2H); 7.24-7.39 (m, 3H); 7.46 (t, 2H, $J=8.0$ Hz); 7.54-7.62 (m, 4H). ^{13}C NMR (100 MHz, $CDCl_3$) δ 21.5, 24.8, 32.6, 32.7, 47.1, 51.0, 109.2, 110.7, 118.4, 119.0, 121.6, 126.7, 127.0, 127.2, 127.4, 127.9, 128.8, 129.3, 137.3, 139.2, 140.7, 170.4. (B) 1H NMR (400 MHz, $CDCl_3$) δ 2.01 (s, 3H, CH_3); 2.93-3.01 (m, 4H, CH_2); 3.63-3.71 (m, 4H, CH_2); 3.76 (s, 3H, CH_3); 6.92 (s, 1H); 7.14-7.19 (m, 2H); 7.24-7.39 (m, 3H); 7.46 (t, 2H, $J=8.2$ Hz); 7.54-7.62 (m, 3H); 7.70 (d, 1H, $J=8.0$ Hz). ^{13}C NMR (100 MHz, $CDCl_3$) δ 23.6, 24.8, 32.7, 35.0, 47.5, 50.1, 109.5, 112.0, 118.9, 119.1, 121.9, 126.9, 127.1, 127.3, 127.5, 128.7, 129.1, 137.0, 138.5, 139.7, 140.9, 170.5. ESIMS m/z calcd for $C_{29}H_{34}N_2 [(M + H)^+]$ 426.27; found 426.35.

General procedure for the synthesis of derivatives 17d-i and 18a-c.

One equivalent of intermediate **16d-i** was dissolved in DCM, then 1.5 eq of the proper acyl chloride and 1.5 eq of TEA, were added to the solution. The reaction was conducted for 20 min at room temperature. The organic phase was washed with water (3 X 50 mL), dried over anhydrous Na_2SO_4 , filtered, concentrated and purified by column chromatography using n-hexane/ethyl acetate (2:1 v/v) as

mobile phase. Final derivatives **17d-i** and **18a-c** were obtained as an atropisomer mixtures in 42-58% yield.

N-(2-(1-methyl-1H-indol-3-yl)ethyl)-N-(naphthalen-2-yl)acetamide (17d).

Overall yield 49%. ¹H NMR (400 MHz, CDCl₃) δ 1.83 (s, 3H, CH₃); 2.99 (t, 2H, *J*=7.6 Hz, CH₂); 3.63 (s, 3H, CH₃); 4.02 (t, 2H, *J*=7.8 Hz, CH₂); 6.80 (s, 1H); 6.97 (t, 1H, *J*=8.0 Hz); 7.12 (t, 1H, *J*=8.0 Hz); 7.16-7.20 (m, 3H); 7.43-7.48 (m, 3H); 7.69-7.72 (m, 1H); 7.80 (d, 2H, *J*=8.0 Hz). ¹³C NMR (100 MHz, CDCl₃) δ 23.4, 23.6, 32.6, 49.9, 109.0, 118.7, 119.0, 121.5, 126.0, 126.7, 126.8, 127.7, 127.9, 129.7, 131.2, 134.5, 134.4, 171.2. ESIMS *m/z* calcd for C₂₃H₂₂N₂O[(M + H)⁺] 342.17; found 342.23.

N-(2-(1-methyl-1H-indol-3-yl)ethyl)-N-(naphthalen-1-yl)acetamide (17e).

Overall yield 42%. ¹H NMR (400 MHz, CDCl₃) δ 1.71 (s, 3H, CH₃); 2.94-3.10 (m, 2H, CH₂); 3.51-3.58 (m, 1H, CH₂); 3.62 (s, 3H, CH₃); 4.43-4.52 (m, 1H, CH₂); 6.78 (s, 1H); 6.96 (t, 1H, *J*= 8.0 Hz); 7.11 (t, 1H, *J*= 8.2 Hz); 7.17 (d, 1H, *J*= 8.0 Hz); 7.23 (d, 1H, *J*= 8.0 Hz); 7.43 (t, 2H, *J*= 8.2 Hz); 7.48 (m, 2H); 7.74-7.77 (m, 1H); 7.78-7.80 (m, 1H); 7.81-7.84 (m, 1H). ¹³C NMR (100 MHz, CDCl₃) δ 22.5, 23.9, 32.5, 49.7, 109.0, 111.5, 118.7, 119.0, 121.5, 122.5, 125.7, 126.3, 126.7, 127.4, 128.6, 128.7, 134.8, 136.9, 139.4, 169.6. ESIMS *m/z* calcd for C₂₃H₂₂N₂O [(M + H)⁺] 342.17; found 342.23.

N-(2-(1-methyl-1H-indol-3-yl)ethyl)-N-(naphthalen-2-ylmethyl)acetamide (17f).

Overall yield 42%. (A) ¹H NMR (400 MHz, CDCl₃) δ 2.23 (s, 3H, CH₃); 3.10 (t, 2H, *J*= 7.4 Hz, CH₂); 3.74 (s, 3H, CH₃); 3.78 (t, 2H, *J*= 7.4 Hz, CH₂); 4.60 (s, 2H, CH₂); 6.89 (s, 1H); 7.09-7.16 (m, 2H); 7.24-7.34 (m, 2H); 7.44-7.50 (m, 3H); 7.65 (s, 1H); 7.80-7.87 (m, 3H). ¹³C NMR (100 MHz, CDCl₃) δ 22.0, 24.5, 32.6, 47.5, 48.4, 109.2, 110.7, 118.4, 118.8, 119.1, 121.8, 124.9, 126.0, 126.4, 126.7, 126.9, 127.7, 127.9, 128.7, 133.3, 134.4, 137.0, 170.9. (B) ¹H NMR (400 MHz, CDCl₃) δ 2.15 (s, 3H, CH₃); 3.02 (t, 2H, *J*= 7.6 Hz, CH₂); 3.58 (t, 2H, *J*= 7.6 Hz, CH₂); 3.74 (s, 3H, CH₃); 4.84 (s, 2H, CH₂); 6.80 (s, 1H); 7.09-7.16 (m, 2H); 7.24-7.34 (m,

2H); 7.44-7.50 (m, 3H); 7.65 (s, 1H); 7.80-7.87 (m, 3H). ¹³C NMR (100 MHz, CDCl₃) δ 21.5, 23.5, 24.5, 48.4, 52.9, 109.3, 109.4, 111.9, 118.8, 118.9, 121.6, 124.5, 125.8, 126.2, 126.5, 126.9, 127.4, 127.7, 128.4, 132.8, 133.4, 135.3, 137.0, 171.1. ESIMS m/z calcd for C₂₄H₂₄N₂O [(M + H)⁺] 356.19; found 356.24.

N-(2-(1-methyl-1H-indol-3-yl)ethyl)-N-(naphthalen-1-ylmethyl)acetamide (17g).

Overall yield 45%. (A) ¹H NMR (400 MHz, CDCl₃) δ 2.25 (s, 3H, CH₃); 3.05-3.11 (m, 2H, CH₂); 3.50 (t, 2H, J=7.6 Hz, CH₂); 3.65 (s, 3H, CH₃); 4.51 (s, 2H, CH₂); 6.83 (s, 1H); 7.07-7.21 (m, 4H); 7.35 (t, 2H, J=7.8 Hz); 7.44-7.53 (m, 5H). ¹³C NMR (100 MHz, CDCl₃) δ 22.5, 24.2, 30.3, 47.7, 51.2, 110.2, 110.9, 120.3, 121.5, 125.3, 137.9, 140.3, 140.6, 143.3, 171.2. (B) ¹H NMR (400 MHz, CDCl₃) δ 2.18 (s, 3H, CH₃); 2.95 (t, 2H, J=7.8 Hz, CH₂); 3.58 (t, 2H, J=7.8 Hz, CH₂); 3.70 (s, 3H, CH₃); 4.70 (s, 2H, CH₂); 6.85 (s, 1H); 7.07-7.21 (m, 4H); 7.35 (t, 2H, J=8.0 Hz); 7.44-7.53 (m, 5H). ¹³C NMR (100 MHz, CDCl₃) δ 21.9, 23.8, 31.5, 48.0, 50.1, 109.1, 111.2, 120.5, 122.7, 126.5, 138.1, 139.5, 142.8, 143.0, 171.2. ESIMS m/z calcd for C₂₄H₂₄N₂O [(M + H)⁺] 356.19; found 356.24.

N-([1,1'-biphenyl]-4-ylmethyl)-N-(2-(1-methyl-1H-indol-3-yl)ethyl)acetamide (17h).

Overall yield 51%. (A) ¹H NMR (400 MHz, CDCl₃) δ 2.10 (s, 3H, CH₃); 2.91-2.99 (m, 2H, CH₂); 3.46 (t, 2H, J=7.8 Hz, CH₂); 3.63 (s, 3H, CH₃); 4.38 (s, 2H, CH₂); 6.80 (s, 1H); 6.99-7.06 (m, 2H); 7.11-7.25 (m, 4H); 7.26 (t, 2H, J=7.8 Hz); 7.41-7.51 (m, 5H). ¹³C NMR (100 MHz, CDCl₃) δ 22.0, 24.4, 29.7, 47.5, 50.8, 109.2, 110.7, 118.4, 119.1, 127.1, 128.6, 136.8, 140.3, 140.6, 170.9. (B) ¹H NMR (400 MHz, CDCl₃) δ 2.01 (s, 3H, CH₃); 2.91-2.99 (m, 2H, CH₂); 3.60 (t, 2H, J=7.4 Hz, CH₂); 3.67 (s, 3H, CH₃); 4.61 (s, 2H, CH₂); 6.73 (s, 1H); 6.99-7.06 (m, 2H); 7.11-7.25 (m, 4H); 7.26 (t, 2H, J=8.0 Hz); 7.36 (d, 1H, J= 8.0 Hz); 7.41-7.51 (m, 4H). ¹³C NMR (100 MHz, CDCl₃) ¹³C NMR (100 MHz, CDCl₃) δ 21.4, 23.4, 32.6, 48.0, 48.7, 52.5, 109.4, 111.7, 118.9, 121.9, 127.3, 136.0, 137.0, 140.5, 140.8, 171.0. ESIMS m/z calcd for C₂₆H₂₆N₂O [(M + H)⁺] 382.20; found 382.27.

N-(2-(1-methyl-1H-indol-3-yl)ethyl)-N-(4-phenoxybenzyl)acetamide (17i).

Overall yield 50%. (A) ¹H NMR (400 MHz, CDCl₃) δ 1.99 (s, 3H, CH₃); 2.88-2.96 (m, 2H, CH₂); 3.43 (t, 2H, *J*=7.6 Hz, CH₂); 3.67 (s, 3H, CH₃); 4.32 (s, 2H, CH₂); 6.80 (s, 1H); 6.89-6.91 (m, 4H); 6.93-7.02 (m, 3H); 7.04-7.17 (m, 3H); 7.19-7.23 (m, 2H); 7.41 (d, 1H, *J*= 8.2 Hz). ¹³C NMR (100 MHz, CDCl₃) δ 21.9, 23.4, 32.7, 47.3, 52.2, 109.1, 118.3, 118.8, 119.0, 121.6, 123.2, 126.9, 127.5, 128.2, 129.6, 129.8, 131.9, 132.6, 133.8, 135.4, 137.2, 169.9. (B) ¹H NMR (400 MHz, CDCl₃) δ 2.10 (s, 3H, CH₃); 2.88-2.96 (m, 2H, CH₂); 3.58 (t, 2H, *J*=7.8 Hz, CH₂); 3.68 (s, 3H, CH₃); 4.54 (s, 2H, CH₂); 6.74 (s, 1H); 6.89-6.91 (m, 4H); 6.93-7.02 (m, 3H); 7.04-7.17 (m, 3H); 7.19-7.23 (m, 2H); 7.43 (d, 1H, *J*= 8.2 Hz). ¹³C NMR (100 MHz, CDCl₃) δ 21.4, 24.4, 32.7, 47.7, 48.6, 109.4, 118.8, 118.9, 119.1, 121.9, 123.2, 126.7, 127.9, 128.4, 129.7, 131.4, 132.3, 133.9, 135.4, 137.1, 170.4. ESIMS *m/z* calcd for C₂₆H₂₆N₂O [(M + H)⁺] 398.20; found 398.25.

N-(2-([1,1'-biphenyl]-4-yl)ethyl)-N-(2-(1-methyl-1H-indol-3-yl)ethyl)cyclohexanecarboxamide (18a).

Overall yield 55%. (A) ¹H NMR (400 MHz, CDCl₃) δ 0.79-0.88 (m, 4H, CH₂); 1.36-1.45 (m, 4H, CH₂); 1.62-1.77 (m, 2H, CH₂); 2.14-2.20 (m, 1H, CH); 2.84 (t, 2H, *J*= 7.4 Hz, CH₂); 3.05 (t, 2H, *J*= 7.4 Hz, CH₂); 3.60-3.69 (m, 4H, CH₂); 3.76 (s, 3H, CH₃); 6.91 (s, 1H); 7.08-7.12 (m, 2H); 7.25-7.41 (m, 5H); 7.47 (t, 2H, *J*= 8.0 Hz); 7.55-7.66 (m, 4H). ¹³C NMR (100 MHz, CDCl₃) δ 23.6, 26.0, 29.4, 32.6, 35.2, 40.9, 47.0, 49.7, 109.2, 112.0, 118.3, 118.8, 121.6, 126.8, 127.0, 127.9, 128.7, 128.8, 129.3, 129.4, 137.0, 137.4, 139.1, 140.8, 176.3. (B) ¹H NMR (400 MHz, CDCl₃) δ 1.09-1.27 (m, 4H, CH₂); 1.47-1.56 (m, 4H, CH₂); 1.62-1.77 (m, 2H, CH₂); 2.01-2.08 (m, 1H, CH); 2.93-2.97 (m, 4H, CH₂); 3.43-3.49 (m, 4H, CH₂); 3.74 (s, 3H, CH₃); 6.80 (s, 1H); 7.08-7.12 (m, 2H); 7.25-7.41 (m, 5H); 7.47 (t, 2H, *J*= 8.0 Hz); 7.55-7.66 (m, 3H); 7.63 (d, 1H, *J*= 8.0 Hz). ¹³C NMR (100 MHz, CDCl₃) δ 25.2, 25.7, 25.8, 29.5, 32.6, 33.8, 40.4, 48.0, 48.7, 109.5, 110.7, 118.8, 119.1, 121.9, 127.1, 127.2, 127.5, 128.8, 129.3, 137.0, 137.1, 138.7, 139.1, 139.8, 141.0, 176.6. ESIMS *m/z* calcd for C₃₂H₃₆N₂O [(M + H)⁺] 464.28; found 464.37.

N-(2-([1,1'-biphenyl]-4-yl)ethyl)-N-(2-(1-methyl-1H-indol-3-yl)ethyl)benzamide (18b).

Overall yield 57%. (A) ^1H NMR (400 MHz, CDCl_3) δ 2.77 (t, 2H, $J= 7,6$ Hz, CH_2); 3.24 (t, 2H, $J= 7.6$ Hz, CH_2); 3.26-3.40 (m, 2H, CH_2); 3.71 (s, 3H, CH_3); 3.86-3.94 (m, 2H, CH_2); 6.68 (s, 1H); 6.91-7.01 (m, 4H); 7.21-7.25 (m, 2H); 7.23-7.37 (m, 8H); 7.44-7.54 (m, 4H). ^{13}C NMR (100 MHz, CDCl_3) δ 23.5, 33.6, 34.9, 46.2, 51.3, 109.2, 118.4, 118.9, 121.7, 126.4, 126.6, 127.0, 127.2, 127.3, 128.3, 128.8, 129.1, 129.4, 137.0, 171.9. (B) ^1H NMR (400 MHz, CDCl_3) δ 2.85 (t, 2H, $J= 7.8$ Hz, CH_2); 3.15 (t, 2H, $J= 7.6$ Hz, CH_2); 3.26-3.40 (m, 2H, CH_2); 3.76 (s, 3H, CH_3); 3.86-3.94 (m, 2H, CH_2); 6.68 (s, 1H); 6.91-7.01 (m, 4H); 7.21-7.25 (m, 2H); 7.23-7.37 (m, 8H); 7.44-7.54 (m, 3H); 7.60 (d, 1H, $J= 8.0$ Hz). ^{13}C NMR (100 MHz, CDCl_3) δ 24.8, 32.6, 34.9, 47.1, 50.6, 109.2, 118.4, 118.9, 121.7, 126.4, 126.6, 127.0, 127.2, 127.3, 128.3, 128.8, 129.1, 129.4, 137.0, 171.9. ESIMS m/z calcd for $\text{C}_{32}\text{H}_{30}\text{N}_2\text{O}$ [(M + H) $^+$] 458.24; found 458.30.

N-(2-([1,1'-biphenyl]-4-yl)ethyl)-N-(2-(1-methyl-1H-indol-3-yl)ethyl)-3-morpholinopropan amide (18c).

Overall yield 48%. (A) ^1H NMR (400 MHz, CDCl_3) δ 2.54 (t, 4H, $J= 7.4$ Hz, CH_2); 2.89-2.95 (m, 4H, CH_2); 2.98-3.06 (m, 4H, CH_2); 3.53-3.59 (m, 4H, CH_2); 3.78 (s, 3H, CH_3); 6.92 (s, 1H); 7.14 (t, 1H, $J= 8.0$ Hz); 7.18 (t, 1H, $J= 8.0$ Hz); 7.20-7.26 (m, 4H); 7.28-7.31 (m, 2H); 7.36-7.62 (m, 5H). ^{13}C NMR (100 MHz, CDCl_3) δ 23.4, 27.3, 32.7, 34.3, 46.9, 47.4, 49.6, 51.6, 53.6, 63.5, 109.3, 110.3, 111.3, 118.8, 119.4, 121.7, 126.7, 127.2, 127.5, 127.7, 128.8, 129.2, 134.0, 137.3, 139.4, 140.1, 168.6. (B) ^1H NMR (400 MHz, CDCl_3) δ 2.66 (t, 4H, $J= 7.6$ Hz, CH_2); 2.89-2.95 (m, 4H, CH_2); 2.98-3.06 (m, 4H, CH_2); 3.69-3.73 (m, 4H, CH_2); 3.79 (s, 3H, CH_3); 6.97 (s, 1H); 7.14 (t, 1H, $J= 8.0$ Hz); 7.18 (t, 1H, $J= 8.0$ Hz); 7.20-7.26 (m, 4H); 7.28-7.31 (m, 2H); 7.36-7.62 (m, 4H); 7.68 (d, 1H, $J=8.0$ Hz). ^{13}C NMR (100 MHz, CDCl_3) δ 24.1, 27.1, 32.9, 33.5, 47.4, 48.6, 51.6, 52.1, 53.1, 63.5, 109.5, 111.3, 119.0, 121.7, 126.7, 127.0, 127.3, 127.6, 128.1, 129.0, 129.9, 137.1, 137.9, 139.5, 140.8, 168.6. ESIMS m/z calcd for $\text{C}_{32}\text{H}_{37}\text{N}_3\text{O}$ [(M + H) $^+$] 495.29; found 495.33.

Synthesis of derivative 18d.

To a mixture of **16a** (1.0 eq.) in DCM, (Boc)₂O (3.0 eq.) was added followed by TEA (1.5 eq.). The mixture was allowed to stir at room temperature for 12 h. Afterward, the reaction mixture was diluted with dichloromethane (20 mL), and the resulting solution was washed with 10% citric acid (2 X 25 mL). The organic phase was dried over Na₂SO₄, and evaporated to dryness. Compound **18d** was obtained as atropisomer mixture after flash chromatography using n-hexane/ethyl acetate 2/1 in 58% yield.

tert-butyl (2-([1,1'-biphenyl]-4-yl)ethyl)(2-(1-methyl-1H-indol-3-yl)ethyl) carbamate (18d).

Overall yield 58%. (**A**) ¹H NMR (400 MHz, CDCl₃) δ 1.26 (s, 9H, CH₃); 2.72-2.91 (m, 4H, CH₂); 3.34-3.40 (m, 4H, CH₂); 3.59 (s, 3H, CH₃); 6.73 (s, 1H); 7.03 (t, 1H, *J* = 8.0 Hz); 7.13-7.23 (m, 6H); 7.30 (t, 2H, *J* = 8.0 Hz); 7.37 (d, 2H, *J* = 8.0 Hz); 7.48 (d, 2H, *J* = 8.0 Hz). ¹³C NMR (100 MHz, CDCl₃) δ 28.4, 32.6, 49.3, 79.3, 109.2, 118.8, 121.6, 126.7, 127.0, 127.1, 127.2, 128.7, 129.3, 137.0, 138.5, 139.2, 141.0, 155.5. (**B**) ¹H NMR (400 MHz, CDCl₃) δ 1.35 (s, 9H, CH₃); 2.72-2.91 (m, 4H, CH₂); 3.34-3.40 (m, 4H, CH₂); 3.59 (s, 3H, CH₃); 6.81 (s, 1H); 7.03 (t, 1H, *J* = 7.8 Hz); 7.13-7.23 (m, 6H); 7.30 (t, 2H, *J* = 7.8 Hz); 7.37 (d, 2H, *J* = 8.0 Hz); 7.48 (d, 2H, *J* = 8.0 Hz). ¹³C NMR (100 MHz, CDCl₃) δ 28.4, 32.6, 49.3, 79.3, 109.2, 118.8, 121.6, 126.7, 127.0, 127.1, 127.2, 128.7, 129.3, 137.0, 138.5, 139.2, 141.0, 155.5. ESIMS *m/z* calcd for C₃₀H₃₄N₂O₂, [(M + H)⁺] 454.26; found 454.31.

7.2 Pharmacology

Antiviral assays

The compounds were evaluated against different herpes viruses, including varicella-zoster virus (VZV) strains Oka and YS, TK VZV strains 07-1 and YS-R, herpes simplex virus type 1 (HSV-1) strain KOS, thymidine kinase-deficient (TK) HSV-1 KOS strain resistant to ACV (ACV_r), herpes simplex virus type 2 (HSV-2) strain G, human cytomegalovirus (HCMV) strains AD-169 and Davis as well as feline herpes virus (FHV), the poxvirus vaccinia virus (Lederle strain), adenovirus-2, parainfluenza-3 virus, reovirus-1, Sindbis virus, Coxsackie virus B4, Punta Toro virus, respiratory syncytial virus (RSV), feline coronavirus (FIPV) and influenza A virus subtypes H1N1 (A/PR/8), H3N2 (A/HK/7/87) and influenza B virus (B/HK/5/72) and human immune deficiency virus (HIV-1 (IIIB) and HIV-2 (ROD)). The antiviral assays were based on inhibition of virus-induced cytopathicity (CPE) or (VZV) plaque formation in human embryonic lung (HEL) fibroblasts, African green monkey kidney cells (Vero), human epithelial cervix carcinoma cells (HeLa), human CD4⁺ T-lymphocyte cells (CEM), Crandell-Rees feline kidney cells (CRFK), or Madin Darby canine kidney cells (MDCK). Confluent cell cultures in microtiter 96-well plates were inoculated with 100 CCID₅₀ of virus (1 CCID₅₀ being the virus dose to infect 50% of the cell cultures) or with 20 VZV plaque forming units (PFU) and the cell cultures were incubated in the presence of varying concentrations of the test compounds. Viral CPE or plaque formation (VZV) was recorded as soon as it reached completion in the control virus-infected cell cultures that were not treated with the test compounds. Antiviral activity was expressed as the EC₅₀, the concentration required to reduce virus-induced cytopathicity or viral plaque formation by 50%.

Cytotoxicity assays

Cytotoxicity measurements were based on the inhibition of HEL cell growth. HEL cells were seeded at a rate of 5 X 10³ cells/well into 96-well microtiter plates and allowed to proliferate for 24 h. Then, medium containing different concentrations of the test compounds was added. After 3 days of incubation at 37° C, the cell

number was determined with a Coulter counter. The 50% cytostatic concentration (CC_{50}) was calculated as the compound concentration required to reduce cell growth by 50% relative to the number of cells in the untreated controls. CC_{50} values were estimated from graphic plots of the number of cells (percentage of control) as a function of the concentration of the test compounds. Cytotoxicity was expressed as the minimum cytotoxic concentration (MCC) or the compound concentration that causes a microscopically detectable alteration of cell morphology.

CHAPTER IV:
Design and synthesis of potential GRK2
inhibitors

1.1 Introduction: GPCR main features

The cellular responses to stimuli act through several control processes, which make cells able to prevent the uncontrolled stimulation. Mechanisms of attenuation include removal of agonist from the extracellular fluid and receptor desensitization, endocytosis and down-regulation. Receptor phosphorylation by specific G protein-coupled receptor kinases (GRKs) plays a key role in triggering rapid desensitization. The GRK-mediated phosphorylation of the agonist-occupied receptor promotes the binding of a member of the family of uncoupling proteins termed β -arrestins, resulting in the uncoupling of the receptor from G proteins.^{124,125,126}

GPCRs are the largest superfamily of cell surface receptor proteins and transmit various signals across biological membranes through the binding and activation of heterotrimeric G proteins, which amplify the signal and activate downstream effectors leading to the biological responses.¹²⁷ There are numerous different types of GPCRs, some 1,000 types are encoded by the human genome and they respond to a diverse range of stimuli, including light, hormones, amines, neurotransmitters, and lipids. Some examples of GPCRs include β -adrenergic receptors, prostaglandin E2 receptors, rhodopsin, H1 histamine receptor (H1R), D3 dopamine receptor (D3R), 5-hydroxytryptamine receptors (5-HT1B and 5-HT2B), muscarinic acetylcholine receptors (M2R and M3R), three nucleoside receptors, including A2A adenosine receptor (A2AAR), P2Y1 purinergic receptor (P2Y1R) and P2Y12 purinergic receptor (P2Y12R); ten peptide receptors, including chemokine receptors CXCR4 and CCR5 and μ -opioid receptor (μ -OR).¹²⁸ They represent the wider class of drug receptors: more than half of all modern drugs are targeted at these receptors.

GPCRs share a common architecture, each consisting of a single polypeptide with an extracellular N-terminus, an intracellular C-terminus and seven hydrophobic transmembrane domains (TM1-TM7) linked by three extracellular loops and three intracellular loops. Based on aminoacid sequence similarity within the seven-transmembrane (7TM) helical segments, GPCRs are divided into five families: the rhodopsin family (class A, 701 members), the secretin family (class B, 15 members), the adhesion family (24 members), the glutamate family (class C, 15

members), and the frizzled/taste family (class F, 24 members).¹²⁹ Despite this great diversity of ligand types, receptor function is generally very modular. In general in the GPCRs, binding of an agonist causes the transition of a GPCR from the inactive state to an active state and this change is necessary for G-protein activation. Activated receptors couple to a subset of the 16 heterotrimeric G protein subtypes, which are functionally grouped into four broad classes: G_s, G_i, G_q, and G₁₂. These G proteins regulate a relatively small number of intracellular G protein effectors.¹²⁹⁻¹³⁰

GPCRs interaction with heterotrimeric G proteins (composed of an α -, β - and γ -subunit), undergoes conformational changes that lead to the exchange of GDP for GTP bound to the α -subunit following receptor activation. Consequently, the G α - and G $\beta\gamma$ -subunits stimulate effector molecules, which include adenylyl and guanylyl cyclases, phosphodiesterases, phospholipase A2 (PLA2), phospholipase C (PLC) and phosphoinositide 3-kinases (PI3Ks), thereby activating or inhibiting the production of a variety of second messengers such as cAMP, cGMP, diacylglycerol, inositol (1,4,5)-trisphosphate [Ins(1,4,5)P3], phosphatidyl inositol (3,4,5)-trisphosphate [PtdIns(3,4,5)P3], arachidonic acid and phosphatidic acid, in addition to promoting increases in the intracellular concentration of Ca²⁺ and the opening or closing of a variety of ion channels (Figure 1).¹³¹

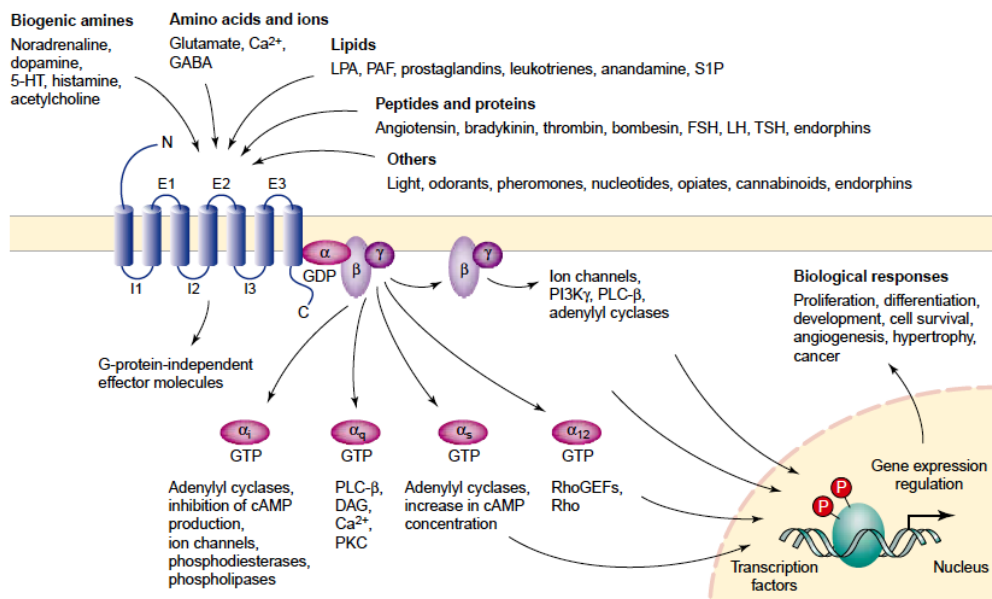


Figure 1. Diversity of G-protein-coupled receptors (GPCRs). A wide variety of ligands, including biogenic amines, amino acids, ions, lipids, peptides and proteins, use GPCRs to stimulate cytoplasmic and nuclear targets through heterotrimeric G-protein-dependent and independent pathways. Such signaling pathways regulate key biological functions such as cell proliferation, cell survival and angiogenesis.

One important mechanism for regulating GPCR responsiveness is the G protein-coupled receptor kinase (GRK)-arrestin pathway. G protein-coupled receptor kinases (GRKs) initiate the homologous desensitization of activated GPCRs leading to signaling termination.

GRKs play a key role in maintaining homeostasis as regulatory proteins and component of chemical signaling mechanisms that provide targets for important drugs and medicinal chemistry development.

1.2 GRKs: main features

Based on the sequence similarity, vertebrate GRKs have been traditionally divided into three subfamilies: GRK1, comprising GRK1 (rhodopsin kinase) and GRK7 (cone opsin kinase) which primarily regulate photoreceptors in the retina; GRK2, comprising GRK2 and 3, both of which are ubiquitously expressed; and GRK4 comprising GRK4, whose expression is primarily in the testis, cerebellum and kidney, 5, and 6, both of which are widely expressed. All GRKs are multidomain proteins¹³¹⁻¹³² consisting of about 30-residue N-terminal region specific for this family, followed by the Regulator of G protein Signaling (RGS) homology domain (RH),¹³³ and a Ser-Thr protein kinase domain (KD) with high similarity to other AGC protein kinases, such as PKA, PKB, and PKC. The C-termini of GRKs contain additional structural elements responsible for their membrane targeting: GRK1 and 7 carry short C-terminal prenylation sequences, GRK2 and 3 contain pleckstrin homology (PH) domain interacting with G protein $\beta\gamma$ -subunits, GRKs 4 and 6 carry palmitoylation sites, whereas GRK5 has positively charged lipid-binding element. (Figure 2).¹³⁴

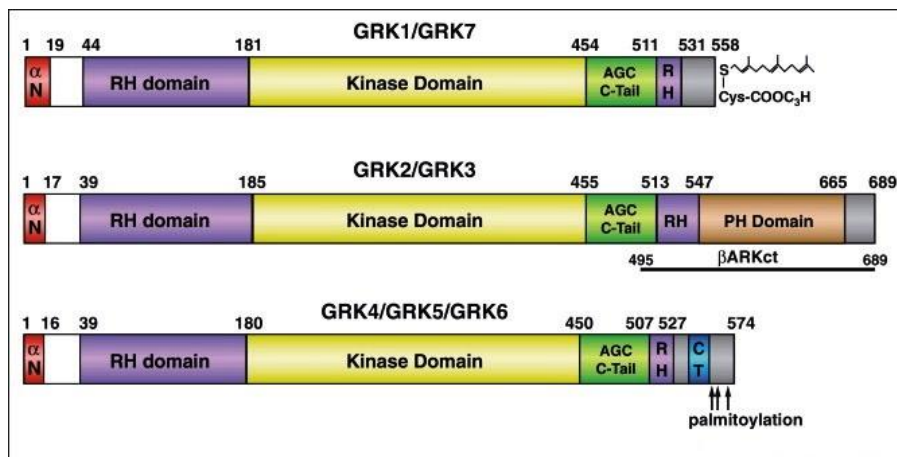


Figure 2. Domain structure of the three mammalian GRK subfamilies.

GRKs recognize activated GPCRs, which leads to catalytic activation of the protein kinase and results in receptor phosphorylation at specific sites on the intracellular loops and carboxyl-terminal tail. Phosphorylated receptors become substrates for binding of arrestin proteins, which prevent the receptor from

activating additional G proteins. This mechanism results in a cessation of G protein signaling, even despite the continued presence of the receptor agonist. The GRK-arrestin pathway also performs other functions, such as facilitating receptor internalization from the cell surface through clathrin-coated pits (Figure 3).¹³⁵

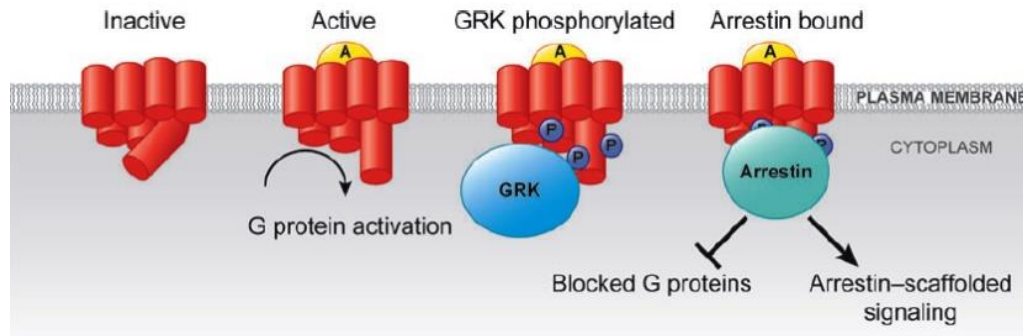


Figure 3. In the absence of an activating agonist ligand (A), the GPCR is in an inactive conformation. When an appropriate agonist binds to the extracellular face of its receptor, it undergoes a conformational change to expose surfaces that act as a guanine nucleotide exchange factor for heterotrimeric G proteins. The activated receptor facilitates release of tightly bound GDP from an inactive G protein bound to the receptor; the receptor then facilitates binding of GTP to the G protein. The GTP-bound G protein undergoes a conformational change that causes its release from the receptor and dissociation into activated α - and $\beta\gamma$ -subunits, which each go on to activate downstream effectors (not shown). As long as the agonist remains bound to the receptor, this activated receptor can continue to activate G proteins. A GRK recognizes the activated conformation of the receptor and phosphorylates the receptor. GRK-phosphorylated receptor binds to an arrestin protein, which desensitizes G protein activation and couples the receptor to the clathrin-coated-pit internalization pathway.

GRKs also regulate GPCR trafficking in a phosphorylation independent manner via direct protein-protein interactions.¹³⁶

1.3 GRK2: physiopathological role

GRK2 is the most widely studied member of this family of kinases and it is ubiquitously expressed, with higher levels found in brain, leukocytes, heart and spleen, followed by lung and kidney. Such expression pattern suggests a particularly important role of GRK2 in neurotransmission, cardiovascular function and immune and inflammatory responses.¹³⁷

1.3.1 GRK2 and the cardiovascular system

GRK2 is directly involved in β -adrenergic receptor (β AR) desensitization mechanism and represents a point of convergence in the pathogenesis of cardiovascular diseases. Constant stimulation of β ARs by catecholamines in heart failure and hypertension leads to selective β AR downregulation and an overall attenuation of β AR-mediated adenylyl cyclase activity.

During the development of heart failure β 1AR density and responsiveness becomes severely compromised as a consequence of the downregulation that takes place during the maladaptive response to chronic stimulation. In addition the dysfunction of the adenylyl cyclase system is favoured by an abnormal functionality of the G_i proteins and of adenylyl cyclase itself.¹³⁸ Several studies confirm that mRNA levels for GRK2 as well as kinase activity are increased almost three-fold in the ventricles of congestive heart failure patients.¹³⁹

GRK2 levels are also altered in mouse models of cardiac hypertrophy and an increased activity has been found in patients with ischemic and idiopathic dilated cardiomyopathy and hypertension.¹⁴⁰ Consistent with a key role for GRK2 in cardiac function, cardiac contractility can be decreased or enhanced in transgenic mice overexpressing GRK2 or GRK2 inhibitor constructs, respectively.¹⁴¹ Moreover, genetic deletion of GRK2 results in marked myocardial hypoplasia and embryonic death in mice, indicating a crucial role for this kinase in cardiac cell growth and differentiation.¹⁴² Among its role in GPCRs regulation, GRK2 is the major kinase responsible for type 1A angiotensin II receptor (AT1A-R) phosphorylation, which mediates cardiovascular effects of angiotensin II, and accordingly for the largest fraction of β -arrestin recruitment and receptor internalization in HEK293 cells.¹⁴³ These data underline the importance of GRK2

levels as a marker of predisposition to cardiac dysfunction and support the idea that GRK2 offers a potential therapeutic target.

1.3.2 GRK2 and the immune system

GRK2 is highly expressed in different cellular types of the immune system and emerges as an important regulator of cell responses during inflammation.¹⁴⁴ GRK2 phosphorylates chemokine receptors such as CCR5, CCR2, CXCR4, CXCR2 and chemotactic receptors for substance P, S1P or formyl-peptide, responsible for leukocyte trafficking to the inflammatory foci, T cell egression from lymphoid organs, leukocyte activation or proliferation.¹⁴⁵ Consistently, splenocytes and T lymphocytes isolated from GRK2^{+/-} mice display increased agonist-induced activation of ERK and PI3K/Akt pathways and increased migration when compared with wild-type littermates in response to certain chemokines (CCL5, CXCL12). In agreement with these data, it has been described that the GRK2 transcriptional down-regulation caused by activation of the Toll-like receptor (TLR)-4 pathway lowers chemokine receptor desensitization augmenting the migratory response of polymorphonuclear leukocytes (PMNs). The modulation of chemokine-mediated induction of ERK activity by altered GRK2 levels seems to involve both kinase-dependent and independent functions, the later related to the ability of GRK2 to interfere the MEK/ERK interface. Further functional interactions of GRK2 with immune cell migration remains to be investigated.¹⁴⁶ All these data suggest an important role for GRK2 in the regulation of immune cells and development of inflammatory diseases.

1.3.3 GRK2: role in cancer

Emerging data indicate changes in GRK2 expression in certain tumors¹⁴⁷ and establish a complex network of functional interactions during the cell cycle. It has been reported that GRK2 interacts with MEK, p38, Mdm2, PI3K, or c-Src¹⁴⁸ which are known to be implicated in several phases of the cell cycle. GRK2 is up-regulated in breast cancer cell lines, in spontaneous tumors in mice, and in a proportion of invasive ductal carcinoma patients. Increased GRK2 functionality promotes the phosphorylation and activation of the Histone Deacetylase 6

(HDAC6) leading to de-acetylation of the Prolyl Isomerase Pin1, a central modulator of tumor progression, thereby enhancing its stability and functional interaction with key mitotic regulators. Cancer cells where GRK2 is enhanced display genetic alterations in PI3KCA and PTEN pathway or hyperstimulation of receptors such as EGFR, HER2, ER. G protein-coupled receptor kinase 2 (GRK2) was recently shown to be a key element in the creation of a permissive microenvironment for tumor progression and necessary for vessel formation and stability. GRK2 modulates transforming growth factor β 1 (TGF β 1)-mediated pathways, which are fundamental for the activation and resolution of angiogenic events and upregulate other key angiogenic modulators.^{149,150} However reduced level of GRK2 in the endothelium accelerates tumor growth in mice, in addition to increasing the size of intratumoral vessels, reducing pericyte coverage, and enhancing macrophage infiltration.

Currently the precise contribution of GRK2 kinase activity to different aspects of cancer progression remains to be determined.¹⁵¹

1.3.4 GRK2 and the insuline resistance

Insulin resistance is characterized by a reduced responsiveness to circulating insulin and is a common feature of obesity that predisposes to several pathological conditions, including hyperinsulinemia, glucose intolerance, hypertension, cardiovascular disease and type 2 diabetes. Physiologically insulin promotes glucose transport by stimulating translocation of insulin-responsive glucose transporter 4 (GLUT4) proteins to the cell surface.¹⁵²

GRK2 overexpression is found in blood mononuclear cells from metabolic-syndrome patients and in different models of insulin resistance, such as human visceral adipocytes, and in white adipose tissue (WAT) and muscle of TNF α -, aging- or high-fat diet (HFD)-induced murine models, suggesting that increased GRK2 levels may contribute to the development of this condition.¹⁵³ Recent evidences suggest that GRK2 inhibits the insulin-stimulated glucose transport system by interacting with the G α q/11/cdc42/PI3-kinase pathway at the G α q/11 step.¹⁵⁴

These data raise the possibility that GRK2 may be an important target for antidiabetic therapy. Chemical inhibitors of GRK2 could act as insulin sensitizers with beneficial effects in a wide variety of insulin-resistant human conditions, including type II diabetes mellitus.¹⁵⁵

2.1 Background and design: 1st series

Because GRK2 modulates multiple cellular responses in various physiological contexts its selectively targeting may represent a new therapeutic strategy to tackle human pathologies involving cardiovascular disorders, uncontrolled cell proliferation, deregulated signaling pathways. Over the past several decade a significant effort was made to develop selective GRK2 inhibitors.

The natural product balanol is a potent, nonselective inhibitor of AGC kinases and exhibits some selectivity among GRK. It acts as a competitive inhibitor of ATP, inhibiting GRK2 and GRK3 at the nanomolar level, even if it also showed activity on other isoforms.¹⁵⁶ Takeda Pharmaceutical Company developed a class of heterocyclic compounds, structurally related to balanol, which exhibit higher selectivity for GRK2 versus PKA, PKC, and Rho kinase.¹⁵⁷ Mayer et al. identified a highly specific RNA aptamer that binds to GRK2 and inhibits its kinase function. This RNA aptamer represents the most potent and selective inhibitor of GRK2 activity reported (IC₅₀ of 4.1 nM). Furthermore, this aptamer might represent a starting point for the development of small molecules that specifically target GRK2.¹⁵⁸

Another class of GRK2 inhibitors is represented by peptides which were designed based on the knowledge that short peptides derived from the catalytic domain of the kinase show inhibiting activity. Several crystallographic and mutational studies have pointed to HJ-G residues (HJ-loop) as being involved in substrate binding and in binding to upstream activators. Seven to ten amino acids of this fragment typically participate in substrate binding and in some cases were shown to determine selectivity toward substrate.¹⁵⁹ Starting from the HJ-loop of GRK2 Anis et al. synthesized short peptides that closely resemble the HJ loop of GRK2/3, in detail two peptides, KRX-683107 and KRX-683124 modulate GRK2/3 activity, enhancing GPCR signal transduction and result in improved glucose homeostasis. These sequence-based peptides have an anti-diabetogenic effect in three different animal models of diabetes and could be useful in the treatment of Type 2 diabetes.¹⁶⁰

My research group has recently found that the deacylated derivatives of KRX-683107 and KRX-683124, selectively inhibit GRK2 in vitro.¹⁶¹ Based on conformation

of the HJ loop within the X-ray structure of GRK2 a small library of cyclic peptides was synthesized. The biological evaluation of this library evidenced that the cyclic peptide **7** was the most active in the GRK2 inhibition (Table 1). Moreover peptide **7** increased the density of β -adrenergic receptors and the β AR stimulated cAMP production in cardiac cells, further confirming the GRK2 control on regulation of β AR signalling.¹⁶²

Table 1. Structure, inhibition activities and analytical data of peptides 2-9.

Com.	Sequence	Inhibition ^a		HPLC ^c k'	ESI-MS (M +H)	
		GRK2 ^b	GRK5 ^b		Calcd	Found
2	GLLRrHS	47.6 \pm 5.5	<5	1.70	836.97	837.66
3	GLLRrHSI	49.6 \pm 6.3	<5	1.72	950.13	950.70
4	[GLLRrHS]	47.8 \pm 6.0	<5	1.70	819.96	820.53
5	[GLLRrHSI]	37.2 \pm 10.7	<5	1.85	933.12	933.80
6	[KLLRrHD]	36.3 \pm 4.4	<5	1.72	919.09	920.13
7	[KLLRrHD]I	55.3 \pm 4.6	<5	1.75	1032.25	1033.11
8	[KLLRGHD]	47.2 \pm 4.5	<5	1.76	819.47	820.51
9	[KLLRGHD]I	33.7 \pm 7.8	<5	1.78	933.12	933.68

^aData represent mean values (\pm SD) of three independent determinations. ^bGRK2 and GRK5 purified proteins activity (50 ng) were tested on rod outer segments (ROS) in presence or absence of 1 mM inhibitors. ^ck' $\frac{1}{4}$ [(peptide retention time solvent retention time)/solvent retention time].

Further studies aimed to point on the structure-activity relationship of this small family of peptides led to the identification of the tetrapeptide LLRr as the minimal sequence which retains GRK2 inhibiting activity. Conformational analysis performed on the isolated sequence indicated that it is characterized by β -turn structure. In order to overcome all the limits linked to peptides administration and stability and, moreover, to obtain more potent and selective derivatives, we decided to synthesize a library of small molecules as potential GRK2 inhibitors. We chose thiazolidine scaffold as template for the design of this series of compounds, because of its ability to induce β -turn conformation, as previously described.¹⁶⁴

The thiazolidine core was derivatized with substituents miming the electronic and structural features of the aminoacids side chains of the above mentioned peptide,

as shown in Figure 4. The relative position of these chain into the bicyclic core would also allow us to study the spatial arrangement/activity relationship.

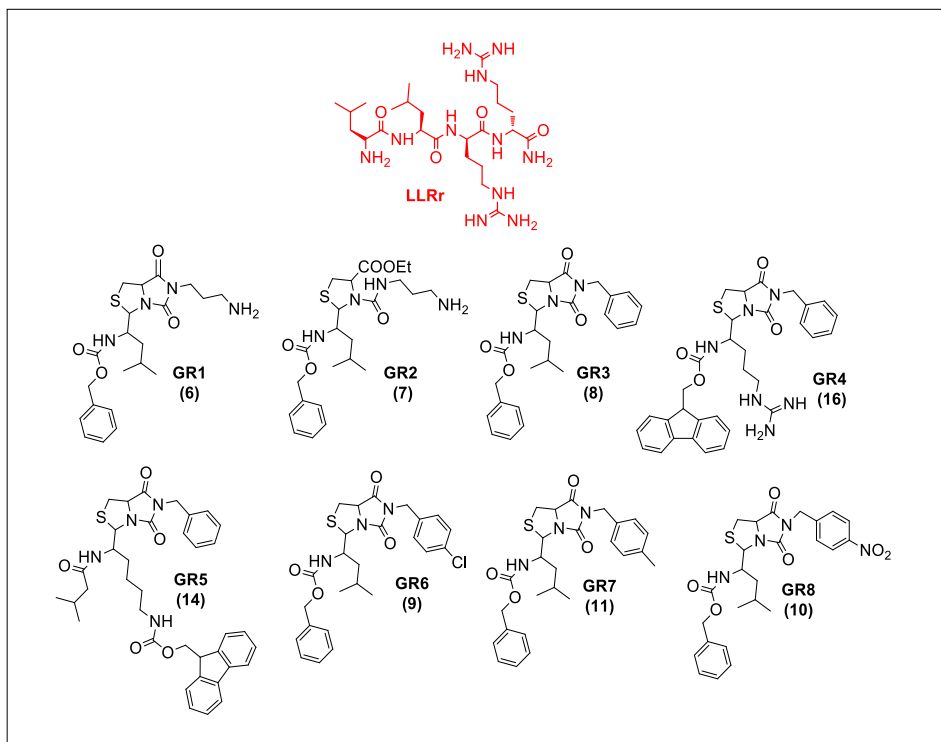
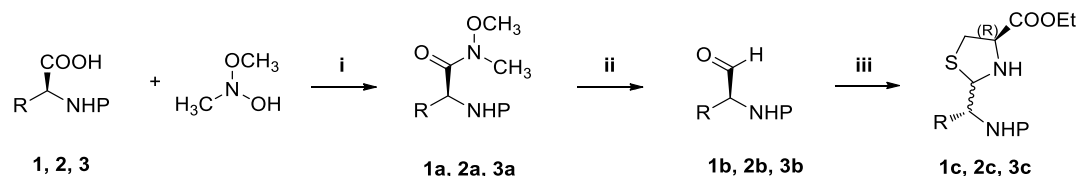


Figure 4. Designed library of potential GRK2 inhibitors. Numbers in parentheses refer to compounds number in the synthetic route.

2.2 Synthesis of 1st series

The synthesis of the new derivatives started from the Weinreb amidation as shown in Scheme 1. The reaction involved three different protected aminoacids (Z-L-Leu-OH, Boc-L-Lys(Fmoc)-OH and Fmoc-L-Arg(Pbf)-OH) that were coupled with N,O-dimethylhydroxylamine. The following treatment of the intermediates with an excess of lithium aluminum hydride led to the aldehydes **1b**, **2b**, **3b**. These aldehydes were reacted with L-Cys-OEt to give the thiazolidine compounds as mixture of cis and trans diastereoisomers.

Scheme 1. Synthesis of intermediates **1c**, **2c**, **3c**.



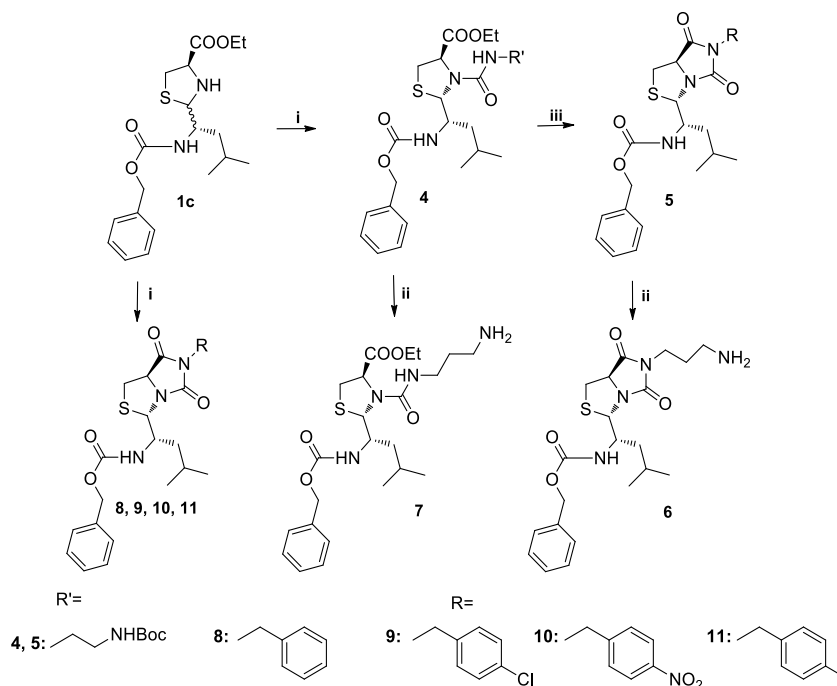
R= **1**, **1a**, **1b**, **1c**: $\text{CH}_2\text{CH}(\text{CH}_3)_2$; **2**, **2a**, **2b**, **2c**: $(\text{CH}_2)_4\text{NHFmoc}$; **3**, **3a**, **3b**, **3c**: $(\text{CH}_2)_3\text{NHC}(\text{NH})\text{NHPbf}$

P= **1**, **1a**, **1b**, **1c**: Bz; **2**, **2a**, **2b**, **2c**: Boc; **3**, **3a**, **3b**, **3c**: Fmoc

Reagents and conditions: i: DCM/DMF, HOBT, HBTU, DIPEA, N,O-dimethylhydroxylamine, 12h, rt; ii: THF dry, LiAlH_4 (1M in THF), N_2 , 10', 0°C; iii: EtOH, L-CysOEt, NaHCO_3 , 12h, rt.

Intermediate **1c** was derivatized using different aliphatic amines through ureidic bond formation. Treatment with triphosgene, benzylamine, 4-chlorobenzylamine, 4-nitrobenzylamine and 4-methylbenzylamine led to derivatives **8-11**, due to spontaneous cyclization to hydantoin promoted by the aromatic moiety. Treatment with N-Boc-1,3-propanediamine led to intermediate **4**, while the hydantoin **5** was obtained by cyclization in methanol/TEA. Deprotection by trifluoroacetic acid in dichloromethane provided the amines **6** and **7**.

Scheme 2. Synthesis of derivatives 6-11.



Reagents and conditions: i: DCM, triphosgene, TEA, RNH₂, 10', rt; ii: DCM/TFA 3/1 TIS, 2h, rt; iii: MeOH/TEA, 10', reflux.

The ureidic intermediates **4** and **7** were stereoselectively converted to the corresponding hydantoin, retaining their configuration during cyclization and leading to the pure diastereoisomer 2*S*,4*R*,1'*S*. The H-3 configuration was assigned on the basis of the NOE correlations observed in the ROESY spectrum of **8**. The *S* configuration assigned to chiral centre 3 is justified by the absence of correlation between H-3 and H-7a of the thiazolidine (Figure 5).

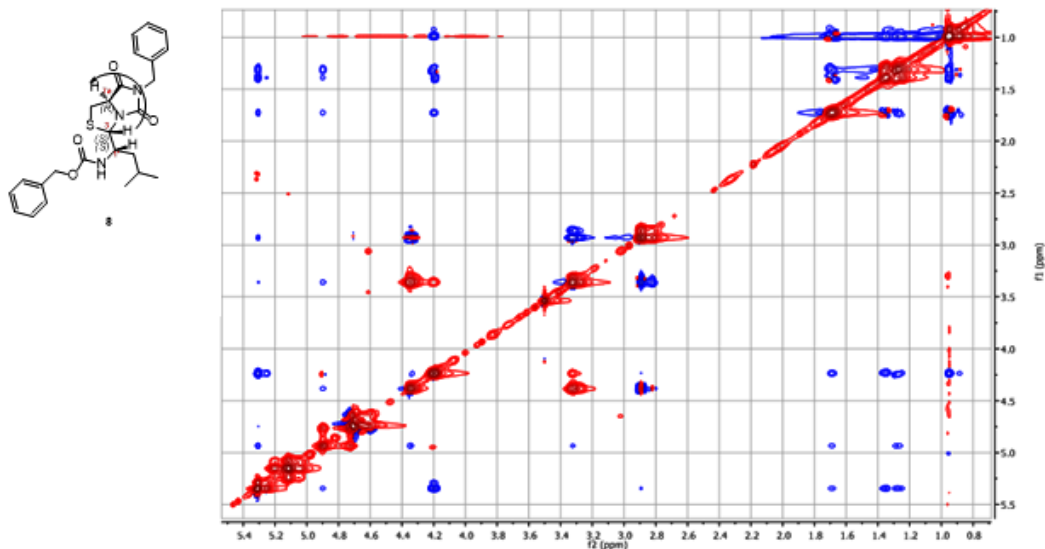
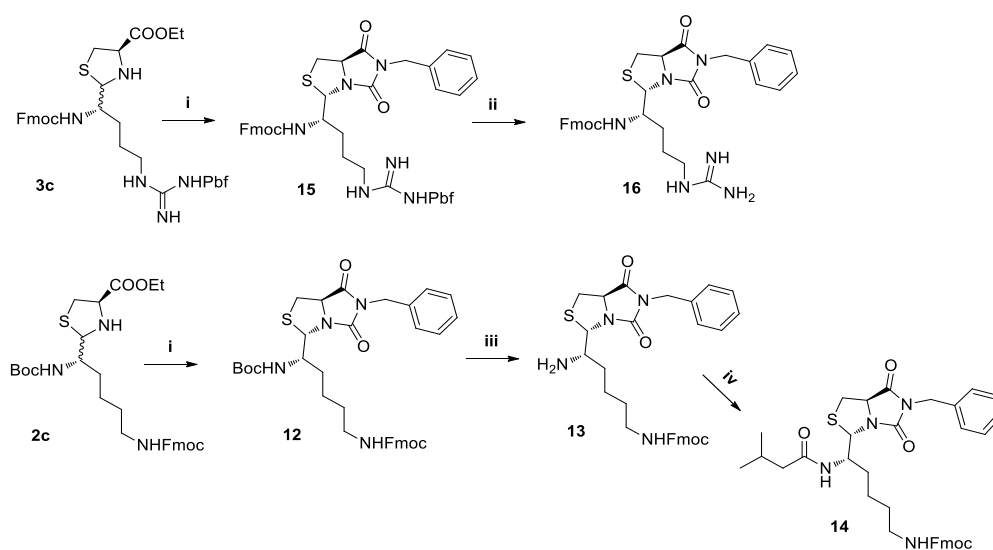


Figure 5. ROESY experiment of compound 8.

Intermediates **2c** and **3c** were converted to the corresponding hydantoin using benzylamine and triphosgene. The selective removal of the N-protecting group of compound **15** and **12** led to final derivative **16** and to intermediate **13**, respectively. Treatment of compound **13** with isovaleryl chloride gave the corresponding acyl derivative **14** (Scheme 3).

Scheme 3. Synthesis of derivatives 14 and 16.



Reagents and conditions: i: DCM, triphosgene, TEA, benzylamine, 10', rt; ii: DCM/TFA 2/1, TIS cat., 2h, rt; iii: DCM/TFA 3/1, TIS, 2h, rt; iv: DCM, isovaleryl chloride, TEA, 30', rt.

3.1 Activity of the thiazolidine derivatives of the 1st series

The synthesized compounds were tested at the Department of Clinical Medicine, Cardiovascular and Immune Sciences of University of Naples Federico II, for their inhibiting activity over GRK2 protein. The results obtained are summarized in Figure 6. All synthesized derivatives were tested at the concentration of 1 μ M by in vitro rhodopsin phosphorylation assay and visualized by autoradiography of dried gels. All the synthesized compounds showed activity in reducing GRK2 phosphorylation. Overall, compound **9 (GR6)** was the most active to inhibit GRK2.

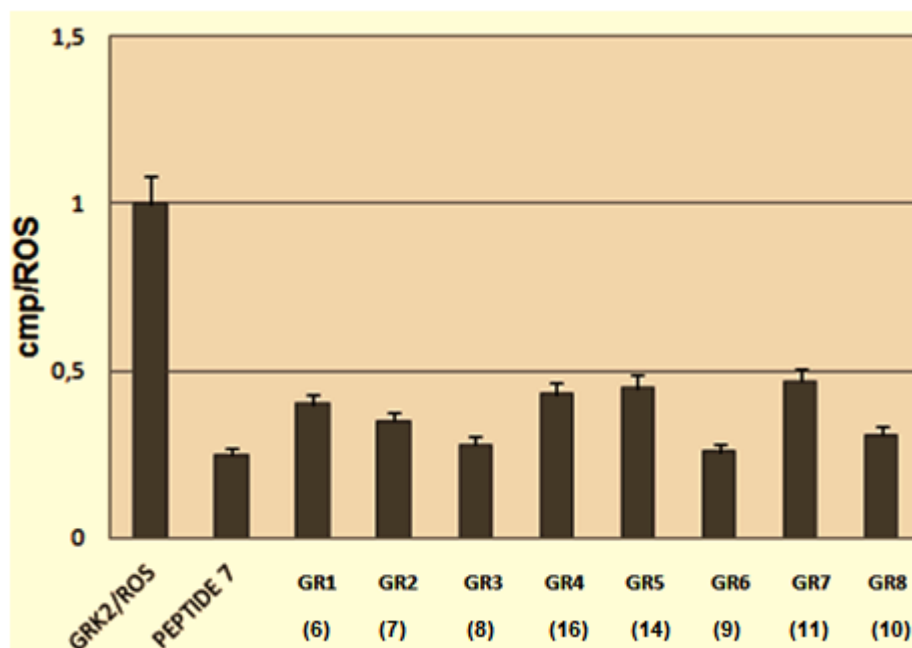


Figure 6. GRK2 purified protein (50ng) was tested on rod outer segments (ROS) in presence of 1 μ M inhibitors. Numbers in parentheses refer to compounds number in the synthetic route.

4.1 Background and design: 2nd series

Starting from the results obtained from the previous series, the aim of my second year of PhD was to identify a more potent GRK2 inhibitor starting from the structure of compound **9**, which showed the best activity in the phosphorylation assay. We thus explored different substitutions at the thiazolidine ring (Figure 7) designing and synthesizing new derivatives bearing different and generally bulkier substituents at the N-1 position. In detail the designed modification included:

- Introduction of aliphatic fragment to verify the importance of hydrophobic interaction
- Increase the distance between the thiazolidine ring and the aromatic group
- Introduction of a guanidine moiety to increase ionic interactions

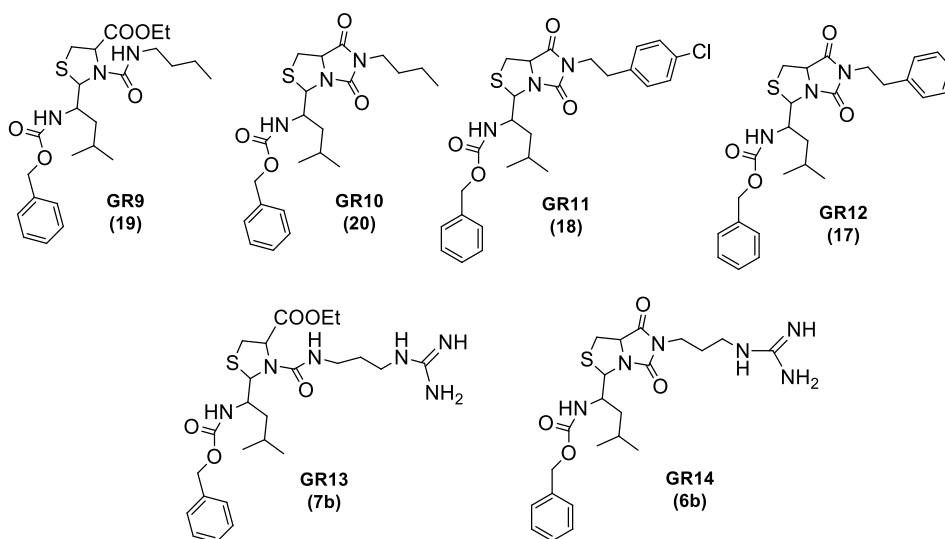
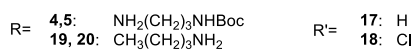
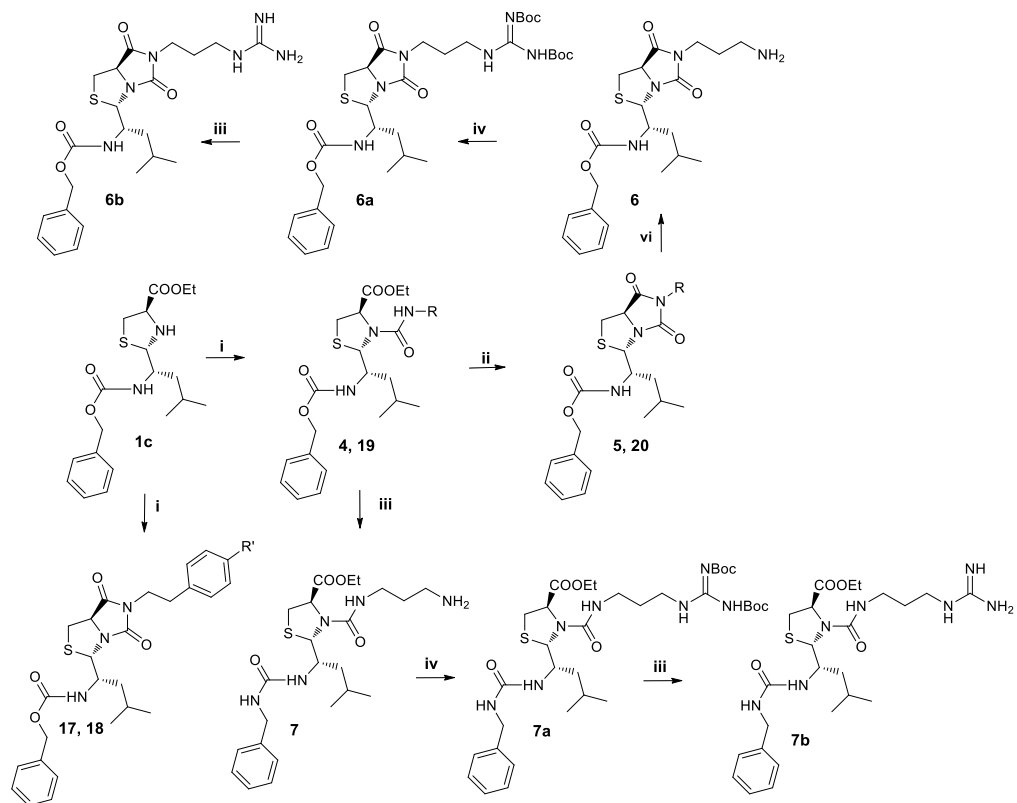


Figure 7. Synthesized compounds of series 2 starting from 9. Numbers in parentheses refer to compounds number in the synthetic route.

4.2 Synthesis of 2nd series

The designed thiazolidine derivatives (**6b**, **7b**, **17-20**) were prepared applying the synthetic route shown in Scheme 4. The starting ethyl 2-(1-(((benzyloxy)carbonyl)amino)-3-methylbutyl)thiazolidine-4-carboxylate intermediate **1c** was obtained as previously described using Z-L-Leu-OH as starting material (Scheme 1). Treatment of **1c** with triphosgene and N-Boc-1,3-propanediamine, 2-phenylethylamine, 2-(4-chlorophenyl)ethylamine or n-butylamine led to compounds **4**, **17-19**. As displayed for the 1st series of derivatives the presence of the aromatic group promoted the spontaneous cyclization to the corresponding hydantoin (**17** and **18**). Hydantoins **5** and **20** were obtained by cyclization of the corresponding ureas in methanol/TEA. Deprotection by trifluoroacetic acid in dichloromethane provided the amines **6** and **7**, which were treated with N,N'-Di-Boc-1H-pyrazole-1-carboxamide as guanidinylation reagent to allow the synthesis of protected guanidines **6a** and **7a**. The removal of the guanidine protecting group led to the final derivatives **6b** and **7b**.

Scheme 4. Synthesis of derivatives 6b, 7b, 17- 20.



Reagents and conditions: i: DCM, triphosgene, TEA, RNH_2 or $\text{R}'\text{NH}_2$, 10', rt; ii: MeOH/TEA, 10', reflux; iii: DCM/TFA 3/1, TIS, 2h, rt; iv: DCM, BPCA, DMAP, TEA, 3h, rt.

5. Activity evaluation of the 2nd series of derivatives

All the synthesized derivatives are current in the process of biological assays to test their activity on GRK2.

6. Conclusions

GRK2 plays a key role in human health and disease, such as in pathological cardiovascular processes. Hence, modulation of its activity could represent a valid strategy for the treatment of many pathological disorders. The present work describes the design and synthesis of potential GRK2 inhibitors thiazolidine-based. The preliminary activity screening evidenced that all synthesized compounds showed inhibitor activity against GRK2. Overall, compound 9 was the most active within the 1st series. Aimed to obtain more potent and selective molecules we synthesized new derivatives currently under biological evaluation.

Experimental section

7.1 Chemistry

Reagents, starting materials, and solvents were purchased from Sigma-Aldrich (Milan, Italy) and used as received. Reactions were carried out with magnetic stirring in round-bottomed flasks unless otherwise noted. Moisture-sensitive reactions were conducted in oven-dried glassware under a positive pressure of dry nitrogen, using predried, freshly distilled solvents. Microwave assisted reactions were performed in a Biotage Initiator+ reactor. Analytical thin layer chromatography (TLC) was performed on precoated glass silica gel plates 60 (F254, 0.25 mm, VWR International). Purifications were performed by flash column chromatography on silica gel (230–400 mesh, Merck Millipore). NMR spectra were recorded on Varian Mercury-400 apparatus. ^1H NMR and ^{13}C NMR spectra were recorded with a Varian-400 spectrometer, operating at 400 and 100 MHz, respectively. Chemical shifts are reported in δ values (ppm) relative to internal Me_4Si , and J values are reported in hertz (Hz). The following abbreviations are used to describe peaks: s (singlet), d (doublet), dd (double double), t (triplet), q (quadruplet), and m (multiplet). ESI-MS experiments were performed on an Applied Biosystem API 2000 triple-quadrupole spectrometer. Combustion microanalyses were performed on a Carlo Erba CNH 1106 analyzer, and results were within 0.4% of calculated values and confirmed >95% purity for the final products. Analytical RP-HPLC was performed on a Phenomenex Synergi Fusion RP-80A (75 mm \times 4.6 mm, 4 μm), with a flow rate of 1 mL/min, using a tunable UV detector at 254 nm. Mixtures of CH_3CN and 0.05% TFA in H_2O were used as mobile phase.

General Procedure for the Synthesis of Derivatives 1c, 2c and 3c.

To a solution of Z-L-Leu-OH, Boc-L-Lys(Fmoc)-OH and Fmoc-L-Arg(Pbf)-OH (**1**, **2**, **3**) (1 mmol) dissolved in DCM/DMF (10/1) 1.2 eq of HOBt, 1.2 eq of HBTU and 2.4 eq of Dipea at room temperature were added. After 30 min 1.2 eq of N,O-dimethylhydroxylamine were added and the reaction was mixed at room temperature over night. Then the crude was washed with water (3 x 20 mL), 10%

aqueous solution of citric acid (3 X 20 mL) and saturated aqueous solution of sodium bicarbonate (3 x 20 mL). The combined organic layer was dried over anhydrous sodium sulfate, filtered, concentrated and purified by flash chromatography in 30:20 n-hexane/ethyl acetate.

The N-methoxy-N-methylcarbamoyl derivative (1 mmol; 90 % yield) was dissolved in dry THF and mixed at 0°C under nitrogen atmosphere. Then 2.5 eq of LiAlH₄ (1 M in THF) were added and the reaction was mixed at 0°C for 6 minutes. The crude was washed with 10% aqueous solution of citric acid (3 X 20 mL), the combined organic layer was dried over anhydrous sodium sulfate, filtered and concentrated. No further purification was performed.

Intermediates **1b**, **2b**, **3b** were dissolved in ethanol, then 1.2 eq of L-Cys-OEt and 1.2 eq of NaHCO₃ were added and the reaction was mixed at room temperature over night. The solvent was removed in vacuo and the crude was diluted with DCM and washed with water (3 X 20 mL). The combined organic layer was dried over anhydrous sodium sulfate, filtered, concentrated and purified by flash chromatography in 40:10 n-hexane/ethyl acetate to obtain final compounds **1c**, **2c**, **3c** (70-75 % yield).

General Procedure for the Synthesis of Derivatives 6-11.

To 1 mmol of intermediate **1c** dissolved in dichloromethane 0.4 eq of triphosgene, 1.2 eq of TEA and 1.2 eq of proper amine (N-Boc-1,3-propanediamine, benzylamine, 4-chlorobenzylamine, 4-nitrobenzylamine and 4-methylbenzylamine) were added. The reaction was mixed at room temperature for 20 minutes. Then the solution was washed with water (3 x 20 mL). The combined organic layer was dried over anhydrous sodium sulfate, filtered, concentrated and purified by flash chromatography in 75:25 n-hexane/ethyl acetate to obtain **6** and **7**. According to Scheme 2 final derivatives **8-11** and intermediate **4** were obtained. Intermediate **5** was synthesized by refluxing **4** in MeOH/TEA for 10 minutes. The removal of the protecting group, using a solution of DCM/TFA in ratio 3:1 (9:3 mL), led to final derivatives **6** and **7** after treatment with saturated aqueous solution of sodium bicarbonate (3 x 20 mL).

General Procedure for the Synthesis of Derivatives **14** and **16**.

To 1 mmol of intermediate **2c** or **3c** dissolved in dichloromethane (20 mL) 0.4 eq of triphosgene, 1.2 eq of TEA and 1.2 eq of benzylamine were added. The reaction was mixed at room temperature for 20 minutes. Then the solution was washed with water (3 x 20 mL). The combined organic layer was dried over anhydrous sodium sulfate, filtered, concentrated and purified by flash chromatography in in 40:10 n-hexane/ethyl acetate to give intermediates **12** and **15**. Final derivative **16** and intermediate **13** were obtained removing the protecting group in a mixture 2/1 and 3/1 DCM/TFA, respectively. To **13** dissolved in dichloromethane 1.2 eq of isovaleryl chloride and 1.2 eq of TEA were added. The reaction was mixed at room temperature for 20 minutes. Then the solution was washed with saturated aqueous solution of sodium bicarbonate (3 x 20 mL) and water (3 x 20 mL). The combined organic layer was dried over anhydrous sodium sulfate, filtered, concentrated and purified by flash chromatography in in 45:5 n-hexane/ethyl acetate to give final derivative **14**.

General Procedure for the Synthesis of Derivatives **6b** and **7b**, **17-20**.

To 1 mmol of intermediate **1c** dissolved in dichloromethane 0.4 eq of triphosgene, 1.2 eq of TEA and 1.2 eq of proper amine (N-Boc-1,3-propanediamine, 2-phenylethylamine, 2-(4-chlorophenyl)ethylamine or n-butylamine) were added. The reaction was mixed at room temperature for 20 minutes. Then the solution was washed with water (3 x 20 mL). The combined organic layer was dried over anhydrous sodium sulfate, filtered, concentrated and purified by flash chromatography in in 70:30 n-hexane/ethyl acetate. According to Scheme 4 final derivatives **17-18** and intermediates **4** and **19** were obtained. Intermediate **5** and final compound **20** were synthesized by refluxing **4** and **19**, respectively, in MeOH/TEA for 10 minutes. The removal of the protecting group, using a solution of DCM/TFA in ratio 3:1 (9:3 mL), led to intermediates **6** and **7** after treatment with saturated aqueous solution of sodium bicarbonate (3 x 20 mL). The amino free compounds were dissolved in dichloromethane and 1 eq of BPCA, 0.1 eq of DMAP and 1 eq of TEA were added. The reaction was mixed at room temperature for 3 hours. Then the solution was washed with water (3 x 20 mL).

The combined organic layer was dried over anhydrous sodium sulfate, filtered, concentrated and purified by flash chromatography using n-hexane/ethyl acetate (80:20 ratio) as mobile phase. The final reaction step was the deprotection of the N-tert-butoxycarbonyl group of intermediates **6a** and **7a**, using a solution of DCM/TFA in ratio 3:1 (9:3 mL). Derivatives **6b** and **7b** were obtained with no further purification.

(2S,4R, 1'S) ethyl 3-((3-aminopropyl)carbamoyl)-2-(1-(((benzyloxy)carbonyl)amino)-3-methylbutyl)thiazolidine-4-carboxylate (7).

Overall Yield 65%. ¹H NMR (400 MHz, CD₃OD) δ 0.89–0.93 (m, 6H, 3CH₃); 1.18-1.26 (m, 7H, 2CH₂, CH₃); 1.63-1.68 (m, 1H, CH); 3.11-3.15 (m, 4H, 2CH₂); 3.35 (d, 1H, H-5a, J = 11.2 Hz); 3.57-3.61 (m, 1H, H-5b); 4.08 (q, 2H, CH₂); 4.55-4.59 (m, 1H, H-1'); 4.75 (d, 1H, H-4, J = 5.6 Hz); 4.98 (d, 1H, CH₂, J' = 12Hz); 5.11 (d, 1H, CH₂); 5.27 (s, 1H, H-2); 7.25-7.38 (m, 5H, Aryl). ¹³C NMR (100 MHz, CD₃OD) δ 20.1(2CH₃); 21.8 (CH₃); 25.1 (CH₂); 23.0 (CH₂); 26.9 (CH); 31.0 (C-5); 38.1 (CH₂); 42.2 (CH₂); 50.0 (C-1'); 62.2 (CH₂); 63.2 (C-4); 67.0 (CH₂ Bz); 69.1 (C-2); 128.0; 128.1; 128.4 (Aryl); 156.1; 168.8; 170.6(CO). ESI-MS *m/z* calcd per C₂₃H₃₆N₄O₅S [(M + H)⁺] 480.19; found, 481.20.

(3S,7aR,1'S) benzyl (1-(6-(3-aminopropyl)-5,7-dioxohexahydroimidazo[1,5-c]thiazol-3-yl)-3-methylbutyl)carbamate (6).

Overall Yield 68%. ¹H NMR (400 MHz, CD₃OD) δ 0.90–0.94 (m, 6H, 2CH₃); 1.25-1.35 (m, 4H, 2CH₂); 1.69-1.72 (m, 1H, CH); 2.66-2.72 (m, 4H, CH₂); 2.87-2.91 (t, 1H, H-1a); 3.24-3.28 (t, 1H, H-1b); 4.10-4.14 (m, 1H, H-1'); 4.20-4.24 (t, 1H, H-7a); 5.11 (dd, 2H, CH₂, J' = 12, J'' = 19.8 Hz); 5.27 (d, 1H, H-3, J = 3.6 Hz); 7.25-7.34 (m, 5H, Aryl). ¹³C NMR (100 MHz, CD₃OD) δ 20.5 (2CH₃); 21.8 (CH₂); 25.2 (CH₂); 28.6 (CH); 34.9 (C-1); 42.7 (CH₂); 44.5 (CH₂); 53.4 (C-1'); 62.3 (C-7a); 65.0 (CH₂ Bz); 66.5 (C-3); 126.1; 127.3; 128.5; 136.3 (Aryl); 157.0; 158.1; 172.9 (CO). ESI-MS *m/z* calcd per C₂₁H₃₀N₄O₄S [(M + H)⁺] 434.12; found, 434.50.

(3*S*,7*aR*,1'*S*) 1-Benzyl-(6-benzyl-5,7-dioxohexahydroimidazo[1,5-*c*]thiazol-3-yl)-3-methylbutyl)carbamate (8).

Overall Yield 72%. ¹H NMR (400 MHz, CDCl₃) δ 0.92 (d, 6H, 2CH₃, J = 8.0 Hz); 1.22-1.36 (m, 2H, CH₂); 1.57-1.68 (m, 1H, CH); 2.86 (t, 1H, H-1a); 3.25-3.29 (m, 1H, H-1b); 4.15-4.17 (m, 1H, H-1'); 4.30 (t, 1H, H-7a); 4.55 (dd, 2H, CH₂, J' = 12, J'' = 19.8 Hz); 5.09 (dd, 2H, CH₂, J' = 12, J'' = 19.8 Hz); 5.27 (d, 1H, H-3, J = 3.6 Hz); 7.25-7.33 (m, 10H, Aryl). ¹³C NMR (100 MHz, CDCl₃) δ 21.8 (2CH₃); 23.1 (CH₂); 24.6 (CH); 32.8 (C-1); 53.6 (C-1'); 63.3 (C-7a); 66.1 (CH₂ Bz); 67.5 (C-3); 124.7; 127.0; 127.0; 127.6; 127.7; 128.1; 128.6 (Aryl); 155.8; 157.8; 170.6; (CO). ESI-MS *m/z* calcd per C₂₅H₂₉N₃O₄S [(M + H)⁺] 467.19; found, 467.50.

(3*S*,7*aR*,1'*S*)-Benzyl 1-(6-(4-chlorobenzyl)-5,7-dioxohexahydroimidazo[1,5-*c*]thiazol-3-yl)-3-methylbutyl)carbamate (9).

Overall Yield 72%. ¹H NMR (400 MHz, CDCl₃) δ 0.93 (d, 6H, 2CH₃, J = 8.0 Hz); 1.22-1.36 (m, 2H, CH₂); 1.57-1.68 (m, 1H, CH); 2.84 (t, 1H, H-1a); 3.25-3.29 (m, 1H, H-1b); 4.15-4.17 (m, 1H, H-1'); 4.28 (t, 1H, H-7a); 4.56 (dd, 2H, CH₂, J' = 12, J'' = 19.8 Hz); 5.09 (dd, 2H, CH₂, J' = 12, J'' = 19.8 Hz); 5.27 (d, 1H, H-3, J = 3.6 Hz); 7.25-7.33 (m, 9H, Aryl). ¹³C NMR (100 MHz, CDCl₃) δ 20.8 (2CH₃); 23.8 (CH₂); 26.6 (CH); 32.8 (C-1); 42.2 (CH₂); 55.6 (C-1'); 65.3 (C-7a); 67.1 (CH₂ Bz); 67.3 (C-3); 128.1; 128.5; 128.9; 130.1; (Aryl); 157.8; 159.8; 171.6; (CO). ESI-MS *m/z* calcd per C₂₅H₂₈ClN₃O₄S [(M + H)⁺] 502.15; found, 502.50.

(3*S*,7*aR*,1'*S*)-benzyl (-3-methyl-1-(6-(4-methylbenzyl)-5,7-dioxohexahydroimidazo[1,5-*c*]thiazol-3-yl)butyl)carbamate (11).

Overall Yield 73%. ¹H NMR (400 MHz, CDCl₃) δ 0.93 (d, 6H, 2CH₃, J = 8.0 Hz); 1.22-1.36 (m, 2H, CH₂); 1.57-1.68 (m, 1H, CH); 2.32 (s, 3H, CH₃); 2.84 (t, 1H, H-1a); 3.24-3.29 (m, 1H, H-1b); 4.14-4.17 (m, 1H, H-1'); 4.27 (t, 1H, H-7a); 4.54 (dd, 2H, CH₂, J' = 12, J'' = 19.8 Hz); 5.09 (dd, 2H, CH₂, J' = 12, J'' = 19.8 Hz); 5.27 (d, 1H, H-3, J = 3.6 Hz); 7.13 (d, 2H, H-3, Aryl, J = 8.0 Hz); 7.24 (d, 2H, Aryl, J = 8.0 Hz); 7.33-7.38 (m, 5H, Aryl). ¹³C NMR (100 MHz, CDCl₃) δ

22.1 ($2CH_3$); 21.8 (CH_3); 23.2 (CH_2); 24.7 (CH); 32.7 (C-1); 42.6 (CH_2); 53.6 (C-1'); 65.4 (C-7a); 67.0 (CH_2 Bz); 67.3 (C-3); 128.1; 128.3; 128.5; 128.6; 128.9; 129.4; (C Aryl); 154.3; 155.9; 173.9; (CO). ESI-MS m/z calcd per $C_{26}H_{31}N_3O_4S$ [(M + H)⁺] 481.2; found, 482.20.

(3S,7aR,1'S)-Benzyl (-3-methyl-1-(6-(4-nitrobenzyl)-5,7-dioxohexahydroimidazo[1,5-c]thiazol-3-yl)butyl)carbamate (10).

Overall Yield 69%. ¹H NMR (400 MHz, CDCl₃) δ 0.96 (d, 6H, 2 CH_3 , J = 12.0 Hz); 1.28-1.36 (m, 2H, CH_2); 1.66-1.72 (m, 1H, CH); 2.90 (t, 1H, H-1a); 3.32-3.35 (m, 1H, H-1b); 4.19-4.22 (m, 1H, H-1'); 4.35 (t, 1H, H-7a); 4.71 (dd, 2H, CH_2 J' = 24, J'' = 36 Hz); 5.10 (dd, 2H, CH_2 , J' = 12, J'' = 24 Hz); 5.33 (d, 1H, H-3, J = 12.0 Hz); 7.36-7.40 (m, 5H, Aryl); 7.54 (d, 2H, H-2, H-6, Aryl, J = 6.0 Hz); 8.22 (d, 2H, H-5, H-3, Aryl, J = 12.0 Hz). ¹³C NMR (100 MHz, CDCl₃) δ 20.8 ($2CH_3$); 23.8 (CH_2); 26.6 (CH); 32.8 (C-1); 55.6 (C-1'); 65.3 (C-7a); 67.1 (CH_2 Bz); 67.33 (C-3); 128.1; 128.5; 128.9; 135.6; 145.1; 147.8; (C Aryl); 157.8; 159.8; 171.6; (CO). ESI-MS m/z calcd per $C_{25}H_{28}N_4O_6S$ [(M + H)⁺] 512.17; found, 512.36.

(3S,7aR,1'S)- (9H-fluoren-9-yl)methyl (-5-(6-benzyl-5,7-dioxohexahydroimidazo[1,5-c]thiazol-3-yl)-5-(3-methylbutanamido)pentyl)carbamate (14).

Overall Yield 62%. ¹H NMR (400 MHz, CDCl₃) δ 0.94 (d, 6H, 2 CH_3 , J = 12 Hz); 1.24-1.27 (m, 2H, CH_2); 1.59-1.64 (m, 4H, 2 CH_2); 1.71-1.75 (m, 1H, CH); 2.10-2.14 (m, 2H, CH_2); 2.99-3.04 (m, 3H, CH_2 , H-1a); 3.28-3.34 (m, 1H, H-1b); 4.07-4.10 (m, 1H, H-1'); 4.32 (t, 1H, H-7a); 4.39 (t, 1H, CH Fmoc); 4.51 (dd, 2H, CH_2 J' = 12, J'' = 19.8 Hz); 4.73-4.80 (m, 3H, CH_2 Fmoc, CH_2); 5.20 (d, 1H, H-3, J = 3.6 Hz); 7.27-7.34 (m, 7H, Aryl); 7.45-7.61 (m, 6H, Aryl). ¹³C NMR (100 MHz, CDCl₃) δ 22.2 ($2CH_3$); 25.8 (CH_2); 26.1 (CH_2); 29.9 (CH_2); 36.8 (C-1); 40.8 (CH_2); 42.5 (CH_2); 47.0 (CH_2); 54.0 (C-1'); 64.3 (C-7a); 67.1 (CH_2); 69.0 (C-3); 120.5; 125.2; 126.2; 126.9; 128.5; 136.7; 142.6; 143.6 (Aryl); 155.6; 156.4; 170.0; 172.6 (CO); ESI-MS m/z calcd per $C_{32}H_{34}N_6O_4S$ [(M + H)⁺] 598.72; found, 599.01.

(3*S*,7*aR*,1'*S*)-2-((9*H*-fluoren-9-yl)oxy)-*N*-(16-benzyl-5,7-dioxohexahydroimidazo[1,5-*c*]thiazol-3-yl)-4-guanidinobutyl)acetamide (16).

Overall Yield 59%. ¹H NMR (400 MHz, CD₃OD) δ 1.50–1.59 (m, 4H, 2CH₂); 2.59 (t, 2H, CH₂); 2.85 (t, 1H, H-1a, J = 19.6 Hz); 3.27-3.31 (m, 1H, H-1b); 4.11-4.13 (m, 1H, H-1'); 4.29 (t, 1H, H-7a, J = 8.0 Hz); 4.37 (t, 1H, CH Fmoc); 4.48 (dd, 2H, CH₂ J' = 12, J'' = 19.8 Hz); 4.77-4.84 (dd, 2H, CH₂ Fmoc, CH₂); 5.24- (d, 1H, H-3, J = 3.6 Hz); 7.25-7.33 (m, 7H, Aryl); 7.48-7.59 (m, 6H, Aryl). ¹³C NMR (100 MHz, CD₃OD) δ 25.8 (CH₂); 26.1 (CH₂); 34.8 (C-1); 41.8 (CH₂); 43.5 (CH₂); 47.0 (CH); 53.5 (C-1'); 64.3 (C-7a); 67.1 (CH₂); 68.56 (C-3); 120.5; 125.2; 126.2; 126.9; 128.5; 136.7; 142.6; 143.6 (Aryl); 155.6; 156.4; 172.6 (CO); 158.2 (CNH). ESI-MS *m/z* calcd per C₃₇H₄₂N₄O₅S [(M + H)⁺] 654.29; found, 654.50.

(2*S*,4*R*,1'*S*)ethyl 2-(1-(((benzyloxy)carbonyl)amino)-3-methylbutyl)-3-((3-guanidinopropyl) carbamoyl) thiazolidine-4-carboxylate (7b).

Overall Yield 61%. ¹H NMR (400 MHz, CD₃OD) δ 0.92–0.96 (m, 6H, 3CH₃); 1.20-1.29 (m, 5H, CH₂, CH₃); 1.55-1.68 (m, 1H, CH); 1.78 (t, 2H, CH₂); 3.23-3.30 (m, 1H, H-5a); 3.33-3.44 (m, 4H, 2CH₂); 3.46-3.50 (m, 1H, H-5b); 4.14-4.25 (m, 3H, H-1', CH₂); 4.75 (t, 1H, H-4); 5.08-5.15 (m, 1H, CH₂); 5.18 (d, 1H, H-2, J = 8 Hz); 7.13-7.30 (m, 5H, Aryl). ¹³C NMR (100 MHz, CD₃OD) δ 20.6 (2CH₃); 22.5 (CH₃); 24.9 (CH₂); 26.0 (CH₂); 31.9 (CH); 37.0 (C-5); 38.3 (CH₂); 41.1 (CH₂); 51.0 (C-1'); 61.4 (CH₂); 65.1 (C-4); 66.1 (CH₂ Bz); 68.6 (C-2); 127.3; 127.4; 127.9 (Aryl); 152.1; 167.8; 170.6 (CO); 160.4 (CNH). ESI-MS *m/z* calcd per C₂₄H₃₈N₆O₅S [(M + H)⁺] 522.26; found 522.48.

(3*S*,7*aR*,1'*S*)-benzyl (1-(6-(3-guanidinopropyl)-5,7-dioxohexahydroimidazo[1,5-*c*]thiazol-3-yl)-3-methylbutyl)carbamate (6b).

Overall Yield 58%. ¹H NMR (400 MHz, CD₃OD) δ 0.87–0.93 (m, 6H, 2CH₃); 1.36-1.41 (m, 2H, CH₂); 1.61-1.67 (m, 1H, CH); 1.79 (t, 2H, CH₂); 3.10 (t, 1H, H-1a); 3.14-3.28 (t, 2H, CH₂); 3.30 (t, 1H, H-1b); 3.50 (t, 2H, CH₂); 3.90-3.97 (m, 1H, H-1'); 4.40 (t, 1H, H-7a); 5.01-5.14 (dd, 2H, CH₂, J' = 12, J'' = 24

Hz); 5.19 (d, 1H, H-3, J = 6.0 Hz); 7.28-7.32 (m, 5H, Aryl). ¹³C NMR (100 MHz, CD₃OD) δ 20.5 (2CH₃); 22.3 (CH₂); 24.6 (CH₂); 26.9 (CH); 35.7(CH-1); 38.3 (CH₂); 40.3 (CH₂); 53.6 (C-1'); 65.1 (C-7a); 66.1 (CH₂ Bz); 67.7 (C-3); 127.2; 127.6; 128.0; (Aryl); 156.1; 156.9; 172.3 (CO); 158.7 (CNH). ESI-MS *m/z* calcd per C₂₂H₃₂N₆O₄S [(M + H)⁺] 476.22; found, 476.35.

3S,7aR,1'S)-Benzyl (1-(6-(4-chlorophenethyl)-5,7-dioxohexahydroimidazo[1,5-c]thiazol-3-yl)-3-methylbutyl)carbamate (17).

Overall Yield 76%. ¹H NMR (400 MHz, CDCl₃) δ 0.93 (d, 6H, 2CH₃, J= 6 Hz); 1.21-1.33 (m, 2H, CH₂); 1.65-1.69 (m, 1H, CH); 2.65-2.70 (m, 1H, H-1a); 2.88-2.91 (t, 2H, CH₂); 3.21-3.24 (m, 1H, H.1b); 3.65-3.68 (t, 2H, CH₂); 4.12-4.23 (m, 2H, H-7a, H-1'); 4.84 -5.10 (m, 2H, CH₂); 5.24 (d, 1H, H-3, J = 4.0 Hz); 7.11 (d, 2H, H-2, H5 Aryl, J'= 12); 7.24-7.37(m, 7H, H-3,H-5, Aryl.). ¹³C NMR (100 MHz, CDCl₃) δ 21.88 (2CH₃); 22.89 (CH₂); 27.90 (CH); 37.26 (C-1); 41.65 (CH₂); 46.38 (CH₂); 53.72 (C-1'); 65.19 (C-7a); 67.46 (CH₂ Bz); 67.08 (C-3); 128.14; 128.33; 128.59; 128.72; 130.30 (Aryl); 152.39; 155.41; 170.97 (CO); ESI-MS *m/z* calcd per C₂₆H₃₀ClN₃O₄S [(M + H)⁺] 515.16; found, 515.27.

(3S,7aR,1'S)-Benzyl (1-(5,7-dioxo-6-phenethylhexahydroimidazo[1,5-c]thiazol-3-yl)-3-methylbutyl)carbamate (18).

Overall Yield 78%. ¹H NMR (400 MHz, CDCl₃) δ 0.95–0.97 (d, 6H, 2CH₃, J=6.0 Hz); 1.27-1.34 (m, 2H, CH₂); 1.67-1.69 (m, 1H, CH); 2.62-2.69 (t, 1H, H.1a); 2.93-2.98 (t, 2H, CH₂, J' = 6.0 Hz); 3.17-3.20 (m, 1H, H,1b); 3.67-3.77 (m, 2H, CH₂); 4.13-4.25 (m, 2H, H-7a, H-1'); 5.13 (s, 2H, CH₂); 5.27- 5.31 (d, 1H, H-3, J = 12.0 Hz); 7.20- 7.37 (m, 10H, Aryl.). ¹³C NMR (100 MHz, CDCl₃) δ 21.89 (2CH₃); 22.89 (CH₂); 28.90 (CH); 38.26 (C-1); 41.40 (CH₂); 46.1 (CH₂); 54.72 (C-1'); 65.19 (C-7a); 67.46 (CH₂ Bz); 67.08 (C-3); 128.14; 128.33; 128.59; 129.72; 132.30 (Aryl); 152.39; 155.41; 172.1 (CO); ESI-MS *m/z* calcd per C₂₆H₃₁N₃O₄S [(M + H)⁺] 481.20; found, 481.38.

(2S,4R,1'S)-Ethyl 2-(-1-(((benzyloxy)carbonyl)amino)-3-methylbutyl)-3-(butylcarbamoyl)thiazolidine-4-carboxylate (19).

Overall Yield 70%. ¹H NMR (400 MHz, CDCl₃) δ 0.84–0.92 (m, 11H, 3CH₃, CH₂); 1.22 (t, 3H, CH₃); 1.29-1.66 (m, 4H, 2CH₂); 1.63-1.68 (m, 5H, CH₂, CH); 3.11-3.22 (m, 3H, CH₂, H-5a); 3.40-3.43 (m, 1H, H-5b); 4.10-4.15 (m, 3H, CH₂, H-1'); 4.55-4.59 (m, 1H, H-1'); 4.64-4.67 (m, 1H, H-4); 5.02 (d, 1H, CH₂, J = 12Hz); 5.13 (d, 1H, CH₂); 5.38 (s, 1H, H-2); 7.26-7.38 (m, 5H, Aryl). ¹³C NMR (100 MHz, CDCl₃) δ 18.2 (2CH₃); 19.04 (CH₃); 20.02(CH₃); 21.9 (CH₂); 23.29 (CH₂); 25.05 (CH); 31.93 (CH₂); 32.34 (C-5); 40.73 (CH₂); 52.06 (C-1'); 62.18 (CH₂); 63.77 (C-4); 66.60 (CH₂ Bz); 68.62 (C-2); 128.01; 128.07; 128.41; 136.55 (Aryl); 156.19; 167.8; 170.99 (CO). ESI-MS *m/z* calcd per C₂₄H₃₇N₃O₅S [(M + H)⁺] 479.25; found, 479.80.

(3S,7aR,1'S)-Benzyl ((S)-1-(6-butyl-5,7-dioxohexahydroimidazo[1,5-c]thiazol-3-yl)-3-methylbutyl)carbamate (20).

Overall Yield 75%. ¹H NMR (400 MHz, CDCl₃) δ 0.90–0.94 (m, 9H, 3CH₃); 1.25-1.35 (m, 4H, 2CH₂); 1.41-1.58 (m, 2H, CH₂); 1.65-1.68 (m, 1H, CH); 2.85-2.90 (t, 1H, H-1a); 3.26-3.31 (t, 1H, H-1b); 3.42-3.46 (t, 2H, CH₂); 4.12-4.15 (m, 1H, H-1'); 4.17-4.28 (t, 1H, H-7a); 5.09 (dd, 2H, CH₂, J' = 12, J'' = 19.8 Hz); 5.28 (d, 1H, H-3, J = 3.6 Hz); 7.25-7.33 (m, 10H, Aryl). ¹³C NMR (100 MHz, CDCl₃) δ 20.1 (2CH₃); 20.88 (CH₃); 21.87 (CH₂); 23.27 (CH₂); 24.71 (CH₂); 29.91 (CH); 32.91 (C-1); 41.66 (CH₂); 53.42 (C-1'); 65.30 (C-7a); 67.04 (CH₂ Bz); 67.42 (C-3); 128.14; 128.31; 128.56; 136.30 (Aryl); 156.01; 156.19; 171.99 (CO). ESI-MS *m/z* calcd per C₂₂H₃₁N₃O₄S [(M + H)⁺] 433. 21; found, 433.42.

7.2 Pharmacology: GRK2 activity in rhodopsin phosphorylation assay

To evaluate the effect of all synthesized derivatives on GRK2 activity we assessed GRK2 purified proteins by light-dependent phosphorylation of rhodopsin-enriched rod outer segment membranes (ROS) using [g - ^{32}P]-ATP. Briefly, 50 ng of active GRK2 were incubated with ROS membranes in presence or absence of inhibitor molecules in reaction buffer (25 ml) containing 10 mM $MgCl_2$, 20mM TriseCl, 2 mM EDTA, 5 mM EGTA, and 0.1 mM ATP and 10 mCi of [^{32}P] g -ATP. After incubation with white light for 15 min at room temperature, the reaction was quenched with ice-cold lysis buffer and centrifuged for 15 min at 13000g. The pelleted material was resuspended in 35 mL protein gel loading dye, electrophoresed and resolved on SDS-PAGE 4-12% gradient (Invitrogen), stained with Coomassie blue, destained, vacuum dried, and exposed for autoradiography. Phosphorylated rhodopsin was visualized by autoradiography of dried gels and quantified using a PhosphorImager (Molecular Dynamics). Alternatively, the ROS pellet was washed twice in ice-cold lysis buffer to remove the unbound [g - ^{32}P]-ATP and then resuspended in 100 mL of buffer and the level of [g - ^{32}P]-ATP incorporation into ROS was determined by liquid scintillation counter.

CHAPTER V:
A continuous flow procedure for the
difluoromethylation of aminoacids

1. Introduction

The synthesis of organofluorine compounds has flourished because of the wide scope of their applications in biological and material sciences in recent years.^{165,166} Currently, the selective incorporation of fluorine atoms or fluorine-containing moieties into organic molecules to modulate their biological properties has become a routine and powerful strategy in drug design.

Difluoromethyl functionalized compounds in particular are employed because of their significantly increased lipophilicity, membrane permeability, aqueous solubility, and metabolic stability, as exemplified by the anesthetic Desflurane, anticancer Gemcitabine, lung disease drug Roflumilast, antiulcer Pantoprazole, antiviral difluoromethoxyquinolone Garenoxacin and herbicide Sulfentrazone (Figure 1).^{167,168}

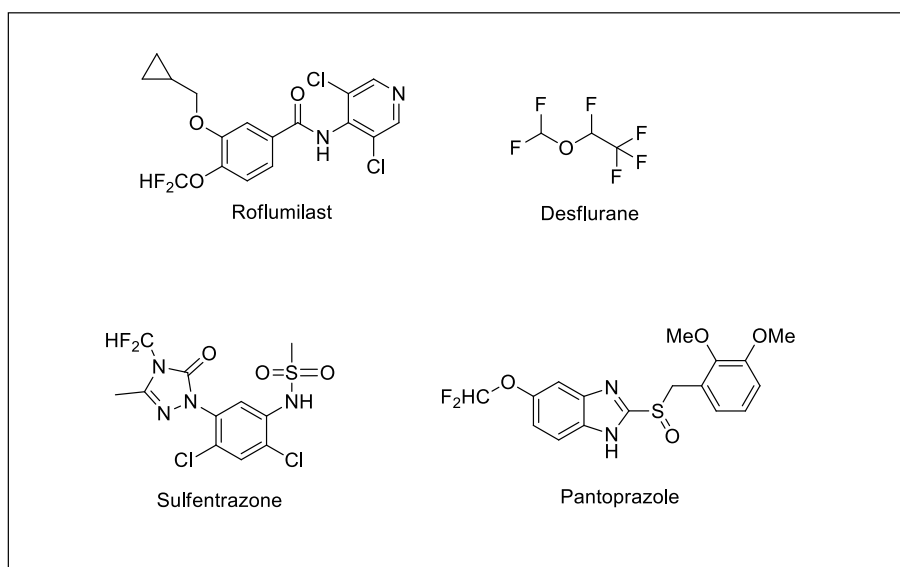


Figure 1. Pharmaceutically active compounds containing difluoromethyl group.

Additionally the difluoromethyl group is known to be isosteric to a carbinol unit, which can act as a lipophilic hydrogen donor through weak hydrogen bonding interactions and makes it an interesting group to the design of bioactive molecules.¹⁶⁹

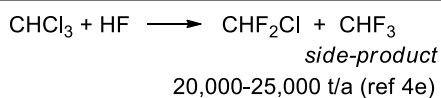
The difluoromethyl compounds thus obtained are biologically and chemically important and, therefore, the introduction of the difluoromethyl functionality into organic compounds is of vital importance, as typically shown in difluoromethyl analogues of α -amino acids.¹⁷⁰

The difluoromethylornithine (DFMO), eflornithine is a mechanism-based inhibitor of ornithine decarboxylase, a pyridoxal-dependent key enzyme of the polyamines biosynthesis from ornithine. Fluorine atoms are essential for the inhibition process. Despite its very low bioavailability, eflornithine is the best therapy for sleeping sickness (trypanosomiasis) in particular, at the cerebral stage due to *Trypanosoma brucei gambiense* parasite.¹⁷¹ Eflornithine is explored as anticancer agent, and it is in clinical use for the treatment of *Pneumocystis carinii pneumonia*, the most frequent opportunistic infection associated with the acquired immune deficiency syndrome (AIDS).¹⁷²

Among the cheapest and most versatile reagents for direct CHF₂-transfer is chlorodifluoromethane (CHF₂Cl, Freon 22). Chlorodifluoromethane is produced on a massive scale, particularly for the production of fluoropolymers, and it is available at relatively little cost. With sufficiently strong bases, CHF₂Cl can be deprotonated. The so-formed carbanion, chlorodifluoromethanide (CF₂Cl⁻), immediately loses chloride to generate an electrophilic singlet difluorocarbene (CF₂Cl⁻ → CF₂ + Cl⁻). The short-lived difluorocarbene can then be trapped with a suitably reactive nucleophilic species to produce the difluoromethylated product (Scheme 1). This reaction has been shown to proceed successfully with a range of compounds.^{173,174,175}

Scheme 1. General routes to the synthesis of difluoromethylaminoacids.

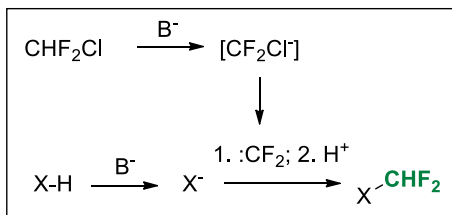
Production of CHF₂Cl:



CHF₂Cl:

- potent greenhouse gas (~1800 times higher than CO₂)
- ozone depleter
- **applications are phased out (Montreal Protocol)**

Difluoromethylation with CHF₂Cl:



CHF₃:

- potent greenhouse gas (~15 000 times higher than CO₂)
- needs capturing from emissions
- **little to no practical use -> incineration**

However, CHF₂Cl is a strong ozone depleting gas and its production and usage has become limited and expensive. Thus, the development of suitable methods for the generation of CHF₂ group is of great practical significance.

It is well known that the fluorine released in the form of fluorine radical and fluoride ion from stratospheric decomposition of fluorocarbons, such as CFCs, HCFCs and HFCs is entirely and rapidly converted to hydrogen fluoride and becomes inert to ozone.¹⁷⁶ Many of the substitute HCFCs and HFCs contain trifluoromethyl groups and it was postulated that the trifluoromethyl radical (CF₃), formed from decomposition of fluorocarbons is rapidly removed by oxidation processes and forms carbonyl difluoride and hydrogen fluoride, both of which are inert as far as ozone depletion is concerned.¹⁷⁷

For this reasons, recently, the use of fluoroform, a non ozone depleting gas, as source of difluorocarbene group was investigated. Fluoroform is a byproduct of Teflon manufacture, but if desired, it could readily be manufactured as a commodity chemical by fluorine/chlorine exchange of chloroform. Recently it had attracted little interest as a synthetic fluorinated building block reagent, in spite of various reports, invoking its use to carry out difluoromethylation reactions.^{178,179,180}

2. Aim of the study

During my PhD research semester abroad, at the University of Graz in the research group of Professor Oliver Kappe, I've been involved in a project based on the use of fluoroform as source of difluorocarbene in the continuous flow synthesis of difluoromethyl compounds. Recent papers reported the fluoroform activation with alkali metal bases. Mikami and co-workers demonstrated that fluoroform can be utilized for the direct difluoromethylation of lithium enolates utilizing strong lithium bases (lithium diisopropylamide (LDA) or lithium hexamethyldisilazide (LiHMDS)).¹⁸¹

The mechanism of the difluoromethylation reaction is believed to resemble that of the corresponding reaction with CHF_2Cl . The direct α -difluoromethylation of **1** with lithium enolates was recently demonstrated via C–F bond activation of **1** (Figure 2). The proposed $\text{S}_{\text{N}}2$ reaction involves the lithium enolate attacking a trifluoromethyl lithium species formed by the deprotonation of fluoroform. This may be possible because the interaction of the enolate lithium with the lithium carbenoid C–F bond is stronger than with the neutral fluoroform C–F bond. The leaving fluoride from the lithium carbenoid may be the driving force for $\text{S}_{\text{N}}2$ -displacement by attraction of the Lewis acidic lithium cation.¹⁸²

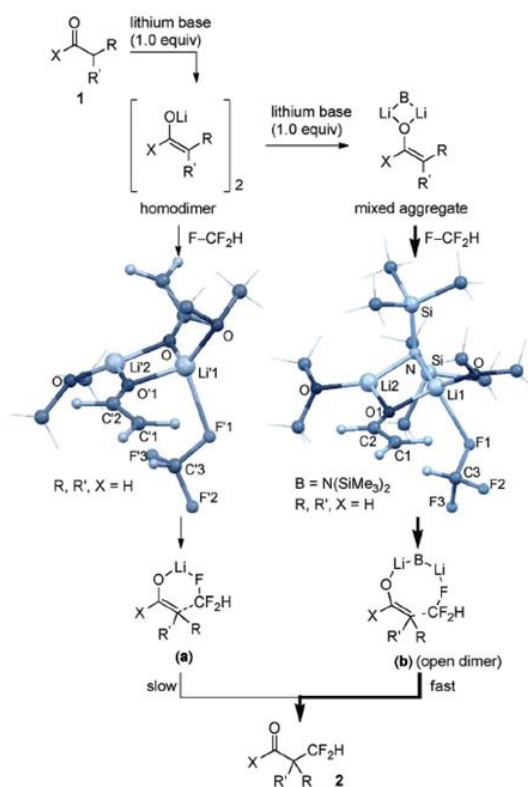


Figure 2. Plausible mechanism of α -difluoromethylation.

The research aim was to establish a scalable, continuous flow synthesis route to $C\alpha$ -difluoromethyl amino acids using fluoroform as the reagent. Continuous processing techniques have had a significant impact in the development of more sustainable manufacturing routes for several pharmaceuticals.¹⁸³ For gas-liquid reactions several specific advantages exist: high pressures operation and fast gas-liquid mass transfer enhances availability of the gaseous reagent in the liquid phase.¹⁸⁴ In addition, the gaseous reagent can be dosed into the liquid phase with precise stoichiometry using mass flow controllers.

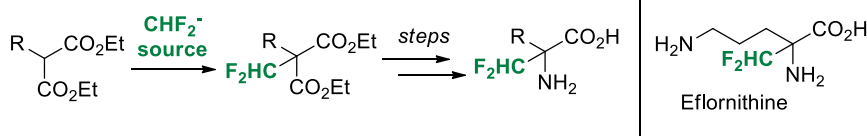
$C\alpha$ -Difluoromethyl amino acids are potent and selective irreversible inhibitors of their respective α -amino acid decarboxylases.¹⁸⁵ Representatives of this class of compounds exhibit a broad spectrum of biological activities, such as antibacterial, antihypertensive, cancerostatic, and cytotoxic activity. Two different strategies can be employed for the generation of $C\alpha$ -difluoromethyl amino acids:

construction of the amino acid from fluorine-containing building blocks (e.g. α -difluoromethyl malonates)^{170b}, or direct substitution of the α -hydrogen of amino acids with a CHF_2 moiety (Scheme 2). The direct $\text{C}\alpha$ -difluoromethylation of Schiff base-protected α -amino acid methyl esters with CHF_2Cl as the reagent has been demonstrated by Bey and others.¹⁸⁶

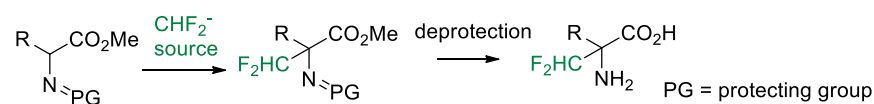
α -Difluoromethylation of protected amino acids with CHF_3 is currently not reported. Indeed, the protocol described herein is, to the best of our knowledge, the first example where fluoroform is utilized for the preparation of α -difluoromethyl aminoacids starting from the parent one.

Scheme 2 Synthesis of D,L- α -difluoromethyl amino acids.

indirect route to α -difluoromethyl amino acids:



direct route to α -difluoromethyl amino acids:



3. Synthesis

The first preliminary batch experiments were performed using diethyl phenylmalonate (**1a**) as starting material (Table 1). The malonate was dissolved in THF and the base was added. After stirring the mixture for a few minutes at the indicated temperatures (t_1 , T_1 in Table 1), fluoroform was slowly passed through the reaction mixture under vigorous stirring (t_2 , T_2 in Table 1). Using phenylmalonate **1a** as substrate, no product was obtained with *n*BuLi, LDA or *t*BuOK as base (entries 1 to 5 in Table 1). We observed no difluoromethylated product using Dolbier and co-workers method (entry 7 in Table 1)¹⁸⁷. According to Dolbier's procedure, the phenylmalonate **1a** is stirred in aqueous KOH for 30 min at room temperature. MeCN or dioxane is then added and fluoroform is bubbled through the solution. Small amounts of the desired product were formed using LiHMDS as base (entry 6 in Table 1). Mikami and co-workers have already shown that fluoroform in combination with LiHMDS can be utilized for the direct difluoromethylation of cyclic amides, cyclic and open esters, and certain simple malonates. According to the authors, the reaction proceeds best with 2 equiv of base and 5 equiv of CHF₃. Reaction times of 6 to 48 h at temperatures of 0 to 25 °C were needed to provide the desired products in good yield.

Table 1. Difluoromethylation of diethyl phenylmalonate **1a** with CHF₃^a.

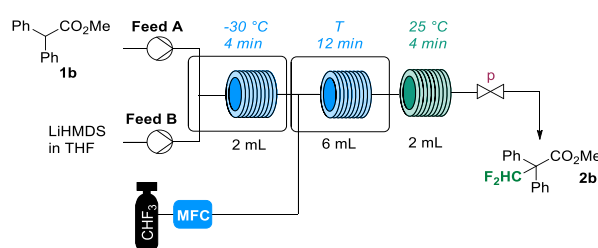
	base (equiv)	t ₁ (min)	T ₁ (°C)	t ₂ (min)	T ₂ (°C)	conv (%) ^b	sel (%) ^b
1	<i>t</i> BuOK (3)	5	25	60	25	28	0
2	<i>t</i> BuOLi (3)	5	25	60	25	4	0
3	LDA (2)	5	25	5	25	0	0
4	<i>n</i> BuLi (2)	5	25	5	25	0	0
5	<i>n</i> BuLi (2)	5	-80	5	-80	0	0
6	LiHMDS (2)	5	25	60	25	2	100
7^c	KOH (15)	30	25	120	25	32 ^d	0

^a Conditions: 0.5 mmol diethyl phenylmalonate **1a** in 0.5 mL THF, base, CHF₃ (balloon). ^b analyzed by HPLC-UV/VIS at 215 nm. ^c method B in ref 9a. ^d 20% ethyl phenylacetate (by hydrolysis and decarboxylation).

Encouraged by this result, a continuous flow protocol was developed. The initial flow setup consisted of two continuous syringe pumps to introduce (i) a 0.5 M solution of substrate in THF (Feed A, Table 2), and (ii) a commercial solution of LiHMDS (Feed B, Table 2). The two feeds were mixed in a Y-shaped connector in a cooling bath. The substrate was deprotonated in a 2 mL residence loop (reactor 1), before the mixture was combined with fluoroform in a second Y-shaped connector in a second cooling bath. The flow rate of the fluoroform stream was controlled using a calibrated mass flow controller (MFC). The combined mixture then went through a second cooled residence loop (reactor 2) and left the flow system through a third residence loop at room temperature (reactor 3) and an adjustable back pressure regulator. With pressures of ~5 bar and temperatures below ~ 25 °C for reactor 2, the fluoroform dissolved completely in the liquid feed. At higher temperatures at this pressure, distinct gas-liquid segments were evidenced. The processed reaction mixture was finally collected in a quench solution of aqueous HCl/Et₂O and the organic phase was analyzed by GC-FID and

^{19}F -NMR. Methyl diphenylacetate **1b** was used as the model substrate for the initial optimization. With flow rates of 300 $\mu\text{L}/\text{min}$ for Feed A, 200 $\mu\text{L}/\text{min}$ for Feed B and 8.3 mL/min for fluoroform, a stoichiometry of 1:1.3:2.5 for substrate/LiHMDS/ CHF_3 and a total residence time of ~ 20 min was obtained. The flow reactions clearly revealed that the conversion increased with decreasing temperature and increasing pressure (Table 2). Also the selectivity increased slightly with decreasing temperatures (Table 2). As already observed by Mikami and co-workers, the best results are obtained with 2 equiv of base. Also, for fluoroform, 2 to 3 equiv were identified as the ideal amount.

Table 2. Difluoromethylation of methyl diphenylacetate **1b** under flow conditions^a.



	T (°C)	P (bar)	Conv (%) ^b	Sel (%) ^b
1	40	5	63	81
2	25	5	65	80
3	-10	5	82	88
4	-15	10	86	91
5	-15	12	92	91

^a Conditions: Feed A: 0.5 M diethyl phenylmalonate **1b** in THF; Feed B: 1 M LiHMDS in THF; with flow rates for Feed A/Feed B/ CHF_3 = 0.30 : 0.20 : 8.3 mL/min, respectively, the following conditions were obtained: LiHMDS (1.33 equiv); CHF_3 (2.5 equiv). ^b analyzed by GC-FID.

The general reaction conditions were suitable for a variety of substrates (Figure 2). Malonates with sterically benign alkyl groups in the α -position performed particularly well (**1d** to **1f** in Figure 2), while the phenyl derivative **1a** resulted in low conversion. The reaction was remarkably clean, with unreacted substrate and tris(trimethylsilyl)amine being the only contamination in the crude mixture after

washing with water. The analytically pure compounds were isolated by preparative thin-layer chromatography (TLC). The yield for the diethyl methylmalonate **2e** was the same as previously reported for the batch protocol, even though the reaction time for the present procedure was significantly shorter (20 min vs 20 h for the batch procedure). The yield for product **2b** was lower than that reported for the batch procedure (39% vs 78% according ^{19}F -NMR). The other difluoromethylated compounds prepared in this work have not been previously reported.

Based on the obtained results we decided to investigate the application of this procedure to Schiff base-protected α -amino acid methyl esters. The N-benzylidene-protected α -amino acid methyl esters were readily available from the parent amino esters using literature procedures¹⁸⁸. Gratifyingly, when the N-benzylidene-protected α -amino acid methyl esters **1g** to **1k** was subjected to the general reaction conditions resulted in >95% conversion to the desired product. Indeed, the reaction was remarkably clean with only one CHF_2 -moiety (two doublets of doublets) detectable in the ^{19}F -NMR spectra of the crude reaction mixtures. Difluoromethylation on the imine carbon, a side reaction typically encountered in reactions with CHF_2Cl as reagent, was not observed. Due to the instability of the Schiff base to hydrolysis, isolation of the intermediate products was not attempted. Instead, the N-benzylidene- and the O-methyl- protecting group were directly removed by heating the crude product in 6N HCl in a microwave batch autoclave (150 °C for 45 min). The released benzaldehyde was removed by extracting with ether and the aqueous phase was concentrated. After recrystallization from MeOH/EtOH, the C α -difluoromethyl amino acids were obtained as their monohydrochloride salts (dihydrochloride salt for product **2k**). The yields were above 70% for all tested amino acids over the two reaction steps, i.e. difluoromethylation and deprotection (Figure 3).

Importantly, eflornithine (**2g**) was isolated in 76% yield after the two reaction steps. The yield of eflornithine for the present chromatography-free method is significantly higher than that previously reported for the less desirable process based on chlorodifluoromethane (37% to 40%).

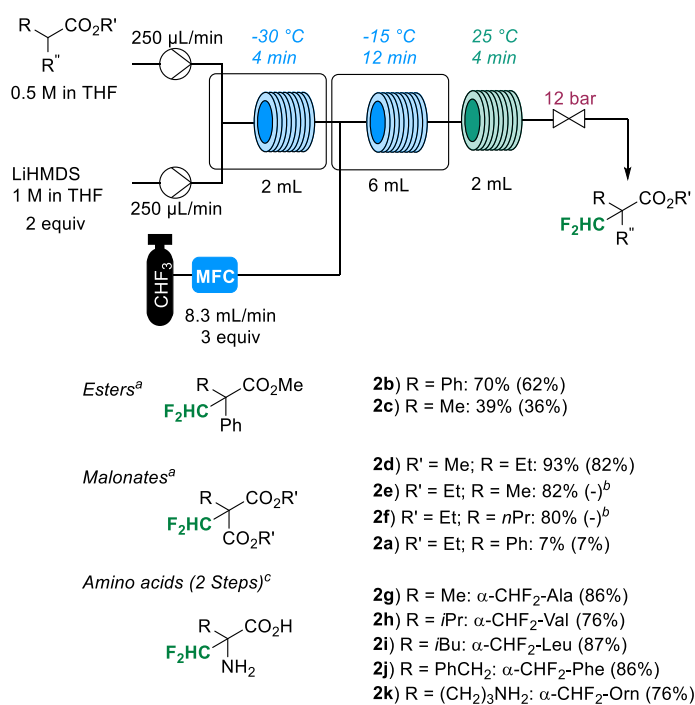


Figure 3. Continuous flow C ^{α} -difluoromethylation with fluoroform. ^a ¹⁹F-NMR yields (trifluorotoluene as internal standard); isolated yields (TLC) in parentheses. ^b isolation was not attempted. ^c isolated yields after 2 steps (C ^{α} -difluoromethylation and hydrolysis of protecting groups).

4. Conclusions

During my PhD course I spent a semester at the University of Graz laboratories, where I took part to a research project concerning the use of fluoroform as source of difluorocarbene in the continuous flow synthesis of difluoromethyl compounds. In detail, the project concerned the design of a gas–liquid continuous flow difluoromethylation protocol employing fluoroform as a reagent. The developed protocol allows this reaction to be performed within very short reaction times. Importantly, the protocol allows the direct C α -difluoromethylation of protected α -amino acids. These compounds are highly selective and potent inhibitors of pyridoxal phosphate-dependent decarboxylases. The starting materials are conveniently obtained from the commercially available α -amino acid methyl esters, and the final products are synthesized in excellent yields and high purities after hydrolysis and precipitation. The developed process appears to be especially appealing for industrial applications, where atom economy, sustainability, reagent cost and reagent availability are crucial factors¹⁸⁹.

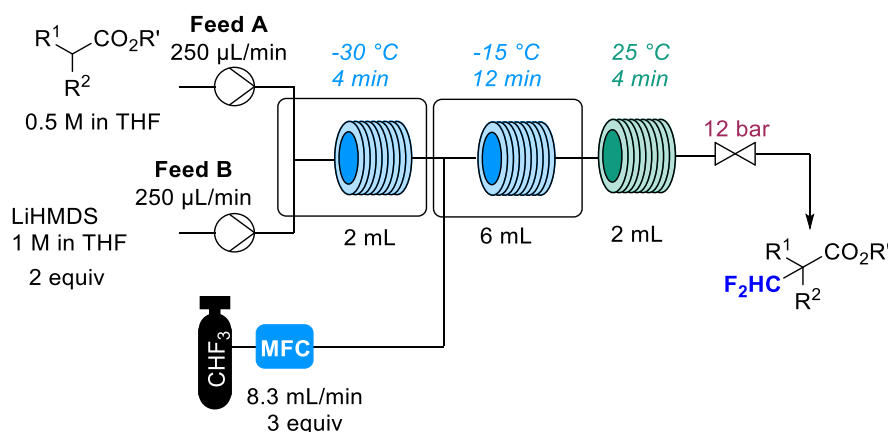
Experimental Section

5. Chemistry

^1H and ^{13}C NMR spectra were recorded on a 300 MHz instrument. Chemical shifts (δ) are expressed in ppm downfield from TMS as an internal standard. The letters s, d, t, q, and m are used to indicate singlet, doublet, triplet, quadruplet, and multiplet, respectively. Analytical HPLC analysis were carried out on a Shimadzu LC20-AD chromatograph equipped with a C18 reversed-phase (RP) analytical column (150 x 4.6mm, particle size 5 μm) at 37 $^\circ\text{C}$ using a mobile phase A (water/acetonitrile 90:10 (v/v) + 0.1% TFA) and B (acetonitrile + 0.1% TFA) at a flow rate of 1.5 mL/min. The following gradient was applied: linear increase from solution 3% B to 25% in 9 minutes, 25% B to 80% in 7 min hold at 80% B for 1 minute. Low resolution mass spectra were obtained on a LC-MS instrument using electrospray ionization (ESI) in positive or negative mode (Shimadzu LCMS-2020). All chemicals, solvents, catalysts, and ligands were obtained from known commercial suppliers and were used without any further purification. Microwave reactions were carried out in a Biotage Initiator+ single-mode microwave instrument. Reaction times refer to hold times at the temperatures indicated, not to total irradiation times. The temperature was measured with an IR sensor on the outside of the reaction vessel. Thin-layer chromatography was performed on tlc silica gel 60 f254 20 x 20 cm. Trifluorotoluene was used as internal standard for ^{19}F NMR.

General procedure for continuous flow difluoromethylation of malonates derivatives (2a-2f).

Scheme 3. Continuous flow setup.



The flow setup consisted of two continuous syringe pumps (Asia Syrris) to introduce (i) a solution of substrate in THF (Feed A), and (ii) a commercial solution of LiHMDS (1.0 M in THF, Sigma-Aldrich); Feed B). Injection loops (perfluoroalkoxy alkanes (PFA), 0.8 mm i.d., 1.59 mm o.d.; internal volume: 2.0 mL (Feed A) and 2.5 mL (Feed B)) were used to deliver the two feeds. To start the experiment, the complete reactor setup was flushed by pumping dry THF with flow rates of Feed A = 250 µL/min and Feed B = 250 µL/min. Fluoroform was introduced into the reactor with a flow rate of 8.3 mL/min using a calibrated Bronkhorst mass flow controller (MFC). The internal pressure of the reactor reached the target pressure of 12 bar after approximately 10 min. Substrate (1.00 mmol) was dissolved in neat THF and diluted to 2.00 mL in a volumetric flask with THF (Feed A). A LiHMDS solution (1.0 M, 2.5 mL) in THF was used as Feed B. Both solutions were loaded into their corresponding injection loops. Feed A and Feed B were pumped from the injection loops in a Y-shaped connector (Y Assembly PEEK 1/4-28 0.040in) in a cooling bath (-30 °C). The combined mixture went through a first residence loop at -30 °C (1/16 in. o.d.; 0.8 mm i.d.;

residence volume V1 = 2.0 mL), before the mixture was combined with fluoroform in a second Y-shaped connector (Y Assembly PEEK 1/4-28 .040in) in a second cooling bath (-15 °C). The combined mixture then went through a second residence loop (1/16 in. o.d.; 0.8 mm i.d.; residence volume V2 = 6.1 mL) and left the flow system through a third residence loop at room temperature (1/8 in. o.d.; 1.6 mm i.d.; residence volume V3 = 2.0 mL) and an adjustable back pressure regulator (Swagelok KCB1H0A2A5P60000, 0–26 bar). The product mixtures were collected and the solvent removed in vacuo. The products were isolated by thin layer chromatography using dichloromethane/hexane as eluent.

Methyl 3,3-(difluoro)-2,2-diphenylpropanoate (2a).

Yield: 173 mg (0.62 mmol, 62%); 93% by ^{19}F NMR; light yellow viscous liquid. ^1H NMR (300 MHz, D_2O): δ = 7.45 – 7.19 (m, 10H), 6.90 (t, $^2J_{\text{HF}}$ = 55.0 Hz, 1H), 3.79 (s, 3H). ^{13}C NMR (75 MHz, D_2O): δ = 171.1, 136.3, 129.8, 128.3, 128.2, 115.6 (t, $^1J_{\text{CF}}$ = 246.2 Hz), 64.7, 53.1. ^{19}F NMR (282 MHz, D_2O): δ = -123.0 (d, $^2J_{\text{HF}}$ = 55.0 Hz).

Diethyl 2-(difluoromethyl)-2-phenylmalonate (2b).

Yield: 21 mg (0.07 mmol, 7%); 7% by ^{19}F NMR; light yellow viscous liquid. ^1H NMR (300 MHz, D_2O): δ = 7.45 – 7.31 (m, 5H), 6.56 (t, $^2J_{\text{HF}}$ = 54.9 Hz, 1H), 4.44 – 4.32 (m, 4H), 1.33 (t, $^3J_{\text{HH}}$ = 7.1 Hz, 6H). ^{13}C NMR (75 MHz, D_2O): δ = 166.2, 129.5, 128.8, 128.3, 114.2 (t, $^1J_{\text{CF}}$ = 251.6 Hz), 62.8, 14.1. ^{19}F NMR (282 MHz, D_2O): δ = -123.57 (d, $^2J_{\text{HF}}$ = 55.0 Hz).

Diethyl 2-(difluoromethyl)-2-phenylmalonate (2c).

Yield: 39% by ^{19}F NMR. ^1H NMR (300 MHz, D_2O): δ = 7.42 – 7.31 (m, 5H), 6.38 (dd, $^2J_{\text{HF}}$ = 56.0, 55.4 Hz, 1H), 3.75 (s, 3H), 1.71 (s, 3H). ^{13}C NMR (75 MHz, D_2O): δ = 136.6, 129.0, 128.3, 126.7, 116.7 (dd, $^1J_{\text{CF}}$ = 247.1, 245.5 Hz), 54.8, 52.8, 14.7. ^{19}F NMR (282 MHz, D_2O): δ = -124.48 (dd, $^2J_{\text{FF}}$ = 277.0, $^2J_{\text{HF}}$ = 55.3 Hz), -129.91 (dd, $^2J_{\text{FF}}$ = 277.1, $^2J_{\text{HF}}$ = 56.1 Hz).

Dimethyl 2-(difluoromethyl)-2-ethylmalonate (2d).

Yield: 172 mg (0.82 mmol, 82%); 93% by ^{19}F NMR ;light yellow viscous liquid. ^1H NMR (300 MHz, D_2O): δ = 6.28 (t, $^2J_{\text{HF}}$ = 54.6 Hz, 1H), 3.79 (s, 6H), 2.14 (q, $^3J_{\text{HH}}$ = 7.5 Hz, 2H), 1.01 (t, $^3J_{\text{HH}}$ = 7.5 Hz, 3H). ^{13}C NMR (75 MHz, D_2O): δ = 167.3 (t, $^3J_{\text{CF}}$ = 4.4 Hz), 115.1 (t, $^1J_{\text{CF}}$ = 247.9 Hz), 62.0 (t, $^2J_{\text{CF}}$ = 21.2 Hz), 53.2, 23.0 (t, $^3J_{\text{CF}}$ = 2.9 Hz), 9.4 (t, $^3J_{\text{CF}}$ = 1.6 Hz). ^{19}F NMR (282 MHz, D_2O): δ = -126.18 (d, $^2J_{\text{HF}}$ = 54.6 Hz).

Diethyl 2-(difluoromethyl)-2-methylmalonate (2e).

Yield: 82% by ^{19}F NMR; light yellow viscous liquid. ^1H NMR (300 MHz, D_2O): δ = 6.32 (t, $^2J_{\text{HF}}$ = 55.4 Hz, 1H), 4.21 (q, $^3J_{\text{HH}}$ = 7.1 Hz, 4H), 1.50 (s, 3H), 1.24 (t, $^3J_{\text{HH}}$ = 7.1 Hz, 6H). ^{13}C NMR (75 MHz, D_2O): δ = 167.0 (t, $^3J_{\text{CF}}$ = 4.9 Hz), 114.6 (t, $^1J_{\text{CF}}$ = 246.2 Hz), 62.4, 58.3 (t, $^2J_{\text{CF}}$ = 22.7 Hz), 13.9, 12.1 (t, $^3J_{\text{CF}}$ = 4.0 Hz). ^{19}F NMR (282 MHz, D_2O): δ = -128.32 (d, $^2J_{\text{HF}}$ = 55.4 Hz).

Diethyl 2-(difluoromethyl)-2-propylmalonate (2f).

Yield: 80% by ^{19}F NMR; ^1H NMR (300 MHz, D_2O): δ = 6.27 (t, $^2J_{\text{HF}}$ = 54.7 Hz, 1H), 4.25 (q, $^3J_{\text{HH}}$ = 7.1 Hz, 4H), 2.07 – 1.98 (m, 2H), 1.49 – 1.33 (m, 2H), 1.27 (t, $^3J_{\text{HH}}$ = 7.1 Hz, 6H), 0.95 (t, $^3J_{\text{HH}}$ = 7.3 Hz, 3H). ^{13}C NMR (75 MHz, D_2O): δ = 166.8 (t, $^3J_{\text{CF}}$ = 4.5 Hz), 115.1 (t, $^1J_{\text{CF}}$ = 247.7 Hz), 62.0, 61.6, 31.4 (t, $^3J_{\text{CF}}$ = 2.4 Hz), 18.0, 14.6, 14.0. ^{19}F NMR (282 MHz, D_2O): δ = -126.10 (d, $^2J_{\text{HF}}$ = 54.7 Hz).

General procedure for continuous flow difluoromethylation of aminoacid derivatives (2g-2k).

The aminoacid derivatives were synthesized according to Scheme 3. Then the reaction mixture was concentrated in vacuo and diluted with 10 mL Et_2O . After filtration the filtrate was concentrated in vacuo and treated with 10 mL 6N HCl. The reaction mixture was heated to 150 °C for 45 min in a microwave reactor and washed with Et_2O (2x20 mL). The aqueous layer was mixed with activated carbon which was subsequently filtered off. After concentrating the crude product in vacuo it was recrystallized from MeOH/EtOH.

α -Difluoromethylalaninehydrochloride (2g).

Yield: 151 mg (0.86 mmol, 86%); colourless powder. mp 272 °C; ^1H NMR (300 MHz, D_2O): $\delta = 6.32$ (t, $^2J_{\text{HF}} = 53.1$ Hz, 1H), 1.60 (s, 3H). ^{13}C NMR (75 MHz, D_2O): $\delta = 169.2$ (d, $^3J_{\text{CF}} = 6.2$ Hz), 114.3 (dd, $^1J_{\text{CF}} = 249.1$ Hz, $^1J_{\text{CF}} = 246.0$ Hz), 61.4 (dd, $^2J_{\text{CF}} = 20.9$ Hz, $^2J_{\text{CF}} = 19.3$ Hz), 16.8 (dd, $^3J_{\text{CF}} = 4.6$ Hz, $^3J_{\text{CF}} = 2.1$ Hz). ^{19}F NMR (282 MHz, D_2O): $\delta = -126.77$ (dd, $^2J_{\text{FF}} = 281.4$, $^2J_{\text{HF}} = 52.7$ Hz), -133.44 (dd, $^2J_{\text{FF}} = 281.6$, $^2J_{\text{HF}} = 53.4$ Hz).

α -Difluoromethylvaline hydrochloride (2h).

Yield: 155 mg (0.76 mmol, 76%); colourless powder. mp 272-282 °C; ^1H NMR (300 MHz, D_2O): $\delta = 6.47$ (t, $^2J_{\text{HF}} = 52.8$ Hz, 1H), 2.33 (h, $^3J_{\text{HH}} = 6.9$ Hz, 1H), 1.07 (d, $^3J_{\text{HH}} = 6.9$ Hz, 3H), 1.02 (d, $^3J_{\text{HH}} = 6.9$ Hz, 3H). ^{13}C NMR (75 MHz, D_2O): $\delta = 168.7$, 114.8 (dd, $^1J_{\text{CF}} = 249.0$ Hz, $^2J_{\text{CF}} = 244.3$ Hz), 68.5 (t, $^2J_{\text{CF}} = 17.5$ Hz), 30.30 (d, $^3J_{\text{CF}} = 4.3$ Hz), 16.6, 15.9. ^{19}F NMR (282 MHz, D_2O): $\delta = -126.46$ (dd, $^2J_{\text{FF}} = 283.9$, $^2J_{\text{HF}} = 52.3$ Hz), -130.72 (dd, $^2J_{\text{FF}} = 281.6$, $^2J_{\text{HF}} = 53.3$ Hz).

α -Difluoromethylleucine hydrochloride (2i).

Yield: 189 mg (0.87 mmol, 87%); colourless powder. mp 242-243 °C; ^1H NMR (300 MHz, D_2O): $\delta = 6.21$ (t, $^2J_{\text{HF}} = 53.4$ Hz, 1H), 1.97-1.84 (m, 1H), 1.07 (m, 2H), 0.93(d, $^3J_{\text{HH}} = 6.5$ Hz, 3H), 0.89(d, $^3J_{\text{HH}} = 6.5$ Hz, 3H). ^{13}C NMR (75 MHz, D_2O): $\delta = 170.0$ (d, $^3J_{\text{CF}} = 5.0$ Hz), 115.3 (dd, $^1J_{\text{CF}} = 249.1$ Hz, $^1J_{\text{CF}} = 246.3$ Hz), 65.3 (dd, $^2J_{\text{CF}} = 20.3$ Hz, $^2J_{\text{CF}} = 16.2$ Hz), 38.7 (d, $^3J_{\text{CF}} = 2.3$ Hz), 23.5, 22.9, 21.4. ^{19}F NMR (282 MHz, D_2O): $\delta = -127.14$ (dd, $^2J_{\text{FF}} = 277.9$, $^2J_{\text{HF}} = 53.0$ Hz), -132.73 (dd, $^2J_{\text{FF}} = 277.9$, $^2J_{\text{HF}} = 53.9$ Hz).

α -Difluoromethylphenylalaninehydrochloride (2j).

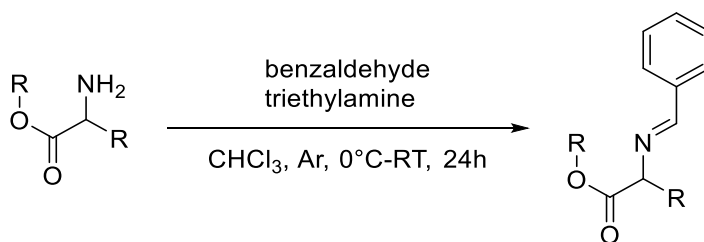
Yield: 216 mg (0.86 mmol, 86%); colourless powder. mp 245 °C; ^1H NMR (300.36 MHz, D_2O): $\delta = 7.40$ -7.32 (m, 3H), 7.26-7.20 (m, 2H), 6.39 (t, $^2J_{\text{HF}} = 53.1$ Hz, 1H), 3.44 (d, $^2J_{\text{HH}} = 14.3$ Hz, 1H), 3.06 (d, $^2J_{\text{HH}} = 14.3$ Hz, 1H). ^{13}C NMR (75 MHz, D_2O): $\delta = 168.6$ (d, $^3J_{\text{CF}} = 5.9$ Hz), 131.5 130.1, 129.2, 128.4, 114.8 (dd, $^1J_{\text{CF}} = 249.0$ Hz, $^1J_{\text{CF}} = 246.4$ Hz), 66.5

(dd, $^2J_{CF} = 20.3$ Hz, $^2J_{CF} = 16.9$ Hz), 36.5 (d, $^3J_{CF} = 2.8$ Hz). ^{19}F NMR (282 MHz, D_2O): $\delta = -127.01$ (dd, $^2J_{FF} = 280.8$, $^2J_{HF} = 52.6$ Hz), -132.02 (dd, $^2J_{FF} = 280.8$, $^2J_{HF} = 53.6$ Hz).

α -Difluoromethylornithinedihydrochloride (**2k**).

Yield: 194 mg (0.76 mmol, 76%) colourless powder. mp 228 °C; ^1H -NMR (300.36 MHz, D_2O): $\delta = 6.33$ (t, $^2J_{HF} = 53.2$ Hz, 1H), 3.02 (t, $^3J_{HH} = 7.6$ Hz, 2H), 2.16-1.53 (m, 4H). ^{13}C NMR (75 MHz, D_2O): $\delta = 168.8$ (d, $^3J_{CF} = 5.9$ Hz), 114.9 (dd, $^1J_{CF} = 248.4$ Hz, $^1J_{CF} = 246.0$ Hz), 65.1 (dd, $^2J_{CF} = 21.3$ Hz, $^2J_{CF} = 16.6$ Hz), 38.7, 27.7 (d, $^3J_{CF} = 5.0$ Hz), 20.9. ^{19}F NMR (282 MHz, D_2O): $\delta = 126.83$ (dd, $^2J_{FF} = 281.6$ Hz, $^2J_{HF} = 52.6$ Hz), -132.39 (dd, $^2J_{FF} = 281.6$ Hz, $^2J_{HF} = 53.8$ Hz).

General procedure for the preparation of benzylidene-protected amino acid esters.



A dry 20 mL vessel with magnetic stirring bar was charged with 1 eq of amino acid ester hydrochloride (**1g** to **1k**), sealed and flushed with argon three times. CHCl_3 was added to afford a 1 M solution followed by the addition of 0.99 eq (1.99 eq in case of ornithine (**1k**)) of benzaldehyde. The resulting stirred solution was cooled to 0°C . After adding 1.1 eq (2.2 eq in case of ornithine (**1k**)) of triethylamine over 10 min, the mixture was gradually warmed to room temperature and stirred for 24 h. The reaction mixture was filtered through Na_2SO_4 and the obtained light yellow filtrate was concentrated under vacuo and treated with Et_2O to precipitate $\text{Et}_3\text{N}\cdot\text{HCl}$. The formed colourless precipitate was filtered off and the obtained filtrate was concentrated in vacuo to give the benzylidene protected amino acid.

Methyl (S)-2-(benzylideneamino)propanoate (1g).

970 mg (6.95 mmol, 1.0 eq) L-Alanine methyl ester hydrochloride, 700 μ L (6.88 mmol, 0.99 eq) benzaldehyde, 1.06 mL (7.65 mmol, 1.1 eq) triethylamine and 7 mL CHCl_3 . Yield: 1.289 g (6.74 mmol, 97%), yellow viscous oil. $^1\text{H-NMR}$ (300 MHz, CDCl_3): δ = 8.31 (s, 1H), 7.81-7.74 (m, 2H), 7.48-7.38 (m, 3H), 4.16 (q, $^3J_{\text{HH}}$ = 6.8 Hz, 1H), 3.75 (s, 3H), 1.53 (d, $^3J_{\text{HH}}$ = 6.8 Hz, 3H). $^{13}\text{C NMR}$ (75 MHz, CDCl_3): δ = 173.1, 163.1, 135.8, 131.3, 128.7, 128.6, 68.2, 52.4, 19.6.

Methyl (S)-2-(benzylideneamino)-3-methylbutanoate (1h).

1.165 g (6.95 mmol, 1.0 eq) L-Valine methyl ester hydrochloride, 700 μ L (6.88 mmol, 0.99 eq) benzaldehyde, 1.06 mL (7.65 mmol, 1.1 eq) triethylamine and 7 mL CHCl_3 . Yield: 1.4925 g (6.80 mmol, 98%), yellow viscous oil. $^1\text{H-NMR}$ (300 MHz, CDCl_3): δ = 8.24 (s, 1H), 7.83 – 7.74 (m, 2H), 7.46 – 7.36 (m, 3H), 3.75 (s, 3H), 3.67 (d, $^3J_{\text{HH}}$ = 7.3 Hz, 1H), 2.39 (dq, $^3J_{\text{HH}}$ = 13.7, $^3J_{\text{HH}}$ = 6.8 Hz, 1H), 0.95 (dd, $^3J_{\text{HH}}$ = 8.9, 6.8 Hz, 6H). $^{13}\text{C NMR}$ (75 MHz, CDCl_3): δ = 172.6, 163.4, 135.8, 131.2, 128.7, 128.7, 80.6, 52.1, 31.9, 19.6, 18.8.

Methyl (S)-2-(benzylideneamino)-4-methylpentanoate (1i).

1.271 g (7.00 mmol, 1.0 eq) L-Leucine methyl ester hydrochloride, 706 μ L (6.93 mmol, 0.99 eq) benzaldehyde, 1.07 mL (7.70 mmol, 1.2 eq) triethylamine and 7 mL CHCl_3 . Yield: 1.609 g (6.90 mmol, 99%), yellow viscous oil. $^1\text{H-NMR}$ (300 MHz, CDCl_3): δ = 8.23 (s, 1H), 7.76 – 7.70 (m, 2H), 7.36 – 7.29 (m, 3H), 4.05 (dd, $^3J_{\text{HH}}$ = 8.5, 5.9 Hz, 1H), 3.65 (s, 3H), 1.90 - 1.73 (m, 2H), 1.61 – 1.46 (m, 1H), 0.87 (dd, $^3J_{\text{HH}}$ = 14.1, 6.6 Hz, 6H). $^{13}\text{C NMR}$ (75 MHz, CDCl_3): δ = 172.5, 162.9, 135.5, 130.9, 128.4, 128.3, 71.3, 51.8, 41.9, 24.2, 23.0, 21.2.

Methyl (S)-2-(benzylideneamino)-3-phenylpropanoate (1j).

1.500 g (6.95 mmol, 1.0 eq) L-Phenylalanine methyl ester hydrochloride, 700 μ L (6.88 mmol, 0.99 eq) benzaldehyde, 1.06 mL (7.65 mmol, 1.1 eq) triethylamine and 7 mL CHCl_3 . Yield: 1.7831 g (6.67 mmol, 96%), yellow viscous oil. $^1\text{H-NMR}$ (300 MHz, CDCl_3): δ = 7.92 (s, 1H), 7.72-7.66 (m, 2H), 7.45-7.35 (m, 3H), 7.28-7.14 (m, 5H), 4.18 (dd, $^3J_{\text{HH}}$ = 8.8, 5.1 Hz, 1H), 3.75 (s, 3H), 3.39 (dd,

$^2J_{\text{HH}} = 13.5$, $^3J_{\text{HH}} = 5.1$ Hz, 1H), 3.16 (dd, $^2J_{\text{HH}} = 13.5$, $^3J_{\text{HH}} = 8.9$ Hz, 1H). ^{13}C NMR (75 MHz, CDCl_3): $\delta = 172.2$, 163.9, 137.5, 135.6, 131.2, 129.9, 128.6, 128.6, 128.4, 126.7, 75.2, 52.4, 39.9.

Methyl (S)-2,5-bis((benzylidene)amino)pentanoate (1k).

1.530 g (7.00 mmol, 1.0 eq) L-Ornithine methyl ester dihydrochloride, 1.42 mL (13.93 mmol, 1.99 eq) benzaldehyde, 2.13 mL (15.4 mmol, 2.2 eq) triethylamine and 7 mL CHCl_3 . Yield: 2.2136 g (6.87 mmol, 98%), yellow viscous oil. $^1\text{H-NMR}$ (300 MHz, CDCl_3): $\delta = 7.68$ -7.56 (m, 4H), 7.47-7.29 (m, 12H), 7.20-7.08 (m, 4H), 4.10 (dd, $^3J_{\text{HH}} = 8.0$ Hz, $^3J_{\text{HH}} = 5.2$ Hz, 1H), 3.71 (s, 3H), 3.33 (t, $^3J_{\text{HH}} = 6.8$ Hz, 2H), 2.07-1.88 (m, 2H), 1.79-1.54 (m, 2H).

REFERENCES

References

1. Raddatz, N.; Castillo, J. P.; Gonzalez, C.; Alvarez, O.; Latorre, R., Temperature and voltage coupling to channel opening in transient receptor potential melastatin 8 (TRPM8). *The Journal of biological chemistry* **2014**, 289 (51), 35438-54.
2. Phelps, C. B.; Gaudet, R., The role of the N terminus and transmembrane domain of TRPM8 in channel localization and tetramerization. *The Journal of biological chemistry* **2007**, 282 (50), 36474-80.
3. Nilius, B.; Owsianik, G., The transient receptor potential family of ion channels. *Genome biology* **2011**, 12 (3), 218.
4. Vay, L.; Gu, C.; McNaughton, P. A., The thermo-TRP ion channel family: properties and therapeutic implications. *British journal of pharmacology* **2012**, 165 (4), 787-801.
5. Venkatachalam, K.; Montell, C., TRP channels. *Annual review of biochemistry* **2007**, 76, 387-417.
6. Gees, M.; Colosoul, B.; Nilius, B., The role of transient receptor potential cation channels in Ca²⁺ signaling. *Cold Spring Harbor perspectives in biology* **2010**, 2 (10), a003962.
7. Tominaga, M., The Role of TRP Channels in Thermosensation. In *TRP Ion Channel Function in Sensory Transduction and Cellular Signaling Cascades*, Eds. Boca Raton (FL), 2007.
8. Patapoutian, A., TRP channels and thermosensation. *Chemical senses* **2005**, 30 Suppl 1, 193-4.
9. Voets, T., TRP channels and thermosensation. *Handbook of experimental pharmacology* **2014**, 223, 729-41.
10. Talavera, K.; Yasumatsu, K.; Voets, T.; Droogmans, G.; Shigemura, N.; Ninomiya, Y.; Margolskee, R. F.; Nilius, B., Heat activation of TRPM5 underlies thermal sensitivity of sweet taste. *Nature* **2005**, 438 (7070), 1022-5.
11. Caterina, M. J., Transient receptor potential ion channels as participants in thermosensation and thermoregulation. *American Journal of Physiology-Regulatory, Integrative and Comparative Physiology* **2007**, 292 (1), R64-R76.

12. Brauchi, S.; Orio, P.; Latorre, R., Clues to understanding cold sensation: Thermodynamics and electrophysiological analysis of the cold receptor TRPM8. *Proceedings of the National Academy of Sciences of the United States of America* **2004**, *101* (43), 15494-15499.
13. Voets, T.; Droogmans, G.; Wissenbach, U.; Janssens, A.; Flockerzi, V.; Nilius, B., The principle of temperature-dependent gating in cold- and heat-sensitive TRP channels. *Nature* **2004**, *430* (7001), 748-754.
14. Zhang, L.; Barritt, G. J., TRPM8 in prostate cancer cells: a potential diagnostic and prognostic marker with a secretory function? *Endocrine-related cancer* **2006**, *13* (1), 27-38.
15. Peier, A. M.; Moqrich, A.; Hergarden, A. C.; Reeve, A. J.; Andersson, D. A.; Story, G. M.; Earley, T. J.; Dragoni, I.; McIntyre, P.; Bevan, S.; Patapoutian, A., A TRP channel that senses cold stimuli and menthol. *Cell* **2002**, *108* (5), 705-715.
16. Latorre, R.; Brauchi, S.; Madrid, R.; Orio, P., A Cool Channel in Cold Transduction. *Physiology* **2011**, *26* (4), 273-285.
17. Phelps, C. B.; Gaudet, R., The role of the N terminus and transmembrane domain of TRPM8 in channel localization and tetramerization. *Journal of Biological Chemistry* **2007**, *282* (50), 36474-36480.
18. Pedretti, A.; Marconi, C.; Bettinelli, I.; Vistoli, G., Comparative modeling of the quaternary structure for the human TRPM8 channel and analysis of its binding features. *Bba-Biomembranes* **2009**, *1788* (5), 973-982.
19. Zhang, L.; Barritt, G. J., TRPM8 in prostate cancer cells: a potential diagnostic and prognostic marker with a secretory function? *Endocrine-related cancer* **2006**, *13* (1), 27-38.
20. Kobayashi, K.; Fukuoka, T.; Obata, K.; Yamanaka, H.; Dai, Y.; Tokunaga, A.; Noguchi, K., Distinct expression of TRPM8, TRPA1, and TRPV1 mRNAs in rat primary afferent neurons with delta/c-fibers and colocalization with trk receptors. *The Journal of comparative neurology* **2005**, *493* (4), 596-606.
21. Yamamura, H.; Ugawa, S.; Ueda, T.; Morita, A.; Shimada, S., TRPM8 activation suppresses cellular viability in human melanoma. *American Journal of Physiology-Cell Physiology* **2008**, *295* (2), C296-C301.

22. Ouadid-Ahidouch, H.; Dhennin-Duthille, I.; Gautier, M.; Sevestre, H.; Ahidouch, A., TRP calcium channel and breast cancer: expression, role and correlation with clinical parameters. *Breast Cancer* **2012**, *99* (6), 655-664.
23. Valero, M. L.; Mello de Queiroz, F.; Stuhmer, W.; Viana, F.; Pardo, L. A., TRPM8 ion channels differentially modulate proliferation and cell cycle distribution of normal and cancer prostate cells. *PloS one* **2012**, *7* (12), e51825.
24. Henshall, S. M.; Afar, D. E. H.; Hiller, J.; Horvath, L. G.; Quinn, D. I.; Rasiah, K. K.; Gish, K.; Willhite, D.; Kench, J. G.; Gardiner-Garden, M.; Stricker, P. D.; Scher, H. I.; Grygiel, J. J.; Agus, D. B.; Mack, D. H.; Sutherland, R. L., Survival analysis of genome-wide gene expression profiles of prostate cancers identifies new prognostic targets of disease relapse. *Cancer Research* **2003**, *63* (14), 4196-4203.
25. Zhang, L.; Barritt, G. J., Evidence that TRPM8 is an androgen-dependent Ca²⁺ channel required for the survival of prostate cancer cells. *Cancer Research* **2004**, *64* (22), 8365-8373.
26. Bidaux, G.; Flourakis, M.; Thebault, S.; Zholos, A.; Beck, B.; Gkika, D.; Roudbaraki, M.; Bonnal, J. L.; Mauroy, B.; Shuba, Y.; Skryma, R.; Prevarskaya, N., Prostate cell differentiation status determines transient receptor potential melastatin member 8 channel subcellular localization and function. *The Journal of Clinical Investigation* **2007**, *117* (6), 1647-1657.
27. Morgentaler, A., Testosterone and prostate cancer: An historical perspective on a modern myth. *European Urology* **2006**, *50* (5), 935-939.
28. Asuthkar, S.; Elustondo, P. A.; Demirkhanyan, L.; Sun, X.; Baskaran, P.; Velpula, K. K.; Thyagarajan, B.; Pavlov, E. V.; Zakharian, E., The TRPM8 Protein Is a Testosterone Receptor I. Biochemical evidence for direct TRPM8-testosterone interactions. *Journal of Biological Chemistry* **2015**, *290* (5), 2659-2669.
29. (a) Siegel, R. E., Galen on Sense Perception: His Doctrines, Observations and Experiments on Vision, Hearing, Smell, Taste, Touch and Pain, and Their Historical Sources. *Karger* **1970**; (b) Proudfoot, C. J.; Garry, E. M.; Cottrell, D. F.; Rosie, R.; Anderson, H.; Robertson, D. C.; Fleetwood-Walker, S. M.;

- Mitchell, R., Analgesia mediated by the TRPM8 cold receptor in chronic neuropathic pain. *Current biology* **2006**, *16* (16), 1591-605.
30. (a) Wright, A., Oil of peppermint as a local anaesthetic. *Lancet* **1870**, *2464*; (b) Bini, G.; Cruccu, G.; Hagbarth, K. E.; Schady, W.; Torebjork, E., Analgesic effect of vibration and cooling on pain induced by intraneural electrical stimulation. *Pain* **1984**, *18* (3), 239-48.
31. Sauls, J., Efficacy of cold for pain: fact or fallacy? *The Online Journal of Knowledge Synthesis for Nursing* **1999**, *6*, 8.
32. Caterina, M. J.; Leffler, A.; Malmberg, A. B.; Martin, W. J.; Trafton, J.; Petersen-Zeitz, K. R.; Koltzenburg, M.; Basbaum, A. I.; Julius, D., Impaired nociception and pain sensation in mice lacking the capsaicin receptor. *Science* **2000**, *288* (5464), 306-313.
33. Caspani, O.; Zurborg, S.; Labuz, D.; Heppenstall, P. A., The Contribution of TRPM8 and TRPA1 Channels to Cold Allodynia and Neuropathic Pain. *PloS one* **2009**, *4* (10).
34. Andersson, D. A.; Chase, H. W. N.; Bevan, S., TRPM8 activation by menthol, icilin, and cold is differentially modulated by intracellular pH. *Journal of Neuroscience* **2004**, *24* (23), 5364-5369.
35. Xing, H.; Chen, M.; Ling, J.; Tan, W. H.; Gu, J. G. G., TRPM8 mechanism of cold allodynia after chronic nerve injury. *Journal of Neuroscience* **2007**, *27* (50), 13680-13690.
36. Premkumar, L. S.; Raisinghani, M.; Pingle, S. C.; Long, C.; Pimentel, F., Downregulation of transient receptor potential melastatin 8 by protein kinase C-mediated dephosphorylation. *Journal of Neuroscience* **2005**, *25* (49), 11322-11329.
37. Su, L.; Wang, C.; Yu, Y. H.; Ren, Y. Y.; Xie, K. L.; Wang, G. L., Role of TRPM8 in dorsal root ganglion in nerve injury-induced chronic pain. *BMC Neuroscience* **2011**, *12*.
38. Tsukimi, Y.; Mizuyachi, K.; Yamasaki, T.; Niki, T.; Hayashi, F., Cold response of the bladder in guinea pig: Involvement of transient receptor potential channel, TRPM8. *Urology* **2005**, *65* (2), 406-410.

39. Stein, R. J.; Santos, S.; Nagatomi, J.; Hayashi, Y.; Minnery, B. S.; Xavier, M.; Patel, A. S.; Nelson, J. B.; Futrell, W. J.; Yoshimura, N.; Chancellor, M. B.; De Miguel, F., Cool (TRPM8) and hot (TRPV1) receptors in the bladder and male genital tract. *Journal of Urology* **2004**, *172* (3), 1175-1178.
40. Kanai, A.; Andersson, K. E., Bladder Afferent Signaling: Recent Findings. *Journal of Urology* **2010**, *183* (4), 1288-1295.
41. Andersson, K. E.; Gratzke, C.; Hedlund, P., The role of the transient receptor potential (TRP) superfamily of cation-selective channels in the management of the overactive bladder. *BJU International* **2010**, *106* (8), 1114-1127.
42. Liu, B. Y.; Qin, F., Functional control of cold- and menthol-sensitive TRPM8 ion channels by phosphatidylinositol 4,5-bisphosphate. *Journal of Neuroscience* **2005**, *25* (7), 1674-1681.
43. Andersson, D. A., Modulation of the Cold-Activated Channel TRPM8 by Lysophospholipids and Polyunsaturated Fatty Acids. *The Journal of Neuroscience*, **2007**, *27* (12), 3347-3355
44. McKemy, D. D., TRPM8: The Cold and Menthol Receptor. In *TRP Ion Channel Function in Sensory Transduction and Cellular Signaling Cascades*, Liedtke, W. B.; Heller, S., Eds. Boca Raton (FL), 2007.
45. McKemy, D. D., Therapeutic Potential of TRPM8 Modulators. *The Open Drug Discovery Journal* **2010**, *2*, 81-88.
46. Chuang, H. H.; Neuhauser, W. M.; Julius, D., The super-cooling agent icilin reveals a mechanism of coincidence detection by a temperature-sensitive TRP channel. *Neuron* **2004**, *43* (6), 859-869.
47. Yang, F.; Vu, S.; Yarov-Yarovoy, V.; Zheng, J., Rational design and validation of a vanilloid-sensitive TRPV2 ion channel. *Proceedings of the National Academy of Sciences of the United States of America* **2016**, *113* (26), E3657-E3666.
48. Premkumar, L. S.; Raisinghani, M.; Pingle, S. C.; Long, C.; Pimentel, F., Downregulation of transient receptor potential melastatin 8 by protein kinase C-mediated dephosphorylation. *Journal of Neuroscience* **2005**, *25* (49), 11322-9.

49. Zhang, X.; Mak, S.; Li, L.; Parra, A.; Denlinger, B.; Belmonte, C.; McNaughton, P. A., Direct inhibition of the cold-activated TRPM8 ion channel by Galphag. *Nature cell biology* **2012**, *14* (8), 851-8.
50. Weil, A.; Moore, S. E.; Waite, N. J.; Randall, A.; Gunthorpe, M. J., Conservation of functional and pharmacological properties in the distantly related temperature sensors TRPV1 and TRPM8. *Molecular pharmacology* **2005**, *68* (2), 518-27.
51. Meseguer, V.; Karashima, Y.; Talavera, K.; D'Hoedt, D.; Donovan-Rodriguez, T.; Viana, F.; Nilius, B.; Voets, T., Transient receptor potential channels in sensory neurons are targets of the antimycotic agent clotrimazole. *Journal of Neuroscience* **2008**, *28* (3), 576-86.
52. Schwarz, G.; Droogmans, G.; Nilius, B., Multiple effects of SK&F 96365 on ionic currents and intracellular calcium in human endothelial cells. *Cell calcium* **1994**, *15* (1), 45-54.
53. DeFalco, J.; Steiger, D.; Dourado, M.; Emerling, D.; Duncton, M. A. J., 5-Benzyloxytryptamine as an antagonist of TRPM8. *Bioorganic Medicinal & Chemistry Letters* **2010**, *20* (23), 7076-7079.
54. Benedikt, J.; Teisinger, J.; Vyklicky, L.; Vlachova, V., Ethanol inhibits cold-menthol receptor TRPM8 by modulating its interaction with membrane phosphatidylinositol 4,5-bisphosphate. *Journal of Neurochemistry* **2007**, *100* (1), 211-224.
55. Journigan, V. B.; Zaveri, N. T., TRPM8 ion channel ligands for new therapeutic applications and as probes to study menthol pharmacology. *Life Sciences* **2013**, *92* (8-9), 425-437.
56. Knowlton, W. M.; Daniels, R. L.; Palkar, R.; McCoy, D. D.; McKemy, D. D., Pharmacological Blockade of TRPM8 Ion Channels Alters Cold and Cold Pain Responses in Mice. *PloS one* **2011**, *6* (9).
57. Than, J., Excitation and modulation of TRPA1, TRPV1, and TRPM8 channel-expressing sensory neurons by the pruritogen chloroquine. *Journal of Biological Chemistry* **2013**, *288*, 12818–12827.
58. Terada, Y.; Kitajima, M.; Taguchi, F.; Takayama, H.; Horie, S.; Watanabe, T., Identification of Indole Alkaloid Structural Units Important for

Stimulus-Selective TRPM8 Inhibition: SAR Study of Naturally Occurring Iboga Derivatives. *Journal of Natural Products* **2014**, *77* (8), 1831-8.

59. Bharate, S. S.; Bharate, S. B., Modulation of Thermoreceptor TRPM8 by Cooling Compounds. *ACS Chemical Neuroscience* **2012**, *3* (4), 248-267.

60. Ostacolo, C.; Ambrosino, P.; Russo, R.; Lo Monte, M.; Soldovieri, M. V.; Laneri, S.; Sacchi, A.; Vistoli, G.; Tagliatela, M.; Calignano, A., Isoxazole derivatives as potent transient receptor potential melastatin type 8 (TRPM8) agonists. *European Journal of Medicinal Chemistry* **2013**, *69*, 659-669.

61. Bertamino, A., Tryptamine-Based Derivatives as Transient Receptor Potential Melastatin Type 8 (TRPM8) Channel Modulators. *Journal of Medicinal Chemistry* **2016**, *59* (5), 2179–2191.

62. Bautista, D. M.; Siemens, J.; Glazer, J. M.; Tsuruda, P. R.; Basbaum, A. I.; Stucky, C. L.; Jordt, S. E.; Julius, D., The menthol receptor TRPM8 is the principal detector of environmental cold. *Nature* **2007**, *448* (7150), 204-208.

63. Lashinger, E. S.; Steingina, M. S.; Hieble, J. P.; Leon, L. A.; Gardner, S. D.; Nagilla, R.; Davenport, E. A.; Hoffman, B. E.; Laping, N. J.; Su, X., AMTB, a TRPM8 channel blocker: evidence in rats for activity in overactive bladder and painful bladder syndrome. *American Journal of Physiology. Renal physiology* **2008**, *295* (3), F803-10.

64. Caterina, M. J.; Leffler, A.; Malmberg, A. B.; Martin, W. J.; Trafton, J.; Petersen-Zeitz, K. R.; Koltzenburg, M.; Basbaum, A. I.; Julius, D., Impaired nociception and pain sensation in mice lacking the capsaicin receptor. *Science* **2000**, *288* (5464), 306-13.

65. Davis, J. B.; Gray, J.; Gunthorpe, M. J.; Hatcher, J. P.; Davey, P. T.; Overend, P.; Harries, M. H.; Latcham, J.; Clapham, C.; Atkinson, K.; Hughes, S. A.; Rance, K.; Grau, E.; Harper, A. J.; Pugh, P. L.; Rogers, D. C.; Bingham, S.; Randall, A.; Sheardown, S. A., Vanilloid receptor-1 is essential for inflammatory thermal hyperalgesia. *Nature* **2000**, *405* (6783), 183-187.

66. Kwan, K. Y., TRPA1 contributes to cold, mechanical, and chemical nociception but is not essential for hair-cell transduction. *Neuron* **2006**, *50* (2), 277-89.

67. McKemy, D. D.; Neuhauser, W. M.; Julius, D., Identification of a cold receptor reveals a general role for TRP channels in thermosensation. *Nature* **2002**, *416* (6876), 52-8.
68. Behrendt, H. J.; Germann, T.; Gillen, C.; Hatt, H.; Jostock, R., Characterization of the mouse cold-menthol receptor TRPM8 and vanilloid receptor type-1 VR1 using a fluorometric imaging plate reader (FLIPR) assay. *British Journal of Pharmacology* **2004**, *141* (4), 737-745.
69. Malkia, A.; Madrid, R.; Meseguer, V.; de la Pena, E.; Valero, M.; Belmonte, C.; Viana, F., Bidirectional shifts of TRPM8 channel gating by temperature and chemical agents modulate the cold sensitivity of mammalian thermoreceptors. *The Journal Of Physiology* **2007**, *581* (1), 155-174.
70. Schrödinger, SiteMap. **2015**.
71. Taberner, F. J.; Lopez-Cordoba, A.; Fernandez-Ballester, G.; Korchev, Y.; Ferrer-Montiel, A., The Region Adjacent to the C-end of the Inner Gate in Transient Receptor Potential Melastatin 8 (TRPM8) Channels Plays a Central Role in Allosteric Channel Activation. *Journal of Biological Chemistry* **2014**, *289* (41), 28579-28594.
72. De Petrocellis, L.; Arroyo, F. J.; Orlando, P.; Moriello, A. S.; Vitale, R. M.; Amodeo, P.; Sanchez, A.; Roncero, C.; Bianchini, G.; Martin, M. A.; Lopez-Alvarado, P.; Menendez, J. C., Tetrahydroisoquinoline-Derived Urea and 2,5-Diketopiperazine Derivatives as Selective Antagonists of the Transient Receptor Potential Melastatin 8 (TRPM8) Channel Receptor and Antiprostata Cancer Agents (vol 59, pg 5661, 2016). *Journal of Medicinal Chemistry* **2016**, *59* (16), 7697-7697.
73. Cox, E. D.; Cook, J. M., The Pictet-Spengler Condensation - a New Direction for an Old Reaction. *Chemical Reviews* **1995**, *95* (6), 1797-1842.
74. Gomez-Monterrey, I. M., Synthesis of Novel Indole-Based Ring Systems by Acid-Catalysed Condensation from α -Amino Aldehydes and L-Trp-OMe. *European Journal of Organic Chemistry* **2008**, 1983-1992.
75. Ambrosino, P., Functional and biochemical interaction between PPAR α receptors and TRPV1 channels: Potential role in PPAR α agonists-mediated analgesia. *Pharmacological Research* **2014**, *87*, 113-122.

76. Sastry, G. M.; Adzhigirey, M.; Day, T.; Annabhimoju, R.; Sherman, W., Protein and ligand preparation: parameters, protocols, and influence on virtual screening enrichments. *Journal of Computational-Aided Molecules Design* **2013**, *27* (3), 221-234.
77. Schrödinger, Protein Preparation Wizard. **2015**.
78. Schrödinger, Epik. **2015**.
79. Schrödinger, Maestro. **2015**.
80. Schrödinger, LigPrep. **2015**.
81. Bowers, K. J., Scalable algorithms for molecular dynamics simulations on commodity clusters. *Proceedings of ACM/IEEE Supercomputing Conference* **2006**.
82. (a) Crich, D.; Banerjee, A., Chemistry of the Hexahydropyrrolo[2,3-b]indoles: configuration, conformation, reactivity, and applications in synthesis. *Accounts of Chemical Research* **2007**, *40* (2), 151-61; (b) Decker, M., Novel inhibitors of acetyl- and butyrylcholinesterase derived from the alkaloids dehydroevodiamine and rutaecarpine. *European Journal of Medicinal Chemistry* **2005**, *40* (3), 305-13; (c) Dong, G.; Sheng, C.; Wang, S.; Miao, Z.; Yao, J.; Zhang, W., Selection of evodiamine as a novel topoisomerase I inhibitor by structure-based virtual screening and hit optimization of evodiamine derivatives as antitumor agents. *Journal of Medicinal Chemistry* **2010**, *53* (21), 7521-31; (d) Dong, G.; Wang, S.; Miao, Z.; Yao, J.; Zhang, Y.; Guo, Z.; Zhang, W.; Sheng, C., New tricks for an old natural product: discovery of highly potent evodiamine derivatives as novel antitumor agents by systemic structure-activity relationship analysis and biological evaluations. *Journal of Medicinal Chemistry* **2012**, *55* (17), 7593-613; (e) Dounay, A. B.; Humphreys, P. G.; Overman, L. E.; Wroblewski, A. D., Total synthesis of the strychnos alkaloid (+)-minfiensine: tandem enantioselective intramolecular Heck-iminium ion cyclization. *Journal of American Chemical Society* **2008**, *130* (15), 5368-77; (f) Hajicek, J.; Taimr, J.; BudAsinsky, M., Revised structure of isoschizogamine. *Tetrahedron Letters* **1998**, *39* (5-6), 505-508; (g) Movassaghi, M.; Schmidt, M. A., Concise total synthesis of (-)-calycanthine, (+)-chimonanthine, and (+)-folicanthine. *Angewandte Chemie International Edition English* **2007**, *46* (20), 3725-8; (h)

Peters, L.; Konig, G. M.; Terlau, H.; Wright, A. D., Four new bromotryptamine derivatives from the marine bryozoan *Flustra foliacea*. *Journal of Natural Products* **2002**, *65* (11), 1633-7; (i) Snider, B. B.; Zeng, H., Total syntheses of (-)-fumiquinazolines A, B, and I. *Organic Letters* **2000**, *2* (25), 4103-6; (j) Zhang, M.; Huang, X.; Shen, L.; Qin, Y., Total synthesis of the akuammiline alkaloid (+/-)-vincorine. *Journal of American Chemical Society* **2009**, *131* (16), 6013-20.

83. Peters, L.; Konig, G. M.; Terlau, H.; Wright, A. D., Four new bromotryptamine derivatives from the marine bryozoan *Flustra foliacea*. *Journal of Natural Products* **2002**, *65* (11), 1633-1637.

84. Wu, P.; Nielsen, T. E., Scaffold Diversity from N-Acyliminium Ions. *Chemical Reviews* **2017**, *117* (12), 7811-7856.

85. (a) Nielsen, T. E.; Le Quement, S.; Meldal, M., Solid-phase synthesis of bicyclic dipeptide mimetics by intramolecular cyclization of alcohols, thiols, amines, and amides with N-acyliminium intermediates. *Organic Letters* **2005**, *7* (17), 3601-3604; (b) Yamashita, T.; Kawai, N.; Tokuyama, H.; Fukuyama, T., Stereocontrolled total synthesis of (-)-Eudistomin C. *Journal of the American Chemical Society* **2005**, *127* (43), 15038-15039.

86. (a) Campos, K. R., Direct sp³ C-H bond activation adjacent to nitrogen in heterocycles. *Chemical Society Reviews* **2007**, *36* (7), 1069-84; (b) Che, X.; Zheng, L. Y.; Dang, Q.; Bai, X., Synthesis of 7,8,9-trisubstituted dihydropurine derivatives via a 'tert-Amino Effect' cyclization. *Synlett* **2008**, (15), 2373-2375; (c) Dieckmann, A.; Richers, M. T.; Platonova, A. Y.; Zhang, C.; Seidel, D.; Houk, K. N., Metal-Free alpha-Amination of Secondary Amines: Computational and Experimental Evidence for Azaquinone Methide and Azomethine Ylide Intermediates. *Journal of Organic Chemistry* **2013**, *78* (8), 4132-4144; (d) Doye, S., Catalytic C-H activation of sp(3) C-H bonds in alpha-position to a nitrogen atom - Two new approaches. *Angewandte Chemie- International Edition* **2001**, *40* (18), 3351-+; (e) Kim, J. T.; Gevorgyan, V., Double cycloisomerization as a novel and expeditious route to tricyclic heteroaromatic compounds: short and highly diastereoselective synthesis of (+/-)-tetraponerine T6. *Organic Letters* **2002**, *4* (26), 4697-9; (f) Matyus, P.; Elias, O.; Tapolcsanyi, P.; Polonka-Balint, A.; Halasz-Dajka, B., Ring-closure reactions of ortho-vinyl-tert-anilines and

(Di)aza-heterocyclic analogues via the tert-amino effect: Recent developments. *Synthesis-Stuttgart* **2006**, (16), 2625-2639; (g) Mergott, D. J.; Zuend, S. J.; Jacobsen, E. N., Catalytic asymmetric total synthesis of (+)-yohimbine. *Organic Letters* **2008**, *10* (5), 745-748; (h) Meth-Cohn, O.; Naqui, M. A., A ready synthesis of dihydrobenzimidazoles. *Chemical Communications (London)* **1967**, (22), 1157; (i) Mitchell, E. A.; Peschiulli, A.; Lefevre, N.; Meerpoel, L.; Maes, B. U. W., Direct alpha-Functionalization of Saturated Cyclic Amines. *Chemical European Journal* **2012**, *18* (33), 10092-10142; (j) Murahashi, S.; Zhang, D., Ruthenium catalyzed biomimetic oxidation in organic synthesis inspired by cytochrome P-450. *Chemical Society Reviews* **2008**, *37* (8), 1490-501; (k) Murahashi, S. I., Synthetic Aspects of Metal-Catalyzed Oxidations of Amines and Related Reactions. *Angewandte Chemie-International Edition in English* **1995**, *34* (22), 2443-2465; (l) Richers, M. T.; Deb, I.; Platonova, A. Y.; Zhang, C.; Seidel, D., Facile Access to Ring-Fused Aminals via Direct alpha-Amination of Secondary Amines with o-Aminobenzaldehydes: Synthesis of Vasicine, Deoxyvasicine, Deoxyvasicinone, Mackinazolinone, and Ruteacarpine. *Synthesis-Stuttgart* **2013**, *45* (13), 1730-1748; (m) Rowland, G. B.; Zhang, H.; Rowland, E. B.; Chennamadhavuni, S.; Wang, Y.; Antilla, J. C., Bronsted acid-catalyzed imine amidation. *Journal of American Chemical Society* **2005**, *127* (45), 15696-7; (n) Seidel, D., The Azomethine Ylide Route to Amine C-H Functionalization: Redox-Versions of Classic Reactions and a Pathway to New Transformations. *Accounts Chemical Research* **2015**, *48* (2), 317-328; (o) Simon, J.; Salzbrunn, S.; Prakash, G. K.; Petasis, N. A.; Olah, G. A., Regioselective conversion of arylboronic acids to phenols and subsequent coupling to symmetrical diaryl ethers. *Journal of Organic Chemistry* **2001**, *66* (2), 633-4; (p) Verboom, W.; Hamzink, M. R. J.; Reinhoudt, D. N.; Visser, R., Novel applications of the "t-amino effect" in heterocyclic chemistry. Synthesis of a pyrrolo[1,2-a]quinazoline and 5H-pyrrolo[1,2-a][3,1]benzothiazines. *Tetrahedron Letters* **1984**, *25* (38), 4309-4312; (q) Wendlandt, A. E.; Suess, A. M.; Stahl, S. S., Copper-Catalyzed Aerobic Oxidative C-H Functionalizations: Trends and Mechanistic Insights. *Angewandte Chemie- International Edition* **2011**, *50* (47), 11062-11087; (r) Yang, J.; Xie, X. G.; Wang, Z. S.; Mei, R. M.; Zheng, H. J.; Wang, X. L.; Zhang, L.; Qi, J.; She, X.

- G., Stereoselective Synthesis of Fused Spiroindolines via Tandem Mannich/Intramolecular Amino Formation. *Journal of Organic Chemistry* **2013**, 78 (3), 1230-1235; (s) Zhang, C.; De, C. K.; Mal, R.; Seidel, D., alpha-amination of nitrogen heterocycles: Ring-fused amins. *Journal of the American Chemical Society* **2008**, 130 (2), 416-+; (t) Zhang, C.; Murarka, S.; Seidel, D., Facile Formation of Cyclic Amins through a Bronsted Acid-Promoted Redox Process. *Journal of Organic Chemistry* **2009**, 74 (1), 419-422; (u) Zhang, Y.; Fu, H.; Jiang, Y.; Zhao, Y., Copper-catalyzed amidation of sp³ C-H bonds adjacent to a nitrogen atom. *Organic Letters* **2007**, 9 (19), 3813-6.
87. Bertamino, A., Ring-Fused Cyclic Amins from Tetrahydro-β-carboline-Based Dipeptide Compounds. *Journal of Organic Chemistry* **2017**, 82 (23), 12014-12027.
88. (a) Li, Z.; Li, C. J., CuBr-catalyzed direct indolation of tetrahydroisoquinolines via cross-dehydrogenative coupling between sp³ C-H and sp² C-H bonds. *Journal of American Chemical Society* **2005**, 127 (19), 6968-9; (b) Sun, M.; Zhang, T.; Bao, W., FeCl₃ catalyzed sp³ C-H amination: synthesis of amins with arylamines and amides. *Tetrahedron Letters* **2014**, 55 (4), 893-896.
89. Maryanoff, B. E.; Zhang, H. C.; Cohen, J. H.; Turchi, I. J.; Maryanoff, C. A., Cyclizations of N-acyliminium ions. *Chemical Reviews* **2004**, 104 (3), 1431-628.
90. Nadmid, S.; Plaza, A.; Lauro, G.; Garcia, R.; Bifulco, G.; Muller, R., Hyalachelins A-C, Unusual Siderophores Isolated from the Terrestrial Myxobacterium *Hyalangium minutum*. *Organic Letters* **2014**, 16 (16), 4130-4133.
91. Vyawahare, N. S.; Hadambar, A. A.; Chothe, A. S.; Jalnapurkar, R. R.; Bhandare, A. M.; Kathiravan, M. K., Effect of novel synthetic evodiamine analogue on sexual behavior in male rats. *Journal of Chemical Biology* **2012**, 5 (1), 35-42.
92. De Petrocellis, L.; Schiano Moriello, A.; Fontana, G.; Sacchetti, A.; Passarella, D.; Appendino, G.; Di Marzo, V., Effect of chirality and lipophilicity in the functional activity of evodiamine and its analogues at TRPV1 channels. *British Journal of Pharmacology* **2014**, 171 (10), 2608-20.

93. Bertamino, A.; Ostacolo, C.; Ambrosino, P.; Musella, S.; Di Sarno, V.; Ciaglia, T.; Soldovieri, M. V.; Iraci, N.; Fernandez Carvajal, A.; de la Torre-Martinez, R.; Ferrer-Montiel, A.; Gonzalez Muniz, R.; Novellino, E.; Tagliatela, M.; Campiglia, P.; Gomez-Monterrey, I., Tryptamine-Based Derivatives as Transient Receptor Potential Melastatin Type 8 (TRPM8) Channel Modulators. *Journal of Medicinal Chemistry* **2016**, *59* (5), 2179-91.
94. (a) Lauro, G.; Manfra, M.; Pedatella, S.; Fischer, K.; Cantone, V.; Terracciano, S.; Bertamino, A.; Ostacolo, C.; Gomez-Monterrey, I.; De Nisco, M.; Riccio, R.; Novellino, E.; Werz, O.; Campiglia, P.; Bifulco, G., Identification of novel microsomal prostaglandin E2 synthase-1 (mPGES-1) lead inhibitors from Fragment Virtual Screening. *European Journal of Medicinal Chemistry* **2017**, *125*, 278-287; (b) Lauro, G.; Tortorella, P.; Bertamino, A.; Ostacolo, C.; Koeberle, A.; Fischer, K.; Bruno, I.; Terracciano, S.; Gomez-Monterrey, I. M.; Tauro, M.; Loiodice, F.; Novellino, E.; Riccio, R.; Werz, O.; Campiglia, P.; Bifulco, G., Structure-Based Design of Microsomal Prostaglandin E2 Synthase-1 (mPGES-1) Inhibitors using a Virtual Fragment Growing Optimization Scheme. *ChemMedChem* **2016**, *11* (6), 612-9.
95. Kumpaty, H. J.; Van Linn, M. L.; Kabir, M. S.; Forsterling, F. H.; Deschamps, J. R.; Cook, J. A., Study of the Cis to Trans Isomerization of 1-Phenyl-2,3-disubstituted Tetrahydro-beta-carbolines at C(1). Evidence for the Carbocation-Mediated Mechanism. *J. Org. Chem.* **2009**, *74* (7), 2771-2779.
96. Maestro, , *version 9.6, Schrödinger, LLC, New York, NY, 2013*.
97. Jorgensen, W. L.; Tirado-Rives, J., The OPLS [optimized potentials for liquid simulations] potential functions for proteins, energy minimizations for crystals of cyclic peptides and crambin. *Journal of American Chemical Society* **1988**, *110* (6), 1657-66.
98. Frisch, M. J. T., G. W.; Schlegel, H. B.; Scuseria, G. E.; Robb, M. A.; Cheeseman, J. R.; Scalmani, G.; Barone, V.; Mennucci, B.; Petersson, G. A.; Nakatsuji, H.; Caricato, M.; Li, X.; Hratchian, H. P.; Izmaylov, A. F.; Bloino, J.; Zheng, G.; Sonnenberg, J. L.; Hada, M.; Ehara, M.; Toyota, K.; Fukuda, R.; Hasegawa, J.; Ishida, M.; Nakajima, T.; Honda, Y.; Kitao, O.; Nakai, H.; Vreven, T.; Montgomery, J. A., Jr.; Peralta, J. E.; Ogliaro, F.; Bearpark, M.; Heyd, J. J.;

Brothers, E.; Kudin, K. N.; Staroverov, V. N.; Kobayashi, R.; Normand, J.; Raghavachari, K.; Rendell, A.; Burant, J. C.; Iyengar, S. S.; Tomasi, J.; Cossi, M.; Rega, N.; Millam, J. M.; Klene, M.; Knox, J. E.; Cross, J. B.; Bakken, V.; Adamo, C.; Jaramillo, J.; Gomperts, R.; Stratmann, R. E.; Yazyev, O.; Austin, A. J.; Cammi, R.; Pomelli, C.; Ochterski, J. W.; Martin, R. L.; Morokuma, K.; Zakrzewski, V. G.; Voth, G. A.; Salvador, P.; Dannenberg, J. J.; Dapprich, S.; Daniels, A. D.; Farkas, Ö.; Foresman, J. B.; Ortiz, J. V.; Cioslowski, J.; Fox, D. J., *Gaussian 09, Revision A.02*, Gaussian, Inc., Wallingford CT, 2009.

99. (a) Sarotti, A. M.; Pellegrinet, S. C., A multi-standard approach for GIAO (13)C NMR calculations. *Journal of Organic Chemistry* **2009**, *74* (19), 7254-60;

(b) Sarotti, A. M.; Pellegrinet, S. C., Application of the multi-standard methodology for calculating ¹H NMR chemical shifts. *Journal of Organic Chemistry* **2012**, *77* (14), 6059-65.

100. (a) Schrödinger, LLC New York NY **2013**; (b) Halgren, T. A.; Murphy, R. B.; Friesner, R. A.; Beard, H. S.; Frye, L. L.; Pollard, W. T.; Banks, J. L., Glide: A new approach for rapid, accurate docking and scoring. 2. Enrichment factors in database screening. *Journal of Medicinal Chemistry* **2004**, *47* (7), 1750-1759; (c) Friesner, R. A.; Banks, J. L.; Murphy, R. B.; Halgren, T. A.; Klicic, J. J.; Mainz, D. T.; Repasky, M. P.; Knoll, E. H.; Shelley, M.; Perry, J. K.; Shaw, D. E.; Francis, P.; Shenkin, P. S., Glide: a new approach for rapid, accurate docking and scoring. 1. Method and assessment of docking accuracy. *Journal of Medicinal Chemistry* **2004**, *47* (7), 1739-49; (d) Friesner, R. A.; Murphy, R. B.; Repasky, M. P.; Frye, L. L.; Greenwood, J. R.; Halgren, T. A.; Sanschagrin, P. C.; Mainz, D. T., Extra precision glide: docking and scoring incorporating a model of hydrophobic enclosure for protein-ligand complexes. *Journal of Medicinal Chemistry* **2006**, *49* (21), 6177-96.

101. Blair, W.; Cox, C., Current Landscape of Antiviral Drug Discovery. *F1000Research* **2016**, *5*.

102. Arvin, A. M., Varicella-zoster virus. *Clinical microbiology reviews* **1996**, *9* (3), 361-81.

103. Arvin, A. M.; Moffat, J. F.; Redman, R., Varicella-zoster virus: aspects of pathogenesis and host response to natural infection and varicella vaccine. *Advances in Virus Research* **1996**, *46*, 263-309.
104. Cohen, J. I.; Brunell, P. A.; Straus, S. E.; Krause, P. R., Recent advances in varicella-zoster virus infection. *Annals of Internal Medicine* **1999**, *130* (11), 922-32.
105. Myers, M. G.; Connelly, B. L., Animal models of varicella. *The Journal of Infectious Diseases* **1992**, *166 Suppl 1*, S48-50.
106. Bouhassira, D.; Chassany, O.; Gaillat, J.; Hanslik, T.; Launay, O.; Mann, C.; Rabaud, C.; Rogeaux, O.; Strady, C., Patient perspective on herpes zoster and its complications: an observational prospective study in patients aged over 50 years in general practice. *Pain* **2012**, *153* (2), 342-9.
107. Che, H.; Lukas, C.; Morel, J.; Combe, B., Risk of herpes/herpes zoster during anti-tumor necrosis factor therapy in patients with rheumatoid arthritis. Systematic review and meta-analysis. *Joint, bone, spine: revue du rhumatisme* **2014**, *81* (3), 215-21.
108. Tanuseputro, P.; Zagorski, B.; Chan, K. J.; Kwong, J. C., Population-based incidence of herpes zoster after introduction of a publicly funded varicella vaccination program. *Vaccine* **2011**, *29* (47), 8580-4.
109. Gonzalez Chiappe, S.; Sarazin, M.; Turbelin, C.; Lasserre, A.; Pelat, C.; Bonmarin, I.; Chosidow, O.; Blanchon, T.; Hanslik, T., Herpes zoster: Burden of disease in France. *Vaccine* **2010**, *28* (50), 7933-8.
110. Johnson, R. W.; Alvarez-Pasquin, M. J.; Bijl, M.; Franco, E.; Gaillat, J.; Clara, J. G.; Labetoulle, M.; Michel, J. P.; Naldi, L.; Sanmarti, L. S.; Weinke, T., Herpes zoster epidemiology, management, and disease and economic burden in Europe: a multidisciplinary perspective. *Therapeutic advances in vaccines* **2015**, *3* (4), 109-20.
111. Mueller, N. H.; Gilden, D. H.; Cohrs, R. J.; Mahalingam, R.; Nagel, M. A., Varicella zoster virus infection: clinical features, molecular pathogenesis of disease, and latency. *Neurologic clinics* **2008**, *26* (3), 675-97, viii.

112. Jeon, Y. H., Herpes Zoster and Postherpetic Neuralgia: Practical Consideration for Prevention and Treatment. *The Korean Journal of Pain* **2015**, 28 (3), 177-84.
113. Snoeck, R.; Andrei, G.; De Clercq, E., Current pharmacological approaches to the therapy of varicella zoster virus infections: a guide to treatment. *Drugs* **1999**, 57 (2), 187-206.
114. (a) Arvin, A.; Abendroth, A., VZV: immunobiology and host response. In *Human Herpesviruses: Biology, Therapy, and Immunoprophylaxis*, Arvin, A.; Campadelli-Fiume, G.; Mocarski, E.; Moore, P. S.; Roizman, B.; Whitley, R.; Yamanishi, K., Eds. Cambridge, 2007; (b) Moffat, J.; Ku, C. C.; Zerboni, L.; Sommer, M.; Arvin, A., VZV: pathogenesis and the disease consequences of primary infection. In *Human Herpesviruses: Biology, Therapy, and Immunoprophylaxis*, Arvin, A.; Campadelli-Fiume, G.; Mocarski, E.; Moore, P. S.; Roizman, B.; Whitley, R.; Yamanishi, K., Eds. Cambridge, 2007.
115. Rabasseda, X., Brivudine: a herpes virostatic with rapid antiviral activity and once-daily dosing. *Drugs of today* **2003**, 39 (5), 359-71.
116. Gilbert, C.; Bestman-Smith, J.; Boivin, G., Resistance of herpesviruses to antiviral drugs: clinical impacts and molecular mechanisms. *Drug resistance update: reviews and commentaries in antimicrobial and anticancer chemotherapy* **2002**, 5 (2), 88-114.
117. Sacks, S. L.; Wanklin, R. J.; Reece, D. E.; Hicks, K. A.; Tyler, K. L.; Coen, D. M., Progressive esophagitis from acyclovir-resistant herpes simplex. Clinical roles for DNA polymerase mutants and viral heterogeneity? *Annals of Internal Medicine* **1989**, 111 (11), 893-9.
118. Bacon, T. H.; Levin, M. J.; Leary, J. J.; Sarisky, R. T.; Sutton, D., Herpes simplex virus resistance to acyclovir and penciclovir after two decades of antiviral therapy. *Clinical Microbiology reviews* **2003**, 16 (1), 114-28.
119. Wagstaff, A. J., Foscarnet. A reappraisal of its antiviral activity, pharmacokinetic properties and therapeutic use in immunocompromised patients with viral infections. *Drugs* **1994**, 48 (2), 199-226.
120. Chono, K.; Katsumata, K.; Kontani, T.; Kobayashi, M.; Sudo, K.; Yokota, T.; Konno, K.; Shimizu, Y.; Suzuki, H., ASP2151, a novel helicase-primase

inhibitor, possesses antiviral activity against varicella-zoster virus and herpes simplex virus types 1 and 2. *The Journal of Antimicrobial Chemotherapy* **2010**, *65* (8), 1733-41.

121. (a) Gable, J. E.; Acker, T. M.; Craik, C. S., Current and potential treatments for ubiquitous but neglected herpesvirus infections. *Chemical Reviews* **2014**, *114* (22), 11382-412; (b) Schnute, M. E., 4-Oxo-4,7-dihydrothieno[2,3-b]pyridines as Non-Nucleoside Inhibitors of Human Cytomegalovirus and Related Herpesvirus Polymerases. *Journal of Medicinal Chemistry* **2005**, *48* (18), 5794–5804.

122. Welsch, M. E.; Snyder, S. A.; Stockwell, B. R., Privileged scaffolds for library design and drug discovery. *Current opinion in chemical biology* **2010**, *14* (3), 347-61.

123. Zhang, M. Z.; Chen, Q.; Yang, G. F., A review on recent developments of indole-containing antiviral agents. *European Journal of Medicinal Chemistry* **2015**, *89*, 421-41.

124. Aragay, A. M.; Ruiz-Gomez, A.; Penela, P.; Sarnago, S.; Elorza, A.; Jimenez-Sainz, M. C.; Mayor, F., Jr., G protein-coupled receptor kinase 2 (GRK2): mechanisms of regulation and physiological functions. *FEBS letters* **1998**, *430* (1-2), 37-40.

125. Palczewski, K., GTP-binding-protein-coupled receptor kinases--two mechanistic models. *European Journal of Biochemistry* **1997**, *248* (2), 261-9.

126. Bohm, S. K., Regulatory mechanisms that modulate signalling by G-protein-coupled receptors. *Biochemical Journal* **1997**, *322* (1), 1–18.

127. Pierce, K. L.; Premont, R. T.; Lefkowitz, R. J., Seven-transmembrane receptors. *Nature reviews. Molecular cell biology* **2002**, *3* (9), 639-50.

128. Zhang, D.; Zhao, Q.; Wu, B., Structural Studies of G Protein-Coupled Receptors. *Molecules and Cells* **2015**, *38* (10), 836-42.

129. Fredriksson, R.; Lagerstrom, M. C.; Lundin, L. G.; Schioth, H. B., The G-protein-coupled receptors in the human genome form five main families. Phylogenetic analysis, paralogon groups, and fingerprints. *Molecular Pharmacology* **2003**, *63* (6), 1256-72.

130. Kenakin, T., Drug efficacy at G protein-coupled receptors. *Annual Review of Pharmacology and Toxicology* **2002**, *49*, 349-79.
131. Marinissen, M. J.; Gutkind, J. S., G-protein-coupled receptors and signaling networks: emerging paradigms. *Trends in pharmacological sciences* **2001**, *22* (7), 368-76.
132. Gurevich, E. V., G protein-coupled receptor kinases: more than just kinases and not only for GPCRs. *Pharmacology & Therapeutics* **2012**, *133* (1), 40-69.
133. Siderovski, D. P.; Hessel, A.; Chung, S.; Mak, T. W.; Tyers, M., A new family of regulators of G-protein-coupled receptors? *Current biology* **1996**, *6* (2), 211-2.
134. Touhara, K.; Inglese, J.; Pitcher, J. A.; Shaw, G.; Lefkowitz, R. J., Binding of G protein beta gamma-subunits to pleckstrin homology domains. *The Journal of Biological Chemistry* **1994**, *269* (14), 10217-20.
135. Premont, R. T.; Gainetdinov, R. R., Physiological roles of G protein-coupled receptor kinases and arrestins. *Annual review of physiology* **2007**, *69*, 511-34.
136. Evron, T.; Daigle, T. L.; Caron, M. G., GRK2: multiple roles beyond G protein-coupled receptor desensitization. *Trends in pharmacological sciences* **2012**, *33* (3), 154-64.
137. Sterne-Marr, R.; Benovic, J. L., Regulation of G protein-coupled receptors by receptor kinases and arrestins. *Vitamins and hormones* **1995**, *51*, 193-234.
138. Penela, P.; Murga, C.; Ribas, C.; Tutor, A. S.; Peregrin, S.; Mayor, F., Jr., Mechanisms of regulation of G protein-coupled receptor kinases (GRKs) and cardiovascular disease. *Cardiovascular research* **2006**, *69* (1), 46-56.
139. Ungerer, M.; Bohm, M.; Elce, J. S.; Erdmann, E.; Lohse, M. J., Altered expression of beta-adrenergic receptor kinase and beta 1-adrenergic receptors in the failing human heart. *Circulation* **1993**, *87* (2), 454-63.
140. Ungerer, M.; Kessebohmer, K.; Kronsbein, K.; Lohse, M. J.; Richardt, G., Activation of beta-adrenergic receptor kinase during myocardial ischemia. *Circulation research* **1996**, *79* (3), 455-60.

141. Koch, W. J.; Rockman, H. A.; Samama, P.; Hamilton, R. A.; Bond, R. A.; Milano, C. A.; Lefkowitz, R. J., Cardiac function in mice overexpressing the beta-adrenergic receptor kinase or a beta ARK inhibitor. *Science* **1995**, *268* (5215), 1350-3.
142. Jaber, M.; Koch, W. J.; Rockman, H.; Smith, B.; Bond, R. A.; Sulik, K. K.; Ross, J., Jr.; Lefkowitz, R. J.; Caron, M. G.; Giros, B., Essential role of beta-adrenergic receptor kinase 1 in cardiac development and function. *Proceedings of the National Academy of Sciences of the United States of America* **1996**, *93* (23), 12974-9.
143. Oppermann, M.; Freedman, N. J.; Alexander, R. W.; Lefkowitz, R. J., Phosphorylation of the type 1A angiotensin II receptor by G protein-coupled receptor kinases and protein kinase C. *The Journal of biological chemistry* **1996**, *271* (22), 13266-72.
144. Eijkelkamp, N.; Heijnen, C. J.; Willemsen, H. L.; Deumens, R.; Joosten, E. A.; Kleibeuker, W.; den Hartog, I. J.; van Velthoven, C. T.; Nijboer, C.; Nassar, M. A.; Dorn, G. W., 2nd; Wood, J. N.; Kavelaars, A., GRK2: a novel cell-specific regulator of severity and duration of inflammatory pain. *Journal of Neuroscience* **2010**, *30* (6), 2138-49.
145. Penela, P.; Murga, C.; Ribas, C.; Salcedo, A.; Jurado-Pueyo, M.; Rivas, V.; Aymerich, I.; Mayor, F., Jr., G protein-coupled receptor kinase 2 (GRK2) in migration and inflammation. *Archives of physiology and biochemistry* **2008**, *114* (3), 195-200.
146. Penela, P.; Murga, C.; Ribas, C.; Lafarga, V.; Mayor, F., Jr., The complex G protein-coupled receptor kinase 2 (GRK2) interactome unveils new physiopathological targets. *British journal of pharmacology* **2010**, *160* (4), 821-32.
147. Luttrell, L. M., Composition and function of g protein-coupled receptor signalsomes controlling mitogen-activated protein kinase activity. *Journal of molecular neuroscience : MN* **2005**, *26* (2-3), 253-64.
148. Ribas, C.; Penela, P.; Murga, C.; Salcedo, A.; Garcia-Hoz, C.; Jurado-Pueyo, M.; Aymerich, I.; Mayor, F., Jr., The G protein-coupled receptor kinase

(GRK) interactome: role of GRKs in GPCR regulation and signaling. *Biochimica et biophysica acta* **2007**, *1768* (4), 913-22.

149. Rivas, V., Developmental and tumoral vascularization is regulated by G protein-coupled receptor kinase 2. *The Journal of Clinical Investigation* **2013**, *123* (11), 4714-30.

150. van Meeteren, L. A.; Goumans, M. J.; ten Dijke, P., TGF-beta receptor signaling pathways in angiogenesis; emerging targets for anti-angiogenesis therapy. *Current pharmaceutical biotechnology* **2011**, *12* (12), 2108-20.

151. Rivas, V.; Nogues, L.; Reglero, C.; Mayor, F., Jr.; Penela, P., Role of G protein-coupled receptor kinase 2 in tumoral angiogenesis. *Molecular & cellular oncology* **2014**, *1* (4), e969166.

152. (a) Kahn, C. R.; Crettaz, M., Insulin receptors and the molecular mechanism of insulin action. *Diabetes/metabolism reviews* **1985**, *1* (1-2), 5-32;

(b) Kahn, C. R., The molecular mechanism of insulin action. *Annual review of medicine* **1985**, *36*, 429-51.

153. Vila-Bedmar, R.; Cruces-Sande, M.; Lucas, E.; Willemen, H. L.; Heijnen, C. J.; Kavelaars, A.; Mayor, F., Jr.; Murga, C., Reversal of diet-induced obesity and insulin resistance by inducible genetic ablation of GRK2. *Science signaling* **2015**, *8* (386), ra73.

154. Usui, I., G Protein-Coupled Receptor Kinase 2 Mediates Endothelin-1-Induced Insulin Resistance via the Inhibition of Both Gαq/11 and Insulin Receptor Substrate-1 Pathways in 3T3-L1 Adipocytes. *Molecular Endocrinology* **2005**, *19* (11), 2760–2768.

155. Usui, I., GRK2 is an endogenous protein inhibitor of the insulin signaling pathway for glucose transport stimulation. *EMBO Journal* **2004**, *23* (14), 2821–2829.

156. Tesmer, J. J.; Tesmer, V. M.; Lodowski, D. T.; Steinhagen, H.; Huber, J., Structure of human G protein-coupled receptor kinase 2 in complex with the kinase inhibitor balanol. *Journal of Medicinal Chemistry* **2010**, *53* (4), 1867-70.

157. Thal, D. M., Molecular mechanism of selectivity among G protein-coupled receptor kinase 2 inhibitors. *Molecular pharmacology* **2011**, *80* (2), 294-303.

158. Mayer, G., An RNA molecule that specifically inhibits G-protein-coupled receptor kinase 2 in vitro. *RNA* **2008**, *14*, 524–534.
159. Niv, M. N., Sequence-based Design of Kinase Inhibitors Applicable for Therapeutics and Target Identification. *The Journal of biological chemistry* **2004**, *279* (2), 1242–1255.
160. Anis, I., Antidiabetic effect of novel modulating peptides of G-protein-coupled kinase in experimental models of diabetes. *Diabetologia* **2004**, *47*, 1232–1244.
161. Gomez-Monterrey, I., SAR study and conformational analysis of a series of novel peptide G protein-coupled receptor kinase 2 (GRK2) inhibitors. *Biopolymers* **2014**, *101* (1), 121-8.
162. Carotenuto, A.; Cipolletta, E.; Gomez-Monterrey, I.; Sala, M.; Vernieri, E.; Limatola, A.; Bertamino, A.; Musella, S.; Sorriento, D.; Grieco, P.; Trimarco, B.; Novellino, E.; Iaccarino, G.; Campiglia, P., Design, synthesis and efficacy of novel G protein-coupled receptor kinase 2 inhibitors. *European Journal of Medicinal Chemistry* **2013**, *69*, 384-92.
163. Cipolletta, E., The G protein coupled receptor kinase 2 plays an essential role in beta-adrenergic receptor-induced insulin resistance. *Cardiovascular Research* **2009**, *84* (3), 407-15.
164. Campiglia, P., Design and Synthesis of Small Libraries of Peptidomimetics Based on a Thiazolidine Moiety. *Letters in Organic Chemistry* **2006**, *3* (7), 539-545.
165. Dolbier, W. R., Organofluorine Compounds: Chemistry and Applications. *Journal of the American Chemical Society*. **2000**, *122* (42), 10492–10492.
166. Okazoe, T., Overview on the history of organofluorine chemistry from the viewpoint of material industry. *Proceedings of the Japan Academy. Series B, Physical and biological sciences* **2009**, *85* (8), 276-89.
167. Jeschke, P.; Baston, E.; Leroux, F. R., alpha-fluorinated ethers as "exotic" entity in medicinal chemistry. *Mini Reviews in Medicinal Chemistry* **2007**, *7* (10), 1027-1034.
168. Wang, J.; Sanchez-Rosello, M.; Acena, J. L.; del Pozo, C.; Sorochinsky, A. E.; Fustero, S.; Soloshonok, V. A.; Liu, H., Fluorine in Pharmaceutical

Industry: Fluorine-Containing Drugs Introduced to the Market in the Last Decade (2001-2011). *Chemical Reviews* **2014**, *114* (4), 2432-2506.

169. Zafrani, Y.; Yeffet, D.; Sod-Moriah, G.; Berliner, A.; Amir, D.; Marciano, D.; Gershonov, E.; Saphier, S., Difluoromethyl Bioisostere: Examining the "Lipophilic Hydrogen Bond Donor" Concept. *Journal of Medicinal Chemistry* **2017**, *60* (2), 797-804.

170. (a) Qiu, X. L.; Meng, W. D.; Qing, F. L., Synthesis of fluorinated amino acids. *Tetrahedron* **2004**, *60* (32), 6711-6745; (b) Smits, R.; Cadicamo, C. D.; Burger, K.; Koksche, B., Synthetic strategies to alpha-trifluoromethyl and alpha-difluoromethyl substituted alpha-amino acids. *Chemical Society reviews* **2008**, *37* (8), 1727-39.

171. Burri, C.; Brun, R., Eflornithine for the treatment of human African trypanosomiasis. *Parasitology research* **2003**, *90 Supp 1*, S49-52.

172. Wordell, C. J.; Hauptman, S. P., Treatment of Pneumocystis carinii pneumonia in patients with AIDS. *Clinical pharmacy* **1988**, *7* (7), 514-27.

173. Nawrot, E.; Jonczyk, A., Difluoromethyltrialkylammonium salts - Their expeditious synthesis from chlorodifluoromethane and tertiary amines in the presence of concentrated aqueous sodium hydroxide. The catalytic process. *Journal of Organic Chemistry* **2007**, *72* (26), 10258-10260.

174. Miller, T. G., The Preparation of Aryl Difluoromethyl Ethers. *J. Org. Chem* **1960**, *25* (11), 2009-2012.

175. Lee, K. N.; Lee, J. W.; Ngai, M. Y., Synthesis of Trifluoromethoxylated (Hetero)Arenes via OCF₃ Migration. *Synlett : accounts and rapid communications in synthetic organic chemistry* **2016**, *27* (3), 313-319.

176. World Meteorological Organization (WMO), Global Ozone Research and Monitoring Project. **1985**, *Reports Nos. 16* (20).

177. Ravishankara, A. R., Do Hydrofluorocarbons Destroy Stratospheric Ozone? *Science* **1994**, *263*, 71-75.

178. Aikawa, K., α -difluoromethylation on sp³ carbon of nitriles using fluoroform and Ruppert-Prakash reagent. *Organic Letters* **2015**, *17* (19), 4882-4885.

179. Aikawa, K., Siladifluoromethylation and Difluoromethylation onto C(sp³), C(sp²), and C(sp) Centers Using Ruppert–Prakash Reagent and Fluoroform. *Organic Letters* **2016**, *18* (14), 3354–3357.
180. Thomason, C. S.; Dolbier, W. R., Use of Fluoroform as a Source of Difluorocarbene in the Synthesis of Difluoromethoxy- and Difluorothiomethoxyarenes. *Journal of Organic Chemistry* **2013**, *78* (17), 8904–8908.
181. Iida, T., Umpolung of Fluoroform by CF Bond Activation: Direct Difluoromethylation of Lithium Enolates *Angewandte Chemie International Edition* **2012**, *51*, 9535–9538
182. Honda, K., Computational SN₂-Type Mechanism for the Difluoromethylation of Lithium Enolate with Fluoroform through Bimetallic C–F Bond Dual Activation. *A European Journal* **2016**, *22* (26), 8796–8800.
183. Porta, R.; Benaglia, M.; Puglisi, A., Flow Chemistry: Recent Developments in the Synthesis of Pharmaceutical Products. *Organic Process Research & Development* **2016**, *20* (1), 2–25.
184. Gutmann, B.; Cantillo, D.; Kappe, C. O., Continuous-flow technology—a tool for the safe manufacturing of active pharmaceutical ingredients. *Angewandte Chemie* **2015**, *54* (23), 6688–728.
185. Ribereau-Gayon, G.; Palfreyman, M. G.; Zraika, M.; Wagner, J.; Jung, M. J., Irreversible inhibition of aromatic-L-amino acid decarboxylase by alpha-difluoromethyl-DOPA and metabolism of the inhibitor. *Biochemical pharmacology* **1980**, *29* (18), 2465–9.
186. Bey, P., Direct synthesis of α -halogenomethyl- α -amino acids from the parent α -amino acids. *The Journal of Organic Chemistry* **1979**, *44* (15), 2732–2742.
187. O'Donnell, M. J., The enantioselective synthesis of alpha-amino acids by phase-transfer catalysis with achiral Schiff base esters. *Accounts of chemical research* **2004**, *37* (8), 506–17.
188. Köckinger, M., Utilization of fluoroform for difluoromethylation in continuous flow: a concise synthesis of α -difluoromethyl-amino acids. *Green Chemistry* **2018**, *20*, 108–112.